


RADIOLOGY
AND
ONCOLOGY



vol.52 no.2
june 2018

NOVO

CABOMETYX®

(kabozantinib) tablete

60 mg | 40 mg | 20 mg

CABOMETYX® pomembno izboljša PFS, OS in ORR v drugi liniji zdravljenja napredovalega karcinoma ledvičnih celic¹

Z mehanizmom delovanja, ki premaga rezistenco na predhodni zaviralec VEGFR, z zaviranjem AXL, MET in VEGFR.¹

AXL: receptor za protein 6, ki specifično zavira rast; MET: receptor za hepatocitni rastni faktor; ORR: objektivna stopnja odziva; OS: celokupno preživetje; PFS: preživetje brez napredovanja bolezni; VEGFR: receptor za VEGF

Referenci:

1. Choueiri TK, Escudier B, Powles T, et al. Cabozantinib versus everolimus in advanced renal cell carcinoma (METEOR): final results from a randomised, open-label, phase 3 trial. *The Lancet Oncology*. 2016;17(7):917-27.
2. Povzetek glavnih značilnosti zdravila Cabometyx.

- ✓ PFS²
- ✓ OS²
- ✓ ORR²

Skrajšani povzetki glavnih značilnosti zdravila

CABOMETYX 20 mg filmsko obložene tablete
CABOMETYX 40 mg filmsko obložene tablete
CABOMETYX 60 mg filmsko obložene tablete
(kabozantinib)

TERAPEVTSKE INDIKACIJE Zdravljenje odraslih bolnikov z napredovalim karcinomom ledvičnih celic (KLC) po predhodnem zdravljenju, usmerjenem v vaskularni endotelijski rastni faktor (VEGF). **ODMERJANJE IN NAČIN UPORABE** Priporočeni odmerek je 60 mg enkrat na dan. Zdravljenje je treba nadaljevati tako dolgo, dokler bolnik več nima kliničnih koristi od terapije ali do pojava nesprejemljive toksičnosti. Pri sumu na neželeno reakcijo na zdravljenje, bodi morda treba zdravljenje začasno prekiniti in/ali zmanjšati odmerek. Če je treba odmerek zmanjšati, se priporoča zmanjšanje na 40 mg na dan in nato na 20 mg na dan. Prekinitev odmerka se priporoča pri obravnavi toksičnosti 3. ali višje stopnje po CTCAE (*common terminology criteria for adverse events*) ali nevzdržni toksičnosti 2. stopnje. Zmanjšanje odmerka se priporoča za dogodke, ki bi lahko čez čas postali resni ali nevzdržni. V primeru pojavnosti neželenih učinkov 1. in 2. stopnje, ki jih bolnik prenaša in jih je možno enostavno obravnavati, prilagoditev odmerjanja običajno ni potrebna. Treba je razmisлити o dodatni podporni oskrbi. V primeru pojavnosti neželenih učinkov 2. stopnje, ki jih bolnik ne prenaša in jih ni mogoče obravnavati z zmanjšanjem odmerka ali podporno oskrbo, je treba zdravljenje prekiniti, dokler neželeni učinki ne izvenijo do ≤ 1. stopnje, uvesti podporno oskrbo in razmisлити o ponovni uvedbi zdravljenja z zmanjšanim odmerkom. V primeru pojavnosti neželenih učinkov 3. stopnje je treba zdravljenje prekiniti, dokler neželeni učinki ne izvenijo do ≤ 1. stopnje, uvesti podporno oskrbo in razmisлити o ponovni uvedbi zdravljenja z zmanjšanim odmerkom. V primeru pojavnosti neželenih učinkov 4. stopnje je treba zdravljenje prekiniti, uvesti ustrezno zdravniško oskrbo, in če neželeni učinki izvenijo do ≤ 1. stopnje, ponovno uvesti zdravljenje z zmanjšanim odmerkom. Če neželeni učinki ne izvenijo, je treba trajno prenehati z uporabo. Pri bolnikih z blago ali zmerno **ledvično okvaro** je treba kabozantinib uporabljati previdno. Uporaba se ne priporoča pri bolnikih s hudo ledvično okvaro. Pri bolnikih z blago ali zmerno **jetrno okvaro** je priporočeni odmerek kabozantiniba 40 mg enkrat na dan. Pri teh bolnikih je treba spremljati neželeno dogodke in po potrebi razmisлити o prilagoditvi odmerka ali prekinitvi dajanja. Uporaba se ne priporoča pri bolnikih s hudo jetrno okvaro. **Način uporabe:** Tablete je treba pogoltniti cele in jih ni dovoljeno drobiti. Bolnikom je treba naročiti, naj vsaj 2 uri pred uporabo zdravila in 1 uro po tem ničesar ne jedo. **KONTRAINDIKACIJE** Preobčutljivost na učinkovino ali katero koli pomožno snov. **POSEBNA OPOZORILO IN PREVIDNOSTNI UKREPI** Večina dogodkov se lahko pojavi zgodaj v teku zdravljenja, zato mora zdravnik bolnika v prvih 8 tednih zdravljenja skrbno spremljati, da oceni, ali je treba odmerek prilagoditi. Dogodki, ki se običajno pojavijo zgodaj, vključujejo hipokalcemijo, hipokaliemijo, trombocitopenijo, hipertenzijo, sindrom palmarno-plantarne eritrodisezije (PPES), proteinurijo in gastrointestinalne dogodke (bolečine v trebuhu, vnetje sluznice, zaprtje, driska, bruhanje). Bolnike, ki imajo vnetno bolezen črevesja (npr. Crohnovo bolezen, ulcerozni kolitis, peritonitis, divertikulitis ali apendicitis), ki imajo tumorsko infiltracijo prebavil ali so imeli pred posegom na prebavilih zaplete (zlasti v povezavi z zapoznelimi ali

▼ Za to zdravilo se izvaja dodatno spremljanje varnosti. Tako bodo hitreje na voljo nove informacije o njegovi varnosti. Zdravstvene delavce naprošamo, da poročajo o katerem koli domnevem neželenem učinku zdravila.

nepopolnim celjenjem), je treba pred uvedbo zdravljenja skrbno oceniti, nato pa natančno spremljati za pojav simptomov perforacij in fistul, vključno z abscesi. Trajna ali ponavljajoča se driska med zdravljenjem je lahko dejavnik tveganja za nastanek analne fistule. Uporaba kabozantiniba je treba pri bolnikih, pri katerih se pojavi gastrointestinalna perforacija ali fistula, ki je ni možno ustrezno obravnavati, prekiniti. Kabozantinib je treba uporabljati previdno pri bolnikih, pri katerih obstaja tveganje za pojav venske tromboembolije, vključno s pljučno embolijo, in arterijske tromboembolije ali imajo te dogodke v anamnezi. Z uporabo je treba prenehati pri bolnikih, pri katerih se razvije akutni miokardni infarkt ali drugi klinično pomembni znaki zapletov arterijske tromboembolije. Kabozantiniba se ne sme dajati bolnikom, ki hudo krvavijo, ali pri katerih obstaja tveganje za hudo krvavitev. Zdravljenje s kabozantinibom je treba ustaviti vsaj 28 dni pred načrtovanim kirurškim posegom, vključno z zobozdravstvenim, če je mogoče. Kabozantinib je treba ukiniti pri bolnikih z zapletom s celjenjem rane, zaradi katerih je potrebna zdravniška pomoč. Pred uvedbo kabozantiniba je treba dobro obvladati krvni tlak. Med zdravljenjem je treba vse bolnike spremljati za pojav hipertenzije in jih po potrebi zdraviti s standardnimi antihipertenzivi. V primeru trdovratne hipertenzije, kljub uporabi antihipertenzivov, je treba odmerek kabozantiniba zmanjšati. Z uporabo je treba prenehati, če je hipertenzija resna ali trdovratna kljub zdravljenju z antihipertenzivi in zmanjšanemu odmerku kabozantiniba. V primeru hipertenzijske krize je treba zdravljenje prekiniti. Pri resni PPES je treba razmisлити o prekinitvi zdravljenja. Nadaljevanje zdravljenja naj se začne z nižjim odmerkom, ko se PPES umiri do 1. stopnje. V času zdravljenja je treba redno spremljati beljakovine v urinu. Pri bolnikih, pri katerih se razvije nefrotični sindrom, je treba z uporabo kabozantiniba prenehati. Pri uporabi kabozantiniba so opazili sindrom reverzibilne posteriorne levkoencefalopatije (RPLS), znan tudi kot sindrom posteriorne reverzibilne encefalopatije (PRES). Na ta sindrom je treba pomisliti pri vseh bolnikih s številnimi prisotnimi simptomi, vključno z epileptičnimi napadi, glavobolom, motnjami vida, zmedenostjo ali spremenjenim mentalnim delovanjem. Pri bolnikih z RPLS je treba zdravljenje prekiniti. Kabozantinib je treba uporabljati previdno pri bolnikih s podaljšanjem intervala QT v anamnezi, pri bolnikih, ki jemljejo antiaritmike, in pri bolnikih z relevantno obstoječo boleznijo srca, bradikardijo ali elektrolitskimi motnjami. Bolniki z redko dedno intoleranco za galaktozo, laponsko obliko zmanjšane aktivnosti laktaze ali malabsorpcijo glukoze/galaktoze ne smejo jemati tega zdravila. **Plodnost, nosečnost in dojenje:** Zenskam v rodni dobi je treba svetovati, da v času zdravljenja s kabozantinibom ne smejo zanositi. Zanositev morajo preprečiti tudi ženske partnerice moških bolnikov, ki uporabljajo kabozantinib. Med zdravljenjem in še vsaj 4 mesece po končanju terapije morajo tako bolniki in bolnice kot tudi njihovi partnerji uporabljati zanesljiv način kontracepcije. Kabozantiniba se ne sme uporabljati med nosečnostjo, razen če zdravljenje ni nujno potrebno zaradi kliničnega stanja ženske. Matere med zdravljenjem s kabozantinibom in še 4 mesece po končanju terapije ne smejo dojeti. Zdravljenje s kabozantinibom lahko predstavlja tveganje za plodnost pri moških in ženskah. **INTERAKCIJE** Kabozantinib je substrat za CYP3A4. Pri sočasni uporabi močnih zaviralcev CYP3A4 (npr. ritonavirja, itrakonazola, eritromicina, klaritromicina, soka grenivke) je potrebna previdnost. Kronični sočasni

uporabi močnih induktorjev CYP3A4 (npr. fenitoina, karbamazepina, rifampicina, fenobarbitala ali pripravkov želiščnega izvora iz šentjanževke) se je treba izogibati. Razmisлити je treba o sočasni uporabi alternativnih zdravil, ki CYP3A4 ne inducirajo in ne zavirajo ali pa inducirajo in zavirajo le neznatno. Pri sočasni uporabi zaviralcev MRP2 je potrebna previdnost (npr. ciklosporin, efavirenz, emtricitabin), saj lahko povzročijo povečanje koncentracij kabozantiniba v plazmi. Učinka kabozantiniba na farmakokinetiko kontraceptivnih steroidov niso preučili, vendar pa se priporoča dodatna kontracepcijska metoda (pregradna metoda). Zaradi visoke stopnje vezave kabozantiniba na plazemske beljakovine je možna interakcija z varfarinom v obliki izpodrivanja iz plazemskih beljakovin, zato je treba spremljati vrednosti INR. Kabozantinib morda lahko poveča koncentracije sočasno uporabljenih substratov P-gp v plazmi. Osebe je treba opozoriti na uporabo substratov P-gp (npr. feksofenadina, aliskirena, ambrisentana, dabigatran eteksilata, digoksin, kolhicin, maravirola, posakonazola, ranolazina, saksaglitina, sitagliptina, talinolola, tolvaptana) sočasno s kabozantinibom. **NEŽELENI UČINKI** Za popolno informacijo o neželenih učinkih, prosimo, preberite celoten povzetek glavnih značilnosti zdravila Cabometyx. Najbolj pogosti resni neželeni učinki so bolečine v trebuhu (3 %), pleuralni izliv (3 %), driska (2 %) in navzea (2 %). Najpogostejši neželeni učinki katere koli stopnje (pojavili so se pri vsaj 25 % bolnikov) vključujejo drisko (74 %), utrujenost (56 %), navzeo (50 %), zmanjšani apetit (46 %), PPES (42 %), hipertenzijo (37 %), bruhanje (32 %), zmanjšanje telesne mase (31 %) in konstipacijo (25 %). **Zelo pogosti (≥ 1/10):** anemija, hipotiroidizem, zmanjšani apetit, hipofosfatemija, hipoalbuminemija, hipomagnezija, hiponatriemija, hipokaliemija, hiperkaliemija, hipokalcemija, hiperbilirubinemija, disgeviija, glavobol, omotica, hipertenzija, disfonija, dispneja, kašelj, driska, navzea, bruhanje, stomatitis, konstipacija, bolečine v trebuhu, dispneja, PPES, izpuščaji, suha koža, bolečine v okončinah, mišični spazmi, artralgiija, proteinurija, utrujenost, vnetje sluznice, astenija, zmanjšanje telesne mase, zvišanje vrednosti ALT, AST in ALP v serumu, zvišanje vrednosti kreatinina, zvišanje vrednosti trigliceridov, hiperglikemija, hipoglikemija, limfopenija, nevropenija, trombocitopenija, povečana vrednost GGT, povečana vrednost amilaze, povečana vrednost holesterola v krvi, povečana vrednost lipaze. **Pogosti (≥ 1/100, < 1/10):** absces, dehidracija, tinitus, pljučna embolija, bolečina zgornjega dela trebuha, gastroezofagealna refluksna bolezen, hemoroidi, pruritus, alopecija, periferni edem. **Občasni (≥ 1/1000, < 1/100):** konvulzije, analna fistula, pankreatitis, holestatični hepatitis, osteonekroza čeljusti. **Vrsta ovojnine in vsebina:** Pastenka vsebuje 30 filmosko obloženih tablet. **Režim izdaje:** Rp/Spec. **Imetnik dovoljenja za promet z zdravilom:** Ipsen Pharma, 65 quai Georges Gorse, 92100 Boulogne-Billancourt, Francija **Pred predpisovanjem, prosimo, preberite celoten povzetek glavnih značilnosti zdravila!** CAB-112017

IPSEN
Innovation for patient care

SAMO ZA STROKOVNO JAVNOST
CABO418-03, april 2018

PharmaSwiss
Choose More Life

Odgovoren za trženje v Sloveniji:
PharmaSwiss d.o.o., Brodišče 32, 1236 Trzin
telefon: +386 1 236 47 00, faks: +386 1 283 38 10



Publisher

Association of Radiology and Oncology

Affiliated with

Slovenian Medical Association – Slovenian Association of Radiology, Nuclear Medicine Society,
Slovenian Society for Radiotherapy and Oncology, and Slovenian Cancer Society
Croatian Medical Association – Croatian Society of Radiology
Societas Radiologorum Hungarorum
Friuli-Venezia Giulia regional groups of S.I.R.M.
Italian Society of Medical Radiology

Aims and scope

Radiology and Oncology is a journal devoted to publication of original contributions in diagnostic and interventional radiology, computerized tomography, ultrasound, magnetic resonance, nuclear medicine, radiotherapy, clinical and experimental oncology, radiobiology, radiophysics and radiation protection.

Editor-in-Chief

Gregor Serša, Institute of Oncology Ljubljana,
Department of Experimental Oncology, Ljubljana,
Slovenia

Executive Editor

Viljem Kovač, Institute of Oncology Ljubljana,
Department of Radiation Oncology, Ljubljana, Slovenia

Editorial Board

Sotirios Bisdas, National Hospital for Neurology
and Neurosurgery, University College London
Hospitals, London, UK

Karl H. Bohuslavizki, Facharzt für
Nuklearmedizin, Hamburg, Germany

Serena Bonin, University of Trieste, Department of
Medical Sciences, Trieste, Italy

Boris Brkljačić, University Hospital “Dubrava”,
Department of Diagnostic and Interventional
Radiology, Zagreb, Croatia

Luca Campana, Veneto Institute of Oncology
(IOV-IRCCS), Padova, Italy

Christian Dittreich, Kaiser Franz Josef - Spital,
Vienna, Austria

Metka Filipič, National Institute of Biology,
Department of Genetic Toxicology and Cancer Biology,
Ljubljana, Slovenia

Maria Gódehy, National Institute of Oncology,
Budapest, Hungary

Janko Kos, University of Ljubljana, Faculty of
Pharmacy, Ljubljana, Slovenia

Robert Jeraj, University of Wisconsin, Carbone
Cancer Center, Madison, Wisconsin, USA

Advisory Committee

Tullio Girdali, University of Trieste, Faculty of
Medicine and Psychology, Trieste, Italy

Vassil Hadjidekov, Medical University,
Department of Diagnostic Imaging, Sofia, Bulgaria

Deputy Editors

Andrej Čör, University of Primorska, Faculty of
Health Science, Izola, Slovenia

Maja Čemažar, Institute of Oncology Ljubljana,
Department of Experimental Oncology, Ljubljana,
Slovenia

Igor Kocijančič, University Medical Centre
Ljubljana, Institute of Radiology, Ljubljana, Slovenia

Karmen Stanič, Institute of Oncology Ljubljana,
Department of Radiation Oncology, Ljubljana, Slovenia

Primož Strojjan, Institute of Oncology Ljubljana,
Department of Radiation Oncology, Ljubljana, Slovenia

Tamara Lah Turnšek, National Institute of
Biology, Ljubljana, Slovenia

Damijan Miklavčič, University of Ljubljana,
Faculty of Electrical Engineering, Ljubljana, Slovenia

Luka Milas, UT M. D. Anderson Cancer Center,
Houston, USA

Damir Miletić, Clinical Hospital Centre Rijeka,
Department of Radiology, Rijeka, Croatia

Håkan Nyström, Skandionkliniken,
Uppsala, Sweden

Maja Osmak, Ruder Bošković Institute,
Department of Molecular Biology, Zagreb, Croatia

Dušan Pavčnik, Dotter Interventional Institute,
Oregon Health Science University, Oregon,
Portland, USA

Geoffrey J. Pilkington, University of
Portsmouth, School of Pharmacy and Biomedical
Sciences, Portsmouth, UK

Ervin B. Podgoršak, McGill University,
Montreal, Canada

Matthew Podgorsak, Roswell Park Cancer
Institute, Departments of Biophysics and Radiation
Medicine, Buffalo, NY, USA

Marko Hočevar, Institute of Oncology Ljubljana,
Department of Surgical Oncology, Ljubljana, Slovenia

Miklós Kásler, National Institute of Oncology,
Budapest, Hungary

Csaba Polgar, National Institute of Oncology,
Budapest, Hungary

Dirk Rades, University of Lubeck, Department of
Radiation Oncology, Lubeck, Germany

Mirjana Rajer, Institute of Oncology Ljubljana,
Department of Radiation Oncology, Ljubljana, Slovenia

Luis Souhami, McGill University, Montreal,
Canada

Borut Štabuc, University Medical Centre Ljubljana,
Department of Gastroenterology, Ljubljana, Slovenia

Katarina Šurlan Popovič, University Medical
Center Ljubljana, Clinical Institute of Radiology,
Ljubljana, Slovenia

Justin Teissié, CNRS, IPBS, Toulouse, France

Gillian M. Tozer, University of Sheffield,
Academic Unit of Surgical Oncology, Royal
Hallamshire Hospital, Sheffield, UK

Andrea Veronesi, Centro di Riferimento
Oncologico - Aviano, Division of Medical Oncology,
Aviano, Italy

Branko Zakotnik, Institute of Oncology Ljubljana,
Department of Medical Oncology, Ljubljana, Slovenia

Stojan Plesničar, Institute of Oncology Ljubljana,
Department of Radiation Oncology, Ljubljana, Slovenia

Tomaž Benulič, Institute of Oncology Ljubljana,
Department of Radiation Oncology, Ljubljana, Slovenia

Editorial office

Radiology and Oncology

Zaloška cesta 2

P. O. Box 2217

SI-1000 Ljubljana

Slovenia

Phone: +386 1 5879 369

Phone/Fax: +386 1 5879 434

E-mail: gsera@onko-i.si

Copyright © Radiology and Oncology. All rights reserved.

Reader for English

Vida Kološa

Secretary

Mira Klemenčič

Zvezdana Vukmirović

Design

Monika Fink-Serša, Samo Rován, Ivana Ljubanović

Layout

Matjaž Lužar

Printed by

Tiskarna Ozimek, Slovenia

Published quarterly in 400 copies

Beneficiary name: DRUŠTVO RADIOLOGIJE IN ONKOLOGIJE

Zaloška cesta 2

1000 Ljubljana

Slovenia

Beneficiary bank account number: SI56 02010-0090006751

IBAN: SI56 0201 0009 0006 751

Our bank name: Nova Ljubljanska banka, d.d.,

Ljubljana, Trg republike 2,

1520 Ljubljana; Slovenia

SWIFT: LJBASIX

Subscription fee for institutions EUR 100, individuals EUR 50

The publication of this journal is subsidized by the Slovenian Research Agency.

Indexed and abstracted by:

- *Celdes*
- *Chemical Abstracts Service (CAS)*
- *Chemical Abstracts Service (CAS) - SciFinder*
- *CNKI Scholar (China National Knowledge Infrastructure)*
- *CNPIEC*
- *DOAJ*
- *EBSCO - Biomedical Reference Collection*
- *EBSCO - Cinahl*
- *EBSCO - TOC Premier*
- *EBSCO Discovery Service*
- *Elsevier - EMBASE*
- *Elsevier - SCOPUS*
- *Google Scholar*
- *J-Gate*
- *JournalTOCs*
- *Naviga (Softweco)*
- *Primo Central (ExLibris)*
- *ProQuest - Advanced Technologies Database with Aerospace*
- *ProQuest - Health & Medical Complete*
- *ProQuest - Illustrata: Health Sciences*
- *ProQuest - Illustrata: Technology*
- *ProQuest - Medical Library*
- *ProQuest - Nursing & Allied Health Source*
- *ProQuest - Pharma Collection*
- *ProQuest - Public Health*
- *ProQuest - Science Journals*
- *ProQuest - SciTech Journals*
- *ProQuest - Technology Journals*
- *PubMed*
- *PubsHub*
- *ReadCube*
- *SCImago (SJR)*
- *Summon (Serials Solutions/ProQuest)*
- *TDOne (TDNet)*
- *Thomson Reuters - Journal Citation Reports/Science Edition*
- *Thomson Reuters - Science Citation Index Expanded*
- *Ulrich's Periodicals Directory/ulrichsweb*
- *WorldCat (OCLC)*

This journal is printed on acid-free paper

On the web: ISSN 1581-3207

<http://www.degruyter.com/view/j/raon>

<http://www.radioloncol.com>

contents

review

- 121 **Radiotherapy of glioblastoma 15 years after the landmark Stupp's trial: more controversies than standards?**
Tomas Kazda, Adam Dziacky, Petr Burkon, Petr Pospisil, Marek Slavik, Zdenek Rehak, Radim Jancalek, Pavel Slampa, Ondrej Slaby, Radek Lakomy

radiology

- 129 **Ultrasound elastography can detect placental tissue abnormalities**
Tomoya Hasegawa, Naoaki Kuji, Fumiaki Notake, Tetsu Tsukamoto, Toru Sasaki, Motohiro Shimizu, Kazunori Mukaida, Hiroe Ito, Keiichi Isaka, Hirotaka Nishi
- 136 **Is carotid stiffness a possible surrogate for stroke in long-term survivors of childhood cancer after neck radiotherapy?**
Lorna Zadavec Zaletel, Matjaz Popit, Marjan Zaletel
- 143 **Perfusion magnetic resonance imaging changes in normal appearing brain tissue after radiotherapy in glioblastoma patients may confound longitudinal evaluation of treatment response**
Markus Fahlström, Erik Blomquist, Tufve Nyholm, Elna-Marie Larsson

experimental oncology

- 152 ***In silico* selection approach to develop DNA aptamers for a stem-like cell subpopulation of non-small lung cancer adenocarcinoma cell line A549**
Mateja Vidic, Tina Smuc, Nika Janez, Michael Blank, Tomaz Accetto, Jan Mavri, Isis C. Nascimento, Arthur A. Nery, Henning Ulrich, Tamara T. Lah

clinical oncology

- 160 **Matrix metalloproteinases polymorphisms as baseline risk predictors in malignant pleural mesothelioma**
Danijela Strbac, Katja Gorcar, Vita Dolzan, Viljem Kovac
- 167 **Glioblastoma in patients over 70 years of age**
Uros Smrdel, Marija Skoblar Vidmar, Ales Smrdel
- 173 **Comparative analysis of clinical and pathological lymph node staging data in head and neck squamous cell carcinoma patients treated at the General Hospital Vienna**
Christina Eder-Czembirek, Birgit Erlacher, Dietmar Thurnher, Boban M. Erovc, Edgar Selzer, Michael Formanek

- 181 **A population-based study of the effectiveness of stereotactic ablative radiotherapy versus conventional fractionated radiotherapy for clinical stage I non-small cell lung cancer patients**
Chih-Yen Tu, Te-Chun Hsia, Hsin-Yuan Fang, Ji-An Liang, Su-Tso Yang, Chia-Chin Li, Chun-Ru Chien
- 189 **Survival and stability of patients with urothelial cancer and spinal bone metastases after palliative radiotherapy**
Robert Foerster, Katharina Hees, Thomas Bruckner, Tilman Bostel, Ingmar Schlamp, Tanja Sprave, Nils H. Nicolay, Juergen Debus, Harald Rief
- 195 **Prognostic value of plasma EBV DNA for nasopharyngeal cancer patients during treatment with intensity-modulated radiation therapy and concurrent chemotherapy**
Chawalit Lertbutsayanukul, Danita Kannarunimit, Anussara Prayongrat, Chakkapong Chakkabat, Sarin Kitpanit, Pokrath Hansasuta
- 204 **Early cardiotoxicity after adjuvant concomitant treatment with radiotherapy and trastuzumab in patients with breast cancer**
Tanja Marinko, Simona Borstnar, Rok Blagus, Jure Dolenc, Cvetka Bilban-Jakopin
- 213 **Ocular changes in metastatic melanoma patients treated with MEK inhibitor cobimetinib and BRAF inhibitor vemurafenib**
Ana Ursula Gavric, Janja Ocvirk, Polona Jaki Mekjavic
- 220 **Sclerosing melanocytic lesions (sclerosing melanomas with nevoid features and sclerosing nevi with pseudomelanomatous features) - an analysis of 90 lesions**
Biljana Grcar-Kuzmanov, Emanuela Bostjancic, Juan Antonio Contreras Bandres, Joze Pizem

radiophysics

- 229 **An evaluation of the ICON® mask fixation: curing characteristics of the thermoplastic fixation and implications for patient workflow**
Samendra Prasad, Matthew Podgorsak, Robert Plunkett, Dheerendra Prasad

slovenian abstracts

Radiotherapy of glioblastoma 15 years after the landmark Stupp's trial: more controversies than standards?

Tomas Kazda^{1,2,3}, Adam Dziacky⁴, Petr Burkon^{1,2}, Petr Pospisil^{1,2}, Marek Slavik^{1,2}, Zdenek Rehak^{5,6,7,8}, Radim Jancalek^{9,10}, Pavel Slampa^{1,2,6}, Ondrej Slaby^{3,7,8}, Radek Lakomy^{7,8}

¹ Department of Radiation Oncology, Masaryk Memorial Cancer Institute, Brno, Czech Republic

² Department of Radiation Oncology, Faculty of Medicine, Masaryk University, Brno, Czech Republic

³ Central European Institute of Technology, Masaryk University, Brno, Czech Republic

⁴ Faculty of Medicine, Masaryk University, Brno, Czech Republic

⁵ Department of Nuclear Medicine and PET Center, Masaryk Memorial Cancer Institute, Brno, Czech Republic

⁶ Regional Center for Applied Molecular Oncology (RECAMO), Masaryk Memorial Cancer Institute, Brno, Czech Republic

⁷ Department of Comprehensive Cancer Care, Faculty of Medicine, Masaryk University, Brno, Czech Republic

⁸ Department of Comprehensive Cancer Care, Masaryk Memorial Cancer Institute, Brno, Czech Republic

⁹ Department of Neurosurgery - St. Anne's University Hospital Brno, Faculty of Medicine, Masaryk University, Brno, Czech Republic

¹⁰ Department of Neurosurgery, St. Anne's University Hospital Brno, Brno, Czech Republic

Radiol Oncol 2018; 52(2): 121-128.

Received 7 November 2017

Accepted 12 March 2018

Correspondence to: Radek Lakomy M.D., Ph.D., Department of Comprehensive Cancer Care, Masaryk Memorial Cancer Institute, Zlutý kopec 7, 656 53 Brno, Czech Republic. Phone: +420 54 31 32 203; Fax: +420 54 31 32 455; E-mail: lakomy@mou.cz

Disclosure: No potential conflicts of interest were disclosed.

Background. The current standard of care of glioblastoma, the most common primary brain tumor in adults, has remained unchanged for over a decade. Nevertheless, some improvements in patient outcomes have occurred as a consequence of modern surgery, improved radiotherapy and up-to-date management of toxicity. Patients from control arms (receiving standard concurrent chemoradiotherapy and adjuvant chemotherapy with temozolomide) of recent clinical trials achieve better outcomes compared to the median survival of 14.6 months reported in Stupp's landmark clinical trial in 2005. The approach to radiotherapy that emerged from Stupp's trial, which continues to be a basis for the current standard of care, is no longer applicable and there is a need to develop updated guidelines for radiotherapy within the daily clinical practice that address or at least acknowledge existing controversies in the planning of radiotherapy.

The goal of this review is to provoke critical thinking about potentially controversial aspects in the radiotherapy of glioblastoma, including among others the issue of target definitions, simultaneously integrated boost technique, and hippocampal sparing.

Conclusions. In conjunction with new treatment approaches such as tumor-treating fields (TTF) and immunotherapy, the role of adjuvant radiotherapy will be further defined. The personalized approach in daily radiotherapy practice is enabled with modern radiotherapy systems.

Key words: glioblastoma; radiation therapy; controversy; target volumes; radiotherapy dosage

Introduction

Despite many advances in the understanding of glioblastoma (GBM) biology in recent decades,

only a few findings were translated into updates in the treatment guidelines for this most aggressive and frequent primary brain tumor of adults. These updates have notably occurred in the manage-

ment of elderly patients, where methylation of the *O6-methylguanine-DNA methyltransferase* (MGMT) gene promoter indicates higher chemosensitivity and higher benefit from administration of alkylating agents such as temozolomide (TMZ).¹⁻⁵ Unlike for the majority of other cancer types in which there have been treatment gains with the advent of targeted therapies, there have not been similar advances in GBM treatment to date. Owing to rich tumor neovascularization, much hope was put especially into anti-angiogenic therapy⁶; however, negative results have been reported in GBM clinical trials that used bevacizumab to target vascular endothelial growth factor.^{7,8} In contrast with negative results from recent GBM trials focused on new pharmacotherapeutics, co-administration of RT with TMZ has nearly tripled the 2-year survival of GBM patients in the last decade from a dismal 10% with RT alone to 27% with the addition of TMZ and quintupled to 47% in patients with MGMT promoter methylation⁹, representing an exciting advance after little progress in previous decades.¹⁰ However, standard post-surgery treatment of newly diagnosed GBM patients has remained unchanged since implementation of the recommendations of the EORTC 26981–22981/NCIC CE3 trial (Stupp regimen) that finished enrolling patients in 2002 and was published in 2005.^{9,11} In this protocol, TMZ (75 mg/m²) is administered on days 1 through 42 with concomitant RT (60 Gy), followed by administration of TMZ alone (150 to 200 mg/m²) on days 1–5 in six consecutive 4-week cycles. Co-administration of TMZ improved survival from 12.1 months (with RT alone) to 14.6 months (with the addition of TMZ).^{11,12}

This educational review considers potentially controversial aspects in the RT of GBM assuming strict application of the current standard of care EORTC 26981–22981/NCIC CE3 protocol for RT planning.

Current updates in glioblastoma treatment

Despite the advance described above, patients in ordinary clinical practice (outside of clinical trials) have now been treated with the same general protocol for more than 10 years. During that time, though, RT itself has experienced rapid evolution due to advances in computing technology, better access to imaging methods, and more sophisticated RT instrumentation.¹³ Today, preparation and application of RT is much more complicated than 10 years ago, but does this complexity bring

any benefits in regards to overall survival of patients with GBM? Even though patients receive a numerically identical dose of 60 Gy, the dosing technique matters as it affects toxicity. There is an obvious difference between conventional 2-dimensional external beam RT (as whole brain irradiation, WBRT) and the 3-dimensional conformal RT or other modern methods of photon RT (*e.g.*, intensity-modulated arc therapy, IMRT). Recently, tumor-treating fields (TTFs) have become recognized as a novel cancer treatment modality with antimitotic effects against rapidly dividing tumor cells.¹⁴ This is caused by alternating electric fields of low-intensity and intermediate-frequency through transducer arrays applied to the shaved head, which are being increasingly thought of as an upcoming new standard of care in GBM, already approved by the U.S. Food and Drug Administration for both newly diagnosed as well as recurrent GBM.¹⁵ A randomized clinical phase 3 trial EF-14 evaluated the effect of TTF plus maintenance TMZ *vs.* maintenance TMZ alone on survival parameters in patients with newly diagnosed GBM.^{16,17} This trial represents the first major advance in the treatment of newly diagnosed GBM in roughly a decade, with a hazard ratio for overall survival of 0.63 being numerically comparable with that seen in the Stupp trial in 2005. Ultimately, aside from health-care payers' points of view, the willingness of patients to undergo the burden of carrying a TTF device non-stop will determine if TTF becomes a new standard of care.¹⁸ Based on the interim analysis, there is no preliminary evidence that health-related quality of life, cognitive, or functional status is adversely affected by continuous usage of TTF.¹⁹

Notably, patients in control (standard therapy) arm of this trial achieved relatively long median survival, as well as in another recent trial (ACT IV trial), where the role of epidermal growth factor receptor EGFRvIII targeted vaccine-based immunotherapy rindopepimut was investigated.²⁰ Compared to a median overall survival (OS) of 14.6 months in the original Stupp trial¹¹, there was reported to be significant increase in median OS (from diagnosis to death) to 19.8 months in the EF-14 trial¹⁷, and to 20.2 months (median 17.4 months from randomization to death + a reported median of 2.8 months from diagnosis to randomization) in the control arm of the rindopepimut ACT IV trial.²⁰ Since the underlying treatment (RT to 60 Gy + concomitant and maintenance TMZ) is the same, it is unclear whether this difference in median OS is the evidence of improved treatment outcomes as

a consequence of modern surgery, improved RT, and up-to-date management of toxicity. Patients in both of these studies were randomized after the completion of concomitant chemoradiotherapy. Thus, more favorable patients were selected compared to the first landmark Stupp trial. For this reason, a selection bias may be responsible for the described difference in OS. 82 out of 1019 (8%) eligible patients for EF-14 trial experienced progressive disease after completion of radiotherapy phase and were excluded.¹⁷ Whether 8% patients with the worst prognosis would have been excluded in EORTC 26981–22981/NCIC CE3 trial, the median overall survival would be roughly 16.5 months from randomization (17.7 months from diagnosis). So without eventual selection bias, it is possible to compare these 17.7 months in the Stupp trial to the 19.8 months in EF-14 and 20.2 months in rindopepimut trials, all with the same treatment RT + TMZ. The difference in more than 2 months is clear improvement in outcomes as a consequence of modern surgery, RT and toxicity management. Or should we utilize approaches in daily RT practice which were employed in the Stupp trial decade ago since this is a “registration” trial for the current standard of care?

The correct total dose

Despite advances in RT over the last 10 to 15 years, certain postulates remain unchanged. One such principle is: “*the correct dose to the correct place.*” Dosage for adjuvant RT of GBM has been same over the last few decades, and it is not typically considered controversial in patients younger than 60–65 years.²¹ The effect of high doses in adjuvant RT of GBM was shown in 1979 by a retrospective analysis performed by the German “Brain Tumor Study Group”.²³ The best result (median overall survival of 42 weeks) was achieved by WBRT with 60 Gy compared to 55 (36 weeks) or 50 Gy (28 weeks)²³ and with significant difference between those receiving 60 versus 50 Gy. Doses above 60 Gy did not lead to any benefit regardless of RT technique used. With WBRT, increasing to 70 Gy was not associated with further survival improvement.²⁴ The later attempts to improve outcomes by an increase of RT dose included combination of 60 Gy WBRT and increased targeted dosage by IMRT²⁵, brachytherapy²⁶, or stereotactic radiosurgery (RTOG 9305).²⁷ Increasing focused radiation dose by hyperfractionation was tested as well.²⁸ Doses above 60 Gy have not proven to be beneficial even in the TMZ era.²⁹

One might conclude that the question of the correct total dose in adjuvant RT is a closed chapter and further studies in this field are not judged. On the other hand, it is possible that the studies mentioned above missed application of increased RT dose to the most malignant tumor cells (a high-density portion of tumor). Such areas are generally considered to be areas with contrast enhancement on CT or MRI. MRI-guided serial biopsy study has proven that tumor cells are present inside but also outside the area of this enhancement, infiltrating at least borders of T2 hyperintensity on MRI.³⁰ Positron emission tomography (PET) has an increasingly important role in the diagnosis, grading, response assessment, and/or guidance of surgery and RT.^{31–33} For example, ¹⁸F-DOPA (3,4-dihydroxy-6-[¹⁸F] fluoro-1-phenylalanine) is an amino acid tracer that identifies areas of high-grade portions of disease as proven by histopathology evaluation of ¹⁸F-DOPA and MRI-guided biopsies with statistically significant difference in tumor-to-normal brain uptake ratio between grade II, III and IV gliomas.³⁴ Dose escalation to not only areas with post-contrast MRI enhancement but also to high-risk areas identified by PET or diffusion/perfusion MRI may improve clinical outcomes of glioma treatment.³⁵ An ongoing phase II clinical trial for high-grade gliomas is evaluating increases in the dose up to 76 Gy with target volume defined by MRI and ¹⁸F-DOPA PET (NCT01991977). Dose-escalated proton beam RT is being evaluated in an ongoing prospective trial as well (NCT02179086). Hence, even if the current RT dosage is well established at 60 Gy in common standard of care, the correct dose of radiation may become controversial shortly with wider availability of advanced MR and PET imaging or proton beam facilities.^{36,37} Furthermore, as we gain additional experience with TTF therapy, effects of concurrent administration of TTF and RT will be questioned, and dose escalation or de-escalation trials may be of substantial interest in the field, further clouding the issue of correct RT dose.

The correct RT target definition

Determination of the ideal target volume for RT represents a trade-off between minimizing treatment-related toxicity and achieving tumor control. With standard structural MRI, there are several comparable methods of contouring clinical target volume (CTV: location of expected or suspected malignant cells). Two basic approaches in target definition are “the American approach” by the Radiation Therapy Oncology Group (RTOG con-

TABLE 1. Recommendations for target definition according to EORTC, RTOG and ESTRO-ACROP

Contouring approach	Dose prescription	GTV	CTV
EORTC single phase	30 x 2.0 Gy	Resection cavity + residual T1 enhancement	GTV + 2 cm
RTOG two phases	23 x 2.0 Gy	GTV1: Resection cavity + residual T1 enhancement + FLAIR abnormality (oedema)	CTV1 = GTV1 + 2 cm (the margin is 2.5 cm in cases where no oedema is presented)
	+ 7 x 2.0 Gy	GTV2: Resection cavity + residual T1 enhancement	GTV2 + 2 cm
ESTRO-ACROP	30 x 2.0 Gy	Resection cavity + residual T1 enhancement + FLAIR abnormality (oedema) for secondary glioblastomas	GTV + 2 cm

Abbreviations: EORTC = European Organisation for Research and Treatment of Cancer; ESTRO-ACROP = European Society for Radiotherapy & Oncology - Advisory Committee on Radiation Oncology Practice; CTV = clinical target volume; FLAIR = Fluid-attenuated Inversion Recovery. GTV = gross tumor volume; RTOG = Radiation Therapy Oncology Group

touring approach) that defines two CTVs accommodating hyperintensity at T2/FLAIR MRI (FLAIR – Fluid-attenuated Inversion Recovery) in addition to T1 contrast-enhanced MRI³⁸ and “the European approach” by the European Organization for Research and Treatment of Cancer (*EORTC single phase contouring approach*) that defines one CTV utilizing mainly T1 post-contrast MRI. The ESTRO-ACROP (European Society for Radiotherapy & Oncology - Advisory Committee on Radiation Oncology Practice) approach resembles EORTC practice, although CTV is defined in certain instances also by T2/FLAIR MRI, especially in the case of secondary, *isocitrate dehydrogenase (IDH)*-mutated GBM³⁹ (Table 1). There has been no randomized comparison of these different consensus practices. Nevertheless, the single phase approach is generally associated with reduced irradiated volume without a significant increase in marginal or distant recurrences.⁴⁰ Reducing target volumes leads to lower irradiation of radiographically normal brain and, thus, possibly to less toxicity, although this remains to be validated prospectively.

In daily clinical practice, the chosen method for contouring depends in part on the planned radiation technique (3-dimensional conformal therapy *vs.* inverse planning of IMRT with steeper dose gradients and higher demand on precision) or on the extent of edema, respective of the tumor itself. Molecular characteristics of gliomas, currently established in the integral diagnosis within the new WHO classification update from 2016, may also influence target definition in the personalized contouring of target volumes.⁴¹ Mutation of the *IDH* gene, the early stable driving mutation in diffuse glioma, is associated with WHO grade II/

III gliomas and a better prognosis, while GBMs are typically *IDH* wild-type. Nonetheless, about 10% of GBMs, formerly named secondary GBMs, are *IDH*-mutated, which probably indicates their dedifferentiation from low-grade gliomas. Because this dedifferentiation may occur anywhere within initial low-grade glioma, a single phase approach with high dose irradiation covering all T2/FLAIR hyperintensity may be deemed suitable. Nevertheless, it is too soon to speak about a predictive marker for RT because no clinical trial or RT planning study so far addressed this issue.

If a two-phase RTOG strategy is applied for a particular patient, the dose for “the larger volume” and the dose for “the smaller volume – the high-risk region” must be determined. This cone-down strategy, also called sequential boost, combines most often 46 + 14 Gy, or possibly 50 + 10 Gy, depending on target volume size. IMRT allows preparation of irradiation for two target volumes simultaneously. This technique, called simultaneous integrated boost (SIB), is sometimes used in clinical practice. However, its usage may be controversial. A common prescription is 30 x 1.7 Gy (51 Gy) for planning target volume #1 and 30 x 2.0 Gy (60 Gy) for planning target volume #2. This is not truly an SIB, because the dose in high-risk subvolume does not exceed standard daily 2.0 Gy; instead, the dose in low-risk subvolume is decreased to daily 1.7 Gy. The advantage is in dose control within individual subvolumes. In the case of the standard sequential 46 + 14 Gy regimen, the low-risk subvolume receives more than the prescribed 46 Gy (Figure 1) because irradiation during the second phase passes through the low-risk subvolume (resulting in a non-homogeneous dose of about 50–57 Gy, of which

first 46 Gy is delivered in 2.0 Gy daily fractions). As long as all dose-volume constraints are met, such an RT plan can be clinically applied. SIB seems to be more beneficial for cases with a large volume of hyperintensity on T2/FLAIR-weighted MRI, because the total dose for low-risk subvolume exactly matches the prescribed dose. Assuming relative radioresistance of glioma cells, the disadvantage is in the low daily dose of 1.7 Gy. There are no clinical studies that prove or disprove superiority of this type of SIB, and therefore its use remains controversial. However, there are also no robust clinical studies demonstrating benefits of IMRT in general.⁴² Some reports exist in the evaluation of classical SIB, where the RT schedule is hypofractionated. For example, Paner-Raymond reported no survival improvement or patterns of failure change in their retrospective analysis of patients treated in 20 fraction of 2.0 Gy delivered to the larger volume while simultaneously boosting gross tumor volume by 3.0 Gy.⁴³ The same RT protocol was used in recently published phase II clinical trial evaluating the role of neoadjuvant TMZ.⁴⁴ Hypofractionated (60 Gy in 20 daily fractions) RT was administered concurrently with TMZ after 2 weeks of prior neoadjuvant TMZ (75 mg/m² per day) and was followed by adjuvant TMZ.⁴⁴ Encouraging median overall survival of 22.3 months warrants further testing of this approach in phase III design. Until then, hypofractionated SIB cannot be considered a standard for daily clinical practice. Generally, there is potential for a planning study and then even maybe a trial (comparison of RTOG *vs.* EORTC contouring approaches, normofractionated or hypofractionated SIB techniques *vs.* cone-down strategy, etc), however only one topic at the time must be addressed.

IMRT is commonly used due to its apparent dosimetric advantages, mainly for tumors localized close to critical organs. The question often asked about expensive particle therapy is also pertinent for IMRT: What evidence do we need for the establishment of a new standard of care in RT techniques? Dosimetric advantages have the potential to translate into the better neurocognitive function as is currently evaluated in the NCT01854554 clinical trial, where IMRT is compared with intensity-modulated proton RT for newly diagnosed GBM.

Lessons from the past: RT approach from Stupp's protocol

The RT planning steps in the original Stupp's protocol were substantially less complicated than those used nowadays. Gross tumor volume (GTV)

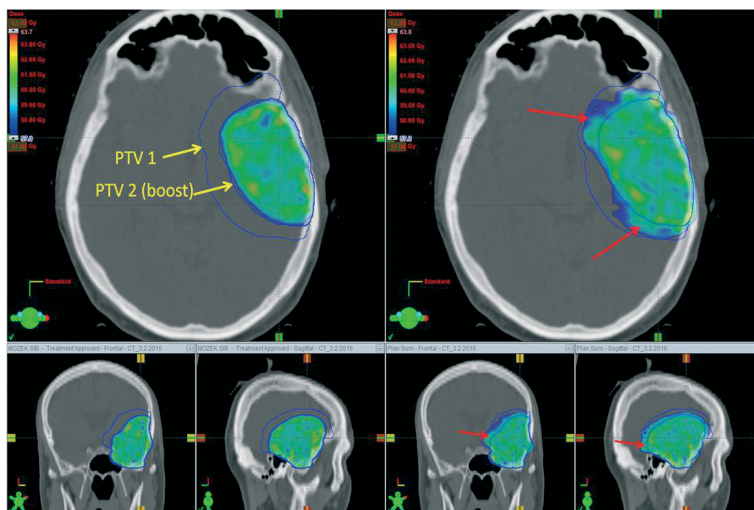


FIGURE 1. An example of an RT treatment plan (color wash display of isodoses with a minimal dose of 57 Gy, that is 95% of the prescribed dose of 60 Gy) in three planes. A RT plan for the same patient was prepared using a simultaneous integrated boost (left) and sequential boost (right). Target volumes are shown in blue contour (yellow labeled arrows). Dose assignment to the "PTV2-boost" target volume is the same in boost cases, 30 x 2.0 Gy. With sequential boost, overtreatment (red arrows) is observed in the area where a lower dose was prescribed.

representing tumor mass, was defined as the area within the primary tumor as measured by post-contrast enhancement on either CT or MRI. In general terms, planning target volume (PTV: margin needed to compensate for inaccuracies) is the GTV enlarged by approximately 2–3 cm.¹¹ Determination of a safety margin for PTV is complicated in daily clinical practice with a slight difference in each patient as several variables must be taken into consideration. The most important are planned technique (classical conformal RT *vs.* IMRT; coplanar *vs.* non-coplanar), quality of immobilization, availability of on-board imaging system, inaccuracy in images registration, compliance, and overall patient's state.

Based on the evaluation of randomly selected individual patients from all participating centers in the EORTC 26981–22981/NCIC CE3 trial, 34% of centers planned RT based solely on pre-operative CT and 62% of centers planned RT on classic 2-dimensional simulator measurements.⁴⁵ Most of the centers (94%) delineated PTV alone or with CTV or GTV.⁴⁵ Would that be considered as a *lege artis* or as a controversial, whether we plan RT for our patient on 2 dimensional RTG simulator without dedicated planning CT (and MRI) scan, since it was employed in a registry study of the current standard of care?

Other controversies in the decision-making of daily RT practice

A few other controversies associated with RT of HGG are mentioned briefly. The issue of reduction of CTV around natural barriers to tumor growth is not standardized. One of the options is to reduce the CTV to as low as zero at the border with fixed barriers such as bone or falx and to as low as few millimeters around non-rigid barriers such as ventricles or brain stem. Another controversial topic is hippocampal sparing with the goal of minimizing the negative effects of RT on cognitive functions.^{46,47} RT in 2 Gy fractions to 40% of the bilateral hippocampi greater than an equivalent dose of 7.3 Gy was associated with long-term memory impairment in patients with low-grade or benign brain tumors.⁴⁷ There is controversy as to whether it might or might not be beneficial to spare the ipsilateral neural stem cell regions as in the hippocampus, owing to accumulating evidence of higher risk of tumor recurrence in the proximity to these regions, which are thought to provide favorable conditions for putative glioma stem cells whose survival is believed to be responsible for tumor recurrence.⁴⁸⁻⁵⁰ Indeed, subventricular zones have been proposed as new key targets for GBM treatment.^{51,52} Whether to spare the contralateral hippocampus remains controversial. Nevertheless, especially when employing inverse RT planning to allow dose control in different parts of the brain, contralateral hippocampal sparing should be at least considered in patients with right-sided low-grade glioma to spare the dominant left hemisphere which may be more related to verbal memory declines after RT.^{53,54}

Conclusion and future perceptivities

To provide state-of-the-art RT for GBM patients in daily clinical practice, it is necessary to acknowledge the capabilities and limitations of current RT techniques in the light of the potential controversies described in this review. With current technical and supportive care advances, it is possible to prolong further the survival of patients with GBM as presented in the control arms of the recent EF-14 and rindopepimut ACT IV trials. In trials enrolling patients who have completed chemoradiotherapy, significant differences in completed upfront treatment may affect results; further confounding influences can be at least partially mitigated if the above-mentioned uncertainties and controversies in daily RT are used as stratifications factors. For

example, for the EF-14 trial, trial protocol amendment V2.0 included an update in the dose of RT (from 60 Gy to 45-70 Gy) to address common variations in the standard of care treatment between individual patients/centers.¹⁶ Although the proportion of patients who received less than 57 Gy was balanced between the TTF and control arms, one must ask what kind of RT should be used in daily clinical practice if the TTF treatment were to become the new standard of care. With the current standard approach of concomitant and adjuvant TMZ, it might not matter which RT procedure is chosen. With new treatment approaches such as TTF or immunotherapy⁵⁵⁻⁵⁷, the role of adjuvant radiotherapy will be further defined.

Acknowledgments and funding

This work was supported in part by the Ministry of Health, Czech Republic – Conceptual Development of Research Organization (MMCI 00209805) and project MEYS-NPS I-LO1413. The results of this research have been acquired within CEITEC 2020 (LQ1601) project with the financial contribution made by the Ministry of Education, Youths and Sports of the Czech Republic within special support paid from the National Programme for Sustainability II funds.

Statement

The paper has not been published or submitted for publication elsewhere. This is the first submission of this paper. All listed authors concur in the submission and are responsible for its content. They agree with publication and have given the corresponding author the authority to act on their behalf in all matters pertaining to publication.

References

1. Roa W, Brasher PM, Bauman G, Anthes M, Bruera E, Chan A, et al. Abbreviated course of radiation therapy in older patients with glioblastoma multiforme: a prospective randomized clinical trial. *J Clin Oncol* 2004; **22**: 1583-8. doi: 10.1200/JCO.2004.06.082
2. Malmström A, Grönberg BH, Marosi C, Stupp R, Frappaz D, Schultz H, et al. Temozolomide versus standard 6-week radiotherapy versus hypofractionated radiotherapy in patients older than 60 years with glioblastoma: the Nordic randomised, phase 3 trial. *Lancet Oncol* 2012; **13**: 916-26. doi: 10.1016/S1470-2045(12)70265-6
3. Wick W, Platten M, Meisner C, Felsberg J, Tabatabai G, Simon M, et al. Temozolomide chemotherapy alone versus radiotherapy alone for malignant astrocytoma in the elderly: The NOA-08 randomised, phase 3 trial. *Lancet Oncol* 2012; **13**: 707-15. doi: 10.1016/S1470-2045(12)70164-X
4. Perry JR, Laperriere N, O'Callaghan CJ, Brandes AA, Menten J, Phillips C, et al. Short-course radiation plus temozolomide in elderly patients with glioblastoma. *N Engl J Med* 2017; **376**: 1027-37. doi: 10.1056/NEJMoa1611977

5. Hegi ME, Diserens AC, Gorlia T, Hamou MF, de Tribolet N, Weller M, et al. MGMT gene silencing and benefit from temozolomide in glioblastoma. *N Engl J Med* 2005; **352**: 997-1003.
6. Wick W, Platten M, Wick A, Hertenstein A, Radbruch A, Bendszus M, et al. Current status and future directions of anti-angiogenic therapy for gliomas. *Neuro Oncol* 2016; **18**: 315-28. doi: 10.1093/neuonc/nov180
7. Chinot OL, Wick W, Mason W, Henriksson R, Saran F, Nishikawa R, et al. Bevacizumab plus radiotherapy-temozolomide for newly diagnosed glioblastoma. *N Engl J Med* 2014; **370**: 709-22. doi: 10.1056/NEJMoa1308345
8. Gilbert MR, Dignam JJ, Armstrong TS, Wefel JS, Blumenthal DT, Vogelbaum MA, et al. A Randomized trial of bevacizumab for newly diagnosed glioblastoma. *N Engl J Med* 2014; **370**: 699-708. doi: 10.1056/NEJMoa1308573
9. Stupp R, Hegi ME, Mason WP, van den Bent MJ, Taphoorn MJB, Janzer RC, et al. Effects of radiotherapy with concomitant and adjuvant temozolomide versus radiotherapy alone on survival in glioblastoma in a randomised phase III study: 5-year analysis of the EORTC-NCIC trial. *Lancet Oncol* 2009; **10**: 459-66. doi: 10.1016/S1470-2045(09)70025-7
10. Uhm JH, Porter AB. Treatment of Glioma in the 21st Century: An exciting decade of postsurgical treatment advances in the molecular era. *Mayo Clin Proc* 2017; **92**: 995-1004. doi: 10.1016/j.mayocp.2017.01.010
11. Stupp R, Mason WP, van den Bent MJ, Weller M, Fisher B, Taphoorn MJB, et al. Radiotherapy plus concomitant and adjuvant temozolomide for glioblastoma. *N Engl J Med* 2005; **352**: 987-96. doi: 10.1056/NEJMoa043330
12. Alexander BM, Cloughesy TF. Adult glioblastoma. *J Clin Oncol* 2017; **35**: 2402-09. doi: 10.1200/JCO.2017.73.0119
13. Halasz BLM, Soltys SG, Breneman JC, Chan MD, Laack NN, Minniti G, et al. Treatment of gliomas: a changing landscape. *Int J Radiat Oncol Biol Phys* 2017; **98**: 255-8. doi: 10.1016/j.ijrobp.2017.02.223
14. Hottinger AF, Pacheco P, Stupp R. Tumor treating fields: a novel treatment modality and its use in brain tumors. *Neuro Oncol* 2016; **18**: 1338-49. doi: 10.1093/neuonc/nov182
15. Mehta M, Wen P, Nishikawa R, Reardon D, Peters K. Critical Reviews in Oncology / Hematology Critical review of the addition of tumor treating fields (TTFields) to the existing standard of care for newly diagnosed glioblastoma patients. *Crit Rev Oncol Hematol* 2017; **111**: 60-5. doi: 10.1016/j.critrevonc.2017.01.005
16. Stupp R, Taillibert S, Kanner AA, Kesari S, Steinberg DM, Toms SA, et al. Maintenance therapy with tumor-treating fields plus temozolomide vs temozolomide alone for glioblastoma. *JAMA* 2015; **314**: 2535-43. doi: 10.1001/jama.2015.16669
17. Stupp R, Taillibert S, Kanner A, Read W, Steinberg DM, Lhermitte B, et al. Effect of Tumor-treating fields plus maintenance temozolomide vs maintenance temozolomide alone on survival in patients with glioblastoma: A randomized clinical trial. *JAMA* 2017; **318**: 2306-16. doi: 10.1001/jama.2017.18718
18. Wick W. TTFields: Where does all the skepticism come from? *Neuro Oncol* 2016; **18**: 303-5. doi: 10.1093/neuonc/nov012
19. Zhu JJ, Demireva P, Kanner AA, Pannullo S, Mehdorn M, Avgeropoulos N, et al. Health-related quality of life, cognitive screening, and functional status in a randomized phase III trial (EF-14) of tumor treating fields with temozolomide compared to temozolomide alone in newly diagnosed glioblastoma. *J Neurooncol* 2017 Aug 28. doi: 10.1007/s11060-017-2601-y. [Epub ahead of print]
20. Weller M, Butowski N, Tran DD, Recht LD, Lim M, Hirte H, et al. Rindopepimut with temozolomide for patients with newly diagnosed, EGFRvIII-expressing glioblastoma (ACT IV): a randomised, double-blind, international phase 3 trial. *Lancet Oncol* 2017; **18**: 1373-85. doi: 10.1016/S1470-2045(17)30517-X
21. Corso CD, Bindra RS, Mehta MP. The role of radiation in treating glioblastoma: here to stay. *J Neurooncol* 2017 Mar 7. doi: 10.1007/s11060-016-2348-x. [Epub ahead of print]
22. Roth P, Gramatzki D, Weller M. Management of elderly patients with glioblastoma. *Curr Neurol Neurosci Rep* 2017; **17**: 35. doi: 10.1007/s11910-017-0740-3
23. Walker MD, Strike TA, Sheline GE. An analysis of dose-effect relationship in the radiotherapy of malignant gliomas. *Int J Radiat Oncol Biol Phys* 1979; **5**: 1725-31. doi: 10.1016/0360-3016(79)90553-4
24. Chang CH, Horton J, Schoenfeld D, Salazer O, Perez-Tamayo R, Kramer S, et al. Comparison of postoperative radiotherapy and combined postoperative radiotherapy and chemotherapy in the multidisciplinary management of malignant gliomas. A joint Radiation Therapy Oncology Group and Eastern Cooperative Oncology Group study. *Cancer* 1983; **52**: 997-1007.
25. Chan JL, Lee SW, Fraass BA, Normolle DP, Greenberg HS, Junck LR, et al. Survival and failure patterns of high-grade gliomas after three-dimensional conformal radiotherapy. *J Clin Oncol* 2002; **20**: 1635-42.
26. Selker RG, Shapiro WR, Burger P, Blackwood MS, Arena VC, Gilder JC, et al. The Brain Tumor Cooperative Group NIH Trial 87-01: a randomized comparison of surgery, external radiotherapy, and carmustine versus surgery, interstitial radiotherapy boost, external radiation therapy, and carmustine. *Neurosurgery* 2002; **51**: 343-57.
27. Souhami L, Seiferheld W, Brachman D, Podgorsak EB, Werner-Wasik M, Lustig R, et al. Randomized comparison of stereotactic radiosurgery followed by conventional radiotherapy with carmustine to conventional radiotherapy with carmustine for patients with glioblastoma multiforme: Report of Radiation Therapy Oncology Group 93-05 protocol. *Int J Radiat Oncol Biol Phys* 2004; **60**: 853-60. doi: 10.1016/j.ijrobp.2004.04.011
28. Werner-Wasik M, Scott CB, Nelson DF, Gaspar LE, Murray KJ, Fischbach JA, et al. Final report of a phase I/II trial of hyperfractionated and accelerated hyperfractionated radiation therapy with carmustine for adults with supratentorial malignant gliomas. Radiation Therapy Oncology Group Study 83-02. *Cancer* 1996; **77**: 1535-43.
29. Badiyan SN, Markovina S, Simpson JR, Robinson CG, DeWees T, Tran DD, et al. Radiation therapy dose escalation for glioblastoma multiforme in the era of temozolomide. *Int J Radiat Oncol Biol Phys* 2014; **90**: 877-85. doi: 10.1016/j.ijrobp.2014.07.014
30. Kelly PJ, Daumas-Duport C, Scheithauer BW, Kall BA KD. Stereotactic histologic correlations of computed tomography- and magnetic resonance imaging-defined abnormalities in patients with glial neoplasms. *Mayo Clin Proc* 1987; **62**: 450-9.
31. Dunet V, Ponomi A, Hottinger A, Nicod-Lalonde M, Prior JO. Performance of 18F-FET versus 18F-FDG-PET for the diagnosis and grading of brain tumors: systematic review and meta-analysis. *Neuro Oncol* 2016; **18**: 426-34. doi: 10.1093/neuonc/nov148
32. Albert NL, Weller M, Suchorska B, Galdiks N, Soffiatti R, Kim MM, et al. Response assessment in Neuro-Oncology working group and European Association for Neuro-Oncology recommendations for the clinical use of PET imaging in gliomas. *Neuro Oncol* 2016; **18**: 1199-208. doi: 10.1093/neuonc/nov058
33. Whitfield GA, Kennedy SR, Djoukadar IK, Jackson A. Imaging and target volume delineation in glioma. *Clin Oncol (R Coll Radiol)* 2014; **26**: 364-76. doi: 10.1016/j.clon.2014.04.026
34. Pafundi DH, Laack NN, Youland RS, Parney IF, Lowe VJ, Giannini C, et al. Biopsy validation of 18 F-DOPA PET and planning and radiotherapy target delineation: results of a prospective pilot study. *Neuro Oncol* 2013; **15**: 1058-67. doi: 10.1093/neuonc/not002
35. Mills SJ, Du Plessis D, Pal P, Thompson G, Buonaccorsi G, Soh C, et al. Mitotic activity in glioblastoma correlates with estimated extravascular extracellular space derived from dynamic contrast-enhanced MR imaging. *Am J Neuroradiol* 2016; **37**: 811-7. doi: 10.3174/ajnr.A4623
36. Brindle KM, Izquierdo-Garcia JL, Lewis DY, Mair RJ, Wright AJ. Brain tumor imaging. *J Clin Oncol* 2017; **35**: 2432-8. doi: 10.1200/JCO.2017.72.7636
37. Niyazi M, Geisler J, Siefert A, Schwarz SB, Ganswindt U, Garny S, et al. FET-PET for malignant glioma treatment planning. *Radiother Oncol* 2011; **99**: 44-8. doi: 10.1016/j.radonc.2011.03.001
38. Sulman EP, Ismaila N, Armstrong TS, Tsien C, Batchelor TT, Cloughesy T, et al. Radiation therapy for glioblastoma: American Society of Clinical Oncology Clinical Practice Guideline Endorsement of the American Society for Radiation Oncology Guideline. *J Clin Oncol* 2017; **35**: 361-9. doi: 10.1200/JCO.2016.70.7562
39. Niyazi M, Brada M, Chalmers AJ, Combs SE, Erridge SC, Fiorentino A, et al. ESTRO-ACROP guideline "target delineation of glioblastomas." *Radiother Oncol* 2016; **118**: 35-42. doi: 10.1016/j.radonc.2015.12.003
40. Minniti G, Amelio D, Amichetti M, Salvati M, Muni R, Bozzao A, et al. Patterns of failure and comparison of different target volume delineations in patients with glioblastoma treated with conformal radiotherapy plus concomitant and adjuvant temozolomide. *Radiother Oncol* 2010; **97**: 377-81. doi: 10.1016/j.radonc.2010.08.020

41. Louis DN, Perry A, Reifenberger G, von Deimling A, Figarella D, Webster B, et al. The 2016 World Health Organization classification of tumors of the central nervous system: a summary. *Acta Neuropathol* 2016; **131**: 803-20. doi: 10.1007/s00401-016-1545-1
42. Chan MF, Schupak K, Burman C, Chui C-S, Ling CC. Comparison of intensity-modulated radiotherapy with three-dimensional conformal radiation therapy planning for glioblastoma multiforme. *Med Dosim* 2003; **28**: 261-5. doi: 10.1016/j.meddos.2003.08.004
43. Panet-Raymond V, Souhami L, Roberge D, Kavan P, Shakibnia L, Muanza T, et al. Accelerated hypofractionated intensity-modulated radiotherapy with concurrent and adjuvant temozolomide for patients with glioblastoma multiforme: a safety and efficacy analysis. *Int J Radiat Oncol Biol Phys* 2009; **73**: 473-8. doi: 10.1016/j.ijrobp.2008.04.030
44. Shenouda G, Souhami L, Petrecca K, Owen S, Panet-Raymond V, Guiot M-C, et al. A phase 2 trial of neoadjuvant temozolomide followed by hypofractionated accelerated radiation therapy with concurrent and adjuvant temozolomide for patients with glioblastoma. *Int J Radiat Oncol Biol Phys* 2017; **97**: 487-94. doi: 10.1016/j.ijrobp.2016.11.006
45. Ataman F, Poortmans P, Stupp R, Fisher B, Mirimanoff RO. Quality assurance of the EORTC 26981/22981; NCIC CE3 intergroup trial on radiotherapy with or without temozolomide for newly-diagnosed glioblastoma multiforme: the individual case review. *Eur J Cancer* 2004; **40**: 1724-30. doi: 10.1016/j.ejca.2004.03.026
46. Kazda T, Jancalek R, Pospisil P, Sevela O, Prochazka T, Vrzal M, et al. Why and how to spare the hippocampus during brain radiotherapy: the developing role of hippocampal avoidance in cranial radiotherapy. *Radiat Oncol* 2014; **9**: 139. doi: 10.1186/1748-717X-9-139
47. Gondi V, Hermann BP, Mehta MP, Tomé WA. Hippocampal dosimetry predicts neurocognitive function impairment after fractionated stereotactic radiotherapy for benign or low-grade adult brain tumors. *Int J Radiat Oncol Biol Phys* 2013; **85**: 348-54. doi: 10.1016/j.ijrobp.2012.11.031
48. Gzell C, Back M, Wheeler H, Bailey D, Foote M. Radiotherapy in glioblastoma: the past, the present and the future. *Clin Oncol (R Coll Radiol)* 2017; **29**: 15-25. doi: 10.1016/j.clon.2016.09.015
49. Smith AW, Mehta MP, Wernicke AG. Neural stem cells, the subventricular zone and radiotherapy: implications for treating glioblastoma. *J Neurooncol* 2016; **128**: 1-10. doi: 10.1007/s11060-016-2123-z
50. Chen L, Chaichana KL, Kleinberg L, Ye X, Quinones-Hinojosa A, Redmond K. Glioblastoma recurrence patterns near neural stem cell regions. *Radiother Oncol* 2015; **116**: 294-300. doi: 10.1016/j.radonc.2015.07.032
51. Khalifa J, Tensaouti F, Lusque A, Plas B, Lotterie J-A, Benouaich-Amiel A, et al. Subventricular zones: new key targets for glioblastoma treatment. *Radiat Oncol* 2017; **12**: 67. doi: 10.1186/s13014-017-0791-2
52. Nourallah B, Diggall R, Jena R, Watts C. Irradiating the subventricular zone in glioblastoma patients: is there a case for a clinical trial? *Clin Oncol (R Coll Radiol)* 2017; **29**: 26-33. doi: 10.1016/j.clon.2016.09.005
53. Pospisil P, Kazda T, Hynkova L, Bulik M, Dobiaskova M, Burkon P, et al. Post-WBRT cognitive impairment and hippocampal neuronal depletion measured by in vivo metabolic MR spectroscopy: results of prospective investigational study. *Radiother Oncol* 2017; **122**: 373-9. doi: 10.1016/j.radonc.2016.12.013
54. Flechl B, Sax C, Ackerl M, Crevenna R, Woehrer A, Hainfellner J, et al. The course of quality of life and neurocognition in newly diagnosed patients with glioblastoma. *Radiother Oncol* 2017; **125**: 228-33. doi: 10.1016/j.radonc.2017.07.027
55. Weller M, Roth P, Preusser M, Wick W, Reardon DA, Platten M, et al. Vaccine-based immunotherapeutic approaches to gliomas and beyond. *Nat Rev Neurol* 2017; **13**: 363-74. doi: 10.1038/nrneurol.2017.64
56. Sampson JH, Maus MV, June CH. Immunotherapy for brain tumors. *J Clin Oncol* 2017; **35**: 2450-6. doi: 10.1200/JCO.2017.72.8089
57. Reznik E, Smith AW, Taube S, Mann J, Yondorf MZ, Parashar B, et al. Radiation and immunotherapy in high-grade gliomas. *Am J Clin Oncol* 2017 Sep 12. doi: 10.1097/COC.0000000000000406. [Epub ahead of print]

Ultrasound elastography can detect placental tissue abnormalities

Tomoya Hasegawa¹, Naoaki Kuji¹, Fumiaki Notake², Tetsu Tsukamoto³, Toru Sasaki¹, Motohiro Shimizu⁴, Kazunori Mukaida¹, Hiroe Ito¹, Keichi Isaka¹, Hirotaka Nishi¹

¹ Department of Obstetrics and Gynecology, Tokyo Medical University, Tokyo, Japan

² Radiation Division, Tokyo Medical University Hachioji Medical Center, Tokyo, Japan

³ Diagnostic Pathology Division, Tokyo Medical University Hachioji Medical Center, Tokyo, Japan

⁴ Obstetrics and Gynecology, Tokyo Medical University Hachioji Medical Center, Tokyo, Japan

Radiol Oncol 2018; 52(2): 129-135.

Received 20 November 2017

Accepted 23 April 2018

Correspondence to: Tomoya Hasegawa, Department of Obstetrics and Gynecology, Tokyo Medical University, 6-7-1, Nishi-Shinjyuku, Shinjyuku, Tokyo, 160-0023, Japan. Phone: +81 3 3342 6111; Fax: +81 3 3342 6112; E-mail: ppppq999@gmail.com

Disclosure: No potential conflicts of interest were disclosed.

Background. In this prospective cohort study, we examined the utility of elastography to evaluate the fetus and placenta.

Patients and methods. Pregnant women in their third trimester of pregnancy, by which time the placenta has formed, were included in this study. A total of 111 women underwent ultrasound examinations, including elastography. Elastographic evaluation was performed using two protocols. First, the placental index (PI) was measured, which quantitatively assesses the hardness of tissue. Second, regions of interest (ROI) were categorized into 3-step scores according to the frequency of the blue area (hardness of placental tissue score [HT score]), which is a qualitative method. After delivery, 40 of the 111 placentas were pathologically examined.

Results. The average PI was 44.3 (\pm 29.4) in the *in utero* SGA group, which was significantly higher than that in the normal group (8.8 (\pm 10.0); $p < 0.01$) during pregnancy. There was a significant correlation between the PI and z score for estimated fetal weight (EFW) ($r = -0.55$; $p < 0.01$). Moreover, a significant positive correlation was observed between the PI and the z score of birth weight ($r = -0.39$; $p < 0.01$). Pathological ischemia findings of the placenta were identified in 67% of the HT score 3 group, representing 6 of the 9 patients, and in 20% of the HT score 1 group, representing only 3 of the 15 patients.

Conclusions. Placental hardness, as determined by elastography, correlates with both lower estimated fetal body weight and birth weight. These results suggest that ultrasound elastography in the placenta may be an additional marker of intrauterine fetal well-being.

Key words: elastography; placenta; small for gestational age; ultrasound

Introduction

When ultrasound elastography was first clinically applied for the evaluation of disease, it was used to differentiate cancer tissue from surrounding normal tissue according to stiffness.¹⁻³ Since the elasticity of tissues and organs can be evaluated objectively, even in inaccessible parts of the living body^{4,5}, this modality has been applied in the clinical diagnosis of breast cancer.⁶

Recently, elastography has been found to be useful for the evaluation of pathological changes in noncancerous tissues. For example, the stiffness of liver tissues is considered to relatively increase with an increase in the density of vessels. In particular, the severity of hepatic fibrosis, as determined by biopsy, actually showed a correlation with a color score found using elastography in the liver area.^{7,8}

Small neonates who did not reach an appropriate weight according to gestational age in weeks

are referred to as small for gestational age (SGA). Perinatal mortality and the incidence of mental deficiency are high for SGA infants compared with non-SGA infants. Therefore, a fetus with SGA represents a high-risk pregnancy.⁹ Screening for SGA in the uterus is important during prenatal exami-

nations; however, pathological conditions vary, and examination methods and indices for discrimination are not sufficient.^{10,11}

Ultrasonography has long been a valuable tool for the diagnosis of pathological conditions during pregnancy when the use of diagnostic radiation imaging or invasive examination is avoided. The ultrasound frequency commonly used for elastography is equivalent to that of B mode, and it is thought that there is little effect on fetuses during pregnancy.¹² Among the few reports of elastography used in obstetrics, some have evaluated the cervix and its correlation with premature labor.¹³⁻¹⁵ Therefore, in this study, we investigated the correlation between the elasticity of placental tissue, as evaluated by ultrasound elastography, and SGA.

Materials and Patients

A prospective cohort study was performed on a total of 111 pregnant women who regularly visit our hospital received examinations. Only cases with anterior-lying placenta were included to avoid the effect of amniotic fluid. Only singleton pregnancies were included. For both fetal biometry and strain elastography, Ascendus (Hitachi Aloka Medical) with Eup-L52 probes were used for ultrasound examinations.

After the regular prenatal examination was performed (biparietal diameter, abdominal circumference, and femur length of the fetus), elastographic evaluation was performed using two protocols. First, the fat lesion ratio (FLR), which expresses the ratio of the elasticity of the target tissues (placenta) to subcutaneous fat (reference), was measured and calculated according to the manufacturer's instructions and defined as the placental index (PI). According to the diagnostic modality used for mammary tissue, two regions of interest (ROI) with 2-cm diameters were randomly set for the fat and placenta for comparison. Second, we made a benchmark to easily determine the hardness of the placenta, and the color mapping patterns of certain ROIs of the placenta were evaluated by an observer. The pattern was categorized into 3-step scores according to the frequency of the blue area (hardness of placental tissue score [HT score]). The HT score was 1 when the blue area in the ROI was <50%, 2 when the blue area was between 50% and 75%, and 3 when the blue area was >75% (Figure 1).

The HT score was evaluated by an obstetrician who was blinded to fetal biometry and perinatal information. Other blinded physician was asked to

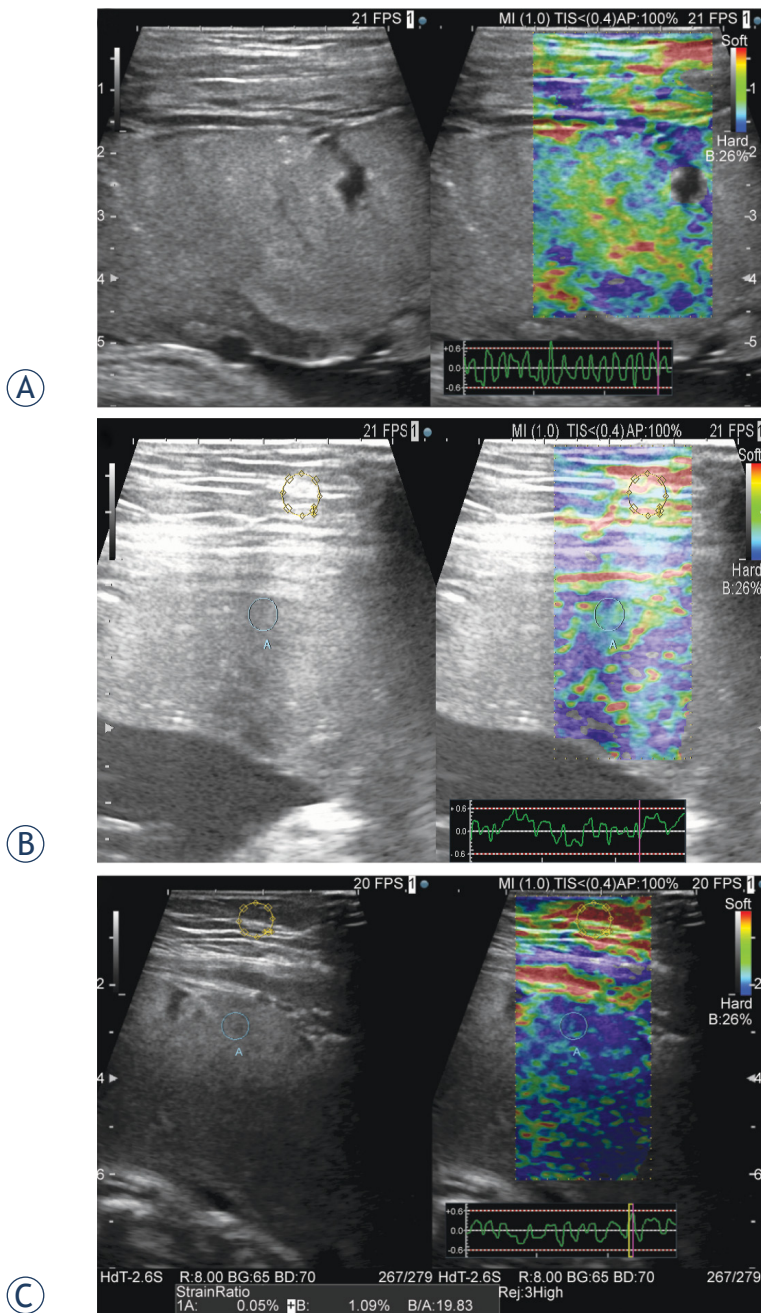


FIGURE 1. Representative ultrasound images of hardness of tissue (HT) score (A) The HT score was 1 when the blue area in the ROI was 50% or less. A strain graph, used to assess proper application of compression, is indicated in the lower right (B) The blue and green areas are shown mixed together in relatively equal percentages in the placenta (C) Most of the placenta is indicated in blue. In the left image, the strain ratio is calculated from the region of interest of the fat and placental tissue. In this case, the placental index is 19.83.

evaluate the score, and a consensus between two examiners was adopted as the HT score for the placenta.

We took measurements by avoiding large blood vessels and thereby avoided bias caused by areas without echo. The ROI was selected within 10 cm from the body surface; areas without tissue elasticity, such as the deep part, were avoided. Also, an attached strain graph was used to confirm whether adequate pressure was applied¹⁶ (Figure 1A, lower right).

The evaluation of reliability in elastography measurements was conducted using intra-class correlation coefficients (ICC). The intra-tester ICC was calculated for the 3 measurements in each placenta.

After delivery, the placentae of 40 patients who agreed to undergo a pathological test were investigated. Pathological examination was done blindly by a pathologist who was unaware about the patient's obstetric information.

Statistical testing was performed using Welch's t-test for patient characteristics and a z score of the estimated fetal weight (EFW) (significance level, 0.05%). Pearson's rank-correlation coefficient was calculated to assess the correlation between the PI and pregnancy outcomes. A multivariate linear regression analysis was performed with the EFW z score as a dependent variable and age, parity, placental weight at delivery, PI, and HT score as independent variables. SPSS version 24.0 was used for all statistical computations.

All procedures performed in studies involving human participants were in accordance with the ethical standards of the institutional and/or national research committee and with the 1964 Helsinki declaration and its later amendments or comparable ethical standards. This study was approved by the Institutional Review Board of the Tokyo Medical University (No. 2949). Informed consent was obtained from all patients before they were enrolled in the study.

Results

The patient characteristics of the normal EFW group and the *in utero* SGA group are shown in Table 1. Five pregnant women from normal groups were randomly selected to evaluate the reliability in elastography measurements. The intra-tester ICC was 0.987, thereby indicating a high reliability.

An EFW with a standard deviation (SD) of -1.5 or lower was defined as SGA.¹⁷ The average PI was

TABLE 1. Population features between the Normal group and SGA group

	Normal group	SGA group	P
Number	101	10	
Maternal age (years)	34.4 (±5.6)	33.6 (±4.7)	NS
Gravidity	0.9 (±1.2)	1.3 (±1.3)	NS
Parity	0.5 (±0.9)	0.6 (±0.7)	NS
Gestational age (weeks)	31.7 (±6.3)	32.8 (±4.2)	NS
EFW (SD)	+0.11 (±0.74)	-2.33 (±0.84)	P<0.01
Placental Index	8.8 (±10.0)	44.3 (±29.4)	P<0.01
HT score	1.56 (±0.68)	2.70 (±0.67)	P<0.01
Birth weight (SD)	0.11 (±1.13)	-2.19 (±1.07)	P<0.01
Placenta weight (g)	562.3 (±119.7)	366 (±120.0)	P<0.01

The above values represent the mean (standard deviation).

EFW = estimated fetal weight; HT = score hardness of tissue score; SGA = small for gestational age

TABLE 2. HT score and pathological findings related to placental ischemia after delivery

HT score	1 (n = 15)	2 (n = 16)	3 (n = 9)
Accelerated maturation of villi (+), (n)	1	2	2
Infarction (+), (n)	2	1	3
Villous inflammation (+), (n)	0	1	1
Total, n, (%)	3 (20)	4 (25)	6 (67)

HT scores were evaluated during elastography. The presence and absence of pathological findings of the placenta after delivery are shown.

8.8 in the normal group and 44.3 in the *in utero* SGA group. The *in utero* SGA group had a higher placenta hardness score than did the normal group.

In this study, significant differences were not observed for the prognosis of cesarean section rate, hemorrhage volume, and Apgar score of the child at delivery during the perinatal period.

The correlation between the PI and z score for EFW is shown in Figure 2. There was a significant correlation between the PI and z score for EFW (correlation coefficient, $r = -0.55$; $p < 0.01$). Moreover, a significant positive correlation was observed between the PI and the z score of birth weight (correlation coefficient, $r = -0.39$; $p < 0.01$) (Figure 3). In the multivariate analysis, HT score and PI were significantly associated with EFW ($\beta = -0.398$, $p = 0.01$; and $\beta = 0.425$, $p = 0.007$, respectively). There was no statistically significant association between the other parameters and EFW. Table 2 shows a correlation between pathological findings of the placenta after delivery and HT score. After delivery, the

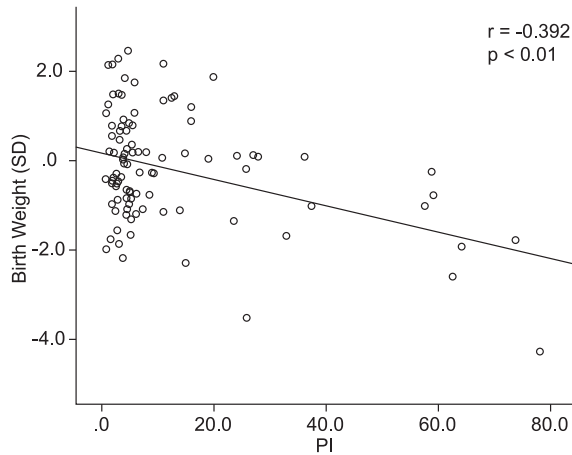


FIGURE 2. The correlation between the placental index (PI) and z score for estimated fetal weight at prenatal examination (EFW). There is a significant correlation between the PI and z score for EFW (correlation coefficient, $r = -0.55$; $p < 0.01$).

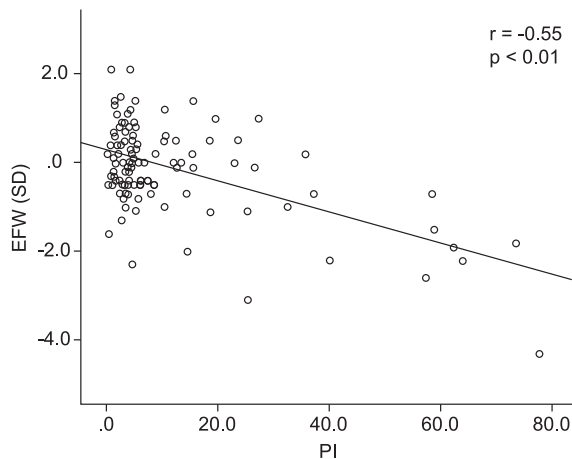


FIGURE 3. A significant positive correlation was observed between the placental index (PI) and z score of birth weight (correlation coefficient, $r = -0.39$; $p < 0.01$).

pathologist checked for three types of accelerated maturation of villi, which reflect vessels that have been reactively increased by ischemia, infarction, and villous inflammation. No significant differences were observed among all HT score groups, but the group with an HT score of 3 tended to have more findings related to ischemia of the placenta.

For the groups with HT scores of 1, 2, and 3, the mean birth weights were -0.11 SD, -0.09 SD, and -0.93 SD, respectively. The differences between HT scores 1 and 2 and between HT scores 2 and 3 were $p = 0.067$ and $p = 0.054$, respectively. Furthermore, when the results of elastography were compared between before and after the 30th week in the same

cases, which allowed us to assess the effect of measurement timing on the HT score, no changes in HT score were observed in the 5 cases that received an elastography examination, except for 1 case.

No obvious maternal or fetal disadvantages, such as premature birth or abruption, developed after the elastography examination.

Discussion

There have been several reports describing the use of elastography to examine the placenta. Recently, Cimsit *et al.* performed elastography by using shear wave imaging; they demonstrated that a placenta affected by pregnancy-induced hypertension was harder than a normal placenta.¹⁸

Using strain elastography with acoustic radiation (ARFI), Sugitani *et al.* discovered that the placenta of fetuses with fetal growth restriction (FGR) seemed harder than normal. They used elastography to study the placenta after delivery and measured the stiffness of the placenta with infarction. In doing so, they found that elastography was able to diagnose fibrogenesis without inflammation and congestion.^{19,20} However, their reports compared the elasticity of placentas from patients with pregnancy-induced hypertension with or without FGR. Furthermore, the safety of shear wave imaging with ARFI in the developing fetus has not been fully established because of the high energy of this modality.²¹

SGA is associated with significant perinatal morbidity and mortality.^{22,23} Although uterine artery Doppler is clinically applied to predict FGR of SGA, its sensitivity, and predictive value are not satisfactory.²⁴ Recently, using a rat model, Quibel *et al.* demonstrated that placentas from fetuses with experimental intrauterine growth restriction demonstrated greater stiffness.²⁵ However, to our knowledge, no report has analyzed the correlation between elasticity of the placenta and SGA in humans in utero. For all of these reasons, we first assumed that the placental hardness correlates with SGA. As seen in Table 1, the backgrounds of the *in utero* SGA group were consistent with those in past reports about FGR.

EFW, birth weight, and placental weight in the *in utero* SGA group were significantly lower than those in the normal group. Furthermore, the PI and HT score in the *in utero* SGA group were significantly higher than those in the normal group in this study. This result suggests that the PI and HT score may be new evaluation items for SGA.

In this study, we first examined PI, which is an objective and quantitative evaluation scale built into the mode used in elastography. The ratio of the elasticity of the abdominal wall fat tissue, which is considered to have the almost constant elasticity to the target tissue, was quantified by a pre-defined algorithm. This approach has been used instead of invasive biopsy in the mammary gland region to enable the diagnosis of mammary gland diseases.²⁶ Statistically significant correlations were found between the PI and z scores of EFW and between the PI and z scores of birth-weight. Furthermore, the multivariate analysis revealed that the HT score and PI were associated with EFW. These results suggest that placental stiffness has a strong relationship with SGA, regardless of the measurement procedure.

The utility of elastography and color mapping has been established in regions such as the mammary gland, prostate gland, and thyroid.^{2,3} Furthermore, color mapping is valuable because it is an intuitive evaluation method. It allows visual determination, even in models without a particular algorithm. Moreover, obstetricians want to confirm the situation of the fetus as efficiently as possible in a short period. Therefore, we secondly developed a novel color mapping score to evaluate the elasticity of the placenta, which we termed the HT score. This score may be a simple screening tool that can be used to identify abnormalities in the placenta.

The HT score failed to show a correlation with the z score for birth weight. Although some additional factors during pregnancy after an HT score examination exist and affect birth weight, it may be possible that a significant difference could be confirmed in a series of cases. Moreover, this study result suggests that HT score does not change based on gestational weeks. Fortunately, it may be convenient to evaluate the stiffness of the placenta using the HT score during pregnancy.

Pathologic examination of placentae of those with FGR revealed fibrin deposits in the intervillous space.²⁷ Also, there have been reports of significant pathological findings of infarction and villous inflammation in the placentas of infants with SGA.²⁸ Therefore, in at least some cases of FGR, hypercoagulability in the placenta will result in blood clots and infarction, leading to a decrease in utero-placental circulation, which contributes to FGR. As shown in Figures 4 and 5, white infarcts were macroscopically observed in parts of the placenta, and complete and incomplete infarction images of the villus were histopathologically observed in the placenta of FGR neonates with HT scores of 3.



FIGURE 4. Gross pathological findings of the placenta. A macro-photograph of the placenta after delivery. The neonate had fetal growth restriction, diagnosed during elastography evaluation at week 28 of pregnancy. White placental infarction is observed at the bottom right of the photo.

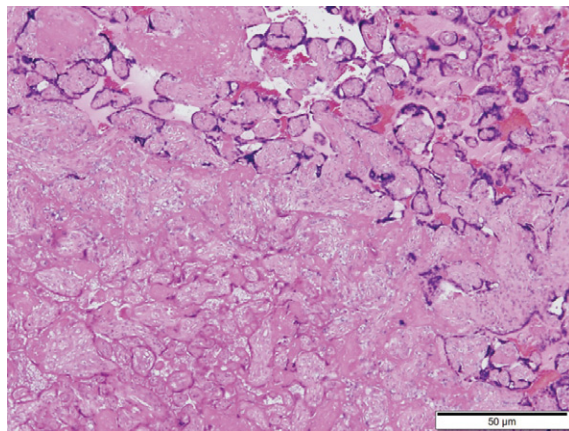


FIGURE 5. Histopathological findings of the placenta. Objective lens with 4× magnification. A micro-photograph of the same case as that shown in Figure 4. Complete infarction and incomplete infarction with remaining nuclear stainability are observed. The outlines of the villus remain in the upper right area.

Regarding the liver region, it has been reported that the pathological degree of fibrogenesis caused by chronic hepatitis and hepatic cirrhosis, and the hardness evaluated by strain elastography, are well correlated.^{8,29} Our findings suggested that the harder the placenta, the more the infarction and villous inflammation tended to be. Thus, elastography may reflect their fibrogenesis of villi resulting from infarction, villous inflammation and insufficient oxygen supply of the placenta in SGA.

However, not all SGAs are pathologically growth restricted but may be constitutionally

small for various other reasons, including genetic causes. Sequential EFW measurements of indices of fetal well-being (e.g., umbilical, middle cerebral, and uterine artery Doppler measurement; amniotic fluid volume, and fetal heart rate monitoring) may facilitate the identification of SGA due to placental insufficiency. Indeed, Karaman *et al.* described a putative association between the uterine artery pulsatility index and elastographic indices of the placenta.³⁰

Another limitation of this study is that strain elastography requires manual compression with the examiner's hands, although it has been reported that reproducible data can be obtained when a single examiner conducts the examination.³¹ Furthermore, only placentas located on the anterior uterine wall could be analyzed by our protocol, since manual compression is nearly impossible for a posteriorly located placenta. Our study also exhibited notably variation in PI values according to measurement locations in the normal and SGA groups. Thus, further studies with standardized elastographic measurements are required to evaluate the condition of the entire placenta.

Despite these limitations, elastography may indicate some characteristics of the placenta. Through the technical development of devices, improvements in evaluation methods, algorithms, and/or combined use with other obstetric examination methods, elastography can become a new evaluation method for the fetus and placenta.¹⁸⁻²⁰

In conclusion, we demonstrate that placental hardness during pregnancy correlates with low birth weight, based upon an assessment of the placenta using a non-invasive approach. Furthermore, hard placentas, as determined by elastography, may be indicative of pathological changes to the placenta in SGA.

References

- Xing P, Wu L, Zhang C, Li S, Liu C, Wu C. Differentiation of benign from malignant thyroid lesions. *J Ultrasound Med* 2011; **30**: 663-9. doi:10.7863/jum.2011.30.5.663
- Itoh A, Ueno E, Tohno E, Kamma H, Takahashi H, Shiina T, et al. Breast disease: Clinical application of US elastography for diagnosis. *Radiology* 2006; **239**: 341-350. doi:10.1148/radiol.2391041676
- Miyayama N, Akaza H, Yamakawa M, Oikawa T, Sekido N, Hinotsu S, et al. Tissue elasticity imaging for diagnosis of prostate cancer: a preliminary report. *Int J Urol* 2006; **13**: 1514-8. doi:10.1111/j.1442-2042.2006.01612.x
- Ophir J, Cespedes I, Ponnekanti H, Yazdi Y, Li X. Elastography: a quantitative method for imaging the elasticity of biological tissues. *Ultrason Imaging* 1991; **13**: 111-34. doi:10.1016/0161-7346(91)90079-W
- Edgebø TM, Økland I, Heien C, Gjessing LK, Romundstad P, Salvesen KÅ. Can ultrasound measurements replace digitally assessed elements of the Bishop score? *Acta Obstet Gynecol Scand* 2009; **88**: 325-31. doi:10.1080/00016340902730417
- Ueno E, Tohno E, Soeda S, Asaoka Y, Itoh K, Bamber JC, et al. Dynamic tests in real-time breast echography. *Ultrasound Med Biol* 1988; **14**: 53-7.
- Tatsumi C, Kudo M, Ueshima K, Kitai S, Takahashi S, Inoue T, et al. Noninvasive Evaluation of Hepatic Fibrosis Using Serum Fibrotic Markers, Transient Elastography (FibroScan) and Real-Time Tissue Elastography. *Intervirolgy* 2008; **51**: 27-33. doi:10.1159/000122602
- Tatsumi C, Kudo M, Ueshima K, Kitai S, Ishikawa E, Yada N, et al. Non-invasive evaluation of hepatic fibrosis for type C chronic hepatitis. *Intervirolgy* 2010; **53**: 76-81. doi:10.1159/000252789
- McIntire DD, Bloom SL, Casey BM, Leveno KJ. Birth weight in relation to morbidity and mortality among newborn infants. *N Engl J Med* 1999; **340**: 1234-8. doi:10.1056/NEJM199904223401603
- Pearce JM, Campbell S. A comparison of symphysis-fundal height and ultrasound as screening tests for light-for-gestational age infants. *Br J Obstet Gynaecol* 1987; **94**: 100-4.
- Duff GB. A randomized controlled trial in a hospital population of ultrasound measurement screening for the small for dates baby. *Aust New Zeal J Obstet Gynaecol* 1993; **33**: 374-8. doi:10.1111/j.1479-828X.1993.tb02113.x
- Makoto Yamakawa, Naotaka Nitta, Tsuyoshi Shiina, Takeshi Matsumura, Satoshi Tamano, Tsuyoshi Mitake, et al. High-speed Freehand Tissue Elasticity Imaging for Breast Diagnosis. *Jpn J Appl Phys* 2003; **42**: 3265. doi:10.1143/JJAP.42.3265
- Wozniak S, Czuczwar P, Szkodziak P, Milart P, Wozniakowska E, Paszkowski T. Elastography in predicting preterm delivery in asymptomatic, low-risk women: a prospective observational study. *BMC Pregnancy Childbirth* 2014; **14**: 238. doi:10.1186/1471-2393-14-238
- Hernandez-Andrade E, Hassan SS, Ahn H, Korzeniewski SJ, Leo Y, Chaiworapongsa T, et al. Evaluation of cervical stiffness during pregnancy using semiquantitative ultrasound elastography. *Ultrasound Obstet Gynecol* 2013; **41**: 152-61. doi:10.1002/uog.12344
- Swiatkowska-Freund M, Traczyk-Łoś A, Preis K, Łukaszuk M, Zielińska K. Prognostic value of elastography in predicting premature delivery. *Ginekol Pol* 2014; **85**: 204-7.
- Shiina T. JSUM ultrasound elastography practice guidelines: basics and terminology. *J Med Ultrason* 2013; **40**: 309-23. doi:10.1007/s10396-013-0490-z
- Shinozuka N, Akamatsu N, Sato S, Kanzaki T, Takeuchi H, Natori M, et al. Ellipse tracing fetal growth assessment using abdominal circumference: JSUM standardization committee for fetal measurements. *J Med Ultrason* 2000; **8**: 87-94.
- Cimsit C, Yoldemir T, Akpınar İN. Shear wave elastography in placental dysfunction. *J Ultrasound Med* 2015; **34**: 151-9. doi:10.7863/ultra.34.1.151
- Arena U, Vizzutti F, Corti G, Ambu S, Stasi C, Bresci S, et al. Acute viral hepatitis increases liver stiffness values measured by transient elastography. *Hepatology* 2007; **47**: 380-4. doi:10.1002/hep.22007
- Colli A, Pozzoni P, Berzuini A, Gerosa A, Canovi C, Molteni EE, et al. Decompensated chronic heart failure: Increased liver stiffness measured by means of transient elastography. *Radiology* 2010; **257**: 872-8. doi:10.1148/radiol.10100013
- Sugitani M, Fujita Y, Yumoto Y, Fukushima K, Takeuchi T, Shimokawa M, et al. A new method for measurement of placental elasticity: Acoustic radiation force impulse imaging. *Placenta* 2013; **34**: 1009-13. doi:10.1016/j.placenta.2013.08.014
- Aucott SW, Donohue PK, Northington FJ. Increased morbidity in severe early intrauterine growth restriction. *J Perinatol* 2004; **24**: 435-40. doi:10.1038/sj.jp.7211116
- Jacobsson B, Ahlin K, Francis A, Hagberg G, Hagberg H, Gardosi J. Cerebral palsy and restricted growth status at birth: population-based case-control study. *BJOG An Int J Obstet Gynaecol* 2008; **115**: 1250-5. doi:10.1111/j.1471-0528.2008.01827.x

24. Cnossen JS, Morris RK, ter Riet G, Mol BWJ, van der Post JAM, Coomarasamy A, et al. Use of uterine artery Doppler ultrasonography to predict pre-eclampsia and intrauterine growth restriction: a systematic review and bivariable meta-analysis. *Can Med Assoc J* 2008; **178**: 701-11. doi:10.1503/cmaj.070430
25. Quibel T, Deloison B, Chammings F, Chalouhi GE, Siauve N, Aliison M, et al. Placental elastography in a murine intrauterine growth restriction model. *Prenat Diagn* 2015; **35**: 1106-11. doi:10.1002/pd.4654
26. Ikeda K, Ogawa Y, Takii M, Sugano K, Ikeya T, Tokunaga S, et al. A role for elastography in the diagnosis of breast lesions by measuring the maximum fat lesion ratio (max-FLR) by tissue Doppler imaging. *Breast Cancer* 2012; **19**: 71-6. doi:10.1007/s12282-011-0274-5
27. Sebire NJ, Backos M, Goldin RD, Regan L. Placental massive perivillous fibrin deposition associated with antiphospholipid antibody syndrome. *BJOG* 2002; **109**: 570-3.
28. Maulik D, Frances Evans J, Ragolia L. Fetal growth restriction: pathogenic mechanisms. *Clin Obstet Gynecol* 2006; **49**: 219-27.
29. Friedrich-Rust M, Ong M-F, Herrmann E, Dries V, Samaras P, Zeuzem S, et al. Real-time elastography for noninvasive assessment of liver fibrosis in chronic viral hepatitis. *Am J Roentgenol* 2007; **188**: 758-64. doi:10.2214/AJR.06.0322
30. Karaman E, Arslan H, Çetin O, Şahin HG, Bora A, Yavuz A, et al. Comparison of placental elasticity in normal and pre-eclamptic pregnant women by acoustic radiation force impulse elastosonography. *J Obstet Gynaecol Res* 2016; **42**: 1464-70. doi:10.1111/jog.13078
31. Ruscalzo A, Steinhard J, Pietro LA, Frohlich C, Bijmens B, Klockenbusch W, et al. Reliability of quantitative elastography of the uterine cervix in at-term pregnancies. *J Perinat Med* 2013; **41**: 421-7. doi:10.1515/jpm-2012-0180

Is carotid stiffness a possible surrogate for stroke in long-term survivors of childhood cancer after neck radiotherapy?

Lorna Zadavec Zaletel¹, Matjaz Popit², Marjan Zaletel²

¹ Radiotherapy Department, Institute of Oncology Ljubljana, Ljubljana, Slovenia

² Department of Vascular Neurology, University Medical Centre Ljubljana, Ljubljana, Slovenia

Radiol Oncol 2018; 52(2): 136-142.

Received 16 October 2017

Accepted 18 December 2017

Correspondence to: Assist. Prof. Lorna Zadavec Zaletel, M.D., Ph.D., Radiotherapy Department, Institute of Oncology Ljubljana, Zaloška 2, SI-1000 Ljubljana. Phone: +386 4 1436 575; Fax: +386 1 5879 304; E-mail: lzaletel@onko-i.si

Disclosure: No potential conflicts of interest were disclosed.

Background. The risk for cerebrovascular late effects among childhood cancer survivors is considerable. According to recent studies it is not clear which marker could be reliable for the screening of cerebrovascular diseases among the long-term survivors of childhood cancer. The purpose of this study is to analyse arterial stiffness and intima-media thickness as possible early markers of later occurring stroke in long-term survivors of childhood cancer after neck radiotherapy.

Patients and methods. Twenty-three patients, treated for Hodgkin disease (HD) in childhood, were included. They had received radiation therapy to the neck with 20–65 (median 30) Gy. Twenty-six healthy controls, matched in age, sex, body mass index, arterial hypertension, smoking history and total cholesterol levels were compared. High-resolution colour-coded duplex sonography and power Doppler sonography of the carotid arteries were performed and intima-media thickness, number and quality of plaques were measured. Arterial stiffness indices were calculated.

Results. Plaque deposits and/or arterial wall calcinations were found in 24 out of 43 (55.8%) irradiated vessels in cancer survivors group and 0 out of 52 vessels in the group of healthy controls ($p < 0.01$). We found significant group differences for all the stiffness parameters we used ($P < 0.05$), but there was no difference in intima-media thickness between cases and controls ($p = 0.92$). In a multivariate model, carotid pulse wave velocity was positively associated with smoking.

Conclusions. The arterial stiffness has appeared as a possible surrogate marker for stroke in long-term survivors of childhood cancer. Smoking habit might have an additional negative influence on vascular aging in the group of patients after neck radiotherapy.

Key words: carotid stiffness; carotid artery disease; childhood cancer survivors; late effects; neck irradiation

Introduction

The survival of children with cancer has improved over the past decades and almost 80% of this population now survives beyond 5 years.^{1,2} But cumulative incidence of a chronic health condition thirty years after the cancer diagnosis is 73% as evidenced by the Childhood Cancer Survivor Study (CCSS).³ Cardiovascular complications are serious late effects in childhood cancer survivors. The risk of stroke is increased in survivors of pae-

diatric Hodgkin disease (HD), leukaemia and brain tumours who received radiation to the brain and/or neck.⁴ Compared with the siblings, the RR of late-occurring stroke among HD survivors was 4.32, among those treated with mantle irradiation the RR was 5.62, for leukaemia survivors the RR of stroke was 6.4 and that one for brain tumour survivors was as high as 29.0 in comparison with siblings.^{5,6} In the CCSS cohort of long-term survivors of childhood cancer (LTSCC) the RR of severe or life-threatening cerebrovascular accident was 9.3 in

comparison with siblings.³ One of possible mechanisms of stroke in young adult survivors of childhood cancer may be a radiation-induced injury to the carotid artery.

The increased risk of carotid artery disease and stroke after radiation therapy (RT) in adult head and neck cancer and HD patients is well documented⁷⁻¹², but these radiation-related late effects have only recently been documented in adult survivors of childhood cancer.¹³⁻¹⁶

The detection of an appropriate surrogate marker for stroke is necessary in order to introduce it into follow-up guidelines. This could enable us to detect LTSCC who are at risk of developing cerebrovascular events. Many studies in adults and some in LTSCC found IMT as possible surrogates. Anyway the results are not consistent. Arterial stiffness was proposed as a possible surrogate for cardiovascular morbidity in LTSCC.^{17,18} However, the stiffness indices were not systematically studied. Therefore, we analysed indices of arterial stiffness besides intima-media thickness as possible early markers of later occurring stroke.

Patients and methods

Subjects

Patients were eligible for the study if they had been treated for HD in Slovenia between 1975 and 1986, under the age of 16, and had received RT to the neck. Fifty-six patients were treated for HD at the age of 16 or less during this time range. Sixteen patients died, 32 out of 40 living patients received neck RT and were eligible for the study. Eight patients refused to participate in the study; one female patient was excluded from the study because she had significant carotid artery stenosis, managed with carotid angioplasty with stenting. Stenting was done 33 years after the patient was treated for HD with a neck RT with 30 Gy and chemotherapy (ChT) with nitrogen mustard, oncovin, procarbazine and prednisolone (MOPP).

None of the patients reported stroke or transient ischemic attack (TIA). Twenty-three (7 females, 16 males) patients were included. They were 3 to 16 (median 11) year old at diagnosis and had evaluation 27 to 38 (median 33) years later at the age of 29 to 48 (median 43) years. They received neck RT with 20 to 65 (median 30) Gy. Eighteen (78%) patients received ChT, only two got ChT with anthracyclines. We recruited 26 healthy controls matched in age, sex, body mass index (BMI), arterial hypertension, smoking history and total cho-

lesterol levels. Study procedures were approved by the National Medical Ethics Committee of the Republic of Slovenia.

Clinical and laboratory investigations

All participants completed a questionnaire to assess cardiovascular risk factors. A positive family history of cerebrovascular disease was defined as a cardiac or cerebral ischemic event in a first-degree relative younger than 65 years. We measured height, weight and blood pressure. Eight hour fasting blood samples were collected for measurement of total cholesterol. Cancer survivors and healthy controls were matched in age, sex, BMI, arterial hypertension, smoking history, total cholesterol levels. Diagnosis and treatment information were abstracted from patient's medical records.

Carotid measurements

High-resolution colour-coded duplex sonography and power Doppler sonography (equipped with an echo tracking system, Alpha 10, Aloka, Tokyo, Japan) of the carotid arteries was performed in all patients. Intima-media thickness (IMT), carotid diameter measurements and arterial stiffness measurements were performed longitudinally, strictly perpendicular to the ultrasound beam, with both walls clearly visualized bilaterally 2 cm below the bifurcation, on the far wall of the common carotid artery (CCA). For reproducible measurements, high-quality images were acquired along a CCA segment of minimum length of 1.5 cm. IMT was measured in accordance with the Mannheim consensus statement. The distances between the characteristic echoes from the lumen-intima and media-adventitia interfaces were measured. The final IMT value was based on the mean value of three maximal IMT measurements in three frames. Arterial stiffness was automatically measured from the modification of the arterial diameter between the systolic and diastolic phases on CCA segments. Carotid diameter waveforms were assessed by means of an ultrasound and converted to carotid pressure waveforms using an empirically derived exponential relationship between pressure and arterial cross section. Blood pressure measurements were obtained simultaneously with ultrasound measurements. The derived carotid pressure waveform was calibrated from brachial end-diastolic and mean arterial pressures by iteratively changing the wall rigidity coefficient.¹⁹ This allowed the calculation of the arterial stiffness in-

TABLE 1. Risk factors in controls and cancer survivors

Characteristics and risk factors	Controls	Survivors	P value
Total	26	23	
Sex (male (%))	6 (77)	7 (70)	0.40
Smoking (%)	8 (30.8)	7 (30.4)	0.613
Family history (%)	5 (20)	0	0.031
Arterial hypertension (%)	4 (15.4)	6 (26.1)	0.354
Diabetes mellitus	0	0	
Age (years)	42.65 ± 5.38	40.22 ± 6.56	0.16
Total cholesterol (mmol/l)	5.7 ± 1.00	5.6 ± 1.01	0.646
Body mass index	25.4 ± 2.98	24.9 ± 1.85	0.595

dices obtained as mean values of the last six measurements:

β , the stiffness index, is relatively independent of transient blood pressure changes:

$$\beta = \ln \frac{P_s}{P_d} \cdot \frac{D_d}{D_s - D_d}$$

where P_s and P_d are systolic and diastolic pressures (in mmHg), and D_s and D_d are systolic and diastolic carotid diameters.²⁰

E_p (kPa), the pressure-strain elasticity modulus, is similar to Young's elastic modulus, regarded as a measure of intrinsic rigidity/stiffness of the arterial wall and inversely related to arterial elasticity^{20,21}:

$$E_p = \frac{(P_s - P_d)D_d}{D_s - D_d}$$

AC, arterial compliance (mm²/kPa), is calculated from the arterial cross-section area and blood pressures. It exhibits an absolute stroke change in arterial lumen area for a given pressure and evaluates the role of the artery as a hollow structure²⁰:

$$AC = \frac{\pi(D_s^2 - D_d^2)}{4(P_s - P_d)}$$

PWV, the one-point pulse wave velocity (m/s), is calculated from the time delay between two adjacent distension waveforms from water hammer equation with the use of the β stiffness parameter²²:

$$PWV = \sqrt{\frac{V\Delta P}{\rho\Delta V}}$$

where ρ is blood density = 1050 kg/m³.

AI, the augmentation index (%), is a simple method commonly used to measure the effects of wave reflection and an indirect index of aortic elasticity²¹:

$$AI = \frac{\Delta P}{PP}$$

where ΔP is the pressure difference between peak systolic pressure and an early inflection point

that indicates the beginning upstroke of the reflected pressure wave, and PP is pulse pressure.²⁰

Beside these indices we examined the carotid arteries for plaque deposits and wall calcinations with the same ultrasound.

Statistical analysis

For the comparison of cases and controls we used chi-square (for categorical variables) and t-test (for continuous variables). In controls we examined carotids from both sides, so we analysed 52 non-irradiated vessels. In cases only carotids on irradiated side of the neck were examined. Twenty patients had bilateral neck RT, 3 unilateral only, so data for 43 vessels was included in our study.

All results were analysed using SPSS Version 21 software (SPSS, Chicago, IL, USA). For the group of cases we performed univariate linear and logistic regression analysis to detect associations between variables. After that we developed multivariate models for carotid PWV and wall calcinations and/or plaques. Variables with P-values < 0.25 from our univariate analysis were introduced into multivariate models.

For intergroup relationships we chose PWV as the most representative and usually used stiffness index and wall calcinations and/or plaques as atherosclerosis surrogate.

Results

Subjects

A total of 49 people (23 cases, 26 controls) were included in our population study. In our comparison of cases and controls no significant group differences were found for age, sex, BMI, total cholesterol, arterial hypertension and smoking history ($P < 0.05$). But there was a difference in family history between both groups ($p = 0.031$). Namely 20% of controls and none of survivors had positive family history (Table 1).

Carotid artery disease

Plaque deposits were present in 9 out of 43 (20.9%) vessels in cancer survivors group and in 0 out of 52 vessels in the group of healthy controls (0%; Figure 1). The results were analysed with the Pearson chi-square test which showed a significant group difference ($p < 0.01$).

Arterial wall calcinations were present in 17 out of 43 (39.5%) vessels in cancer survivors group

and in 0 out of 52 vessels in the group of healthy controls (0%; Figure 1). These results were also analysed with the Pearson chi-square test which showed a significant group difference ($p < 0.01$).

Plaque deposits and/or arterial wall calcinations were found in 24 out of 43 (55.8%) vessels in cancer survivors group and 0 out of 52 vessels in the group of healthy controls (0%; Figure 1) (significant group difference ($p < 0.01$)).

As a measure of carotid stiffness the following parameters were used: beta stiffness index, pressure-strain elastic modulus (Ep), augmentation index (AI), pulse-wave velocity (PWV) and arterial compliance (AC). We analysed the results with the t-test, which showed significant group differences for all the stiffness parameters we used ($P < 0.05$; Table 2), but there was no difference in IMT between cases and controls ($p = 0.92$).

Univariate and multivariate models for the group of cancer survivors

Among cancer survivors, we found a positive association between carotid PWV and gender ($P = 0.03$). No significant relationships were found for smoking, arterial hypertension, total cholesterol, age at diagnosis, age at evaluation, BMI, chemotherapy (yes, no) and size of RT dose (higher than 30 Gy or lower/equal to 30 Gy) (Table 3). In a multivariate model of carotid PWV only smoking was a significant factor; PWV was higher in smokers (Table 4). In a univariate and multivariate model of wall calcination and/or plaque, none of the factors had significant relationships (Tables 3, 5).

Discussion

The principal finding of present study is statistically significant higher values of carotid artery stiffness parameters in LTSCC of HD after neck RT. This is in agreement with two recent studies^{16,17} Vatanen *et al.* found increased carotid artery stiffness in the cohort of 19 high-risk neuroblastoma patients compared with the control group, no differences in stiffness parameters were observed when comparing total body RT with non-total body RT survivors, but the number of patients in the two groups was small.¹⁷ Krystal *et al.* evaluated carotid-femoral PWV in a cohort of 68 LTSCC, including non-irradiated patients, and healthy controls. LTSCC >18 years old at evaluation had significantly higher PWV compared to controls >18 years old and 70% of LTSCC >18 years had elevat-

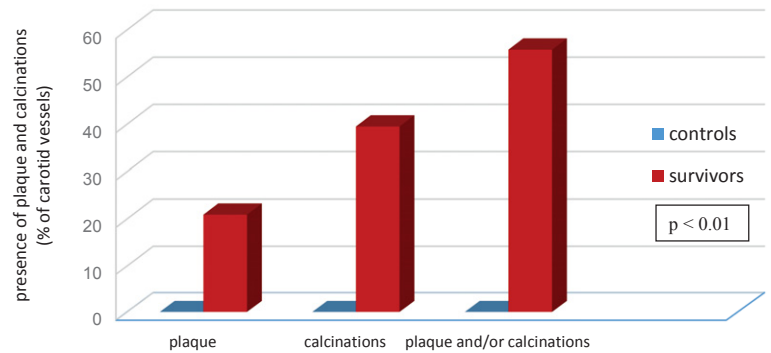


FIGURE 1. Plaques and wall calcinations in cancer survivors and controls.

ed PWV compared to established norms. In a univariate analysis, only exposure to RT and time off therapy were significantly associated with greater PWV. These associations did not hold after adjusting for age, sex, and BMI z-score.¹⁸ In the present study all included patients were treated for HD with neck RT with or without ChT. Therefore, our group is more homogeneous regarding primary diagnosis, type of treatment in comparison with the above-mentioned studies, and it is population based. According to these observations it seems that PWV might be a surrogate marker for stroke in long-term survivors of HD after neck RT.

IMT did not show up as a possible surrogate marker for stroke in survivors of HD after neck RT. Namely, in our study there was no significant difference in IMT between the group of survivors and controls. Many authors offered IMT as a possible surrogate marker for stroke¹⁴⁻¹⁷, however there are

TABLE 2. T-test for IMT and stiffness parameters

	Group	N	Mean	Std. dev.	P value
IMT	0	52	0.546	0.056	0.92
	1	43	0.548	0.132	
Beta stiffness	0	52	6.732	1.437	0.008
	1	43	8.014	3.035	
Ep	0	52	88.149	20.348	0.008
	1	43	109.767	53.331	
AC	0	52	0.774	0.264	0.034
	1	43	0.651	0.293	
AI	0	52	6.722	6.820	0.000
	1	43	20.130	12.833	
PWV	0	52	5.733	0.702	0.009
	1	43	6.300	1.334	

In the second column controls are coded with 0 and cases with 1. AC = arterial compliance; AI = augmentation index; Ep = pressure-strain elastic modulus; IMT = intima-media thickness; PWV = pulse-wave velocity

TABLE 3. Univariate model for carotid pulse-wave velocity (PWV) and wall calcinations and/or plaque

	PWV		Wall calcinations and/or plaque	
	Linear regression estimate (SE)	p value	Odds ratio (95%CI)	p value
Gender	0.055 (0.448)	0.03	1.121 (0.303–4.145)	0.864
Smoking	0.741 (0.424)	0.088	2.679 (0.681–10.534)	0.158
Arterial hypertension	-0.037 (0.472)	0.938	0.570 (0.143–2.268)	0.425
Age at Dg (years)	0.019 (0.052)	0.718	1.094 (0.936–1.278)	0.258
Age at evaluation (years)	-0.047 (0.032)	0.151	1.078 (0.975–1.192)	0.143
Total cholesterol	0.021 (0.205)	0.920	0.702 (0.381–1.294)	0.257
Body mass index	0.021 (0.118)	0.862	0.926 (0.655–1.309)	0.664
Chemo (yes/no)	0.365 (0.484)	0.455	0.455 (0.100–2.072)	0.309
RT (2 groups*)	-0.551 (0.431)	0.208	1.680 (0.452–6.249)	0.439

*Size of radiotherapy dose (higher than 30 Gy or lower/equal to 30 Gy)

some contradictions. Indeed, in a cohort of LTSCC Krawczuk *et al.* failed to find any differences in IMT between irradiated and nonirradiated females.²³ In another article authors did not observe significant differences in IMT between cancer survivors treated with chemotherapy only versus those treated with chemotherapy and radiotherapy.²⁴ Beside that in articles with significant differences in IMT between irradiated and nonirradiated patients those differences were very small and still in a normal range.

In the present population based study, 56% of long-term survivors of HD after neck RT had morphological carotid wall changes as calcinations and/or plaques and none of controls. Many authors reported on higher incidence of atherosclerotic changes in patients treated with neck RT for head and neck cancers or HD in adulthood^{7-12,24,25}, and in LTSCC who were treated with RT as well.^{13-15,17}

But to our knowledge this study is the first population based study of long-term survivors of HD after neck RT.

The high percentage of morphological carotid wall changes in patients of our cohort after neck RT show that atherosclerotic changes are accelerated by neck RT. All patients with morphological carotid wall changes were asymptomatic regarding stroke or TIA. But one female patient was excluded from the study because she experienced hemodynamically significant carotid artery stenosis, managed with carotid angioplasty with stenting. Stenting was done 33 years after the patient was treated for Hodgkin disease with neck RT with 30 Gy and MOPP chemotherapy. Carotid artery disease is a progressive vascular disease, so we can expect that patients with morphological carotid wall changes can be at a higher risk for carotid disease.

Inside the group of survivors we studied the relationship between the size of RT dose and PWV and found out that there was no significant association between the two in the univariate analysis. Also there was no significant relation between them in our multivariate analysis. To our knowledge, no study on LTSCC exists studying the influence of the size of RT dose on stiffness. Meeske *et al.* failed to observe the relationship between radiation doses and intima-media thickness in young patients who received lower (18 Gy) and higher (>30 Gy) doses of RT.¹⁵ In addition, we found no correlation between the size of RT dose and plaque deposits and/or arterial wall calcinations in a univariate analysis. It seems that even a low dose of RT induces premature vascular changes. This is in concordance with the report of Vatanen *et al.* who described premature vascular aging (decreased ar-

TABLE 4. Multivariate model for carotid pulse-wave velocity (PWV)

	Estimate (SE)	p value
Sex	-0.538 (0.471)	0.261
Smoking	0.937 (0.436)	0.031
Age at evaluation (years)	-0.050 (0.034)	0.155
RT (2 groups*)	-0.622 (0.439)	0.165

*Size of RT dose (higher than 30 Gy or lower/equal to 30 Gy)

TABLE 5. Multivariate model for wall calcinations and/or plaque

	Odds ratio (95%CI)	p value
Smoking	2.765 (0.680–1.238)	0.155
Age at evaluation (years)	1.081 (0.974–1.201)	0.144

terial lumen, arterial plaques and increased IMT) in adolescents and young adult survivors of neuroblastoma even after TBI of 10–12 Gy.¹⁷

We analysed the influence of treatment with ChT inside the group of patients as well and there was no significant association between treatment with ChT and PWV or plaque deposits and/or arterial wall calcinations. We were not able to sub-analyse the influence of ChT containing anthracyclines, because only 2 of our patients got it. Our observation is in agreement with the report of Krystal *et al.* who did not find anthracycline dose or chemotherapy exposure to be a risk factor for elevated PWV among LTSCC.¹⁸ Brouwer *et al.* in LTSCC even found a negative association between carotid IMT and treatment with anthracyclines, both as categorical variables [yes/no] and per 100mg/m² cumulative dose.²² Further, Bowers *et al.* observed no association between ChT and the risk of stroke in patients treated for HD in childhood.⁵ To our knowledge, only one study dealing with LTSCC suggested that anthracyclines causes impaired endothelial function, which is early event in atherogenesis.²⁶ In adult patients with breast cancer, Kalabova *et al.* found an association between anthracycline based ChT and increase laboratory risk factors as well as progression of atherosclerosis. They proposed that antracyclines induces oxidative stress that can lead to higher incidence of cardiovascular events.²⁷

Inside the group of survivors we studied the association between traditional cerebrovascular risk factors and PWV. In a multivariate analysis, we found a significant association between smoking and PWV; it was pointed out that smoking habit might have an additional negative influence on vascular aging in the group of patients after neck RT. Interestingly, this finding is in accordance with report of Bowers *et al.* who found out that cigarette smoking may be related to an increased risk of stroke among survivors of HD in childhood. Namely, in this study smoking was undoubtedly recognized as a powerful and independent risk factor for stroke.⁵

We are aware of the limitations of our study. It included only 23 cases and 26 healthy controls, therefore further studies with a bigger sample are needed. The groups matched in the most common risk factors, except in family history of cardiovascular diseases. Further, we could not analyse the influence of follow-up time in the group of survivors, since all of them were treated in a 12-year period.

Patients with carotid disease are asymptomatic in early stages of the disease, and stroke is often the first sign. It would be reasonable to screen patients after neck RT with ultrasound for these radiation-related late effects. To our knowledge, among available long-term follow-up guidelines only current COG guidelines recommend that LTSCC who had neck RT with 40 Gy should undergo yearly neurologic examination and assessment for diminished pulses and the presence of carotid bruits and Doppler of carotid vessels if clinically indicated (<http://www.survivorshipguidelines.org>). It is obvious that recommendations for screening of carotid stenosis in those patients have to be adjusted. One of the possible screening tools in the future could be PWV, but further research in this field is needed. What is more, even a very low dose of RT can cause atherosclerotic changes, therefore we should change cut-off dose of 40 Gy to a lower one. However, it is beyond dispute that atherogenesis in LTSCC with controlling cardiovascular risk factors can be slowed down. This is very important because it was reported that LTSCC are predisposed to obesity, hypertension, dyslipidaemia and glucose intolerance^{16,17}, therefore carefully monitoring and correction of the common vascular risk factors such as diabetes, smoking, obesity, hyperlipidaemia, hypertension is mandatory. Promotion of healthy life style in long-term follow-up clinics is of vital importance as well.

Acknowledgement

Thanks to Slovenian Research Agency for funding and to Slovenian Cancer Registry for data. Thanks to Vesna Savić, dr. med. for help with data collection.

References

1. Gatta G, Botta L, Rossi S, Aareleid T, Bielska-Lasota M, Clavel J, et al. Childhood cancer survival in Europe 1999-2007: results of EUROCare-5 - a population-based study. *Lancet Oncology* 2014; **15**: 35-47. doi: 10.1016/S1470-2045(13) 70548-5
2. Perme MP, Jereb B. Trends in survival after childhood cancer in Slovenia between 1957 and 2007. *Pediatr Hematol Oncol* 2009; **26**: 240-51. doi: 10.1080/08880010902900437
3. Oeffinger KC, Mertens AC, Sklar CA, Kawashima T, Hudson MM, Meadows AT, et al. Chronic health conditions in adult survivors of childhood cancer. *N Engl J Med* 2006; **355**: 1572-82. doi: 10.1056/NEJMSa060185
4. Morris B, Partap S, Yeom K, Gibbs IC, Fisher PG, King AA, et al. Cerebrovascular disease in childhood cancer survivors. A Children's Oncology Group Report. *Neurology* 2009; **73**: 1906-13. doi: 10.1212/WNL.0b013e3181c17ea8

5. Bowers DC, McNeil DE, Liu Y, Yasui Y, Stovall M, Gurney JG, et al. Stroke as a late treatment effect of Hodgkin's disease: a report from the childhood cancer survivor study. *J Clin Oncol* 2005; **23**: 6508-15. doi: 10.1200/JCO.2005.15.107
6. Bowers DC, Liu Y, Leisenring W, McNeil E, Stovall M, Gurney JG, et al. Late-occurring stroke among long-term survivors of childhood leukemia and brain tumors: a report from the childhood cancer survivor study. *J Clin Oncol* 2006; **24**: 5277-82. doi: 10.1200/JCO.2006.07.2884
7. Cheng SW, Wu LL, Ting AC, Ting AC, Lau H, Lam LK, Wei WI. Irradiation-induced extracranial carotid stenosis in patients with head and neck malignancies. *Am J Surg* 1999; **178**: 323-8.
8. Dorresteijn LD, Kappelle AC, Boogerd W, Klokman WJ, Balm AJM, Willem J. Klokman WJ, Keus RB, et al. Increased risk of ischemic stroke after radiotherapy of the neck in patients younger than 60. *J Clin Oncol* 2002; **20**: 282-8. doi: 10.1200/JCO.2002.201.282
9. Carmody BJ, Arora S, Avena R, Curry KM, Simpkins J, Cosby K, et al. Accelerated carotid artery disease after high-dose head and neck radiotherapy: is there a role for routine carotid duplex surveillance? *J Vasc Surg* 1999; **30**: 1045-51. doi: 10.1016/S0741-5214(99)70042-X
10. Elerding SC, Fernandez RN, Grotta J, Lindberg RD, Causay LC, McMurtrey MJ. Carotid artery disease following external cervical irradiation. *Ann Surg* 1981; **194**: 609-15.
11. Wethal T, Nedregaard B, Andersen R, Fosså A, Lund MB, Günther A, et al. Atherosclerotic lesions in lymphoma survivors treated with radiotherapy. *Radiation Oncol* 2013; **110**: 448-54. doi: 10.1016/j.radonc.2013.10.029
12. Hull MC, Morris CG, Pepine CJ, Mendenhall NP. Valvular dysfunction and carotid, subclavian, and coronary artery disease in survivors of Hodgkin lymphoma treated with radiation therapy. *JAMA* 2003; **290**: 2831-7. doi: 10.1001/jama.290.21.2831
13. Meeske KA, Nelson MD, Lavey RS, Gee S, Nelson MB, Bernstein L, et al. Premature carotid artery disease in long-term survivors of childhood cancer treated with neck irradiation: Five case reports. *J Pediatr Hematol Oncol* 2007; **29**: 480-4. doi: 10.1097/MPH.0b013e3180601029
14. King LJ, Hasnain SN, Webb JA, Kingston JE, Shafford EA, Lister TA, et al. Asymptomatic carotid arterial disease in young patients following neck radiation therapy for Hodgkin lymphoma. *Radiology* 1999; **213**: 167-72. doi: 10.1148/radiology.213.1.r99oc07167
15. Meeske KA, Siegel ES, Gilsanz V, Bernstein L, Nelson MB, Spoto R, et al. Premature carotid artery disease in pediatric cancer survivors treated with neck irradiation. *Pediatr Blood Cancer* 2009; **53**: 615-21. doi: 10.1002/pbc.22111
16. Brouwer CAJ, Postma A, Hooimeijer HLH, Smit AJ, Vonk JM, van Roon AM, et al. Endothelial damage in long-term survivors of childhood cancer. *J Clin Oncol* 2013; **31**: 3906-13. doi: 10.1200/JCO.2012.46.6086
17. Vatanen A, Sarkola T, Ojala TH, Turanlahti M, Jahnukainen T, Saarinen-Pihkala UM. Radiotherapy related premature arterial aging in young adult and adolescent. Long-term survivors of high-risk neuroblastoma. *Pediatr Blood Cancer* 2015; **62**: 2000-6. doi: 10.1002/pbc.25616
18. Krystal JI, Reppucci M, Mayr T, Fish JD, Sethna C. Arterial stiffness in childhood cancer survivors. *Pediatr Blood Cancer* 2015; **62**: 1832-7. doi: 10.1002/pbc.25547
19. Meinders JM, Hoeks APG. Simultaneous assessment of diameter and pressure waveforms in the carotid artery. *Ultrasound Med Biol* 2004; **30**: 147-54. doi: 10.1016/j.ultrasmedbio.2003.10.014
20. Rhee MY, Lee HY, Park YB. Measurements of arterial stiffness: Methodological aspects. *Korean Circ J* 2008; **38**: 343-50. doi: 10.4070/kcj.2008.38.7.343
21. Laurent S, Cockcroft J, Van Bortel L, Boutouyrie P, Giannattasio C, Hayoz D, et al. Expert consensus document on arterial stiffness: methodological issues and clinical applications. *Eur Heart J* 2006; **27**: 2588-605. doi: 10.1093/eurheartj/ehl254
22. Jaroch J, Łoboz Grudziński K, Bociąga Z, Kowalska A, Kruszyńska E, Wilczyńska M, et al. The relationship of carotid arterial stiffness to left ventricular diastolic dysfunction in untreated hypertension. *Kardiol Pol* 2012; **70**: 223-31.
23. Krawczuk-Rybak M, Tomczuk-Ostapczuk M, Panasiuk A, Gosciak E. Carotid intima-media thickness in young survivors of childhood cancer. *J Med Imaging Radiat Oncol* 2017; **61**: 85-92. doi: 10.1111/1754-9485.12510
24. Sadurska E, Brodzisz A, Zaucha-Prażmo A, Kowalczyk J. The estimation of intima-media thickness and cardiovascular risk factors in young survivors of childhood cancer. *J Pediatr Hematol Oncol* 2016; **38**: 549-54. doi: 10.1097/MPH.0000000000000513
25. Silverberg GD, Britt RH, Goffinet DR. Radiation-induced carotid artery disease. *Cancer* 1978; **41**: 130-7. doi: 10.1002/1097-0142(197801)41:1<130::AID-CNCR 2820410121>3.0.CO;2-X
26. Chow AY, Chin C, Dahl G, Rosenthal DN. Anthracyclines cause endothelial injury in pediatric cancer patients: a pilot study. *J Clin Oncol* 2006; **24**: 925-8. doi: 10.1200/JCO.2005.03.5956
27. Kalabova H, Melichar B, Ungermann L, Doležal J, Krčmova L, Kašparova M. Intima-media thickness, myocardial perfusion and laboratory risk factors of atherosclerosis in patients with breast cancer treated with anthracycline-based chemotherapy. *Med Oncol* 2011; **28**: 1281-7. doi: 10.1007/s12032-010-9593-1

Perfusion magnetic resonance imaging changes in normal appearing brain tissue after radiotherapy in glioblastoma patients may confound longitudinal evaluation of treatment response

Markus Fahlström¹, Erik Blomquist², Tufve Nyholm³, Elna-Marie Larsson¹

¹ Department of Radiology, Surgical Sciences, Uppsala University, Uppsala, Sweden

² Department of Experimental and Clinical Oncology, Immunology, Genetics and Pathology, Uppsala University, Uppsala, Sweden

³ Department of Radiation Physics and Biomedical Engineering, Radiation Sciences, Umeå University, Umeå, Sweden

Radiol Oncol 2018; 52(2): 143-151.

Received 17 January 2018

Accepted 4 April 2018

Correspondence to: Markus Fahlström, Department of Surgical Sciences, Akademiska Sjukhuset, SE-75185 Uppsala, Sweden. Phone: +467 02 869 961; E-mail: markus.fahlstrom@radiol.uu.se

Disclosure: Professor Elna-Marie Larsson has received speaker honoraria from Bayer AG, Berlin, Germany. Remaining authors declared they have no conflict of interest.

Background. The aim of this study was assess acute and early delayed radiation-induced changes in normal-appearing brain tissue perfusion as measured with perfusion magnetic resonance imaging (MRI) and the dependence of these changes on the fractionated radiotherapy (FRT) dose level.

Patients and methods. Seventeen patients with glioma WHO grade III-IV treated with FRT were included in this prospective study, seven were excluded because of inconsistent FRT protocol or missing examinations. Dynamic susceptibility contrast MRI and contrast-enhanced 3D-T1-weighted (3D-T1w) images were acquired prior to and in average (standard deviation): 3.1 (3.3), 34.4 (9.5) and 103.3 (12.9) days after FRT. Pre-FRT 3D-T1w images were segmented into white- and grey matter. Cerebral blood volume (CBV) and cerebral blood flow (CBF) maps were calculated and co-registered patient-wise to pre-FRT 3D-T1w images. Seven radiation dose regions were created for each tissue type: 0–5 Gy, 5–10 Gy, 10–20 Gy, 20–30 Gy, 30–40 Gy, 40–50 Gy and 50–60 Gy. Mean CBV and CBF were calculated in each dose region and normalised (nCBV and nCBF) to the mean CBV and CBF in 0-5 Gy white- and grey matter reference regions, respectively.

Results. Regional and global nCBV and nCBF in white- and grey matter decreased after FRT, followed by a tendency to recover. The response of nCBV and nCBF was dose-dependent in white matter but not in grey matter.

Conclusions. Our data suggest that radiation-induced perfusion changes occur in normal-appearing brain tissue after FRT. This can cause an overestimation of relative tumour perfusion using dynamic susceptibility contrast MRI, and can thus confound tumour treatment evaluation.

Key words: perfusion MRI; radiation-induced changes; normal-appearing brain tissue; malignant gliomas

Introduction

Radiation-induced changes in brain tissue can be divided into acute, early delayed and late effects.¹⁻⁴ Several publications suggest that vascular damage is the primary cause of acute and early delayed

effects.^{3,5} Both acute and early delayed effects are considered reversible, manifesting as dilation and thickening of blood vessels, decrease in vessel density, endothelial cell damage and disruption of the blood-brain-barrier in normal appearing brain tissue.^{1,3,4,6}

Few studies have assessed radiation-induced changes in brain perfusion in normal appearing brain tissue after fractionated radiotherapy (FRT) or stereotactic radiosurgery.^{5,7-14} Contradictory results have been published, however, perfusion techniques and post-processing methods differ extensively between studies. Overall, the published data show a reduction of both cerebral blood volume (CBV) and cerebral blood flow (CBF) after completion of FRT or single fraction stereotactic radiosurgery, with an inverse dose-response relationship.

Perfusion MRI is useful in the diagnostic evaluation of gliomas as well as for longitudinal response assessment and prognostication, with dynamic susceptibility contrast (DSC)-MRI being the most widely applied perfusion MRI technique in clinical practice.¹⁵⁻²⁰ DSC-MRI is also one of several physiological imaging techniques that has the potential to be incorporated into the Response Assessment in Neuro-Oncology (RANO) criteria as proposed by the RANO working group.^{21,22} DSC-MRI can assess perfusion parameters like CBV and CBF but has several limitations, leading to both quantification and reproducibility issues.¹⁸ These limitations are related to acquisition and post-processing of the data.^{15,16,18,23-26} Generally, only relative measurements, *i.e.* normalised to a reference region in normal appearing brain tissue, are feasible in clinical practice.^{19,26} However, this improves the reproducibility of measurements, which is important for longitudinal comparison.¹⁶ Reference tissue can be defined in several ways, but most commonly, contralateral normal-appearing white matter (WM) is used.^{19,27} We hypothesize that vascular damages in normal appearing brain tissue secondary to radiation exposure can confound DSC-MRI measurements. Since DSC-MRI is an extensively applied perfusion imaging technique in brain tumours it is important to determine if normalisation to reference tissue is affected by radiation exposure. Consequently, the aim of this prospective study was to assess acute and early delayed radiation-induced changes in normal appearing brain tissue measured with DSC-MRI and the dependence of these changes on the radiation dose given.

Patients and methods

Patients

Seventeen patients, 18 years or older, with newly detected glioma WHO grade III-IV proven by histopathology and scheduled for FRT and chemotherapy were included prospectively. This study was

done in accordance with the declaration of Helsinki and was approved by the local ethical committee (*Regionala etikprövningsnämnden i Uppsala*, approval number 2011/248). Written informed consent was obtained from all patients. All patients had undergone surgical resection or biopsy. Baseline MRI was performed prior to FRT (pre-FRT) and post-FRT examinations were scheduled consecutively after the completion of FRT (FRT_{Post-1}, FRT_{Post-2} and FRT_{Post-3}). The FRT was delivered using 6 megavolt photons with intensity-modulated radiation therapy or volumetric arc therapy. Concomitant chemotherapy was administered daily during FRT with temozolomide followed by adjuvant chemotherapy starting 4 weeks after completed FRT according to Stupp *et al.*²⁸ In cases of tumour progression or recurrence, a combination of temozolomide, bevacizumab and/or procarbazine, lomustine and vincristine (in combination further known as PCV) was administered.

Exclusion criteria

Exclusion criteria were inconsistent or missing MRI examinations and/or deviation from a prescribed total radiation dose of 60 Gray (Gy).

Image acquisition

All MR examinations were performed with a consistent imaging protocol on a 1.5 T scanner (Avanto Fit, Siemens Healthcare, Erlangen, Germany) and included DSC perfusion and contrast-enhanced 3D-T1-weighted (3D-T1w) images.

Imaging parameters:

- DSC-MRI (2D-EPI, gradient-echo; Repetition time/Echo time/Flip angle = 1340/30/90; 128 × 128 matrix; 1.8×1.8×5 mm³; time resolution = 1.34 s; 18 slices). A bolus of 5 ml gadolinium-based contrast agent (GBCA) (Gadovist, Bayer AG, Berlin, Germany) was administered for a DCE-MRI and was also regarded as a pre-bolus to diminish the effects of contrast agent extravasation^{15,18} for the following DSC-MRI. For the actual DSC-MRI, a second standard dose bolus of 5 ml GBCA was administered. The contrast agent was administered using a power-injector at a rate of 2 ml/s for the first injection and 5 ml/s for the second injection.
- 3D-T1w image (3D-gradient Echo; Repetition time/Echo Time/Inversion time/Flip angle = 1170/4.17/600/15; 256 × 256 matrix: 1×1×1 mm³: 208 slices)

CT imaging for radiotherapy planning was acquired with a Philips, Brilliance Big Bore (Philips Healthcare, Best, the Netherlands) with a voxel size of $0.525 \times 0.525 \times 2 \text{ mm}^3$.

Perfusion analysis

Signal to concentration time curves conversion has been described previously.^{29,30} Concentration time curves were visually inspected before analysis. CBV was determined as the ratio of areas under the tissue and arterial concentration time curves. CBF was determined through deconvolution as the initial height of the tissue impulse function.^{24,29} Deconvolution was carried out using standard singular value decomposition (sSVD) with Tikhonov regularisation with an iterative threshold.^{29,31-33} A patient-specific arterial input function (AIF) was defined in the middle cerebral artery branches in the hemisphere contralateral to the tumour¹⁹ in the pre-FRT examination, the same AIF was then applied to the patient's following post-FRT examinations. Contrast agent leakage correction was applied according to the method described by Boxerman *et al.*, 2006.³⁴ Vessel segmentation was performed using an iterative five-class k-means cluster analysis to exclude large arteries and veins.³⁵ Calculation of DSC data was performed in NordicICE (NordicNeurolabs, Bergen, Norway).

Data post-processing

CBV and CBF maps were co-registered to the pre-FRT 3D-T1w images for each patient and examination using the SPM12 toolbox (Wellcome Trust Centre for Neuroimaging, London, UK). Planned radiation dose levels for each region were acquired by rigidly transforming the dose-planning CT (including related radiation dose plans) to the pre-FRT 3D-T1w images using the standard Elastix registration toolbox.³⁶

Grey matter (GM) and WM probability maps were segmented from the 3D-T1w images, for each examination, using the segmentation tool in the SPM12 toolbox. WM and GM maps were defined as partial volume fraction above 70%. Contrast-enhancing tissue, oedema, resection cavity, tumour progression and recurrence, if present, were excluded, reviewed by an experienced neuroradiologist. Registered radiation dose plans were divided as follows: 0–5 Gy, 5–10 Gy, 10–20 Gy, 20–30 Gy, 30–40 Gy, 40–50 Gy and 50–60 Gy, creating a total of seven binary dose regions for each tissue

type, (mean volume and standard deviation for each dose region is presented in S1 Table).

Statistical analysis

Mean CBV and CBF were calculated in each dose region and normalised (nCBV and nCBF) to the mean CBV and CBF in 0–5 Gy WM and GM regions, respectively. Super- and subscripts are used to distinguish between tissue type from which measurements were derived (superscript) and reference tissue type used for normalisation (subscript), *i.e.* $nCBV_{WM}^{GM}$, $nCBV_{WM}^{WM}$ and $nCBV_{GM}^{GM}$ (same for nCBF). For descriptive analysis, average mean, 95% confidence interval (CI) and standard error of mean (SEM) were calculated region-wise, outlined by radiation dose regions (regional nCBV and nCBF), and globally, incorporating all regional values irrespective of received radiation dose (global nCBV and nCBF). A Wilcoxon matched-pairs signed ranks test was used to compare post-FRT data with pre-FRT data under the null hypothesis: there is no change in nCBV and nCBF after FRT. This was performed for regional values and global values and for GM and WM, respectively. Derived *P*-values are two-sided and presented as exact values, unless lower than 0.001, in this case they are presented as <0.001 . *P*-values lower than 0.05 were considered significant. Relative change was further defined as:

$$200 \times \frac{(nCBV_{post} - nCBV_{pre})}{(nCBV_{post} + nCBV_{pre})} \text{ same for nCBF}$$

Mean relative change and standard deviation (SD) were calculated and presented as a part of the descriptive analysis. A linear regression model was applied to assess a possible dose-response relationship between relative change and received radiation dose. Graphpad Prism 7 for Mac (Graphpad Software, La Jolla California USA) was used for statistical analysis and graph design.

Results

Patients

Seven patients were excluded due to inconsistent or missing pre-FRT examinations ($n = 5$) or deviation from the prescribed total dose of 60 Gy ($n = 2$). Data from 10 patients were analysed (mean age 55.8 years, SD 8.0 years). All had a histopathological diagnosis of glioblastoma (WHO grade IV). All patients analysed were prescribed a total dose of 60 Gy, however, nine patients had received a fraction

TABLE 1. Mean, standard error of mean (SEM) and change relative pre-fractionated radiotherapy (pre-FRT) for global nCBV and nCBF. Global normalised cerebral blood volume (nCBV) and normalised cerebral blood flow (nCBF) (mean and SEM), change in percentage relative pre-FRT (mean and SD) and derived *P*-values from a Wilcoxon matched-pair signed ranks test comparing post-FRT data with pre-FRT data. Corresponding table for regional nCBV and nCBF can be found in S2 Table

nCBV _{WM} ^{GM}				
	Pre-FRT	FRT _{Post-1}	FRT _{Post-2}	FRT _{Post-3}
nCBV	1.63±0.03	1.53±0.04	1.49±0.05	1.53±0.03
ΔnCBV (%)		-6.7±7.7	-4.6±11.7	-6.0±9.3
p-value		<0,0001	0,0535	<0,0001
nCBF _{WM} ^{GM}				
	Pre-FRT	FRT _{Post-1}	FRT _{Post-2}	FRT _{Post-3}
nCBF	1.60±0.03	1.53±0.03	1.37±0.04	1.46±0.03
ΔnCBF (%)		-5.1±11.7	-12.5±11.4	-7.5±8.2
p-value		0,0057	<0,0001	<0,0001
nCBV _{WM} ^{WM}				
	Pre-FRT	FRT _{Post-1}	FRT _{Post-2}	FRT _{Post-3}
nCBV	1.10±0.03	1.06±0.03	1.03±0.03	1.05±0.03
ΔnCBV (%)		-4.3±7.6	0.7±11.7	-3.6±11.9
p-value		0,0003	0,3818	0,1197
nCBF _{WM} ^{WM}				
	Pre-FRT	FRT _{Post-1}	FRT _{Post-2}	FRT _{Post-3}
nCBF	1.09±0.02	1.08±0.03	0.96±0.03	1.05±0.03
ΔnCBF (%)		-3.1±7.7	-7.4±10.5	-3.4±10.3
p-value		0,0166	0,0002	0,2267
nCBV _{GM} ^{GM}				
	Pre-FRT	FRT _{Post-1}	FRT _{Post-2}	FRT _{Post-3}
nCBV	1.00±0.01	0.99±0.01	1.02±0.02	1.0±0.02
ΔnCBV (%)		-0.9±4.0	1.7±5.7	-0.4±6.8
p-value		0,1629	0,184	0,6445
nCBF _{GM} ^{GM}				
	Pre-FRT	FRT _{Post-1}	FRT _{Post-2}	FRT _{Post-3}
nCBF	1.02±0.01	1.01±0.01	1.00±0.01	1.02±0.01
ΔnCBF (%)		-0.1±5.1	-2.8±4.7	0.0±4.5
p-value		0,4922	0,0073	0,9252

dose of 2.0 Gy/fraction and one patient 2.2 Gy/fraction. Seven post-FRT examinations were missing, yielding a total of 33 MR-examinations. Pre-FRT examination was performed in average (SD, number of patients) 9.0 (7.4, 10 patients) days prior to start of FRT and three post-FRT examinations were

performed 3.1 (3.3, 9 patients), 34.4 (9.5, 5 patients) and 103.3 (12.9, 9 patients) days after end of FRT. Five patients were administrated temozolamide after FRT_{Post-1} and three patients after FRT_{Post-2}. PCV and bevacizumab/lomustine were administrated after FRT_{Post-1} in two patients respectively.

Changes in nCBV and nCBF after radiation treatment

A representative dose region distribution map with corresponding pre-FRT 3D-T1w image are displayed in Figure 1. Global nCBV and nCBF with 95% CI and derived *P*-values are graphically described in Figure 2. Mean and SEM of global nCBV and nCBF together with mean relative change and SD and derived *P*-values are presented in Table 1. Both nCBV_{WM}^{GM} and nCBF_{WM}^{GM} decreased at FRT_{Post-1} decreased further at FRT_{Post-2} and recovered at FRT_{Post-3} however, still below corresponding values at pre-FRT. Significant differences were found for all values except nCBV_{WM}^{GM} at FRT_{Post-2}; nCBV_{WM}^{WM} and nCBF_{WM}^{WM} showed the same tendency. Only small variations between pre-FRT and post-FRT examinations were present in nCBV_{GM}^{GM} and nCBF_{GM}^{GM} implying no change after FRT. Comprehensive figures over regional nCBV and nCBF and derived *P*-values are provided in S1 and S2 Figures and S2 Table. In summary, similar responses were seen in regional nCBV and nCBF after FRT as in global nCBV and nCBF, but they were less pronounced and mostly non-significant.

Dose-response relationship

Using a linear regression model, both nCBV_{WM}^{WM} and nCBF_{WM}^{WM} demonstrated an inverse response to radiation dose, *i.e.* larger reductions in nCBV with increasing radiation dose; nCBV_{WM}^{GM} and nCBF_{WM}^{GM} demonstrated a varied response to radiation dose. Furthermore, the same tendency could be seen for nCBV_{GM}^{GM} and nCBF_{GM}^{GM}. In Figure 3, relative change and derived linear regression curve and equation for regional nCBV is illustrated (corresponding for nCBF can be found in S3 Figure).

Discussion

In this study, we found decreasing perfusion values indicating acute and early delayed effects in normal appearing brain tissue after FRT. We also observed a dose-response relationship in WM but not in GM.

Petr *et al.* reported a 9.8% decrease in contralateral normal appearing GM CBF measured with arterial spin labelling -MRI 4.8 months after FRT. An assessment of how the radiation dose given affects the decrease in CBF indicated that the decrease is larger with higher radiation dose *i.e.* an inverse dose-response relationship.¹⁰ A good correlation has previously been reported between arterial spin labelling -MRI and DSC-MRI with regard to measuring regional CBF^{13,37}, however, an analysis of white matter was not included. Price *et al.* found a dose-related decrease in relative CBV and relative CBF in normal appearing WM after FRT.¹¹ However, only four patients were studied, and normalisation was performed to periventricular normal-appearing WM measured before FRT. Webber *et al.* reported no radiation-induced change in CBF, measured with DSC and arterial spin labelling MRI, after stereotactic radiosurgery in regions restricted to <0.5 Gy up to five times after FRT.¹³ Lee *et al.* studied CBV measured with DSC in WM and found a response that was similar to our results. The dose regions were larger, up to 60 Gy, in steps of 15 Gy. CBV was normalised to voxels receiving 0–15 Gy. A tendency towards an inverse dose-response relationship was reported.⁹ In summary, these results were in fair agreement with ours.

A number of contradictory findings have been reported in the literature. Jakubovic *et al.* evaluated relative CBV and relative CBF measured with DSC

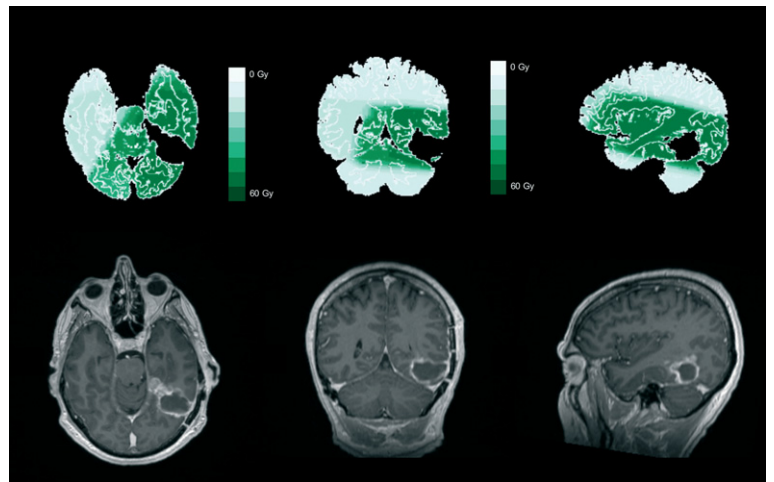


FIGURE 1. Dose region distribution with corresponding pre-fractionated radiotherapy (pre-FRT) Gd-T1w image. Representative dose region distribution with corresponding pre-FRT Gd-T1w image for one patient. Dose distribution was divided into seven binary regions (0–5 Gy, 5–10 Gy, 10–20 Gy, 20–30 Gy, 30–40 Gy, 40–50 Gy and 50–60 Gy). Resection cavity, post-FRT effects and tumour tissue were excluded.

in patients undergoing single fraction stereotactic radiosurgery. They reported increasing rCBV and rCBF in both GM and WM.⁸ This discrepancy compared to our results can be explained by use of different radiation treatment methods and that normalisation was done only to pre-stereotactic radiosurgery CBV and CBF values. Fuss *et al.* evaluated CBV in GM and WM after FRT in patients

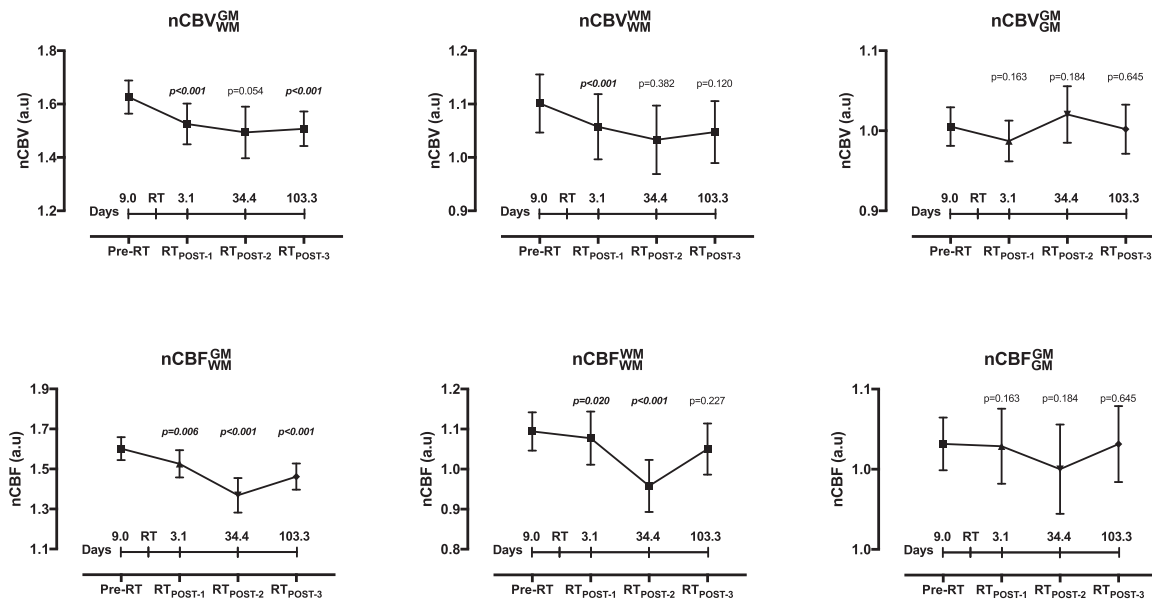


FIGURE 2. Longitudinal change in global normalised cerebral blood volume (nCBV) and normalised cerebral blood flow (nCBF). Global nCBV and nCBF (mean and 95% CI) graphically displayed for the different examinations in consecutive order. Derived *P*-values are included, and emphasised in bold and italics if less than 0.05. Corresponding table for regional nCBV and nCBF can be found in S1 and S2 Figures.

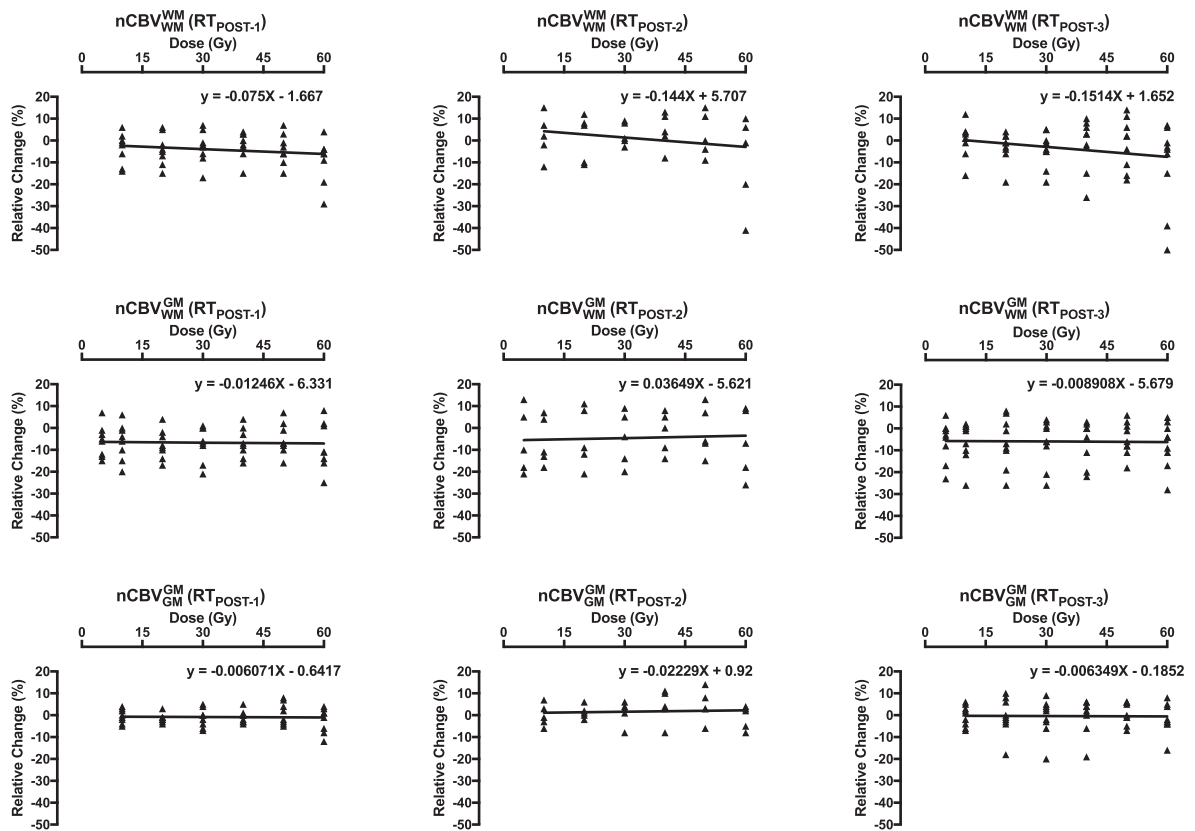


FIGURE 3. Dose-dependent relative change and linear regression model for normalised cerebral blood volume (nCBV). Shows regional relative change for nCBV and derived line regression (line and equation).

Corresponding figure for normalised cerebral blood flow (nCBF) can be found in S3 Figure.

with low-grade astrocytomas. Decrease of CBV up to 30% was seen 24 months after FRT in both GM and WM. Smaller decrease was seen 6 months after FRT.⁷ In another study, CBV change was evaluated 15 months after FRT in GM and WM. CBV after FRT was found to be significantly lower than before FRT.¹⁴ However, in both these studies, the DSC analysis was not described in detail, and the time period used in these studies did not coincide with ours. As absolute values were reported, the results presented in these studies could be affected largely by the limitations in absolute quantification of DSC-MRI-derived perfusion measures. Taki *et al.* reported a 7% decrease in global CBF in GM 2 weeks and 3 months after stereotactic radiosurgery. This is in agreement with our results. However, large decreases were detected in GM receiving < 5 Gy (up to 22%).¹² This contradicting result could be explained by reproducibility errors between examinations. Non-normalised blood flow measured with ^{99m}Tc-HMPAO SPECT is affected by large variations between examinations compared to normal-

ised blood flow.³⁸ In this study, the authors do not describe if normalisation is used or not. Different radiation treatment methods and dose must also be considered as confounding factors when our results are compared with their findings.

Radiation-induced vascular structural changes, such as dilation and thickening of vessels, decreased vessel density, blood-brain-barrier disruption, endothelial cell damages may introduce thrombosis, tortuosity and occlusion. This could affect the perfusion and together with decreased vessel density and may partly explain our results.^{3,4,9} Furthermore, the recovery in nCBV and nCBF seen in our results agrees with the theory of acute and early delayed effects being reversible.^{1,3,4} However, radiation-induced changes in brain tissue is a complex process involving several tissue elements. Moreover, histopathology has mainly been studied in rodent models or single dose experiments.^{3,5,45} Interpreting findings from animal models and applying them to humans should be done with caution.

Our findings suggest that the GM response to the administrated treatment is independent of the radiation dose received; however, there is still an apparent reaction to radiation. This suggestion is based on two preliminary findings; first, a linear regression of relative difference in regional $nCBV_{WM}^{GM}$ and $nCBF_{WM}^{GM}$ demonstrated both positive and negative slopes, with small β values compared to WM tissue. Second, the resulting linear regression for $nCBV_{GM}^{GM}$ and $nCBF_{GM}^{GM}$ is also small and close to zero. This is to be expected if no dose-response relationship exists in GM, and furthermore, the use of radiation-induced changes in low-dose WM as reference tissue can be rejected as a confounding factor in this specific case because GM was used as the reference tissue. To the best of our knowledge, we are the first to report a perfusion decrease independent of radiation dose in GM using DSC. Several publications have shown that grey matter volume decreases after fractionated radiotherapy increasing with radiation dose⁴⁶⁻⁴⁹, since both CBV and CBF are tissue volume dependent parameters, we believe that the dose-independency found in grey matter is a result of decreased grey matter volume instead of an actual response in CBV and CBF independent on radiation dose given.

Despite encouraging results, some potential limitations need to be addressed. First, the patient number is small and for the evaluation of perfusion on examination FRT_{Post-2} only five data sets were analysed. The severity of the disease significantly contributed to the high number of excluded patients through drop-outs and terminating examinations, which was beyond our control. Our efforts to keep a consistent FRT protocol and imaging time frame also contributed to exclusions. However, since we investigated response to radiation dose over time, it was necessary to keep both radiation dose and imaging time point consistent in the patient material. Secondly, concomitant and adjuvant chemotherapy was given to all patients. While there are no reports of temozolomide or PCV affecting brain perfusion, a recent publication reported that bevacizumab may decrease CBF in contralateral normal appearing GM.⁵⁰ However, only one patient was given bevacizumab during the examinations analysed, it is therefore unlikely that our data are affected by the adjuvant chemotherapy given.

The limitations of DSC-MRI are, in the present study, considered by several post-processing selections. The use of patient-specific AIF in DSC measurements has been shown to increase the reproducibility between examinations, minimis-

ing the effects on reproducibility inherent in partial volume effects and noise.⁵¹ This approach also confronts the concern regarding misleading results due to radiation-induced changes in pixels defined as the AIF.⁹ Vessel segmentation was performed to eliminate macro vessel signal contributions causing overestimation of CBV and CBF. We used pre-bolus administration and contrast agent leakage correction as suggested.^{15,18} Furthermore, post-FRT effects such as oedema were excluded from the dose regions during segmentation, and can thereby not influence our results.

In summary, significant decrease of global $nCBV$ and $nCBF$ between pre-FRT and post-FRT examinations was found in our study. As proposed by Petr *et al.*, perfusion variations in healthy tissue can represent a possible bias with regard to reference region selection.¹⁰ Acute and early delayed effects from FRT would, based on our results and other publications, introduce an overestimation of tumour CBV and CBF since the reference normal appearing brain tissue CBV and CBF are the denominator in the ratio. Thus, information from radiation dose plans may assist the selection of a reference WM region, avoiding GM to, if possible, define a region that received as low dose as possible.

Conclusions

Our findings suggest that radiation-induced perfusion changes occur in normal-appearing brain tissue after FRT. This can cause an overestimation of relative tumour perfusion using DSC-MRI, and thus, can confound tumour treatment evaluation.

Acknowledgement

Disclaimer: The views and opinions expressed in this article are those of the authors and do not necessarily express an official position of the institution or funder. This work was funded by Bayer, AG, Berlin, Germany and the Swedish Cancer Society.

References

1. Kim JH, Jenrow KA, Brown SL. Mechanisms of radiation-induced normal tissue toxicity and implications for future clinical trials. *Radiat Oncol J* 2014; **32**: 103-15. doi: 10.3857/roj.2014.32.3.103
2. Price RE, Langford LA, Jackson EF, Stephens LC, Tinkey PT, Ang KK. Radiation-induced morphologic changes in the rhesus monkey (*Macaca mulatta*) brain. *J Med Primatol* 2001; **30**: 81-7. doi: 10.1034/j.1600-0684.2001.300202.x

3. Sundgren PC, Cao Y. Brain irradiation: effects on normal brain parenchyma and radiation injury. *Neuroimaging Clin N Am* 2009; **19**: 657-68. doi: 10.1016/j.nic.2009.08.014
4. Greene-Schloesser D, Robbins ME, Peiffer AM, Shaw EG, Wheeler KT, Chan MD. Radiation-induced brain injury: a review. *Front Oncol* 2012; **2**: 73. doi: 10.3389/fonc.2012.00073
5. Cao Y, Tsien CI, Sundgren PC, Nagesh V, Normolle D, Buchtel H, et al. Dynamic contrast-enhanced magnetic resonance imaging as a biomarker for prediction of radiation-induced neurocognitive dysfunction. *Clin Cancer Res* 2009; **15**: 1747-54. doi: 10.1158/1078-0432.CCR-08-1420
6. Adair JC, Baldwin N, Kornfeld M, Rosenberg GA. Radiation-induced blood-brain barrier damage in astrocytoma: relation to elevated gelatinase B and urokinase. *J Neurooncol* 1999; **44**: 283-9.
7. Fuss M, Wenz F, Scholdei R, Essig M, Debus J, Knopp MV, et al. Radiation-induced regional cerebral blood volume (rCBV) changes in normal brain and low-grade astrocytomas: quantification and time and dose-dependent occurrence. *Int J Radiat Oncol Biol Phys* 2000; **48**: 53-8. doi: 10.1016/S0360-3016(00)00590-3
8. Jakubovic R, Sahgal A, Ruschin M, Pejovic-Milic A, Milwid R, Aviv RI. Non tumor perfusion changes following stereotactic radiosurgery to brain metastases. *Technol Cancer Res Treat* 2014. doi: 10.7785/ctrtexp.2013.600279
9. Lee MC, Cha S, Chang SM, Nelson SJ. Dynamic susceptibility contrast perfusion imaging of radiation effects in normal-appearing brain tissue: changes in the first-pass and recirculation phases. *J Magn Reson Imaging* 2005; **21**: 683-93. doi: 10.1002/jmri.20298
10. Petr J, Platzek I, Seidlitz A, Mutsaerts HJ, Hoffheinz F, Schramm G, et al. Early and late effects of radiochemotherapy on cerebral blood flow in glioblastoma patients measured with non-invasive perfusion MRI. *Radiother Oncol* 2016; **118**: 24-8. doi: 10.1016/j.radonc.2015.12.017
11. Price SJ, Jena R, Green HA, Kirkby NF, Lynch AG, Coles CE, et al. Early radiotherapy dose response and lack of hypersensitivity effect in normal brain tissue: a sequential dynamic susceptibility imaging study of cerebral perfusion. *Clin Oncol (R Coll Radiol)* 2007; **19**: 577-87. doi: 10.1016/j.clon.2007.04.010
12. Taki S, Higashi K, Oguchi M, Tamamura H, Tsuji S, Ohta K, et al. Changes in regional cerebral blood flow in irradiated regions and normal brain after stereotactic radiosurgery. *Ann Nucl Med* 2002; **16**: 273-7.
13. Weber MA, Gunther M, Lichy MP, Delorme S, Bongers A, Thilmann C, et al. Comparison of arterial spin-labeling techniques and dynamic susceptibility-weighted contrast-enhanced MRI in perfusion imaging of normal brain tissue. *Invest Radiol* 2003; **38**: 712-8. doi: 10.1097/01.rli.0000084890.57197.54
14. Wenz F, Rempp K, Hess T, Debus J, Brix G, Engenhart R, et al. Effect of radiation on blood volume in low-grade astrocytomas and normal brain tissue: quantification with dynamic susceptibility contrast MR imaging. *AJR Am J Roentgenol* 1996; **166**: 187-93. doi: 10.2214/ajr.166.1.8571873
15. Paulson ES, Schmainda KM. Comparison of dynamic susceptibility-weighted contrast-enhanced MR methods: recommendations for measuring relative cerebral blood volume in brain tumors. *Radiology* 2008; **249**: 601-13. doi: 10.1148/radiol.2492071659
16. Jafari-Khouzani K, Emblem KE, Kalpathy-Cramer J, Bjornerud A, Vangel MG, Gerstner ER, et al. Repeatability of cerebral perfusion using dynamic susceptibility contrast MRI in glioblastoma patients. *Transl Oncol* 2015; **8**: 137-46. doi: 10.1016/j.tranon.2015.03.002
17. Law M, Young RJ, Babb JS, Peccerelli N, Chheang S, Gruber ML, et al. Gliomas: predicting time to progression or survival with cerebral blood volume measurements at dynamic susceptibility-weighted contrast-enhanced perfusion MR imaging. *Radiology* 2008; **247**: 490-8. doi: 10.1148/radiol.2472070898
18. Lacerda S, Law M. Magnetic resonance perfusion and permeability imaging in brain tumors. *Neuroimaging Clin N Am* 2009; **19**: 527-57. doi: 10.1016/j.nic.2009.08.007
19. Jarnum H, Steffensen EG, Knutsson L, Frund ET, Simonsen CW, Lundbye-Christensen S, et al. Perfusion MRI of brain tumours: a comparative study of pseudo-continuous arterial spin labelling and dynamic susceptibility contrast imaging. *Neuroradiology* 2010; **52**: 307-17. doi: 10.1007/s00234-009-0616-6
20. Choi SH, Jung SC, Kim KW, Lee JY, Choi Y, Park SH, et al. Perfusion MRI as the predictive/prognostic and pharmacodynamic biomarkers in recurrent malignant glioma treated with bevacizumab: a systematic review and a time-to-event meta-analysis. *J Neurooncol* 2016; **128**: 185-94. doi: 10.1007/s11060-016-2102-4
21. Vogelbaum MA, Jost S, Aghi MK, Heimberger AB, Sampson JH, Wen PY, et al. Application of novel response/progression measures for surgically delivered therapies for gliomas: Response Assessment in Neuro-Oncology (RANO) Working Group. *Neurosurgery* 2012; **70**: 234-43; discussion 43-4. doi: 10.1227/NEU.0b013e318223f5a7
22. Tensaouti F, Khalifa J, Lusque A, Plas B, Lotterie JA, Berry I, et al. Response Assessment in Neuro-Oncology criteria, contrast enhancement and perfusion MRI for assessing progression in glioblastoma. *Neuroradiology* 2017; **59**: 1013-20. doi: 10.1007/s00234-017-1899-7
23. Bjornerud A, Emblem KE. A fully automated method for quantitative cerebral hemodynamic analysis using DSC-MRI. *J Cereb Blood Flow Metab* 2010; **30**: 1066-78. Epub 2010/01/21. doi: 10.1038/jcbfm.2010.4
24. Knutsson L, Stahlberg F, Wirestam R. Absolute quantification of perfusion using dynamic susceptibility contrast MRI: pitfalls and possibilities. *MAGMA* 2010; **23**: 1-21. doi: 10.1007/s10334-009-0190-2
25. Mouridsen K, Christensen S, Gyldensted L, Ostergaard L. Automatic selection of arterial input function using cluster analysis. *Magn Reson Med* 2006; **55**: 524-31. doi: 10.1002/mrm.20759
26. Petersen ET, Zimine I, Ho YC, Golay X. Non-invasive measurement of perfusion: a critical review of arterial spin labelling techniques. *Br J Radiol* 2006; **79**: 688-701. doi: 10.1259/bjr/67705974
27. Emblem KE, Bjornerud A. An automatic procedure for normalization of cerebral blood volume maps in dynamic susceptibility contrast-based glioma imaging. *AJNR Am J Neuroradiol* 2009; **30**: 1929-32. doi: 10.3174/ajnr.A1680
28. Stupp R, Mason WP, van den Bent MJ, Weller M, Fisher B, Taphoorn MJ, et al. Radiotherapy plus concomitant and adjuvant temozolomide for glioblastoma. *N Engl J Med* 2005; **352**: 987-96. doi: 10.1056/NEJMoa043330
29. Ostergaard L. Principles of cerebral perfusion imaging by bolus tracking. *J Magn Reson Imaging* 2005; **22**: 710-7. doi: 10.1002/jmri.20460
30. Simonsen CZ, Ostergaard L, Vestergaard-Poulsen P, Rohl L, Bjornerud A, Gyldensted C. CBF and CBV measurements by USPIO bolus tracking: reproducibility and comparison with Gd-based values. *J Magn Reson Imaging* 1999; **9**: 342-7. doi: 10.1002/(SICI)1522-2586(199902)9:2<342::AID-JMRI29>3.0.CO;2-B
31. Emblem KE, Bjornerud A, Mouridsen K, Borra RJ, Batchelor TT, Jain RK, et al. T(1)- and T(2)(*)-dominant extravasation correction in DSC-MRI: part II-predicting patient outcome after a single dose of cediranib in recurrent glioblastoma patients. *J Cereb Blood Flow Metab* 2011; **31**: 2054-64. doi: 10.1038/jcbfm.2011.39
32. Ostergaard L, Sorensen AG, Kwong KK, Weisskoff RM, Gyldensted C, Rosen BR. High resolution measurement of cerebral blood flow using intravascular tracer bolus passages. Part II: Experimental comparison and preliminary results. *Magn Reson Med* 1996; **36**: 726-36. doi: 10.1002/mrm.1910360511
33. Calamante F, Gadian DG, Connelly A. Quantification of bolus-tracking MRI: improved characterization of the tissue residue function using Tikhonov regularization. *Magn Reson Med* 2003; **50**: 1237-47. doi: 10.1002/mrm.10643
34. Boxerman JL, Schmainda KM, Weisskoff RM. Relative cerebral blood volume maps corrected for contrast agent extravasation significantly correlate with glioma tumor grade, whereas uncorrected maps do not. *AJNR Am J Neuroradiol* 2006; **27**: 859-67.
35. Emblem KE, Due-Tonnessen P, Hald JK, Bjornerud A. Automatic vessel removal in gliomas from dynamic susceptibility contrast imaging. *Magn Reson Med* 2009; **61**: 1210-7. doi: 10.1002/mrm.21944
36. Klein S, Staring M, Murphy K, Viergever MA, Pluim JP. Elastix: a toolbox for intensity-based medical image registration. *IEEE Trans Med Imaging* 2010; **29**: 196-205. doi: 10.1109/TMI.2009.2035616
37. White CM, Pope WB, Zaw T, Qiao J, Naeini KM, Lai A, et al. Regional and voxel-wise comparisons of blood flow measurements between dynamic susceptibility contrast magnetic resonance imaging (DSC-MRI) and arterial spin labeling (ASL) in brain tumors. *J Neuroimaging* 2014; **24**: 23-30. doi: 10.1111/j.1552-6569.2012.00703.x

38. Jonsson C, Pagani M, Johansson L, Thurfjell L, Jacobsson H, Larsson SA. Reproducibility and repeatability of ⁹⁹Tcm-HMPAO rCBF SPET in normal subjects at rest using brain atlas matching. *Nucl Med Commun* 2000; **21**: 9-18.
39. Li YQ, Chen P, Haimovitz-Friedman A, Reilly RM, Wong CS. Endothelial apoptosis initiates acute blood-brain barrier disruption after ionizing radiation. *Cancer Res* 2003; **63**: 5950-6.
40. Lyubimova N, Hopewell JW. Experimental evidence to support the hypothesis that damage to vascular endothelium plays the primary role in the development of late radiation-induced CNS injury. *Br J Radiol* 2004; **77**: 488-92. doi: 10.1259/bjr/15169876
41. Cao Y, Tsien CI, Shen Z, Tatro DS, Ten Haken R, Kessler ML, et al. Use of magnetic resonance imaging to assess blood-brain/blood-glioma barrier opening during conformal radiotherapy. *J Clin Oncol* 2005; **23**: 4127-36. doi: 10.1200/JCO.2005.07.144
42. Brown WR, Thore CR, Moody DM, Robbins ME, Wheeler KT. Vascular damage after fractionated whole-brain irradiation in rats. *Radiat Res* 2005; **164**: 662-8.
43. Coderre JA, Morris GM, Micca PL, Hopewell JW, Verhagen I, Kleiboer BJ, et al. Late effects of radiation on the central nervous system: role of vascular endothelial damage and glial stem cell survival. *Radiat Res* 2006; **166**: 495-503. doi: 10.1667/RR3597.1
44. Wong CS, Van der Kogel AJ. Mechanisms of radiation injury to the central nervous system: implications for neuroprotection. *Mol Interv* 2004; **4**: 273-84. doi: 10.1124/mi.4.5.7
45. Yuan H, Gaber MW, Boyd K, Wilson CM, Kiani MF, Merchant TE. Effects of fractionated radiation on the brain vasculature in a murine model: blood-brain barrier permeability, astrocyte proliferation, and ultrastructural changes. *Int J Radiat Oncol Biol Phys* 2006; **66**: 860-6. doi: 10.1016/j.ijrobp.2006.06.043
46. Prust MJ, Jafari-Khouzani K, Kalpathy-Cramer J, Polaskova P, Batchelor TT, Gerstner ER, et al. Standard chemoradiation for glioblastoma results in progressive brain volume loss. *Neurology* 2015; **85**: 683-91. doi: 10.1212/WNL.0000000000001861
47. Karunamuni RA, Moore KL, Seibert TM, Li N, White NS, Bartsch H, et al. Radiation sparing of cerebral cortex in brain tumor patients using quantitative neuroimaging. *Radiother Oncol* 2016; **118**: 29-34. doi: 10.1016/j.radonc.2016.01.003
48. Petr J, Platzek I, Hofheinz F, Mutsaerts H, Asllani I, van Osch MJP, et al. Photon vs. proton radiochemotherapy: effects on brain tissue volume and perfusion. *Radiother Oncol* 2018. doi: 10.1016/j.radonc.2017.11.033
49. Karunamuni R, Bartsch H, White NS, Moiseenko V, Carmona R, Marshall DC, et al. Dose-dependent cortical thinning after partial brain irradiation in high-grade glioma. *Int J Radiat Oncol Biol Phys* 2016; **94**: 297-304. doi: 10.1016/j.ijrobp.2015.10.026
50. Andre JB, Nagpal S, Hippe DS, Ravanpay AC, Schmiedeskamp H, Bammer R, et al. Cerebral blood flow changes in glioblastoma patients undergoing bevacizumab treatment are seen in both tumor and normal brain. [Abstract] *Neuroradiol J* 2015; **28**: 112-9. doi: 10.1177/1971400915576641
51. Mouridsen K, Emblem K, Bjørnerud A, Jennings D, Sorensen AG. Subject-specific AIF optimizes reproducibility of perfusion parameters in longitudinal DSC-MRI. *Proc Intl Soc Mag Reson Med* 2011; **19**: 376.

In silico selection approach to develop DNA aptamers for a stem-like cell subpopulation of non-small lung cancer adenocarcinoma cell line A549

Mateja Vidic^{1,2*}, Tina Smuc^{3**}, Nika Janez³, Michael Blank⁴, Tomaz Accetto⁵, Jan Mavri^{3**}, Isis C. Nascimento⁶, Arthur A. Nery⁶, Henning Ulrich⁶, Tamara T. Lah^{1,7}

¹ Department of Genetic Toxicology and Cancer Biology, National Institute of Biology, Ljubljana, Slovenia

² Jožef Stefan International Postgraduate School, Ljubljana, Slovenia

³ Centre of Excellence for Biosensors, Instrumentation and Process Control, Centre for Biotechnology, Ajdovščina, Slovenia

⁴ AptalT GmbH, Munich, Germany

⁵ Department of Animal sciences, Biotechnical Faculty, University of Ljubljana, Slovenia

⁶ Department of Biochemistry, Institute of Chemistry, University of São Paulo, Brazil

⁷ Department of Biochemistry, Faculty of Chemistry and Chemical Technology, University of Ljubljana, Slovenia

* Current address: Aptamer Group, York YO10 5NY, United Kingdom

** Current address: Lek-Sandoz Company, Ljubljana, Slovenia

Radiol Oncol 2018; 52(2): 152-159.

Received 24 November 2017

Accepted 26 February 2018

Correspondence to: Prof. Henning Ulrich, Department of Biochemistry, Institute of Chemistry, University of São Paulo, Av. Prof. Lineu Prestes 748, São Paulo, 05508-000 SP, Brazil. E-mail: henning@iq.usp.br and Prof. Tamara T. Lah, National Institute of Biology, Večna pot 111, 1000 Ljubljana, Slovenia. E-mail: Tamara.lah@nib.si

Disclosure: No potential conflicts of interest were disclosed.

Background. Detection of circulating lung cancer cells with cancer-stem like characteristics would represent an improved tool for disease prognosis. However, current antibodies based methods have some disadvantages and therefore cell SELEX (Systematic Evolution of Ligands by Exponential Enrichment) was used to develop DNA aptamers, recognizing cell surface markers of non-small lung carcinoma (NSLC) cells.

Materials and methods. The human adenocarcinoma cell line A549 was used for selection in seven cell SELEX cycles. We used human blood leukocytes for negative selection, and lung stem cell protein marker CD90 antibody binding A549 cells for positive selection.

Results. The obtained oligonucleotide sequences after the seventh SELEX cycle were subjected to *in silico* selection analysis based on three independent types of bioinformatics approaches, selecting two closely related aptamer candidates in terms of consensus sequences, structural motifs, binding affinity (Kd) and stability (ΔG). We selected and identified the aptamer A155_18 with very good binding characteristics to A459 cells, selected CD90 antibody binding. The calculated phylogenetic tree showed that aptamers A155_18 and the known A549 cell aptamer S6 have a close structural relationship. MEME sequence analysis showed that they share two unique motifs, not present in other sequences.

Conclusions. The novel aptamer A155_18 has strong binding affinity for A549 lung carcinoma cell line subpopulation that is expressing stem cell marker CD90, indicating a possible stemness, characteristic for the A459 line, or a subpopulation present within this cell line. This aptamer can be applied as diagnostic tool, identifying NSLC circulating cells.

Key words: aptamers; cell-SELEX; circulating tumour cells; non-small lung cancer; computational biology

Introduction

DNA aptamers acquire oligonucleotides' tertiary structures that allow them to bind to various target macromolecules, such as proteins, via non-covalent binding. Aptamer binding affinity to cell surface epitopes is in the range of monoclonal antibodies.^{1,2} When designed to bind to the whole cell, it is assumed that aptamers bind either to specific proteins or other complex molecular structures. The tight binding aptamers are selected by an *in vitro* selection method in a stepwise process from a starting combinatorial library of 10¹⁵ random oligonucleotides by a process called SELEX (Systematic Evolution of Ligands by Exponential Enrichment), reviewed by Šmuc and Ulrich.³ In brief, the SELEX process comprises five main steps: binding, partition, elution, amplification, and conditioning in a reiterative and stepwise manner, which is narrowed down to a homogeneous population of high-target affinity and selectivity sequences.⁴ The here used Cell-SELEX approach is a modification of the original of the original method, where a selection of aptamers binding to cell surface epitopes of target cells, i. e. tumor cells, is followed by a negative selection step against a non-target cells in order to remove any sequences, which commonly bind to epitopes, expressed by both cell types. Finally obtained aptamers shall be selective for the desired cell type.^{5,6}

Although basic mechanisms of aptamer target binding are known, theoretic prediction of individual oligonucleotide binding to cellular surfaces cannot be done. However, novel bioinformatics tools have been developed recently that can discriminate among an already selected set of aptamers with the lowest dissociation constant and the highest binding energy. In cancer, aptamers have been suggested to replace the antibodies mostly for diagnostic purposes, as they are more reliable in terms of reproducibility, stability, and costs of production⁷.

The detection of circulating tumour cells (CTC) in body fluids prior to, or at the first medical intervention, would represent a particular challenge for the prediction of disease progression⁸. The two technologies used for CTC enumeration, the Cell Search System[®] based on the detection of cancer cell membrane protein markers by antibodies⁹ and the platform ISET (Isolation by Size of Epithelial Tumour cells), based on cell size exclusion, are neither by themselves, nor used complementarily sufficient for CTC based diagnosis⁹, therefore new approaches are needed. Lung cancer incidence and

death rates are still increasing. The subgroup of NSCLC appears to have the highest incidence rates and is mostly locally advanced or metastatic at the time of diagnosis.¹⁰ Therefore we have used the cell line A549, established from the primary tumour of a NSCLC patient, to raise the aptamers. There have been several successful attempts so far to target NSCL cells in the blood circulation (lung CTC) by specific aptamers.¹¹⁻¹³ However, these did not address the potential stemness of CTC, which appeared to discriminate among cells with the highest tumorigenic potential and is thus more relevant for aggressive progression and worse prognosis of lung cancer. These lung cancer stem cells (CSC) express high levels of CD44^{high} and CD90⁺ protein.¹⁴ Furthermore, it has been shown that CD90⁺ A549 cells also express CSC markers, such as Oct4, Sox2 and some others.¹⁴ These cells had higher proliferation rates and tumorigenic capacities, and Yan *et al.* assumed that among lung cancer patients a subpopulation of lung CSC cells exists, which could be detected by specific aptamers. The aim of this study was thus the development of DNA aptamers that would also bind cancer-stem like cell surface biomarkers and would be suitable to detect stem cell-like CTC in blood circulation. The novelty in this study is a more efficient development, of aptamer binding to target cell surface based also on a *in silico* selection by novel bioinformatics tools used for the first time, and suggests their application in future aptamer identifications.

Materials and methods:

Cell culture and reagents

Human lung carcinoma cell line A549 (ATCC[®] CCL-185TM, ATCC, Manassas, VA) at passage 60 was cultured in DMEM (Millipore Sigma, Burlington, USA) supplemented with 10% foetal bovine serum until they reached about 80% confluence. Cells were washed to remove residuals of medium and then detached from the bottles with 2mM EDTA solution (Millipore Sigma, Burlington, MA). The cell line authentication was performed with IdentiCell STR allele protocol and showed a 100% match with A549 cells (IdentiCell, Department of Molecular Medicine, Aarhus, Denmark).

Cell-SELEX library design

A random library (5'-FITC- GCC TGT TGT GAG CCT CCT-N34-CGC TTA TTC TTG TCT CCC-3')

regions for the binding of primers during the PCR amplification reactions was used.¹⁵ The forward primer was 5'-BBB-GCC TGT TGT GAG CCT CCT-3', where BBB indicates 3 subsequent biotin moieties, while the reverse primer was labelled with a 6-FAM or Fluorescein Isothiocyanate (FITC-5'-GGG AGA CAA GAA TAA GCG-3'). Before the first selection cycle, the library was amplified by a PCR reaction (PCR Conditions described in Supplementary material), subjected to denaturation and the fluorescence single-stranded DNA was purified by denaturation PAGE. At the beginning of the SELEX cycle, the aptamer pool in selection buffer was denatured at 95°C for 10 min and then placed immediately on ice for 10 min followed by 20 min incubation at room temperature.

Selection of aptamers

The incubation of cells with the aptamers was followed by the BRAZIL technique with a centrifugation of a mixture of cells and oligonucleotides through a dibutyl phthalate: cyclohexane (9:1 [v:v]; d=1.03 g.ml⁻¹) layer¹⁶.

Briefly, the cells with bound aptamers were collected from the pellet of the organic phase and separated by centrifugation (13,000 g for 10 min (Hettich Universal 32R centrifuge, HETTICH Instruments LP, Beverly, MA). The pellet containing aptamers was extracted by phenol/chloroform (1:1) for purification of obtained DNA followed by PCR as detailed above and strand separation for the next cycle of SELEX. To perform selection of ligands with higher affinity, the stringency of the selection was gradually increased in each cycle by adding 0.3 – 3 mg/ml tRNA for reducing nonspecific binding and increasing the ratio of DNA molecules over cells (10⁶ – 10⁵ cells).

In the seventh cycle the first negative selection with human blood cells (erythrocytes, leukocytes, and thrombocytes in the amount of 10⁷ cells) was performed, followed by a positive selection step against 10⁵ A549 cells. Blood cells were separated from plasma by density gradient separation.¹⁷ A selection step against a CD90⁺ A549 cells was done following cell sorting purification of this subpopulation.

Flow cytometry analysis of aptamer binding to A549 cells

These assays were performed with live A549 cells, which not been treated with fixation agents according to Nascimento *et al.* (2016).¹⁸ Pools were incu-

bated in binding buffer (1.25mM HEPES, 0.27mM KCl, 0.14mM CaCl₂, 0.06mM MgCl₂, 7.19mM NaCl, 0.9% glucose) for 10 min at 95°C and then immediately placed on ice for 10 min and maintained for 20 min at room temperature. For the interaction between single-stranded DNA molecules and cells, the solution containing the aptamers was gently mixed with cells (10⁶ cells /microtube) to a final volume of 100 µl and 200 pM concentration of aptamers. The mixture was incubated for 30 min at room temperature with gentle shaking. The mixture was centrifuged at 200 X g and the supernatant was discarded. A wash was performed with binding buffer, the mixture was again centrifuged and the supernatant discarded. Then 500 µl of binding buffer was added, followed by flow cytometry analysis. For analysis of double-labelled cells, the anti-CD90 antibody (1: 1,000) was added to the cells along with the oligonucleotide pools. For cell sorting the same procedure was followed, and a gate was determined to collect the double-labelled cells for CD90 expression and aptamer oligonucleotides.

The pool from the seventh cycle contained aptamers with enhanced binding to the subpopulation of A549 cells, expressing CD90, as was detected by increased fluorescence signals. Since the identified subpopulation demonstrated stem-like cells characteristics¹³, cell sorting was used to isolate the identified fraction of cells. A fraction of 2,500 cells was successfully collected and aptamers were purified for PCR amplification (data not shown).

Sequencing

Selection pool aptamers obtained in each cycle were tested with restriction analysis (RFLP – Restriction Fragment Length Polymorphism) for the presence of conserved restriction sites. Different bands were obtained representing fragments of DNA with conserved restriction sites, thus showing selective enrichment of specific groups of oligonucleotides during SELEX (Suppl. Figure S1).

The sequences from last three cycles were used for Sanger and Next generation sequencing (Supplementary material). Selected sequences were further analysed with different bioinformatics approaches.

Bioinformatics analysis

Three different *in silico* selection procedures were used for processing the selected sequences: CLC Genomics Workbench software, Shell script in

combination with pipelined use programs for processing nucleotide sequences- MEME¹⁹, MEGA6²⁰ and UnaFold²¹ and COMPAS software (AptaIT GbmH, Planegg, Germany).²²

We have compared molecular evolutionary relations (with MEGA6 program²⁰) and motif similarity (with MEME suite¹⁹) of chosen four best binding candidates (A155_18, A452_3, A373_4, A218_12) and already published aptamer S6 binding to A549 cells (5'-GTG GCC AGT CAC TCA ATT GGG TGT AGG GGT GGG GAT TGT GGG TTG-3').¹¹

Validation of selected candidates *in vitro*

Preparation of aptamers: Aptamers were dissolved at 0.5 μ M final concentration in binding buffer, containing 25mM HEPES (Millipore Sigma) 5.4 mM KCl, 2.8 mM CaCl₂, 3.2 mM MgCl₂ and 144 mM NaCl in ddH₂O and denaturated at 95°C and renatured at room temperature, each for 20 min. Further, the cells were incubated for 20 min at 25°C with 0.5 μ M 6-Carboxyfluorescein (6-FAM) labelled aptamer solution in 200 μ l of binding buffer with gentle agitation. Then the cells were washed twice with binding buffer before flow cytometry analysis of A459 cell-aptamer bindings. For determination of unspecific binding, we used a 6'-FAM oligonucleotide with a random region of 34 nucleotides. To determine whether binding between aptamer and the target cells would depend on temperature, binding assays were also carried out at 4°C and 37°C.

CD90 antibody binding to A549 cells: To determine CD90 protein expression in A549 cells, they were incubated with the anti-CD90/Thy1 antibody (PE/Cy5) (ab95698) and for negative control assays with Isotype Control Mouse IgG1, Kappa monoclonal (PE/Cy5) (ab67435) obtained from AbCam (Cambridge, UK). The cells were detached by 0.02% EDTA and filtered through a 70 μ m sieve to avoid doublets. Cells – 300,000 per assay were washed three times with ice cold phosphate-buffered saline (PBS) and incubated for 30 min at 4°C and then re-suspended in 500 μ l ice cold PBS before flow cytometry analysis.

Preparation of blood cells for negative control: As the aim of aptamer developments was to detect NSCLC cells in the blood as CTC, the blood cells were isolated from a healthy donor (male, 40 years) lysed with buffer, containing 150 mM NH₄Cl, 10mM NaHCO₃ and 0.1mM EDTA and centrifuged at 300 \times g for 5 min at room temperature. The blood cells were re-suspended in binding buffer and used as binding target for the negative selection step with previous-

ly eluted SELEX pool DNA to separate aptamers with affinity to the tumour cell target and to discard sequences also binding to control blood cells. The remaining target cell specific sequences were further PCR amplified to form the starting pool for the final round of positive selection.

Flow cytometry: We measured 30,000 events per sample using the flow cytometry device MACSQuant Analyser 10 (Miltenyi Biotec GmbH, Bergisch Gladbach, Germany) or the Attune flow cytometer (Thermo Fisher Scientific Inc., Waltham, MA). For setting the gates we used unlabelled A459 cells.

To determine the equilibrium dissociation constants (K_d) of aptamer binding to A549 cells, mean fluorescence emissions were calculated for each of seven different concentrations (50, 100, 300, 500, 800, 1,000 and 1,200 nM). The dissociation constants were calculated using one-site non-competitive binding; nonlinear curve regression was performed using GraphPad Prism 5 (GraphPad Software, Inc., San Diego, CA). Cell sorting was performed on the FACSARIA I/II equipment (Becton & Dickinson, Franklin Lakes, NJ).

Results

Preparation of aptamer pool for A549 cell line by cell-SELEX

Here we aimed to develop aptamer probes targeting NSCLC circulating tumour cells due to their potential diagnostic, prognostic and predictive capacity. For the development of NSCLC specific aptamers, we have chosen the most commonly used human lung adenocarcinoma A549 cells as target for cell-SELEX. Human blood cells were adopted as a negative control for cell SELEX to increase the selectivity of generated aptamers to A459 cells.

In the selection process, the cultured A549 cells were first incubated with a 70-base synthetic single stranded DNA library. The DNA sequences that bound to the A549 cells were then eluted and separated with the BRAZIL technique, as described in Material and Methods.

We have compared aptamer pools from the original library, the sixth cycle and the negative selection. Regarding the percentage of labelled cells for each pool, no significant difference was observed. We observed that the population of cells that were positive for the aptamer pool from negative selection had higher fluorescence, as shown by the shift to the right in the density plot and the overlap of the histograms (Figure 1A). Furthermore, we per-

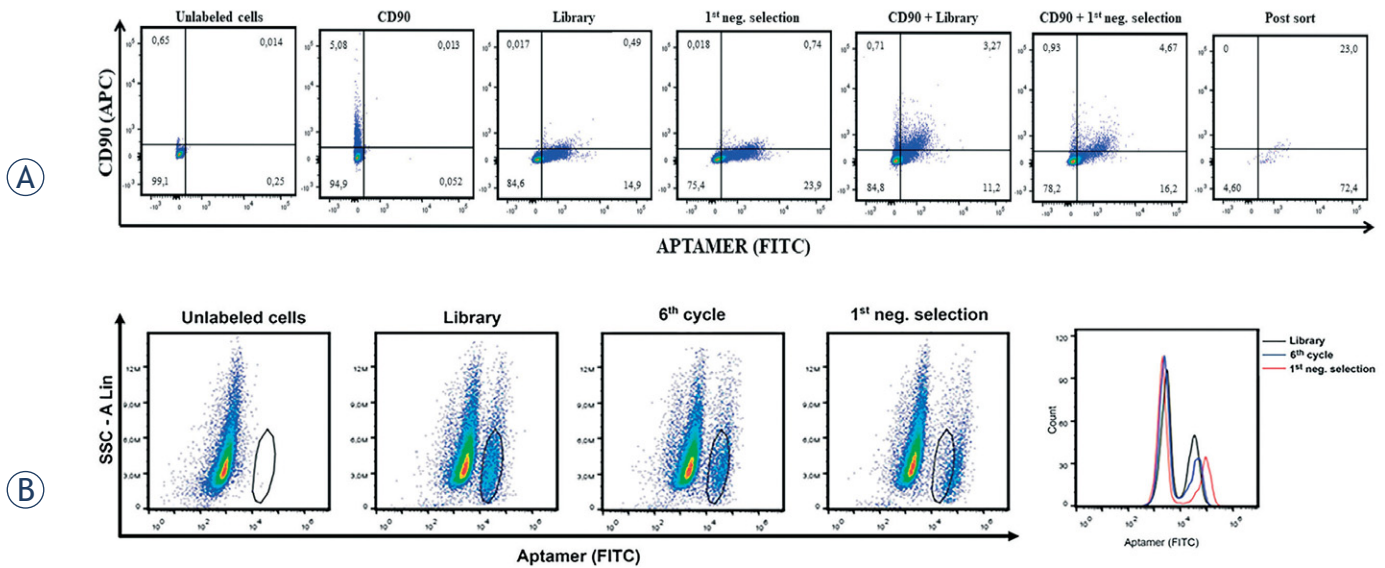


FIGURE 1. Flow cytometry of cells double labelled with CD90 and aptamers. **(A)** Flow cytometry was performed for FITC-labelled aptamer pools (comparing binding to A549 cell binding of the pool of the library), the sixth cycle and the pool following negative selection against blood cells. The density plots are showing that there was no difference in the percentage of labelled cells for each of the pools. Displacement of the population in the density plot, and shift of position on the histograms for the cells labelled with the pool, which followed the negative selection against blood cells, was observed, showing a cell population with increased fluorescence intensity compared to the cells labelled with the initial library or pool of 6th cycle. **(B)** CD90 binding and cell sorting: After adjustment of cellular gates for un-labelled cells, CD90+, the library and the pool following negative selection, the double-labelled cells labelled for CD90/library and CD90/negative selection pool were compared. Here, the gate was set to collect the most intensely labelled cells with the aptamer pool following negative selection. To confirm the profile of the isolated population, the sorted cells were analysed again by flow cytometry (post sort). The density plots show the presence of a well-defined secondary population that was double labelled, suggesting that aptamers were recognizing a sub-population of CD90, which was positive for stem cells within the A549 cell population.

formed flow cytometry using antibody for CD90 detection in A549 cells and we observed a well-defined population that was positive for CD90 and aptamers (Figure 1A). This population of cells was sorted out and bound aptamers were eluted and amplified by PCR. Figure 1B reports the increase in cell labelling of the sixth selection pool following a negative selection against blood cells.

The obtained aptamer pool after the negative selection against blood cells and sorting out aptamers binding to the CD90⁺ subpopulation was used for further sequencing in order for identification aptamer candidates with conserved structural motifs.

Bioinformatics analysis

The sequencing of the seventh cycle pool by Ion Torrent PGM next generation sequencing technology resulted in 239,713 reads, from which 151,814 reads were unique. *In silico* selection of aptamers from the NGS data was accomplished using three different procedures as described in Supplementary material (Table S1).

Using CLC Genomics Workbench software, the starting pool of 239,713 reads was narrowed down

to 16 representative sequences having the highest number of sequence members, ranging from 1 080 to 142 copies per representative sequence. They were subjected to further selection based on the presence of conserved sequence motifs. Aptamers A786_1, A574_2, A278_8 were selected for *in vitro* validation, each carrying a unique motif.

In the second *in silico* aptamer selection, using online available nucleotide sequence processing programs, reads having ambiguous bases or incorrect or no sequence of the library primers were first filtered out. In the remaining high quality sequence set 80,312 reads were unique and 81.7% of the reads appeared in the set only once (no copies). Twenty sequences with the highest numbers of copies (reads), ranging from 786 to 138 copies, were ranked with regard to stability of the computed folding, using ΔG (kcal/mol) as a measure of stability, and the stability of putative loop in the three most stable computed foldings as given by the UnaFold tool. Aptamers A155_18, A452_3, A373_4, A218_12 were selected for *in vitro* validation.

In the third *in silico* selection procedure, that was executed using COMPASS software, the reads

were first clustered in 998 families with defining patterns in the loop space region. Each family was represented by a sequence (one with the highest number of repetitions) and we selected the 21 most frequent among them for further analysis. Grouping families into respective clans was depended on loop space similarity - 12 of the 21 most frequent families were positioned in 10 different family clans. Further scoring for structure stability was applied in terms of melting temperature in addition to pattern ranking and similar to the second selection procedure aptamer sequences, A155_18 and A452_3 were again selected as the best binding candidates.

The selected aptamer candidates were additionally compared with aptamer S6. The constructed dendrogram (Supplementary material, Figure S1) shows clusters of aptamer sequence candidates, where aptamer A155_18 and positive control S6 clustered together. Among the selected aptamer candidates, A155_18 and S6 are also the only two sharing two same motifs: GGTGG/CG and GCCAGT; according to the Unafold-predicted secondary structure, the motifs are placed into the comparable structural sequences between the loops (Supplementary material). The possibility of cross-contamination was excluded as the seventh SELEX pool was sequenced before the positive control S6 was purchased.

In vitro validation of selected candidates

The selected and fluorescence-labelled four candidates, A155_18, A452_3, A373_4, A218_12, together with known binder S6 and the negative control sequence (the sequence with an unknown random region with the length of 34 nucleotides, and flanked by known primers) were used in an *in vitro* binding test to determine the binding characteristics. Binding to A549 cells was demonstrated with flow cytometry analysis. All four selected aptamers (Figure 1A) showed enhanced binding to target the cell line versus the unselected control (CTRL_N34.012), according to the percentage of fluorescently labelled cells as measured by flow cytometry. Kd values of all four selected aptamers are in nanomolar range (Figure 2).

In comparison with control random aptamer, highest specific binding rates of 26% to A549 cells was obtained with A155_18. Flexible binding of aptamers at different temperatures can expand their repertoire of applications. Since the selection was performed at room temperature (25°C), we performed binding assays also at 4°C and 37°C. There


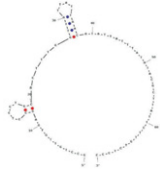
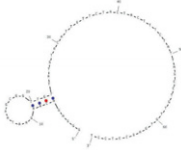

NAME	PREDICTED SECONDARY STRUCTURE	ΔG	Kd (nM)
A155_18		-5.15	160.8 ± 92.69
A452_3		-2.5	129.7 ± 81.18
A373_4		-0.36	18.65 ± 49.51
A218_12		-6.8	134 ± 123.3

FIGURE 2. Predicted secondary structures of four aptamer candidates selected for *in vitro* experiments. The secondary structures of sequences were enabling formation of complementary wrapping around their target. The unpaired bases were responsible for binding events where Watson-Crick paired bases were giving the aptamer stability. Predicted secondary structures were calculated with Unafold, the presented are the ones with lowest ΔG , i.e. the highest stability (energy rules: DNA, temperature 24°C, 14.4 mM NaCl, 3.2 mM MgCl). Equilibrium dissociation constants Kd (nM) were calculated using GraphPad Prism 5, under the non-linear fit model, one-site non-competitive binding to fluorescent population ratio at used aptamer concentrations. See the Supplementary Materials for further details.

was observed no difference in binding of aptamer A155_18 (data not shown). This is particularly important as the clinical application of aptamers will be carried out under physiological conditions.

During the cell selection aptamers are interacting specifically with the outer plasma cell membranes of targeted cells. In our cell-SELEX selection the targeted cell line A549 was enriched by the expression of the stemness marker, the membrane-bound protein CD90. This subpopulation was selected by flow sorting against CD90 in A549 cell population. The latter indicates aptamer ability of recognizing CD90-positive cells, which may be part of the tumor-initiating circulating cells.

Discussion

Cancer treatment is based on surrogate markers reflecting tumour progression and, after medical intervention, also the response to therapy. Another problem that hinders the development of new therapeutic approaches for lung cancer patients relates to the sampling of the representative (lung) tumour specimens.^{22,23,24} Circulating tumour cells (CTC) are promising as they provide an easily accessible liquid biopsy sample for real-time detection of the presence of micro-metastases. Besides their enumeration and characterization, CTC analysis offers the opportunity of mechanistic studies of malignant cancer progression⁷. It has only recently been recognized that cancer stem cells (CSC), residing in peri-arteriolar niches, undergo epithelial-mesenchymal like transition, and from there invade vascular basement membrane entering blood circulation and become CTC. In addition, a large body of evidence has accumulated on the plasticity of CSCs and the intra-tumour heterogeneity, due mainly to the presence of CSC of different subtypes and degrees of differentiation. It would thus be a nearly impossible task to target all these sub-clones by a single event. Thus, the aptamers that we developed here as biomarkers of NSCLC CTC would recognize at least one NSCLC stem cell marker, and we have succeeded in designing an aptamer recognizing a subpopulation of A549 NSCLC, expressing the CD90/Thy-1 CSC marker¹³. Indeed, following the last cycle of SELEX and sorting for CD90 positive cells, we have shown about 30 % cells are positive for this marker among the A549 cell population.

All previous aptamers developed to target NSCLC have been selected on the basis of the cell-SELEX procedure, starting with a single-stranded DNA library and proceeding with 25, 18, and 11 rounds by Zhao *et al.*, Jimenez *et al.* and Zamay *et al.*¹⁰⁻¹², respectively. All selected aptamers bind to their targets in the nanomolar range of Kd. The sequences selected by Zhao *et al.*¹⁰, the S1, S6, S11e and S15 aptamers, all had the ability to bind to A549 cells and to differentiate between normal and carcinoma lung cells. After pre-treating target cells with trypsin, the binding of selected aptamer vanished, strongly indicating that the target molecules of those aptamers were or were strongly associated with membrane proteins; however, we have not analysed them further. The target for selection used by Jimenez *et al.*¹¹ was the adenocarcinoma cell line H23, although their best binders (aptamers EJ4 and ADE1) have also shown good binding

potential for the cell line A549. However, they were not lung cancer selective, as they also recognised the colon adenocarcinoma cell line TOV21G. As possible reason for that, those aptamers recognised a more general human carcinoma cell-surface marker, of the tested cell lines were all of epithelial origin. Zamay *et al.*¹² selected DNA aptamers for lung adenocarcinoma cells derived from postoperative tissues without prior knowledge of protein biomarkers, stating that aptamers specific to the surface protein of cultured cells may not bind to tumour cells in clinical samples because of the difference in the protein expression between cultured and primary tumour cells. For cell-SELEX, these authors have used the postoperative tissue samples and have shown that the selected aptamers did not bind to healthy lung cells and the A549 lung adenocarcinoma cell line. After successful selection, they have recognized eight candidate biomarkers associated with four selected aptamers.

We have chosen the published aptamer S6, specific for A549 cells binding with low Kd value, as the positive binding control¹¹, having high selectivity for NSCLC with no binding potential against SCLC and squamous cell carcinoma cells. Its structure is similar to our selected aptamer, with 45 nucleotides in a random region, flanked by 20 nucleotide-long constant regions on both sites. As expected, aptamer S6 showed good binding potential for A549 cells also when using our protocol. The aptamer S6 was selected after 25 rounds, whereas in our SELEX procedure only seven rounds were needed. Therefore, we improved the selection process by reducing the number of selection rounds, using the bioinformatics approach. The aptamer S6 was used as a control, not only with respect to the nucleotide sequence, but also the structural motifs present, as these are crucial for binding to the selected target cell.

The *in silico* selection of aptamers was carried out after the seventh SELEX cycle, including negative selection against blood cells and yielded a satisfactory quality of sequencing reads. We were able to filter out several high-quality reads using different filters, from length to the base composition (ambiguous bases and library primers). We expected a high variability of unique sequences as there are lot of different epitopes (proteins, glycoproteins, etc.) on the A549 cells that could be potentially recognized by aptamers. The low copy number of the most abundant reads was unexpected, as for example in another cell-SELEX development, using complex bacterial spores, as SELEX targets, we obtained 10 times more copies (COBIK, un-

published). Based on the criteria used to select aptamer candidates, we suggest that physicochemical properties of computed folding (ΔG , T_m , composition of bases in the loop) are a suitable criterion to evaluate oligonucleotides obtained by only a few rounds of SELEX.

In conclusion, we have selected the aptamer A155_18, binding to a A549 lung adenocarcinoma cell line subpopulation, expressing stemness markers, such as CD90. This aptamer sequence, with two very similar motifs indicating overlapping activity with the positive control (aptamer S6), provides the proof of principle of novel approaches. Methodologically, we highly improved the reproducibility of cell-SELEX methodology when paired with bioinformatics tools. We have also shown that the use of bioinformatics reduced the number of selection cycles, thus indicating the great potential of computational biology.

Acknowledgements

We acknowledge Prof. Dr. Tanja Čufer, Dr. Ana Koren and Prof. Dr. Peter Korošec, the University Clinic of Pulmonary and Allergic Diseases Golnik, Slovenia for valuable discussions. This work was supported the Slovenian Research Agency (Program P1-0245 to TLT and the young researches fellowship to MV) and by a collaborative grant from the National Council for Scientific and Technological Development (CNPq), Brazil / Ministry of Higher Education, Science and Technology (MHEST), Slovenia, Project No. 490536/2011-5 awarded to H.U. and T.S. as well as by a grant from the São Paulo Research Foundation FAPESP (Project No. 2012/50880-4), Brazil, awarded to H.U. I.C.N. acknowledges a postdoctoral fellowship from FAPESP (Project No. 2015/18730-0). A.A.N.'s Ph.D. thesis was supported by a fellowship by FAPESP.

References

- Shigdar S, Luczo J, Wei MQ, Bell R, Danks A, Liu K, et al. Aptamer therapeutics: the 21st century's magic bullet of nanomedicine. *Open Conf Proc J* 2010; **1**: 118-24. doi: 10.2174/2210289201001001001118
- Baird GS. Where are all the aptamers? *Am J Clin Pathol* 2010; **134**: 529-31. doi: 10.1309/AJCPFU4CG2WGJJKS
- Šmuc T, Ahn IY, Ulrich H. Nucleic acid aptamers as high affinity ligands in biotechnology and biosensors. *J Pharm Biomed Anal* 2013; **81-82**: 210-7. doi: 10.1016/j.jpba.2013.03.014
- Zhou J, Rossi JJ. Cell-specific aptamer-mediated targeted drug delivery. *Oligonucleotides* 2011; **21**: 1-10. doi: 10.1089/oli.2010.0264
- Ulrich H, Wrenger C. Disease-specific biomarker discovery by aptamers. *Cytometry A* 2009; **75**: 727-33. doi: 10.1002/cyto.a.20766
- Nery AA, Wrenger C, Ulrich H. Recognition of biomarkers and cell-specific molecular signatures: aptamers as capture agents. *J Sep Sci* 2009; **32**: 1523-30. doi:10.1002/jssc.200800695
- Ni S, Yao H, Wang L, Lu J, Jiang F, Lu A, et al. Chemical modifications of nucleic acid aptamers for therapeutic purposes. *Int J Mol Sci* 2017; pii: **E1683**. doi: 10.3390/ijms18081683.
- Ulrich H, Tárnok A. Flow cytometry detection of circulating tumor cells: achievements and limitations as prognostic parameters. *Cytometry A* 2014; **85**: 201-2. doi: 10.1002/cyto.a.22441
- Krebs MG, Hou J-M, Sloane R, Lancashire L, Priest L, Nonaka D, et al. Analysis of circulating tumor cells in patients with non-small cell lung cancer using epithelial marker-dependent and -independent approaches. *J Thorac Oncol* [Internet]. 2012; **7**: 306-15.
- Zhao Z, Xu L, Shi X, Tan W, Shangguan D. Recognition of subtype non-small cell lung cancer by DNA aptamers selected from living cells. *Analyst* 2009; **134**: 1808-14. doi: 10.1039/B904476K
- Jimenez E, Sefah K, Lopez-Colon D, Van Simaey D, Chen HWI, Tockman MS, et al. Generation of lung adenocarcinoma DNA aptamers for cancer studies. *PLoS One* 2012; **7**: 1-7. doi: 10.1371/journal.pone.0046222
- Zamay GS, Kolovskaya OS, Zamay TN, Glazyrin YE, Krat AV, Zubkova O, et al. Aptamers selected to postoperative lung adenocarcinoma detect circulating tumor cells in human blood. *Mol Ther* 2015; **23**: 1486-96. doi: 10.1038/mt.2015.108
- Wang P, Gao Q, Suo Z, Munthe E, Solberg S, Ma L, et al. Identification and characterization of cells with cancer stem cell properties in human primary lung cancer cell lines. *PLoS One* 2013; **8**: e57020. doi: 10.1371/journal.pone.0057020
- Yan X, Luo H, Zhou X, Zhu B, Wang Y, Bian X. Identification of CD90 as a marker for lung cancer stem cells in A549 and H446 cell lines. *Oncol Rep* 2013; **30**: 2733-40. doi: 10.3892/or.2013.2784
- Daniels DA, Chen H, Hicke BJ, Swiderek KM, Gold L. A tenascin-C aptamer identified by tumor cell SELEX: systematic evolution of ligands by exponential enrichment. *Proc Natl Acad Sci U S A*; **100**: 15416-21. doi: 10.1073/pnas.2136683100
- Giordano RJ, Cardó-Vila M, Lahdenranta J, Pasqualini R, Arap W. Biopanning and rapid analysis of selective interactive ligands. *Nat Med* 2001; **7**: 1249-53. doi: 10.1038/nm1101-1249
- Telez A, Rubinstein P. Rapid method for separation of blood cells. *Transfusion* 1970; **10**: 223-5. doi: 10.1111/j.1537-2995.1970.tb00733
- Nascimento IC, Nery AA, Bassaneze V, Krieger JE, Ulrich H. Applications of aptamers in flow and imaging cytometry. *Methods Mol Biol* 2016; **1380**: 127-34. doi: 10.1007/978-1-4939-3197-2_10
- Bailey TL, Johnson J, Grant CE, Noble WS. The MEME suite. *Nucleic Acids Res* 2015; **43**: W39-49. doi: 10.1093/nar/gkv416
- Tamura K, Stecher G, Peterson D, Filipksi A, Kumar S. MEGA6: Molecular evolutionary genetics analysis version 6.0. *Mol Biol Evol* 2013; **30**: 2725-9. doi: 10.1093/molbev/mst197
- Markham NR, Zuker M. UNAFold: Software for nucleic acid folding and hybridization. *Methods Mol Biol* 2008; **453**: 3-31. doi: 10.1007/978-1-60327-429-6_1
- Kinghorn AB, Fraser LA, Tanner JA. Aptamer bioinformatics. *Int J Mol Sci* 2017; pii: **E2561**. doi: 10.3390/ijms18122516
- Berghmans T, Pasleau F, Paesmans M, Bonduelle Y, Cadranet J, Toth IC, et al. Surrogate markers predicting overall survival for lung cancer: ELCWP recommendations. *Eur Respir J* 2012; **39**: 9-28. doi: 10.1183/09031936.00190310
- Eberhard DA, Giaccone G, Johnson BE. Biomarkers of response to epidermal growth factor receptor inhibitors in non-small-cell lung cancer working group: standardization for use in the clinical trial setting. *J Clin Oncol* 2008; **26**: 983-94. doi: 10.1200/JCO.2007.12.9858

Matrix metalloproteinases polymorphisms as baseline risk predictors in malignant pleural mesothelioma

Danijela Strbac¹, Katja Goricar², Vita Dolzan², Viljem Kovac¹

¹ Institute of Oncology Ljubljana, Ljubljana, Slovenia

² Pharmacogenetics Laboratory, Institute of Biochemistry, Faculty of Medicine, University of Ljubljana, Ljubljana, Slovenia

Radiol Oncol 2018; 52(2): 160-166.

Received: 10 December 2017

Accepted: 17 December 2017

Correspondence to: Assist. Prof. Viljem Kovač, M.D., Ph.D., Institute of Oncology Ljubljana, Zaloška 2, SI-1000 Ljubljana, Slovenia. Phone: +386 1 5879 117; Fax: +386 1 5879 400; E-mail: vkovac@onko-i.si

Disclosure: No potential conflicts of interest were disclosed

Background. Malignant mesothelioma (MM) is a rare disease, linked to asbestos exposure in more than 80% of the cases. Matrix metalloproteinases (MMPs) have been identified as modulators of the tumour microenvironment and carcinogenesis. Polymorphisms of selected MMPs have been studied as potential biomarkers of time to progression (TTP) and overall survival (OS) in MM. The aim of our study was to investigate selected MMP polymorphisms as baseline risk predictors in MM development in combination with other well known risk factors, such as asbestos exposure.

Patients and methods. The study included 236 patients and 161 healthy blood donors as the control group. Ten different polymorphisms in three MMP genes were genotyped using a fluorescence-based competitive allele-specific assay (KASPar): MMP2 rs243865, rs243849 and rs7201, MMP9 rs17576, rs17577, rs2250889 and rs20544, and MMP14 rs1042703, rs1042704 and rs743257. In statistical analyses continuous variables were described using median and range (25%–75%), while frequencies were used to describe categorical variables. Deviation from the Hardy-Weinberg equilibrium (HWE) was assessed using the standard chi-square test. The additive and dominant genetic models were used in statistical analyses. The association of genetic polymorphism with MM risk were examined by logistic regression to calculate odds ratios (ORs) and their 95% confidence intervals (CIs).

Results. Carriers of at least one polymorphic MMP2 rs243865 allele tended to have a decreased risk for MM (OR = 0.66, 95% CI = 0.44–1.00; P = 0.050). The association was more pronounced in patients with known asbestos exposure: carriers of at least one polymorphic allele had significantly lower MM risk (OR = 0.55, 95% CI = 0.35–0.86; P = 0.009). None of the other tested polymorphisms showed association with the risk of malignant pleural mesothelioma.

Conclusions. The MMP2 rs243865 polymorphism may have a protective role in malignant pleural mesothelioma development. This finding is even more evident in patients exposed to asbestos, implying a strong gene-environment interaction.

Key words: matrix metalloproteinases; genetic polymorphism; malignant mesothelioma

Introduction

Malignant mesothelioma (MM) is a rare disease, linked to asbestos exposure in more than 80% of the cases. The latency period can last up to thirty years and estimated median survival is 9–12 months. The worldwide incidence of mesothelioma is slowly rising, with approximately 94 000

new cases per year. The most affected areas are parts of Europe, Australia and the USA.¹ The rise in the MM incidence has been noticed in the Slovene population as well. The Slovenian national registry follows the data on MM since 1961. The incidence in 2014 was 37 new cases per year in a population of approximately 2 million.²

Several preclinical studies have identified matrix metalloproteinases (MMPs) as modulators of the tumour microenvironment and having an important role in carcinogenesis.³ MMPs are calcium-dependent, zinc-containing endopeptidases, with three common domains containing the propeptide, catalytic and haemopexin-like C-terminal domain.⁴ They are involved in tissue remodelling by interfering with the cell-cell and cell-extracellular matrix interactions. Studies have shown that MMPs, particularly MMP-2 and MMP-9, play a role in tumour angiogenesis, invasion and metastasis.⁵ The studies performed thus far show that MMPs and their inhibitory molecules, tissue inhibitors of metalloproteinases (TIMPs), have an important role in proliferation and progression of MM and some other, more frequent malignancies, such as colon and breast cancer. Different MMP genes (*MMP2*, *MMP9*, *MMP11*, *MMP14*) and their expression were studied in mesothelioma tissue as potential prognostic markers.⁶ In a previous paper we studied the possible role of single nucleotide polymorphisms (SNPs) as potential markers of treatment response.⁷ We identified *MMP9* rs2250889, *MMP9* rs20544, *MMP14* rs1042703 as statistically significantly associated with overall survival (OS) in MM. Carriers of the polymorphic *MMP9* rs2250889 and *MMP14* rs1042703 alleles had shorter OS, compared to non-carriers, while carriers of polymorphic *MMP9* rs20544 allele had longer OS.⁷

Many studies investigated the role of *MMP* polymorphisms in the baseline genetic risk for common diseases and tumours, however, the role of *MMP* polymorphisms was found to be conflicting in different diseases. In a large nested case-control study investigating skin cancer risk, *MMP9* Arg668Gln polymorphism has been associated with a decreased risk of squamous cell skin cancer (SCC).⁸

The opposite effect was observed in T-cell acute lymphoblastic leukaemia (T-ALL), where *MMP2* rs243865 and *MMP9* rs3918242 polymorphisms were associated with an increased risk of T-ALL.⁹

The data from the literature, linking *MMP* polymorphisms with tumour risk and the statistically significant associations between the selected *MMP2*, *MMP9* and *MMP14* SNPs and time to progression (TTP) and OS in MM, led us to further investigate their potential role in baseline genetic risk of MM development. Our aim was to investigate selected *MMP* polymorphisms as baseline risk predictors in MM development in combination with other well known risk factors, such as asbestos exposure.

Patients and methods

Patients

Patients with histologically confirmed pleural or peritoneal mesothelioma diagnosed and treated between 2007 and 2016 were included in this retrospective study. Patients were diagnosed mostly at the University Clinic Golnik and at the Department of Thoracic Surgery of the University Medical Centre Ljubljana. Patients were treated and followed-up at the Institute of Oncology Ljubljana, Slovenia.

Most patients included in the study were also participating in previous studies on pharmacogenomics of MM treatment, conducted at the Institute of Oncology Ljubljana, Slovenia. Some of the patients were also included in the clinical trial AGILI (Trial registration ID: NCT01281800).¹⁰

Clinical characteristics at diagnosis were obtained from medical records or assessed during clinical interview. Regarding asbestos exposure, patients were divided in two groups: patients with no known asbestos exposure and patients with known occupational or environmental exposure.

The control group consisted of 161 unrelated healthy Slovenian blood donors, aged 49 to 65.

The study was approved by the Slovenian National Medical Ethics Committee and was carried out according to the Declaration of Helsinki.

DNA extraction and genotyping

Genomic DNA was extracted from frozen whole-blood samples collected at the inclusion in any of the above mentioned studies using the Qiagen FlexiGene Kit (Qiagen, Hilden, Germany) in accordance with the manufacturer's instructions.

Ten different polymorphisms in three *MMP* genes were genotyped: *MMP2* rs243865, rs243849 and rs7201, *MMP9* rs17576, rs17577, rs2250889 and rs20544, and *MMP14* rs1042703, rs1042704 and rs743257. Predicted function of these polymorphisms was assessed using SNP Function Prediction tools.¹¹

The genotyping of all the SNPs was carried out using a fluorescence-based competitive allele-specific assay (KASPar), according to the manufacturer's instructions (LGC Genomics, UK).

For all investigated polymorphisms, 15% of samples were genotyped in duplicates. Genotyping quality control criteria included 100% duplicate call rate and 90% SNP-wise call rate.

TABLE 1. Patients' characteristics (N = 236)

Characteristic		N (%)
Gender	Male	174 (73.7)
	Female	62 (26.3)
Age	Median (25%-75%)	66 (58-72)
Stage	I	18 (7.6)
	II	60 (25.4)
	III	70 (29.7)
	IV	67 (28.4)
	Peritoneal	20 (8.5)
	Not determined	1 (0.4)
Histological type	Epithelioid	169 (71.6)
	Biphasic	27 (11.4)
	Sarcomatoid	26 (11.0)
	Not characterized	14 (5.9)
ECOG performance status	0	15 (6.4)
	1	114 (48.3)
	2	92 (39.0)
	3	15 (6.4)
Metastases	No	206 (87.3)
	Yes	30 (12.7)
Asbestos exposure	Not exposed	61 (26.5) [6]
	Exposed	169 (73.5)
Smoking	No	123 (57.7)
	Yes	106 (46.3)

Numbers in square brackets denote the number of patients with missing data.
ECOG = Eastern Cooperative Oncology Group

TABLE 2. Variant allele characteristics, frequencies and agreement with HWE

Gene	SNP	SNP characteristics	Variant allele frequency	P _{HWE}
MMP2	rs243865	c.-1306C>T	0.24	0.165
	rs243849	c.999C>T, p.Asp333=	0.14	0.798
	rs7201	c.*260A>C	0.41	0.441
MMP9	rs17576	c.836A>G, p.Gln279Arg	0.36	0.785
	rs2250889	c.836A>G, p.Gln279Arg	0.05	0.535
	rs17577	c.2003G>A, p.Arg668Gln	0.15	0.096
	rs20544	c.*3C>T	0.44	0.445
MMP14	rs1042703	c.22T>C, p.Pro8Ser	0.26	0.164
	rs1042704	c.817G>A, p.Asp273Asn	0.20	0.830
	rs743257	c.*83C>T	0.50	0.519

HWE = Hardy-Weinberg equilibrium; SNP = single nucleotide polymorphism

Statistical analyses

Continuous and categorical variables were described using median and range (25%-75%) and frequencies, respectively. Deviation from the Hardy-Weinberg equilibrium (HWE) was assessed using the standard chi-square test. The additive and dominant genetic models were used in statistical analyses. The associations of genetic polymorphisms with MM risk were examined by logistic regression to calculate odds ratios (ORs) and their 95% confidence intervals (CIs).

All statistical analyses were carried out by IBM SPSS Statistics, version 21.0 (IBM Corporation, Armonk, NY, USA). Haplotypes were reconstructed and analysed using Thesias software, version 3.1. The most frequent haplotype was used as the reference. All statistical tests were two sided and the level of significance was set to $P = 0.05$. Due to the exploratory nature of the study, no adjustments for multiple comparisons were used.

Results

Patient characteristics

In total, we included 236 patients with MM and 161 healthy blood donors as a control group. Clinical characteristics of patients are summarized in Table 1. Among controls, 125 (77.6%) were male and 36 (22.4%) were female. Median age was 55 (52–58.5) years. There were no significant differences between cases and controls regarding gender ($P = 0.375$), however, controls were significantly younger than MM patients ($P < 0.001$).

Genotyping analysis

Variant allele frequencies for investigated SNPs are presented in Table 2. The distributions of all the investigated SNPs in the control group were in agreement with the Hardy-Weinberg equilibrium.

Duplicate call rate was 100% for all SNPs. With the exception of one SNP that had a call rate of 92%, all SNPs had a call rate above 97%.

Genotype frequencies for cases and controls are presented in Table 3. Carriers of at least one polymorphic *MMP2* rs243865 allele tended to have a decreased risk for MM (OR = 0.66, 95% CI = 0.44–1.00; $P = 0.050$). The association was more pronounced in patients with known asbestos exposure: carriers of at least one polymorphic allele had significantly lower MM risk (OR = 0.55, 95% CI = 0.35–0.86; $P = 0.009$). As the number of homozygotes for poly-

TABLE 3. The association of investigated SNPs with risk for malignant mesothelioma

SNP	Genotype	Controls N (%)	Cases N (%)	OR (95% CI)	P	Cases exposed to asbestos N (%)	OR (95% CI)	P
MMP2 rs243865	CC	90 (55.9)	155 (65.7)	Ref.		118 (69.8)	Ref.	
	CT	65 (40.4)	77 (32.6)	0.69 (0.45-1.05)	0.081	48 (28.4)	0.56 (0.35-0.89)	0.015
	TT	6 (3.7)	4 (1.7)	0.39 (0.11-1.41)	0.150	3 (1.8)	0.38 (0.09-1.57)	0.181
	CT+TT	71 (44.1)	81 (34.3)	0.66 (0.44-1.00)	0.050	51 (30.2)	0.55 (0.35-0.86)	0.009
MMP2 rs243849	CC	108 (75.0) [17]	163 (71.5) [8]	Ref.		116 (71.2) [6]	Ref.	
	CT	33 (22.9)	57 (25.0)	1.14 (0.70-1.87)	0.592	42 (25.8)	1.18 (0.70-2.00)	0.527
	TT	3 (2.1)	8 (3.5)	1.77 (0.46-6.81)	0.408	5 (3.1)	1.55 (0.36-6.65)	0.554
	CT+TT	36 (25.0)	65 (28.5)	1.20 (0.74-1.92)	0.459	47 (28.8)	1.22 (0.73-2.02)	0.451
MMP2 rs7201	AA	56 (35.9) [5]	78 (33.5) [3]	Ref.		63 (37.5) [1]	Ref.	
	AC	71 (45.5)	114 (48.9)	1.15 (0.73-1.81)	0.539	78 (46.4)	0.98 (0.60-1.58)	0.923
	CC	29 (18.6)	41 (17.6)	1.02 (0.56-1.82)	0.960	27 (16.1)	0.83 (0.44-1.56)	0.560
	AC+CC	100 (64.1)	155 (66.5)	1.11 (0.73-1.70)	0.622	105 (62.5)	0.93 (0.59-1.47)	0.765
MMP9 rs17576	AA	64 (40.3) [2]	100 (42.9) [3]	Ref.		74 (44.3) [2]	Ref.	
	AG	75 (47.2)	114 (48.9)	0.97 (0.63-1.49)	0.900	79 (47.3)	0.91 (0.57-1.44)	0.691
	GG	20 (12.6)	19 (8.2)	0.61 (0.30-1.23)	0.165	14 (8.4)	0.61 (0.28-1.30)	0.196
	AG+GG	95 (59.8)	133 (57.1)	0.90 (0.59-1.35)	0.599	93 (55.7)	0.85 (0.55-1.31)	0.458
MMP9 rs2250889	GG	146 (90.7)	212 (90.2) [1]	Ref.		152 (89.9)	Ref.	
	GA	15 (9.3)	23 (9.8)	1.06 (0.53-2.09)	0.876	17 (10.1)	1.09 (0.52-2.26)	0.820
MMP9 rs17577	GG	113 (70.2)	169 (72.8) [4]	Ref.		119 (71.3) [2]	Ref.	
	GA	47 (29.2)	60 (25.9)	0.85 (0.54-1.34)	0.490	45 (26.9)	0.91 (0.56-1.47)	0.699
	AA	1 (0.6)	3 (1.3)	2.01 (0.21-19.53)	0.549	3 (1.8)	2.85 (0.29-27.79)	0.368
	GA+AA	48 (29.8)	63 (27.2)	0.88 (0.56-1.37)	0.565	48 (28.7)	0.95 (0.59-1.53)	0.831
MMP9 rs20544	CC	33 (20.6) [1]	38 (16.3) [3]	Ref.		29 (17.4) [2]	Ref.	
	CT	74 (46.3)	121 (51.9)	1.42 (0.82-2.46)	0.210	82 (49.1)	1.26 (0.70-2.27)	0.441
	TT	53 (33.1)	74 (31.8)	1.21 (0.68-2.18)	0.518	56 (33.5)	1.20 (0.64-2.25)	0.563
	CT+TT	127 (79.4)	195 (83.7)	1.33 (0.79-2.24)	0.275	138 (82.6)	1.24 (0.71-2.15)	0.453
MMP14 rs1042703	TT	90 (57.0) [3]	147 (63.4) [4]	Ref.		109 (65.7) [3]	Ref.	
	TC	54 (34.2)	67 (28.9)	0.76 (0.49-1.18)	0.225	44 (26.5)	0.67 (0.41-1.09)	0.110
	CC	14 (8.9)	18 (7.8)	0.79 (0.37-1.66)	0.530	13 (7.8)	0.77 (0.34-1.71)	0.518
	TC+CC	68 (43.0)	85 (36.6)	0.77 (0.51-1.16)	0.204	57 (34.3)	0.69 (0.44-1.08)	0.108
MMP14 rs1042704	GG	103 (64.0)	160 (68.1) [1]	Ref.		113 (66.9)	Ref.	
	GA	51 (31.7)	64 (27.2)	0.81 (0.52-1.26)	0.346	47 (27.8)	0.84 (0.52-1.35)	0.475
	AA	7 (4.3)	11 (4.7)	1.01 (0.38-2.69)	0.982	9 (5.3)	1.17 (0.42-3.26)	0.761
	GA+AA	58 (36.0)	75 (31.9)	0.83 (0.55-1.27)	0.395	56 (33.1)	0.88 (0.56-1.39)	0.581
MMP14 rs743257	CC	40 (26.0) [7]	59 (25.1) [1]	Ref.		41 (24.4) [1]	Ref.	
	CT	73 (47.4)	104 (44.3)	0.97 (0.59-1.59)	0.892	76 (45.2)	1.02 (0.59-1.75)	0.955
	TT	41 (26.6)	72 (30.6)	1.19 (0.68-2.07)	0.538	51 (30.4)	1.21 (0.67-2.21)	0.526
	CT+TT	114 (74.0)	176 (74.9)	1.05 (0.66-1.67)	0.848	127 (75.6)	1.09 (0.66-1.80)	0.746

Numbers in square brackets denote the number of patients with missing data. Significant values are printed in bold. CI = confidence interval; OR = odds ratio; SNP = single nucleotide polymorphism

TABLE 4. The association of haplotypes with frequencies above 5% for investigated genes with risk for malignant mesothelioma in patients with asbestos exposure

Gene	Haplotype	Estimated frequency	OR (95% CI)	P
MMP2	CCA	0.377	Ref.	
	CCC	0.272	1.14 (0.77 - 1.68)	0.518
	CTA	0.144	1.14 (0.70 - 1.85)	0.599
	TCC	0.144	0.77 (0.48 - 1.25)	0.291
	TCA	0.056	0.59 (0.26 - 1.38)	0.223
MMP9	ACGT	0.572	Ref.	
	GCGC	0.204	0.86 (0.59 - 1.26)	0.440
	GCAC	0.137	0.81 (0.52 - 1.26)	0.353
MMP14	TGC	0.338	Ref.	
	TGT	0.267	1.39 (0.94 - 2.06)	0.103
	CGT	0.125	0.85 (0.52 - 1.37)	0.494
	TAT	0.110	1.23 (0.71 - 2.12)	0.461
	CGC	0.080	1.33 (0.71 - 2.46)	0.371

The single nucleotide polymorphisms are ordered from the 5'- to 3'-end as follows: MMP2:rs243865, rs243849, rs7201; MMP9:rs17576, rs17577, rs2250889, rs20544; MMP14:rs1042703, rs1042704, rs743257.

CI = confidence interval; OR = odds ratio

morphic allele was low, we only observed a significant association with decreased MM risk for heterozygotes in the additive model (Table 3).

In haplotype analysis, no significant associations with MM risk were observed, even when asbestos exposure was taken into account (Table 4). Nevertheless, haplotypes that included the polymorphic MMP2 rs243865 allele had slightly lower risk, consistent with single SNP analysis, but the association did not reach statistical significance.

Discussion

This study investigated the influence of MMP2, MMP9 and MMP14 gene polymorphisms on baseline risk for MM in comparison with healthy control subjects. Carriers of MMP2 rs243865 CT or CT/TT genotypes had significantly decreased risk for developing MM in comparison with CC homozygous genotype, especially in patients with known asbestos exposure.

MMP2 rs243865 (c.-1306C>T) is a promoter polymorphism and our prior *in silico* analysis has shown that it may influence binding of transcription factors and may alter chromatin states.⁷ The data on whether the MMP2 rs243865 T allele has a protective function or if it contributes to higher risk for cancer, is somewhat conflicting for different malignancies.

MMP polymorphisms have been extensively studied in many different common and rarer malignancies.^{12,13} The most attractive and most significant MMPs in risk assessment studies were MMP2, MMP9 and MMP3 polymorphisms. MMP2 rs243865, that was associated with modified cancer risk in our study, had the greatest influence on cancer risk in general. In accordance with our study, two meta-analysis presented the results showing that MMP2 rs243865 polymorphism had a protective role in lung cancer susceptibility in both dominant and recessive models, which is consistent with our results. Seventeen studies were included in the meta-analysis and reported that the MMP2 rs243865 polymorphism had a protective role only in the Asian population.^{12,13}

Considering that lung cancer is the most common thoracic malignancy, these results can be parallel to a less common thoracic malignancy such as MM. However, MMP polymorphisms in other common malignancies in the Asian population have been frequently studied. A meta-analysis of 12 publications studying urinary (renal and bladder) cancers showed a lower risk for bladder cancer with the T allele of MMP2 rs243865 in Asian patients but not in the Caucasian population.¹⁴

All of the above discussed publications present the MMP2 rs243865 T allele as having a somewhat protective role in cancer. There are publications that suggest the opposite effect of the T allele in MMP2 rs243865. A control based study that included a Caucasian population investigated six different polymorphisms in MMPs and TIMPs in bladder cancer patients. They concluded that the combined genotype carrying MMP2 rs243865 allele T with MMP9 rs3918242 allele T was found to increase bladder cancer risk.¹⁵ These results are the opposite to the previously mentioned Asian based metaanalysis.¹⁴

According to the db SNP and HapMap data on rs243865 frequency in genetically different populations, the C allele is more common in Caucasian populations. That can perhaps contribute to the different results in different studied populations.¹⁶

Nevertheless, all of the cited studies find that MMP2 rs243865 could play a role as a risk factor in a variety of different malignancies. With regard to the MMP2 rs243865, T allele containing genotypes seem to have a protective role in predominantly thoracic malignancies, such as lung cancer and MM.

Genome Wide Associated Study (GWAS) of 759 subjects in the Northern Italian population investigated 15 different SNPs in several genes, and

one of them was *MMP14* rs2236304. Almost all of these SNPs had either a significant positive (higher risk after asbestos exposure) or negative (lower risk after asbestos exposure) interaction with asbestos exposure, even after statistical corrections (Bonferroni) had been applied. But, the study has some limitations, such as the small sample size, the age unbalanced control group and the possible rare genetics variants that could have been excluded from the GWAS statistical analysis.¹⁷

The *MMP2* rs243865, T allele genotypes seem to have a protective role in predominantly thoracic malignancies, such as lung cancer and MM. Moreover, thoracic malignancies are also well known to have a strong environmental component (eg. smoking, asbestos exposure).¹⁸ The gene-environment interactions have been studied extensively in MM. The study that investigated the role of microsomal epoxide hydrolase (*mEH*), glutathione S-transferases (*GSTM1*, *GSTT1*), N-acetyltransferase 2 (*NAT2*), and cytochrome P1A1 (*CYP1A1*) genotypes concluded that the presence of synergisms between genotypes, i.e., *mEH* and *NAT2*, *mEH* and *GSTM1*, and *NAT2* and *GSTM1* combined with the interaction observed with exposure to asbestos, suggests the presence of gene-environment and gene-gene interactions in the development of MM.¹⁹

Our results suggest a combined effect of asbestos exposure and *MMP2* rs243865. Gene-environment interactions in asbestos related diseases have been previously studied in enzymes such as catalase (CAT), superoxide dismutase (SOD 2, SOD3) and inducible nitric oxide synthase (iNOS), which are part of the enzymatic defence system against reactive oxygen species (ROS). Besides gene-gene interactions between *MnSOD* Ala -9Val and CAT -262 C>T polymorphisms as well as *iNOS* and CAT -262 C>T polymorphisms and the risk of asbestosis, gene-environment interactions were also reported. A strong interaction was reported between *GSTM1*-null polymorphism and smoking, *iNOS* (CCTTT)_n polymorphism and smoking, and between *iNOS* (CCTTT)_n polymorphism and cumulative asbestos exposure, suggesting that interactions between different genotypes, genotypes and smoking, and between genotypes and asbestos exposure have an important influence on the development of asbestosis.²⁰ These studies on asbestosis suggest, that gene-environment interactions should be investigated also in other asbestos related diseases, including MM, since asbestos exposure is a proven environmental risk factor in MM.

Despite some limitations of our study, such as a small sample size and a control group that was not appropriately age balanced, low rate of patient asbestos exposure and lacking this data of the control group, our results reached statistical significance and showed that there could be a genetic predisposition of certain MMP SNPs for MM and that there is a potential gene-environment interaction between MMP SNPs and asbestos that is a major risk factor for MM.

In conclusion, our data suggests that *MMP2* rs243865 polymorphism may have a protective role in malignant pleural mesothelioma. This finding is even more pronounced in patients exposed to asbestos, implying a strong gene-environment interaction.

Acknowledgments

Barbara Možina MSc, the head of the Biochemical Laboratory at the Institute of Oncology Ljubljana, provided valuable help in blood sample collection and storage as well as logistical help in managing the blood samples.

References

1. Delgermaa V, Takahashi K, Park EK, Le GV, Hara T, Sorahan T. Global mesothelioma deaths reported to the World Health Organization between 1994 and 2008. *Bull World Health Organ* 2011; **89**: 716-24. doi: 10.2471/BLT.11.086678
2. *Cancer in Slovenia 2014*. Ljubljana: Institute of Oncology Ljubljana, Epidemiology and Cancer Registry, Cancer Registry of Republic of Slovenia; 2017.
3. Kessenbrock K, Plaks V, Werb Z. Matrix metalloproteinases: regulators of the tumor microenvironment. *Cell* 2010; **141**: 52-67. doi: 10.1016/j.cell.2010.03.015
4. Rawlings ND, Barrett AJ. Evolutionary families of metalloproteinases. *Methods Enzymol* 1995; **248**: 183-228.
5. Mineo TC, Ambrogio V. Malignant pleural mesothelioma: factors influencing the prognosis. *Oncology (Williston Park)* 2012; **26**: 1164-75.
6. Deraco M, Nonaka D, Baratti D, Casali P, Rosai J, Younan R, et al. Prognostic analysis of clinicopathologic factors in 49 patients with diffuse malignant peritoneal mesothelioma treated with cytoreductive surgery and intraperitoneal hyperthermic perfusion. *Ann Surg Oncol* 2006; **13**: 229-37. doi: 10.1245/ASO.2006.03.045
7. Štrbac D, Goričar K, Dolžan V, Kovač V. Matrix metalloproteinases polymorphisms as prognostic biomarkers in malignant pleural mesothelioma. *Dis Markers* 2017; **2017**: 8069529. Epub 2017 Sep 12. doi: 10.1155/2017/8069529.
8. Nan H, Niu T, Hunter DJ, Han J. Missense polymorphisms in matrix metalloproteinase genes and skin cancer risk. *Cancer Epidemiol Biomarkers Prev* 2008; **17**: 3551-7. doi: 10.1158/1055-9965.EPI-08-0606
9. Lin CM, Zeng YL, Xiao M, Mei XQ, Shen LY, Guo MX, et al. The relationship between *MMP2* -1306C>T and *MMP9* -1562C>T polymorphisms and the risk and prognosis of T-cell acute lymphoblastic leukemia in a Chinese population. *Cell Physiol Biochem* 2017; **42**: 1458-68. doi: 10.1159/000479210

10. Kovač V, Zwitter M, Štrbac D, Goričar K, Rozman A, Kern I, Rajer M. Cisplatin with pemetrexed or gemcitabine in prolonged infusion for inoperable mesothelioma: a phase II randomized trial. [Abstract]. 17th World Conference on Lung Cancer, 4-7 December 2016, Vienna, Austria. *J Thorac Oncol* 2017; **12**(Suppl 1): S715.
11. National Institute of Environmental Health Sciences. SNP Function Prediction (Func Pred). [Internet]. Available at <https://snpinfo.nih.gov/snpinfo/snpfunc.html>. Accessed 15 Jan 2017.
12. Wang J, Cai Y. Matrix metalloproteinase 2 polymorphisms and expression in lung cancer: a meta-analysis. *Tumour Biol* 2012; **33**: 1819-28. doi: 10.1007/s13277-012-0441-0
13. Hu C, Wang J, Xu Y, Li X, Chen H, Bunjhoo H, et al. Current evidence on the relationship between five polymorphisms in the matrix metalloproteinases (MMP) gene and lung cancer risk: a meta-analysis. *Gene* 2013; **517**: 65-71. doi: 10.1016/j.gene.2012.12.085
14. Tao L, Li Z, Lin L, Lei Y, Hongyuan Y, Hongwei J, et al. MMP1, 2, 3, 7, and 9 gene polymorphisms and urinary cancer risk: a meta-analysis. *Genet Test Mol Biomarkers* 2015; **19**: 548-55. doi: 10.1089/gtmb.2015.0123
15. Wieczorek E, Reszka E, Jablonowski Z, Jablonska E, Beata Krol M, Grzegorzczuk A, et al. Genetic polymorphisms in matrix metalloproteinases (MMPs) and tissue inhibitors of MPs (TIMPs), and bladder cancer susceptibility. *BJU Int* 2013; **112**: 1207-14. doi: 10.1111/bju.12230
16. Sherry ST, Ward MH, M. Kholodov, Baker J, Phan L, Smigielski EM, et al. dbSNP: the NCBI database of genetic variation. *Nucleic Acids Res* 2001; **29**: 308-11.
17. Tunesi S, Ferrante D, Mirabelli D, Andorno S, Betti M, Fiorito G, et al. Gene-asbestos interaction in malignant pleural mesothelioma susceptibility. *Carcinogenesis* 2015; **36**: 1129-35. doi: 10.1093/carcin/bgv097
18. Franko A, Kotnik N, Goricar K, Kovac V, Dodic-Fikfak M, Dolzan V. The influence of genetic variability on the risk of developing malignant mesothelioma. *Radiol Oncol* 2018; **52**: 105-111. doi: 10.2478/raon-2018-0004.
19. Neri M, Filiberti R, Taioli E, Garte S, Paracchini V, Bolognesi C, et al. Pleural malignant mesothelioma, genetic susceptibility and asbestos exposure. *Mutat Res* 2005; **592**: 36-44. doi: 10.1016/j.mrfmmm.2005.06.003
20. Franko A, Dolzan V, Arnerić N, Dodić-Fikfak M. The influence of gene-gene and gene-environment interactions on the risk of asbestosis. *Biomed Res Int* 2013; **2013**: 405743. doi: 10.1155/2013/405743

Glioblastoma in patients over 70 years of age

Uros Smrdel¹, Marija Skoblar Vidmar¹, Ales Smrdel²

¹ Department of Radiotherapy, Institute of Oncology Ljubljana, Ljubljana, Slovenia

² Faculty of Computer and Information Science, University of Ljubljana, Slovenia

Radiol Oncol 2018; 52(2): 167-172.

Received 11 November 2017

Accepted 18 November 2017

Correspondence to: Assist. Uroš Smrdel, M.D., Ph.D., Department of Radiotherapy, Institute of Oncology Ljubljana, Zaloška cesta 2, 1000 Ljubljana, Slovenia. Phone: +386 1 5879 504; Fax: +386 1 5879 400; Email: usmrdel@onko-i.si

Disclosure: No potential conflicts of interest were disclosed.

Background. Glioblastoma has in last 20 years seen the steady increase of incidence, which is most prominent in the group of older patients. These older than 70 years have significantly poorer prognosis than other patients and are considered a distinct group of glioblastoma patients. Modified prognostic factors are being used in these patients and this information is lately supplemented with the genetic and epigenetic information on tumour. The therapy is now often tailored accordingly. The aim of our study was to analyse the current treatment of the glioblastoma patients over 70 years of age to determine the impact of clinical prognostic factors.

Patients and methods. Among patients treated at the Institute of Oncology Ljubljana between 1997 and 2015, we found that 207 were older than 70 years. We analysed their survival, clinical prognostic factors (age, performance status) treatment modalities (extent of surgery, radiation dose, chemotherapy).

Results. Median survival of patients older than 70 years was 5.3 months which was statistically significant inferior to the survival of younger patients ($p < 0.001$). The clinical prognostic factors that influenced survival the most were performance status ($p < 0.001$), extent of surgical resection ($p < 0.001$), addition of temozolomide ($p < 0.001$) and addition of radiotherapy ($p = 0.006$). Patients receiving concomitant radiochemotherapy with temozolomide followed by adjuvant temozolomide, had same median survival as patients receiving adjuvant temozolomide after completion of radiotherapy.

Conclusions. The increase of the number of older patients with glioblastoma corresponds to the increase in the life expectancy but in Slovenia also to the increased availability of diagnostic procedures. Clinical prognostic markers are helpful in decision on the aggressiveness of treatment. Radiotherapy and temozolomide have the biggest impact on survival, but the radiotherapy dose seems to be of secondary importance. In selected patients, chemotherapy alone might be sufficient to achieve an optimal effect. Patients that were fitter, had more aggressive surgery, and received temozolomide fared the best. The scheduling of the temozolomide seems to have limited impact on survival as in our study, there was no difference whether patients received temozolomide concomitant with radiotherapy or after the radiotherapy. Thus far, our findings corroborate the usefulness of recursive partitioning analysis (RPA) classes in clinical decisions.

Key words: glioblastoma; age group over 70 years; elderly; prognostic factors; treatment

Introduction

Glioblastoma is the most common primary brain tumour. And while it accounts in Slovenia only for around 1.5 % of all tumours, it is also responsible for 2.5 % of cancer related deaths. The incidence of glioblastoma is slowly increasing, but marked increase of the incidence in the older population;

especially in the over 70 year of age has been noted.¹⁻⁷

Unlike many other tumours, the natural history of glioblastoma is also changing with the age of the patients. While prognosis in the patients under 50 is relatively favourable, with significant portion of the patients living past 2 years after the diagnosis, quite opposite is true for those over 70. In this

group, the median survival is well under a year, and it has not changed significantly in recent times. Along with the improved knowledge of the molecular and genetic characteristic of the glioblastoma, which show that the majority of tumours in elderly belong to the so called primary glioblastoma subgroup, with the characteristic mutation profile, and short disease history. These tumours are characterized on the genetic level by the mutation of *EGFR*, *Rb2*, and amplification of *MDM2*, gain in chromosome 7 and *LoH* of chromosome 10.⁸⁻¹⁰

Patients with these tumours have short history between the onset of the first symptoms and the situation leading to the diagnosis. Quite often, for some time, the patient's mental deterioration is being assigned to other conditions and only quick deterioration in the period of some weeks is the signal prompting the start of diagnostic process.¹¹

The treatment of the elderly patients is in many aspects identical to the treatment of other glioblastoma patients¹², with the exemption, that since many of them are co-morbid and in poorer performance status as the younger ones, there is some reluctance in offering them all treatment modalities. Accordingly, fewer patients have gross total removal of the tumour, and fewer are receiving chemotherapy. Nevertheless, they are not a single homogeneous group. Though age is being recognized as a single most important factor in survival of glioblastoma patients, the glioblastoma peak incidence in the 6th decade of life, lead for a considerable time to neglect regarding the influence of the patients age in the oldest category. So Radiation Therapy Oncology Group (RTOG) has introduced the most widely used classification of glioblastoma patients using the already recognized clinical parameters, dividing them into groups based on age under or over 50, performance status, surgery, radiotherapy dose level and mental status.^{13,14} This, so called recursive partitioning analysis (RPA) classification has proved to be a useful tool in predicting prognosis of the patients and also a tool to help clinician deciding upon the treatment offered to the patient. This classification though has a major drawback, not differentiating the patients in the oldest age group. Therefore RPA analysis regarding only patients over 70 has been made. It has proved that these patients also fall into four distinct groups regarding survival.¹⁴ In this analysis, the main focus has been given to the extent of resection, dividing the patients on the basis of surgical resection versus the biopsy into two distinct groups. The group where resection has been performed has been divided further on the basis

of the patients' age (1 < 75.5; 2 >75.5) and the biopsy group regarding the performance status (3 ≥ Karnofsky performance status [KPS] 70; 4 < KPS 70). The patient, which had a resection and were younger than 75.5 years, don't fare worse than the patients in group 5 of RTOG RPA analysis, but other fare worse, especially those biopsied and in poor performance status.

As the incidence of the glioblastoma in elderly has risen, the interest in these patients has grown and two large studies, NOA 08 in Germany and Nordic in Scandinavia, had shown that there is a chance, that the same effect on survival might be achieved with less aggressive approach.^{15,16} The results of these studies had proven that in elderly, the same survival benefit might be achieved solely with the chemotherapy using temozolomide. The effect of temozolomide is primarily marked in patients, which have methylated methylguaninemethyltransferase (MGMT) promoter region, thus disabling the tumour cells to repair the alkylation of tumour DNA.

In Slovenia, we are also noting the increase of the number of elderly glioblastoma patients.^{5,6} Our strategy so far has been to assign patients either to radical treatment with radiochemotherapy with adjuvant temozolomide, palliative radiotherapy or supportive care. Since the methylation status in patients over 70, is now routinely determined, and the patients are now being offered treatment also on the basis of it, we have analysed our results of the past years, with the aim of obtaining our population data, so that it could serve as a benchmark for assessment of the further treatment strategies in this group of patients.

Patients and methods

Between the 1997 and the end of 2015, 1019 patients, diagnosed with glioblastoma have been referred to the Institute of Oncology Ljubljana. They represent the majority of the patients who were diagnosed with the glioblastoma in Slovenia in this time period. The only exceptions are the patients that have died or were not fit enough for referral.

Among these patients, we have searched for those, which were older than 70 years at the time of diagnosis. For these, we calculated their survival, compared it to the survival of the younger patients and then made the analysis of the survival and patients and treatment relating factors. We also determined RPA classes for those older than 70 according to classes described by Scott *et al.*¹⁴

TABLE 1. Patients' and treatment characteristics

Age (median) (SD)	73 years 3.7 years
Gender	
Female	99 (47.8%)
Male	108 (52.2%)
Surgery	
No	5 (2.5%)
Biopsy	69 (33.3%)
Reduction	96 (46.4%)
Gross total resection	37 (17.9%)
Performance status WHO	
0	3 (1.5%)
I	53 (25.6%)
II	65 (31.4%)
III	70 (33.8%)
IV	16 (7.7%)
Radiotherapy	158 (76.3%)
> 50 Gy	57 (27.5%)
40–50 Gy	33 (15.9%)
≤ 40 Gy	68 (32.8%)
Temozolomide	62 (30.0%)

SD = standard deviation

For the statistical analysis we used SPSS software package. We calculated demographic characteristics, frequencies of patients in the corresponding RPA groups, changes of frequencies during the analysed period and the frequencies of treatment characteristics. We used Kaplan-Maier analysis and Cox regression for survival analysis. We also performed a multivariate analysis using R. The significance level was at 0.05 for all statistics.

Ethical considerations

The study is retrospective analysis. It is a spinoff of an earlier analysis, which was approved by the Commission for Medical Ethics of the Republic of Slovenia.

Results

The median age of 1019 patients, treated for glioblastoma at the Institute of the Oncology Ljubljana between 1997 and 2015, was 60 years (standard deviation [SD] 11.8 years; min. 18 years, max. 86 years) (Table 1). Their overall survival was 10 months (SD 0.4 months). Of these patients, 207 were older than 70 years, and their median survival was 5.3 months

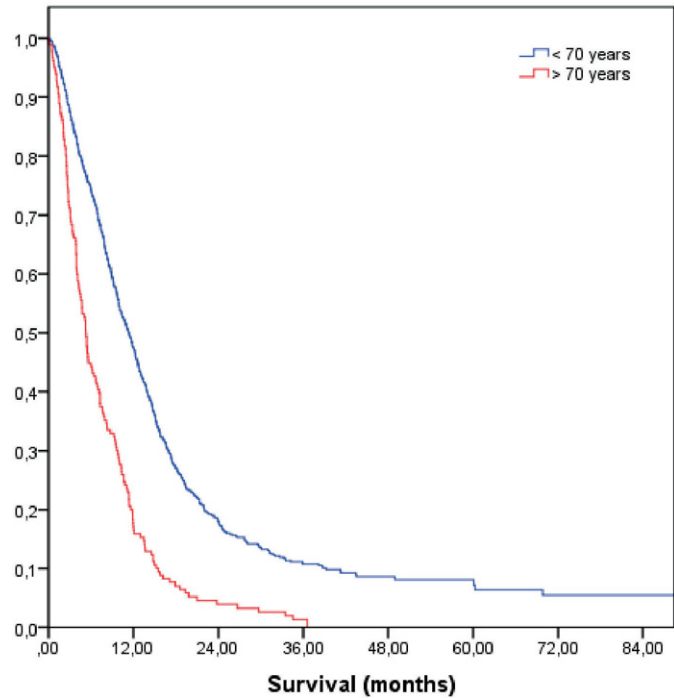


FIGURE 1. Survival of patients with glioblastoma according to the age below and over 70).

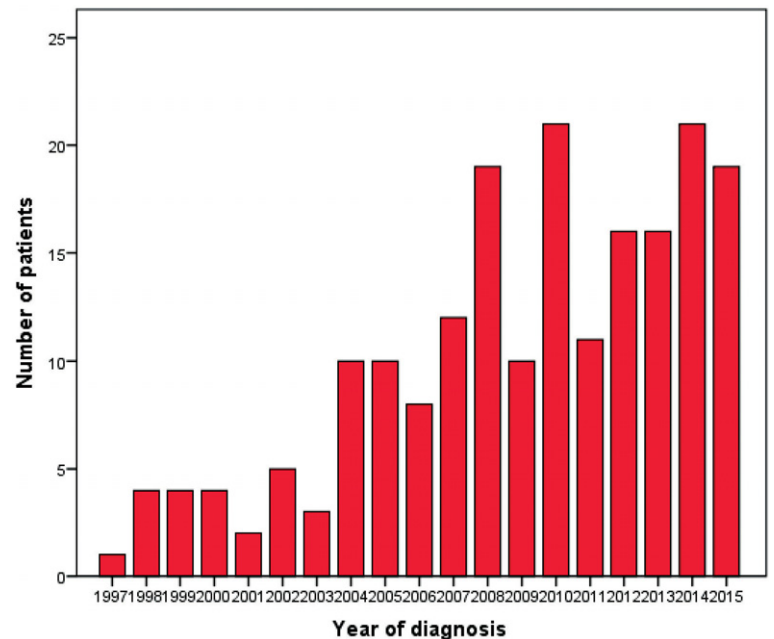


FIGURE 2. The number of patients older than 70 from 1997 to 2015).

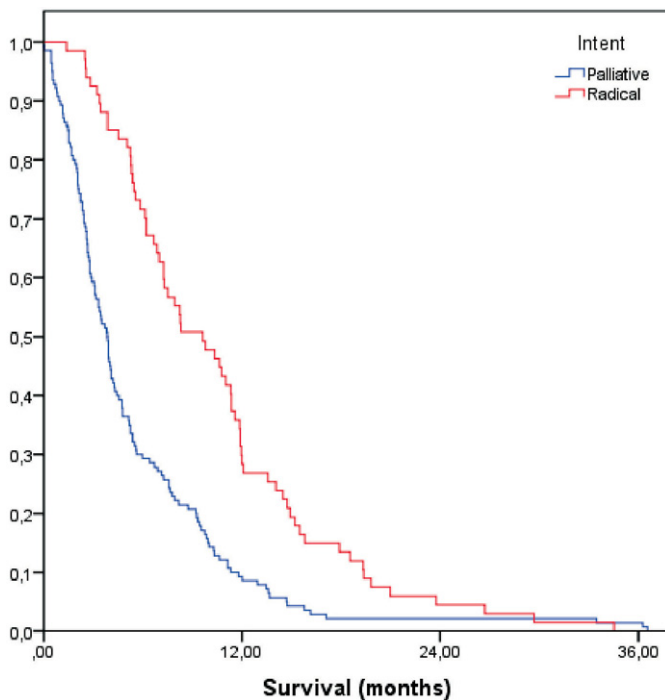


FIGURE 3. Survival of glioblastoma patients older than 70 according to intent of treatment.

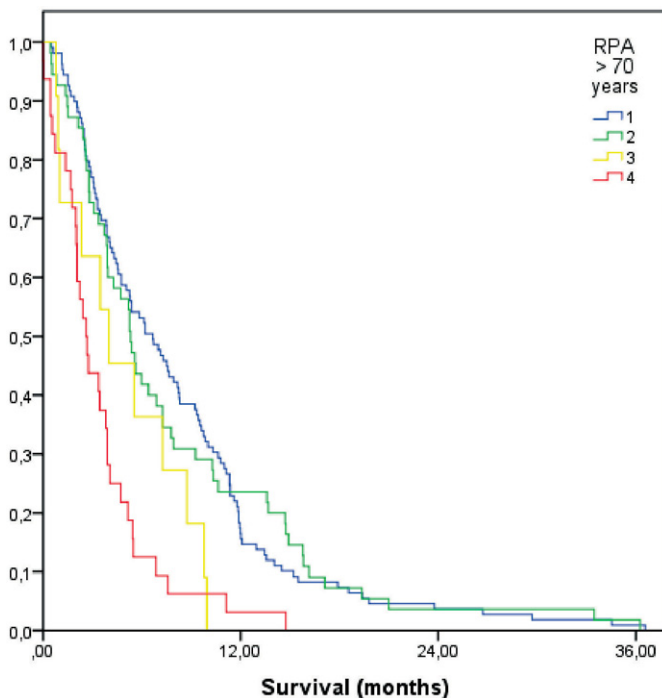


FIGURE 4. Survival of glioblastoma patients older than 70 according to prognostic recursive partitioning analysis (RPA) classes.

(SD 0.4 months). When comparing the groups of the patients younger than 70 with those older, the difference in median survival between groups was statistically significant at $p < 0.001$, with median survival of those younger than 70 years 12 months (SD 0.5 months) (Figure 1).

The number of patients older than 70 has increased over the observed years (Figure 2). The percent has risen from less than 10% in 1997 to more than 20% since the middle of 2000s.

Of the 207 patients older than 70 years, 99 were females and 108 males (1 : 1.1). The majority of whom had a surgical resection (69 gross total resections and 96 reductions), while less had biopsy only. For 5 patients, multidisciplinary team (MDT) decided, that any kind of surgical intervention would be too risky, so the diagnosis was decided upon radiological criteria. Except for this group, in which patients were somewhat older, the groups were identical regarding age and performance status.

The usual treatment following surgery was radiotherapy, 158 (76.3%) of patients were irradiated. Of those, who were not, majority were in poor performance status (WHO 3 and 4), some refused any further treatment and couple of them deteriorated rapidly. Only 2 of them received chemotherapy with temozolomide instead of radiotherapy.

Of the 207 patients, 67 were deemed suitable for "radical" treatment, and they proceeded with conventional radiochemotherapy 60 Gy in 30 fractions in 6 weeks with concomitant temozolomide, followed by adjuvant temozolomide. Others received either radiotherapy alone, radiotherapy followed by temozolomide, lower dose radiotherapy (45 Gy) with temozolomide or supportive care.

While overall survival for the group was 5 months, the median survival of those treated with radical intent was significantly higher (9.6 months, SD 1.5; $p < 0.001$) (Figure 3).

Also, the patients in good performance status fared better, from 8 months for the patients in WHO performance status 1 to 1.5 months for patients in performance status of 4 ($p < 0.001$).

Extent of surgical resection also proved to have a significant impact on survival. When neurosurgeon described a gross total resection, median survival was 7.1 months, in reduction 5.2 and in patients with the biopsy only 2.8 months ($p < 0.001$).

While patients over 70 fare worse than younger, the age does not seem to have such an impact in this group.

RPA classes were calculated, based on age, performance status and extent of surgical resection.

The survival was as predicted best in those with resection and younger than 75.5 years and worst for patients with biopsy in poor performance status ($p < 0.001$) (Figure 4).

We also looked in the impact treatment modalities have on survival. Patients receiving radiotherapy had a better survival, 6.1 months with radiotherapy and 3 months without ($p = 0.006$). And so is true for the addition of temozolomide with 10.4 months with the temozolomide and 3.8 without ($p < 0.001$). However, it seems, that concomitant temozolomide is no better than other schedules, as the survival remains the same, (10.3 and 10.6 months respectively, $p = 0.64$) in patients receiving concomitant temozolomide followed by adjuvant and adjuvant only.

In multivariate analysis, the significant impact on survival is retained by extent of operation ($p < 0.001$, HR 1.5 for biopsy), performance status ($p < 0.006$, hazard ratio [HR] 1.2 for WHO performance status > 1), and temozolomide ($p < 0.001$ HR 0.6 for temozolomide).

Discussion

In the last decade, we are observing a surge in the number of glioblastomas in the elderly population. This is being observed worldwide, and we demonstrated it for Slovenia. In our analysis, the rise is seemingly greater than in other reports. The rise is surely coming from the fact that the lifespan has extended considerably from the old threescore and ten. In Slovenia in the observed period, the life expectancy was 74.6 years in 1997, but in the 2015 it was 81.1 years.¹⁷ The other thing, we can assume could be responsible for the increase we are observing is the availability of diagnostic procedures for instance according to Organisation for Economic Cooperation and Development (OECD) data, the number of CT scanners in Slovenia has risen from 18 in 2004 to 28 in 2016, and this can be seen also in the number of MRI scanners (2004–2010; 2016–2017)¹⁸, thus diagnosis has become much more affordable. Admittedly, the direct proof of the later is lacking, but it is a plausible hypothesis.

In the analysis, we have shown that the median survival is worse for the elderly patients. But the therapeutic nihilism is ill warranted¹⁹, as with the appropriate treatment we can at least approach the median survival of some patients to the median survival of those in more favourable groups. The impact of good surgery in elderly is marked²⁰, so it is the impact of radiotherapy and chemothera-

py, the key is probably to tailor the postoperative therapy to individual patients. After surgery, all patients deserve a good radiotherapy if they are fit to receive it; more questionable is this approach in those which were only biopsied, or even had a diagnosis of malignant glioma established only by radiology. But even in those, some kind of palliative radiotherapy might result in better symptom control.²¹ Data, which has been published has shown, that there has been no significant detrimental effect of radiotherapy on cognitive status²², but the tests used have only limited sensitivity for more subtle changes. In the period we are describing, routine MGMT methylation testing haven't been performed in Slovenia²³, so the impact of alkylating agents is harder to determine, but the inclusion of temozolomide in treatment schedule, has resulted in improved median survival even in unknown methylation status.

Interesting find was that the patients receiving concomitant chemoradiotherapy and adjuvant chemotherapy had identical survival to those receiving radiotherapy followed by adjuvant temozolomide. This may be due to the fact, that more fragile patients haven't been exposed to such aggressive treatment, which might produce detrimental effect, but had benefited from systemic therapy as the performance improved. Of course, with the routine MGMT methylation assessment, with which we have started in 2016, group benefiting the most from temozolomide might be singled out, so we will not be giving the potentially non effective therapy to frail, while we will be able to avoid radiotherapy in those, where chemotherapy alone would suffice for the best palliative effect.

Conclusions

Glioblastoma is becoming ever more important problem in the population of patients aged over 70 years. While we are not able to cure these patients, we are able at least in the portion of them to prolong the survival and ameliorate the symptoms. The means we have at disposal towards this goal are essentially the same as the means we are utilising in the younger patients, the poorer performance status, arising not only due to the tumour related factors, but also due to the patients' comorbidity in elderly patients is forcing us to use them right. Up until now, the clinical prognostic factors have been our sole tool, with which we have accomplished our goals with a measure of success. The epigenetic and possibly even genetic

markers will hopefully improve our decision making capabilities and maybe improve the lot of some of these patients.

References

1. Cancer Research UK. Brain cancer (C71): 2010-2011. One-, five- and ten-year net survival (%), adults aged 15-99, England & Wales. [cited 2017 Aug 15]. Available at: <http://info.cancerresearchuk.org/cancerstats/faqs/#How>.
2. Arora RS, Alston RD, Eden TO, Estlin EJ, Moran A, Geraci M, et al. Are reported increases in incidence of primary CNS tumours real? An analysis of longitudinal trends in England, 1979–2003. *Eur J Cancer* 2010; **46**: 1607-16. doi: 10.1016/j.ejca.2010.02.007
3. Dolecek TA, Propp JM, Stroup NE, Kruchko C. CBTRUS statistical report: primary brain and central nervous system tumors diagnosed in the United States in 2005–2009. *Neuro Oncol* 2012; **14**(Suppl 5): v1–49. doi: 10.1093/neuonc/nos218
4. Ostrom QT, Gittleman H, Fulop J, Liu M, Blanda R, Kromer C, Wolinsky Y, et al. CBTRUS statistical report: primary brain and central nervous system tumors diagnosed in the United States in 2008-2012. *Neuro Oncol* 2015; **17**(Suppl 4): iv1-62. doi: 10.1093/neuonc/nov189
5. *Cancer incidence in Slovenia 1997-2006*. Ljubljana: Institute of Oncology Ljubljana, Epidemiology and Cancer Registry, Cancer Registry of Republic of Slovenia; 2000-2009.
6. *Cancer in Slovenia 2007-11*. Ljubljana: Institute of Oncology Ljubljana, Epidemiology and Cancer Registry, Cancer Registry of Republic of Slovenia; 2010-2014.
7. Smrdel U, Kovac V, Popovic M, Zwitter M. Glioblastoma patients in Slovenia from 1997 to 2008. *Radiol Oncol* 2014; **48**: 72-9. doi: 10.2478/raon-2014-0002
8. Ohgaki H, Dessen P, Jourde B, Horstmann S, Nishikawa T, Di Patre P-L, et al. Genetic pathways to glioblastoma: a population-based study. *Cancer Res* 2004; **64**: 6892-9. doi: 10.1158/0008-5472.CAN-04-1337
9. Steinfeld AD, Donahue B, Walker I. Delay in the diagnosis of glioblastoma multiforme: is age a factor? *Cancer Invest* 1996; **14**: 317-9.
10. Crespo I, Vital AL, Gonzalez-Tablas M, Patino M del C, Otero A, Lopes MC, et al. Molecular and genomic alterations in glioblastoma multiforme. *Am J Pathol* 2015; **185**: 1820-33. doi: 10.1016/j.ajpath.2015.02.023
11. De Groot JF, Aldape KD CH. High-grade astrocytomas. In: Schiff D, On B, editors. *Principles of neuro-oncology*. New York: McGraw Hill; 2005. p. 259-88.
12. Biau J, Dalloz P, Durando X, Hager MO, Ouédraogo ZG, Khalil T, et al. [Elderly patients with glioblastoma: state of the art],[French]. *Bull Cancer* 2015; **102**: 277-86. doi: 10.1016/j.bulcan.2015.02.002
13. Li J, Wang M, Won M, Shaw EG, Coughlin C, Curran WJ, et al. Validation and simplification of the Radiation Therapy Oncology Group recursive partitioning analysis classification for glioblastoma. *Int J Radiat Oncol Biol Phys* 2011; **81**: 623-30. doi: 10.1016/j.ijrobp.2010.06.012
14. Scott JG, Bauchet L, Fraum TJ, Nayak L, Cooper AR, Chao ST, et al. Recursive partitioning analysis of prognostic factors for glioblastoma patients aged 70 years or older. *Cancer* 2012; **118**: 5595-600. doi: 10.1002/cncr.27570
15. Arvold ND, Reardon DA. Treatment options and outcomes for glioblastoma in the elderly patient. *Clin Interv Aging* 2014; **9**: 357-67. doi: 10.2147/CIA.S44259
16. Lönn S, Klæboe L, Hall P, Mathiesen T, Auvinen A, Christensen HC, et al. Incidence trends of adult primary intracerebral tumors in four Nordic countries. *Int J Cancer* 2004; **108**: 450-5. doi: 10.1002/ijc.11578
17. Statistical Office, Republic of Slovenia. Births and deaths. [Internet]. [cited 2017 Nov 19]. Available at: <http://www.stat.si/StatWeb/Field/Index/17/95>
18. OECDLibrary. Health at a glance 2017. [Internet]. OECD Publishing; 2017 [cited 2017 Nov 19]. Available at: http://www.oecd-ilibrary.org/social-issues-migration-health/health-at-a-glance-2017_health_glance-2017-en
19. Fiorentino A, De Bonis P, Chiesa S, Balducci M, Fusco V. Elderly patients with glioblastoma: the treatment challenge. *Expert Rev Neurother* 2013; **13**: 1099-105. doi: 10.1586/14737175.2013.840419
20. Reardon D, Arvold N. Treatment options and outcomes for glioblastoma in the elderly patient. *Clin Interv Aging* 2014; **9**: 357-67. doi: 10.2147/CIA.S44259
21. Zouaoui S, Darlix A, Fabbro-Peray P, Mathieu-Daudé H, Rigau V, Fabro M, et al. Oncological patterns of care and outcomes for 265 elderly patients with newly diagnosed glioblastoma in France. *Neurosurg Rev* 2014; **3**: 415-23. doi: 10.1007/s10143-014-0528-8
22. Keime-Guibert F, Chinot O, Taillandier L, Cartalat-Carel S, Frenay M, Kantor G, et al. Radiotherapy for glioblastoma in the elderly. *N Eng J Med* 2007; **356**: 1527-35. doi: 10.1056/NEJMoa065901
23. Smrdel U, Popovic M, Zwitter M, Bostjancic E, Zupan A, Kovac V, et al. Long-term survival in glioblastoma: methyl guanine methyl transferase (MGMT) promoter methylation as independent favourable prognostic factor. *Radiol Oncol* 2016; **50**: 394-401. doi: 10.1515/raon-2015-0041

Comparative analysis of clinical and pathological lymph node staging data in head and neck squamous cell carcinoma patients treated at the General Hospital Vienna

Christina Eder-Czembirek¹, Birgit Erlacher², Dietmar Thurnher³, Boban M. Erovic⁴, Edgar Selzer⁵, Michael Formanek²

¹ Department of Cranio-, Maxillofacial and Oral Surgery, Medical University of Vienna, Vienna, Austria

² Department of Otorhinolaryngology and Phoniatriy, Hospital St. John of God and Vienna Sigmund Freud University (Medical Faculty), Austria

³ University Clinic of Otorhinolaryngology and Phoniatriy, Medical University of Graz, Graz, Austria

⁴ Department of Ear, Nose and Throat Diseases, Medical University of Vienna, Vienna, Austria

⁵ University Clinic of Radiotherapy, Medical University of Vienna, Vienna, Austria

Radiol Oncol 2018

Received 29 January 2018

Accepted 4 April 2018

Correspondence to: Edgar Selzer, M.D., Medical University of Vienna, Vienna General Hospital, Waehringer Guertel 18-20, A-1090 Vienna, Austria, Europe. Phone: +43 1 40400 26920; Fax: +43 1 40400 26660; E-mail: edgar.selzer@meduniwien.ac.at

Disclosure: No potential conflicts of interest were disclosed.

Background. Results from publications evaluating discrepancies between clinical staging data in relation to pathological findings demonstrate that a significant number of head and neck squamous cell carcinoma (HNSCC) patients are not correctly staged. The aim of this retrospective study was to analyze potential discrepancies of radiological assessment versus pathological data of regional lymph node involvement and to compare the results with data published in the literature.

Patients and methods. In a retrospective analysis we focused on patients with HNSCC routinely treated by surgery plus postoperative radiotherapy between 2002 and 2012. For inclusion, complete pre-operative clinical staging information with lymph node status and patho-histological information on involved lymph node regions as well as survival outcome data were mandatory. We included 87 patients (UICC stage III-IV 90.8%) for which the aforementioned data obtained by CT or MRI were available. Overall survival rates were estimated by the Kaplan–Meier method. The Pearson correlation coefficient and Spearman's rank correlation coefficient (non-linear relationship) was calculated.

Results. Discrepancies at the level of overall tumour stage assessment were noticed in 27.5% of all cases. Thereof, 5.7% were assigned to patho-histological up-staging or down-staging of the primary tumour. At the lymph node level, 11.5% of the patients were downstaged, and 10.3% were upstaged.

Conclusions. The study showed that in approximately one-fifth (21.8%) of the patients, lymph node assessment by CT or MRI differs from the pathologic staging, an outcome that corresponds well with those published by several other groups in this field.

Key words: lymph node staging; head and neck squamous cell cancer; clinical staging; pathological staging

Introduction

Methods for staging of head and neck squamous cell carcinoma patients rely primarily on the assessment by CT, PET-CT or MRI in combination

with a clinical examination by endoscopy and the use of ultrasound.¹⁻⁴ Head and neck carcinoma are usually treated, depending on the stage of disease, as well as based on various risk factors, by surgery, radiotherapy (RT), chemotherapy, cetuximab and

combinations thereof.⁵⁻⁸ While the location, as well as the extent of the primary tumour, is usually known with a sufficient degree of precision, most of the uncertainties about the evaluation of the exact tumour spread are related to the regional lymph node status. Disparities between pathological and clinical nodal staging data for head and neck carcinoma have been described in the literature by several authors.⁹⁻¹² In order to maximally utilize the tumour dose escalation as well as the normal tissue sparing potential of modern radiation technologies, it is important to be able to correctly delineate the target volume based on preclinical imaging data as well as on the statistical likelihood of microscopic tumour spread.¹³⁻¹⁵ It is therefore of importance to be aware of the potential extent of disparity that may exist between pathological and clinical staging methods. Also, it should be kept in mind that additional factors may impact correct diagnosis, in particular, the utilization of different imaging modalities as well as the different professional expertise of the examiners.^{16,17}

In this study, we assessed clinical (pre-treatment) as well as post-surgery (patho-histological) staging data in a retrospective series of patients who were treated with surgery and postoperative radiotherapy (PORT) at the Vienna General Hospital. We aimed to conduct a comparative analysis of clinical and pathological data of regional lymph node involvement and to compare our results with published data from the literature.

Patients and methods

Patient selection

A retrospective review of clinical data was conducted from a series of patients (squamous cell carcinoma, $n = 87$) treated by surgery plus PORT between 2002 and 2012, for which complete pre-operative clinical staging information including explicit description of lymph node involvement, complete patho-histological information on involved lymph node regions as well as survival outcome data were available.

Tumour staging

Tumour staging was conducted according to the 7th Edition TNM Classification for Head and Neck Cancer. Pre-therapeutic staging examinations were routinely performed with contrast agent enhanced CT scans of the head and neck. Alternatively, MRI scans, alone or in combination with CT scans (*e.g.*,

in cases of allergy, or according to the physicians' preferences) were performed. CT examinations alone were conducted in 55, MRI in 21, and both CT and MRI scans were done in 11 patients. In case of discordant diagnoses between the imaging modalities, the ultimate staging was based on the results of the CT scans. In cases of suspicious findings in the chest X-ray or after abdominal sonography, additional thoracic or abdominal CT scans were indicated. Only patients who were treated with curative intent without evidence of previous or accompanying malignancies, and who were operated and irradiated at the Vienna General Hospital, were included in this retrospective analysis.

Patho-histological files and existing pre-treatment imaging reports were compared, and congruence of the data was evaluated by an experienced head and neck oncologist and cross-checked by a non-physician member of the team with experience in clinical trial documentation. A nodal region was scored as positive if at least one lymph node was diagnosed as positive in the patho-histological or clinical diagnosis. The absolute number of positive or negative lymph nodes per nodal region was not assessed.

Radiotherapy and surgery

Surgery was performed at the Department of Ear, Nose and Throat Diseases of the Medical University of Vienna. 88.5% of the patients were operated bilaterally. Patients with clinical N0 status had elective ipsilateral selective neck dissection (13% of the cases) including the submandibular (level I), upper jugular (level II), and midjugular (level III) nodes. In patients with N+ disease, a modified radical neck dissection was performed by additionally including the lower jugular (level IV) and posterior triangle (level V) nodes (87% of the cases). PORT was indicated routinely for UICC stage III and IV cases. Lower disease stages were treated with postoperative radiotherapy if additional risk factors were present, such as large T2 tumours, or if, despite a patho-histological R0-status, according to the surgeon the resection status was uncertain. Postoperatively irradiated patients received a standard fractionation RT (2D/3D, 50–66 Gy total dose, mean dose 58 Gy) at 2 Gy per fraction. IMRT technique was not used on a routine basis. The prescribed dose depended on well-established risk factors such as patho-histological resection status and tumour stage. In the case of extracapsular spread or positive microscopic resection margins, cisplatin (100 mg/sqm) was added to postoperative

radiotherapy (week one and three) and the total radiation dose was escalated up to 66 Gy. Spinal cord dose was limited to a maximum of 50 Gy. All patients included in this retrospective analysis were presented at the Institutional Tumour Board of the Vienna General Hospital before treatment start and after surgery

Follow-up

Patients receiving PORT were clinically monitored weekly during treatment. After completion of therapy, follow-up examinations consisted of clinical examination, a CT or MRI scan of the head and neck region, chest X-ray and/or CT-scan, and upper abdominal sonography according to our institutional guidelines. Initial intervals were three months in the first post-therapeutic year followed by six-month intervals for the next four years. After that, follow-up interval was one year. Follow-up was conducted at the Department of Radiotherapy, at the Department of Ear, Nose and Throat Diseases and the Department of Internal Medicine in the case of additional chemotherapy treatment according to the institutional guidelines.

Statistical analysis

Overall survival rates were estimated by using the Kaplan-Meier method. The Pearson correlation coefficient and Spearman's rank correlation coefficient (non-linear relationship) was calculated to evaluate a possible statistical relationship between various data sets as described below. The software package SPSS Version 23.0 (IBM®) was used for statistical analysis.

Ethics statement

This study was conducted following the Helsinki Declaration on medical protocol and ethics in its most recently amended version and approved by the hospital's Ethic Review Board (Medical University of Vienna - study reference number 612/2009).

Results

A total of 87 patients was included in this retrospective analysis. Basic characteristics of patients included in the analysis according to pathological versus clinical staging data are shown in Table 1A

TABLE 1A. Patient characteristics

Characteristic	abs. (rel.) 87 (100)
Age (mean/median) years	58.4/59.0
Male	67 (77.0)
Female	20 (23.0)
Primary tumour site	
Oropharynx	33 (37.9)
Oral cavity	30 (34.5)
Larynx	9 (10.3)
Hypopharynx	15 (17.2)
Localization	
right	42 (48.3)
left	40 (46.0)
midline	5 (5.7)

TABLE 1B. Pre- and postoperative staging results

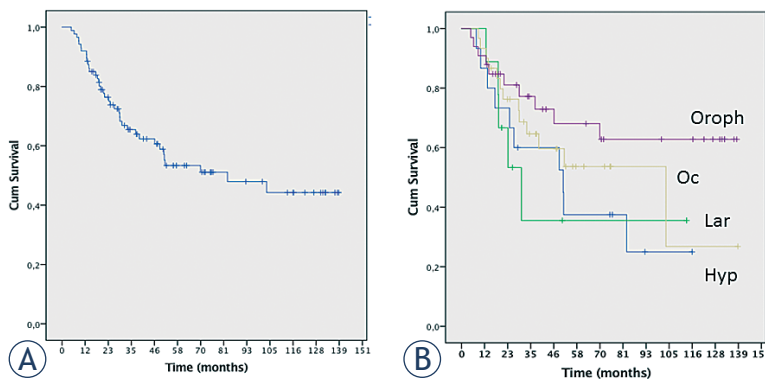
Stage	Pathological staging	Clinical staging	p-value
T			
1	19 (21.8)	19 (21.8)	0.000 ^a
2	42 (48.3)	34 (39.1)	
3	14 (16.1)	19 (21.8)	
4	12 (13.8)	15 (17.2)	
N			
0	21 (24.1)	17 (19.5)	0.000 ^a
1	15 (17.2)	15 (17.2)	
2a	2 (2.3)	6 (6.9)	
2b	34 (39.1)	24 (27.6)	
2c	13 (14.9)	25 (28.7)	
3	2 (2.3)	0 (0)	
UICC			
I	4 (4.6)	2 (2.3)	0.000 ^a
II	12 (13.8)	6 (6.9)	
III	11 (12.6)	17 (19.5)	
IV	60 (69)	62 (71.3)	

^aPearson correlation (significance 2-tailed). Correlations are significant below the 0.01 level

and 1B. 37.9% of the patients analyzed had oropharyngeal, 34.5% oral cavity, 10.3% laryngeal, and 17.2% hypopharyngeal cancer. Primary tumour site localization was well balanced with 48.3% of the carcinomas originating at the right side, 46% on

TABLE 1C. Clinical and pathological lymph node staging results in relation to the type of neck dissection performed

Stage	Bilateral neck dissection	Unilateral neck dissection	Total
pN0	15	6	21
pN1	13	2	15
pN2a	2	0	2
pN2b	32	2	34
pN2c	13	0	13
pN3	2	0	2
Total	77	10	87
cN0	14	3	17
cN1	11	4	15
cN2a	6	0	6
cN2b	21	3	24
cN2c	25	0	25
Total	77	10	87

**FIGURE 1.** Kaplan Meier curves for the complete patient group (A) and according to primary tumour sites (B).

Hyp = hypopharyngeal carcinoma; Lar = laryngeal carcinoma; Oc = oral cavity carcinoma; Oroph = oropharyngeal carcinoma

TABLE 2A. Discrepancies of pathological and clinical findings according to imaging type

Number of discrepant results per patient	CT (n = 55)	MRI (n = 21)	CT/MRI (n = 11)	Total (n = 87)
0	43.6%	38.1%	36.4%	36 (41.4%)
1	25.5%	23.8%	45.5%	24 (27.6%)
2	18.2%	23.8%	9.1%	16 (18.4%)
3	5.5%	9.5%	0.0%	5 (5.7%)
4	7.3%	4.8%	0.0%	5 (5.7%)
5	0.0%	0.0%	9.1%	1 (1.1%)

the left side, and 5.7% midline tumours. Most of the patients (90.8%) had stage III/IV carcinomas. None of the patients was lost to follow-up. In Table 1C, cross-tabulated pathological and clinical N-staging data according to the type of dissection (unilateral versus bilateral) are presented.

Estimate (Kaplan-Meier) of median overall survival for the whole treatment group was 85.9 months (SE 31.9; 95% CI 23.4–148.3). The patient collective investigated corresponds with regard to overall survival (64.5% after 3-years) to previously published results derived from larger data sets (N = 148; OS 69% after 3-years) at our institution.¹⁸ Kaplan-Meier curves for the entire patient collective, as well stratified according to the primary tumour, are shown in Figure 1. To directly compare the results of pathological and clinical staging data, patho-histological files were compared with pre-operative staging examinations (CT or MRI).

Table 2 shows results regarding congruency of patho-histological and clinical staging data. The numbers and percentage of discrepantly staged lymph node levels per patient according to the type of imaging performed (CT, MRI, CT&MRI) are shown in Table 2A. No statistically significant association between type of preoperative imaging modality (MRI, CT, CT&MRI) and clinical staging data was observed (data not shown). Cross-tabulation data (concordance) of patho-histological lymph node stage versus clinical lymph node stage findings are presented in Table 2B. This table shows the initial clinical lymph node staging data (left column) and the corresponding corrected pathological staging results. Of note, in two cases a cN2c stage was upstaged to pN3. Table 3A shows the percentage of patients according to the origin of the primary tumour and pathologically positive lymph node levels (level I to V). Nodal level I was involved in 16.1%, level II in 59.8%, level III in 40.2%, level IV in 20.7%, and level V in 9.2% of the patients. As expected, levels II and III were predominantly involved.

We performed a statistical analysis of the correlation of regional pathological lymph node involvement and asked, whether the involvement of a given lymph node level is statistically correlated with an involvement of any other node level in the ipsilateral neck. The corresponding data are shown in Table 3B. Detailed staging data for all cases in which a discrepant finding between the clinical and pathological involvement of lymph node regions as well as of the primary tumours was found necessitating a re-assessment of the overall tumour stage are shown in Table 4.

Discussion

We retrospectively investigated the correlation of pre-therapeutic clinical staging data with the findings of the patho-histological examination of the lymph nodes of the neck in patients with squamous cell carcinoma of the head and neck who underwent surgery plus postoperative radiotherapy. The principal intention of the study was to determine the possible extent of disparity between the findings of clinical versus pathological staging procedures. Also we sought to compare the results from our institution, at which such a comparative analysis has not been conducted to date, with those from other groups.

We are aware of certain limitations regarding our study, as this analysis was performed in a retrospective manner and data were accumulated over almost ten years. It is possible that changes in the quality of diagnostic imaging as well as variations in the professional experience, amongst others, may have contributed to unknown biases in our analysis.

One of the most comprehensive comparative analysis of clinical and pathological staging data in head and neck carcinoma patients (results from Intergroup Study ECOG 4393/RTOG 9614) was published by Koch *et al.*¹² The authors found disparities between the staging procedures in almost 50% of 501 investigated patients. In summary, a perfect match between clinical and pathological T-, N-classification and the overall stage was found in 52.2%, 53.5%, and 54.9%, respectively. Nevertheless, Koch *et al.*¹² found that both clinical and pathological staging methods showed an association of stage with overall survival. They concluded that both staging methods are useful in predicting survival, although staging after neck dissection regarding nodal metastases allowed further refinement in prognostic results. They found that only 69.7% of the patients judged to be clinically metastasis-free were pathologically N0, corresponding to 30.3% false-negative clinical staging. The percentage of CT versus MRI was not reported in this publication.

Other investigators found a 34% rate of occult lymph node disease in cN0 oral tongue carcinoma patients.¹⁰ Buckley *et al.*¹⁹ investigated the prevalence and distribution of cervical lymph node metastases in 100 laryngeal and hypopharyngeal patients who were treated by neck dissection for either N0 or N+ disease. They found 36% nodal metastases of the ipsilateral neck and 27% of the contralateral neck in clinically staged N0 cases. In

TABLE 2B. Concordance of pathological and clinical findings according to N stage

Clinical stage N = 87	Pathological stage					
	pN0	pN1	pN2a	pN2b	pN2c	pN3
cN0 (N = 17)	11	3	0	1	2	0
cN1 (N = 15)	4	6	0	3	2	0
cN2a (N = 6)	1	2	1	2	0	0
cN2b (N = 24)	3	2	0	18	1	0
cN2c (N = 25)	2	2	1	10	8	2
cN3 (N = 0)	0	0	0	0	0	0

TABLE 3A. Prevalence of regional lymph node involvement according to tumour site

Lymph Node Level	Primary tumour localization				% of total collective
	Hypopharynx (n = 15)	Larynx (n = 9)	Oral cavity (n = 30)	Oropharynx (n = 33)	
I	2 (13.3%)	1 (11.1%)	5 (16.7%)	6 (18.2%)	14 (16.1%)
II	8 (53.3%)	4 (44.4%)	22 (73.3%)	18 (54.4%)	52 (59.8%)
III	3 (20%)	4 (44.4%)	13 (43.3%)	15 (45.5%)	35 (40.2%)
IV	4 (26.7%)	2 (22.2%)	7 (23.3%)	5 (15.2%)	18 (20.7%)
V	2 (13.3%)	1 (11.1%)	4 (13.3%)	1 (3%)	8 (9.2%)

TABLE 3B. Statistical analysis of the correlation of involvement of adjacent lymph-node levels

N = 87		LI	LII	LIII	LIV	LV
LI	Corr.	1				
LII	Corr. Sig.	0.029 0.791	1			
LIII	Corr. Sig.	0.040 0.711	0.325 ^a 0.001	1		
LIV	Corr. Sig.	-0.069 0.524	0.113 0.297	0.449 ^a 0.000	1	
LV	Corr. Sig.	-0.139 0.198	0.088 0.419	0.145 0.182	0.427 ^a 0.000	1

^a Pearson correlation (significance 2-tailed). Correlations are significant below the 0.01 level.

N+ cases, prevalence was 90% ipsilateral and 37% contra-lateral, respectively. The imaging technique in this study used was CT only.

A clinically significant discrepancy between pathological and clinical neck staging (N = 256) was reported by Henriques *et al.*²⁰ Their results suggested that in 62% of the cases a clinical up-staging after pathological assessment of the lymph nodes was necessary.

Our data show that 67% of the patients were staged correctly at the lymph node level when N2a,

TABLE 4. List of all cases associated with up- or down-staging according to the pre- and postoperative regional lymph-node status

No.	cT	cN	Overall clinical stage	pT	pN	Overall pathological stage
Down-staging according to pN status n = 10 (11.5%)						
1	2	1	III	1	0	I
2	1	2a	IV	1	0	I
3	2	2b	IV	1	0	I
4	2	1	III	2	0	II
5	2	1	III	2	0	II
6	2	2b	IV	2	0	II
7	1	2b	IV	2	0	II
8	3	2c	IV	2	0	II
9	3	2b	IV	2	1	III
10	2	2c	IV	2	1	III
Up-staging according to pN status N = 9 (10.3%)						
1	2	0	II	2	1	III
2	3	0	III	4	1	IV
3	2	1	III	2	2b	IV
4	2	1	III	2	2b	IV
5	3	0	III	3	2b	IV
6	2	1	III	2	2b	IV
7	2	1	III	3	2c	IV
8	1	0	I	1	2c	IV
9	1	2b	III	1	2c	IV

N2b, and N2c data were pooled into a single variable. Further sub-classification into N2a, N2b, and N2c leads to an increase in the fraction of discrepantly staged patients (48%). Of these, 25% had to be up-staged, and 23% were down-staged.

A statistical analysis of the correlation of lymph node level involvement was performed, as well as the frequency of pathological involvement according to the primary tumour site was calculated. As expected, level II was the most frequently involved node level (59.8% for all primary tumour sites combined). Level V (9.2% combined) was rarely involved. One patient presented with clinically and pathologically positive lymph nodes in level VI. We performed further statistical analyses of the lymph node data. Positivity in level I involvement was not found to be correlated to positivity or negativity in any other level investigated. As is shown in Table 3B, positivity only of the respective adjacent levels II and III, III and IV, and

level IV and V was significantly correlated. The correlation of positive involvement between level II and III was calculated to be 0.352, between level III and IV 0.449, and between level IV and V 0.427. These results may be explained by the well-known fact that metastasis preferentially proceeds along lymph node levels and rarely bypasses or skips the succeeding level. As has been pointed out by other authors, spreading of metastatic cells along cervical lymph nodes is somewhat consistent, and the risk of involvement increases for each level if the neighboring level is affected.^{15,21}

Some authors attempted to represent current data of nodal involvement in mathematical models.^{22,23} However, such models are - at least for the time being - not of clinical significance. From a clinical point of view, the most relevant question to answer is, in how many cases an up- or down-staging of the overall tumour stage, after reclassification based on the patho-histological examination of lymph node levels, might be necessary. In summary, in 11.5% (10/87) of the cases a down-staging and in 10.3% (9/87) of the cases an up-staging was the consequence after pathological re-assessment of the lymph node involvement. These results correspond nicely to those recently published derived from larger retrospective data sets of 252²⁴ and 392²⁵ oral squamous cell cancer patients, respectively. Choi *et al.*²⁴ reported an 82.5% agreement between the overall pathological and clinical lymph node status, compared to 78% in our collective. The patients in this study had CT or MRI to evaluate the primary tumour and cervical nodal status. PET/CT was performed in all subjects. Underestimation of tumour stage based on clinical assessment was observed by Choi *et al.*²⁴ in 13% of the patients, compared to 10.3% in our collective. The concordance between the pathological and clinical staging for the N-classification was found to be 59% in the study by Kreppel *et al.*²⁵, who compared each cN and pN stage separately. By comparison, sub-classification of our data into N2a, N2b, and N2c results in a comparable percentage of 52% concordantly staged patients. All the patients included in this study had CT as well as MRI scans. Of interest and in context with our study, we recently found, that after preoperative radio-chemotherapy of locally advanced head and neck carcinoma patients, a patho-histological response assessment by CT was associated with a substantial fraction of the patients with either false positive (13%) or false negative (22%) diagnoses.¹¹

In our patient group, 55 (63%) patients had a CT scan only, 21 (24%) patients an MRI scan, and in 11

(13%) cases both an MRI and CT scan was available. Statistical analysis showed that the type of imaging modality used (CT, MRI, CT & MRI) was not correlated with the percentage of discrepant results. Of note, more than one discrepantly diagnosed lymph-node level was identified in 30.9% of all patients.

In summary, our results indicate that in a substantial percentage of patients a patho-histological assessment of lymph node involvement may differ from the clinical evaluation by CT, MRI or despite the combination of CT and MRI. The percentage of patients in which staging had to be either up or down-migrated was very similar. Over- or understaging of lymph-nodes occurred in our collective in a similar percentage of the patients. Other authors²⁵ reported a higher percentage (86%) of overstaging. As the authors discussed in their publication, differences in the clinical assessment of lymph-nodes in the area of functional imaging modalities, such as PET-CT and DW-MRI, may be related directly or indirectly to the biology of malignant lymph-nodes, such as inflammatory processes, vascularization, and the extent of necrosis and hypoxia, which may affect the uptake of contrast agents. Also, the process of obtaining and manipulating the specimen per se, as well as the exactitude of the patho-histological workup, such as the number of resected lymph-nodes^{12,26} may affect the final staging results. Of note, the mean number (N = 22) of resected lymph-nodes in our study was similar to the number published by another group.²⁶

Due to the insufficient number of events in our collective, as defined by the number of cases that had to be up- or down-staged, a statistically valid comparison of the survival rates between these patient groups is not possible. However, three patients were down-staged from stage III/IV to stage I, and two patients were up-staged from stage I/II to stage III/IV. It is very likely that such massive changes in staging affect the prognosis as well as the type treatment of the individual patient affected. The study findings should also be seen in light of the increasing trend to spare healthy tissues or to selectively increase radiation doses using modern treatment techniques such as IMRT/VMAT and stereotactic radiation treatments.²⁷

Conclusions

Results in the study indicated that an under or overestimation of clinical tumour stage may occur in approximately up to 20–30% of HNSCC patients.

Acknowledgement

The authors declare that they have no competing interests. This research did not receive any specific grant from funding agencies in the public, commercial, or not-for-profit sectors.

References

1. Abraham J. Imaging for head and neck cancer. *Surg Oncol Clin N Am* 2015; **24**: 455-71. doi: 10.1016/j.soc.2015.03.012
2. Johnson JT, Branstetter BFT. PET/CT in head and neck oncology: State-of-the-art 2013. *Laryngoscope* 2014; **124**: 913-5. doi: 10.1002/lary.23942
3. Liao LJ, Hsu WL, Wang CT, Lo WC, Lai MS. Analysis of sentinel node biopsy combined with other diagnostic tools in staging cN0 head and neck cancer: A diagnostic meta-analysis. *Head Neck* 2016; **38**: 628-34. doi: 10.1002/hed.23945
4. Zygogianni A, Kyrgias G, Kouvaris J, Pistevo-Gompaki K, Kouloulis V. A new role of PET/CT for target delineation for radiotherapy treatment planning for head and neck carcinomas. *Hell J Nucl Med* 2012; **15**: 139-43.
5. Cmelak AJ. Current issues in combined modality therapy in locally advanced head and neck cancer. *Crit Rev Oncol Hematol* 2012; **84**: 261-73. doi: 10.1016/j.critrevonc.2012.04.004
6. Kavanagh BD, Haffty BG, Tepper JE. Radiation oncology: a snapshot in time, 2014. *J Clin Oncol* 2014; **32**: 2825-6. doi: 10.1200/JCO.2014.57.3071
7. Pryor DJ, Solomon B, Porceddu SV. The emerging era of personalized therapy in squamous cell carcinoma of the head and neck. *Asia Pac J Clin Oncol* 2011; **7**: 236-51. doi: 10.1111/j.1743-7563.2011.01420.x
8. Thariat J, Hannoun-Levi JM, Sun Myint A, Vuong T, Gerard JP. Past, present, and future of radiotherapy for the benefit of patients. *Nat Rev Clin Oncol* 2013; **10**: 52-60. doi: 10.1038/nrclinonc.2012.203
9. Biron VL, O'Connell DA, Seikaly H. The impact of clinical versus pathological staging in oral cavity carcinoma - a multi-institutional analysis of survival. *J Otolaryngol Head Neck Surg* 2013; **42**: 28. doi: 10.1186/1916-0216-42-28
10. Greenberg JS, El Nagggar AK, Mo V, Roberts D, Myers JN. Disparity in pathologic and clinical lymph node staging in oral tongue carcinoma. Implication for therapeutic decision making. *Cancer* 2003; **98**: 508-15. doi: 10.1002/ncr.11526
11. Klug C, Keszthelyi D, Ploder O, Sulzbacher I, Voracek M, Wagner A, et al. Neoadjuvant radiochemotherapy of oral cavity and oropharyngeal cancer: evaluation of tumor response by CT differs from histopathologic response assessment in a significant fraction of patients. *Head Neck* 2004; **26**: 224-31. doi: 10.1002/hed.10373
12. Koch WM, Ridge JA, Forastiere A, Manola J. Comparison of clinical and pathological staging in head and neck squamous cell carcinoma: results from Intergroup Study ECOG 4393/RTOG 9614. *Arch Otolaryngol Head Neck Surg* 2009; **135**: 851-8. doi: 10.1001/archoto.2009.123
13. Gregoire V, Ang K, Budach W, Grau C, Hamoir M, Langendijk JA, et al. Delineation of the neck node levels for head and neck tumors: a 2013 update. DAHANCA, EORTC, HKNPCSG, NCIC CTG, NCRI, RTOG, TROG consensus guidelines. *Radiother Oncol* 2014; **110**: 172-81. doi: 10.1016/j.radonc.2013.10.010
14. Gregoire V, Levendag P, Ang KK, Bernier J, Braaksma M, Budach V et al. CT-based delineation of lymph node levels and related CTVs in the node-negative neck: DAHANCA, EORTC, GORTEC, NCIC, RTOG consensus guidelines. *Radiother Oncol* 2003; **69**: 227-36. doi: 10.1016/j.radonc.2003.09.011
15. Vorwerk H, Hess CF. Guidelines for delineation of lymphatic clinical target volumes for high conformal radiotherapy: head and neck region. *Radiat Oncol* 2011; **6**: 97. doi: 10.1186/1748-717x-6-97
16. Bhargava P, Rahman S, Wendt J. Atlas of confounding factors in head and neck PET/CT imaging. *Clin Nucl Med* 2011; **36**: e20-9. doi: 10.1097/RLU.0b013e318212c872
17. Morgan B. Opportunities and pitfalls of cancer imaging in clinical trials. *Nat Rev Clin Oncol* 2011; **8**: 517-27. doi: 10.1038/nrclinonc.2011.62

18. Selzer E, Grah A, Heiduschka G, Kornek G, Thurnher D. Primary radiotherapy or postoperative radiotherapy in patients with head and neck cancer: comparative analysis of inflammation-based prognostic scoring systems. *Strahlenther Onkol* 2015; **191**: 486-94. doi: 10.1007/s00066-014-0803-1
19. Buckley JG, MacLennan K. Cervical node metastases in laryngeal and hypopharyngeal cancer: a prospective analysis of prevalence and distribution. *Head Neck* 2000; **22**: 380-5.
20. Henriques V, Breda E, Monteiro E. Discrepancy between clinical and pathological neck staging in oral cavity carcinomas. *Acta Otorrinolaringologica Espanola* 2017; **69**: 67-73. doi: 10.1016/j.otorri.2017.02.008
21. Candela FC, Kothari K, Shah JP. Patterns of cervical node metastases from squamous carcinoma of the oropharynx and hypopharynx. *Head Neck* 1990; **12**: 197-203.
22. Benson N, Whipple M, Kalet IJ. A Markov model approach to predicting regional tumor spread in the lymphatic system of the head and neck. *AMIA Annu Symp Proc* 2006; 31-5.
23. Kalet IJ, Whipple M, Pessah S, Barker J, Austin-Seymour MM, Shapiro LG. A rule-based model for local and regional tumor spread. *Proc AMIA Symp* 2002; 360-4.
24. Choi N, Noh Y, Lee EK, Chung M, Baek CH, Baek KH, et al. Discrepancy between cTNM and pTNM staging of oral cavity cancers and its prognostic significance. *J Surg Oncol* 2017; **115**: 1011-18. doi: 10.1002/jso.24606
25. Kreppel M, Nazarli P, Grandoch A, Safi AF, Zirk M, Nickenig HJ et al. Clinical and histopathological staging in oral squamous cell carcinoma - Comparison of the prognostic significance. *Oral Oncol* 2016; **60**: 68-73. doi: 10.1016/j.oraloncology.2016.07.004
26. Safi AF, Kauke M, Grandoch A, Nickenig HJ, Drebber U, Zoller J et al. Clinicopathological parameters affecting nodal yields in patients with oral squamous cell carcinoma receiving selective neck dissection. *J Craniomaxillofac Surg* 2017; **45**: 2092-96. doi: 10.1016/j.jcms.2017.08.020
27. Gregoire V, Langendijk JA, Nuyts S. Advances in Radiotherapy for Head and Neck Cancer. *J Clin Oncol* 2015; **33**: 3277-84. doi: 10.1200/JCO.2015.61.2994

A population-based study of the effectiveness of stereotactic ablative radiotherapy versus conventional fractionated radiotherapy for clinical stage I non-small cell lung cancer patients

Chih-Yen Tu^{1,5,#}, Te-Chun Hsia^{1,6,#}, Hsin-Yuan Fang^{2,#}, Ji-An Liang^{3,#}, Su-Tso Yang^{4,7,#}, Chia-Chin Li³, Chun-Ru Chien^{3,5}

¹ Division of Pulmonary and Critical Care Medicine, Department of Internal Medicine, China Medical University Hospital, Taiwan

² Department of Chest Surgery, China Medical University Hospital, Taiwan

³ Department of Radiation Oncology, China Medical University Hospital, Taiwan

⁴ Department of Radiology, China Medical University Hospital, Taiwan

⁵ School of Medicine, College of Medicine, China Medical University, Taiwan

⁶ Department of Respiratory Therapy, College of Health Care, China Medical University, Taiwan

⁷ School of Chinese Medicine, China Medical University, Taiwan

Radiol Oncol 2018; 52(2): 181-188.

Received 28 July 2017

Accepted 18 September 2017

Correspondence to: Chun-Ru Chien, M.D., Ph.D., School of Medicine, College of Medicine, China Medical University, No.91 Hsueh-Shih Road, North District, Taichung 40402, Taiwan. Phone: +886 4 22052121 7450; Fax: +886 4 22052121 7460; E-mail: d16181@gmail.com

Disclosure: No potential conflicts of interest were disclosed.

The authors contributed equally to this work.

Background. Stereotactic ablative radiotherapy (SABR) is a promising option for non-operated early-stage non-small cell lung cancer (NSCLC) compared to conventional fractionated radiotherapy (CFRT). However, results from conclusive randomized controlled trials are not yet available. The aim of our study was to explore the effectiveness of SABR vs. CFRT for non-operated early-stage NSCLC.

Patients and methods. We used a comprehensive population-based database to identify clinical stage I non-operated NSCLC patients in Taiwan diagnosed from 2007 to 2013 who were treated with either SABR or CFRT. We used inverse probability weighting and the propensity score as the primary form of analysis to address the nonrandomization of treatment. In the supplementary analyses, we constructed subgroups based on propensity score matching to compare survival between patients treated with SABR vs. CFRT.

Results. We identified 238 patients in our primary analysis. A good balance of covariates was achieved using the propensity score weighting. Overall survival (OS) was not significantly different between those treated with SABR vs. CFRT (SABR vs. CFRT: probability weighting adjusted hazard ratio [HR] 0.586, 95% confidence interval 0.264–1.101, $p = 0.102$). However, SABR was significantly favored in supplementary analyses.

Conclusions. In this population-based propensity-score adjusted analysis, we found that OS was not significantly different between those treated with SABR vs. CFRT in the primary analysis, although significance was observed in the supplementary analyses. Our results should be interpreted with caution given the database (i.e., nonrandomized) approach used in our study. Overall, further studies are required to explore these issues.

Keywords: stereotactic ablative radiotherapy; conventional fractionated radiotherapy; non-small cell lung cancer

Introduction

Surgery is the cornerstone for treating early-stage non-small cell lung cancer (NSCLC), although rad-

ical radiotherapy may be used for medically inoperable cases.^{1,2} In recent years, stereotactic ablative radiotherapy (SABR, or so-called stereotactic body radiotherapy) has been used to deliver radiothera-

py instead of conventional fractionated radiotherapy (CFRT).²⁻⁵ Promising results have been reported for medically inoperable and operable cases and even other cancers.⁶⁻⁹

However, a recent randomized phase II study (the SPACE trial) challenged the general belief that SABR is superior to CFRT, as also mentioned in a 2017 systematic review.^{5,10} It showed that disease control and overall survival were similar for SABR and CFRT, although SABR was better considering some side effects and quality of life. However, this study had limited power (67%), and a larger randomized controlled trial (RCT) is required.¹⁰

Statement of general knowledge

PubMed for published reports using the keywords ([*stereotactic radiotherapy*] OR [*stereotactic body radiotherapy*] OR [*stereotactic ablative radiotherapy*] OR [SBRT] OR [SABR]) AND ([*non-small cell lung cancer*] OR [NSCLC]) AND ([*survival*] OR [OS]) was searched on Sep 2nd 2017, for evidence regarding the efficacy of SABR *vs.* CFRT. In addition to the

aforementioned SPACE trial, we identified another small (n = 50) randomized study showing better treatment efficacy for SABR compared to CFRT in peripheral NSCLC.¹¹ However, patients of various stages (stages I–IV) were included in the study, and the results of stage I patients were not reported. We also found a meta-analysis (published in 2010) that reported better overall survival (OS) for SABR compared to CFRT, but all of the included studies were nonrandomized.¹² In addition, none of the included studies directly compared SABR and CFRT.¹² We also found four subsequent single institutional nonrandomized studies from Europe or North America and two subsequent population-based studies from North America.¹³⁻¹⁸ However, to the best of our knowledge, no population-based study from Asia has compared SABR *vs.* CFRT for treating early-stage NSCLC.

Study aim

Given the relatively limited evidence on this topic, we investigated the effectiveness of SABR *vs.* CFRT

TABLE 1. Patient characteristics for the whole study population

		SABR		CFRT		Standardized difference (rounded)*	
		Number or mean (sd) [†]	(%) [‡]	Number or mean (sd) [†]	(%) [‡]	Before IPW	After IPW
Age		77.81 (7.85)		75.40 (9.96)		0.27	0.24
Sex	Female	20	(29)	44	(26)	0.07	0.07
	Male	49	(71)	125	(74)		
Residency	Non-north	32	(46)	93	(55)	0.17	0.19
	North	37	(54)	76	(45)		
Comorbidity	Without	9	(13)	43	(25)	0.32	0.25
	With [†]	60	(87)	126	(75)		
Histology	Adenocarcinoma	40	(58)	82	(49)	0.19	0.24
	Non-adenocarcinoma	29	(42)	87	(51)		
T stage	T1	38	(55)	49	(29)	0.55	0.08
	T2	31	(45)	120	(71)		
Period	2007–2009	15	(22)	65	(38)	0.37	0.22
	2010–2013	54	(78)	104	(62)		
Use of PET	Yes	37	(54)	55	(33)	0.44	0.09
	No	32	(46)	114	(67)		
Use of systemic therapy	Yes	10	(14)	73	(43)	0.67	0.17
	No	59	(86)	96	(57)		
Previous cancer	Yes	9	(13)	16	(9)	0.11	0.06
	No	60	(87)	153	(91)		

CFRT = conventional fractionated radiotherapy; IPW = inverse probability weighting; PET = positron emission tomography; SABR = stereotactic ablative radiotherapy; sd = standard deviation; [†]modified Carlson comorbidity score ≥ 1 ; [‡]rounded at the second

for non-operated early-stage NSCLC in a population-based sample from Taiwan.

Patients and methods

Data source

The Health and Welfare Data Science Center (HWDC) database is a set of databases providing complete information regarding the Taiwan cancer registry, death registry, and reimbursement data for the whole Taiwanese population provided by the Bureau of National Health Insurance (NHI).¹⁹ The high quality of this cancer registry has been reported.²⁰ NHI is a single-payer, compulsory social insurance program that provides insurance coverage to the majority of citizens in Taiwan.²¹ All of the above data were included in the HWDC with deidentified personal identifiers.

Identification of study cases and study design

A flowchart showing the identification of study cases appears in Figure 1 as suggested by the Strengthening the Reporting of Observational Studies in Epidemiology (STROBE) guideline.²² Briefly, we identified stage I histology-documented NSCLC patients diagnosed from 2007 to 2013 who received either CFRT or SABR without surgery. We used the date of diagnosis as the index date. We determined the explanatory variable of interest (CFRT *vs.* SABR) based on the record in the cancer registry using the dose/fractionation recommended by the National Comprehensive Cancer Network (NCCN) NSCLC guideline (CFRT: 60–70 Gy in 1.8–2 Gy/fraction; SABR: 25–34 Gy/1 fraction, or 45–60 Gy/3 fractions, or 48–50 Gy/4 fractions, or 50–55 Gy/5 fractions, or 60–70 Gy/8–10 fractions).¹ We also collected other covariate and outcome data from the HWDC. We decided on covariates (age, sex, residency, comorbidity, histology, T stage, period, use of positron emission tomography [PET], use of systemic therapy, and previous cancer) based on our clinical and HWDC-related research experiences as well as previous reports.^{23–25} The covariates were defined as follows. Patient residency was classified as northern Taiwan or elsewhere. We included this covariable because geographic practice variation had been report in the literature²⁶ and we felt it might influence treatment choice in our clinical and research experiences.²⁴ Comorbidity was defined as with or without a modified Carlson comorbidity score ≥ 1 , as used in our previous

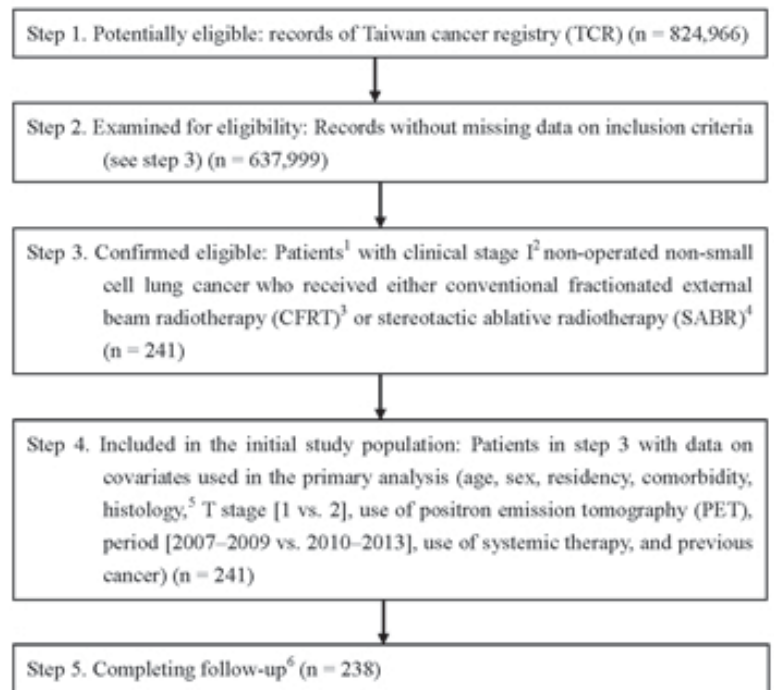


FIGURE 1. The Strengthening the Reporting of Observational Studies in Epidemiology (STROBE) study flowchart and the number of individuals at each stage of the study.

¹ We only included those treated (class 1–2) at a single institution to ensure data consistency. ² Sixth (2007–2009) or Seventh (2010–2013) American Joint Committee on Cancer. ³ 60–70 Gy in 1.8–2 Gy/fraction, $\pm 10\%$ in dose. ⁴ Dose/fraction compatible with National Comprehensive Cancer Network non-small cell lung cancer guideline 2017 v8 [i.e., 25–34 Gy/1 fraction, or 45–60 Gy/3 fractions, or 48–50 Gy/4 fractions, or 50–55 Gy/5 fractions, or 60–70 Gy/8–10 fractions], $\pm 10\%$ in dose. ⁵ Adenocarcinoma or non-adenocarcinoma. ⁶ Without missing information in the Taiwan cancer registry and death registry.

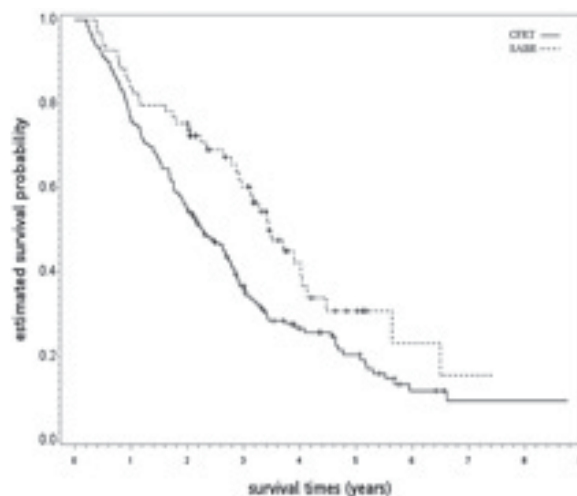


FIGURE 2. Kaplan-Meier survival curve for the whole study population.

CFRT = conventional fractionated radiotherapy; SABRT = stereotactic ablative radiotherapy

NHI cancer study.²⁴ Histology was classified as adenocarcinoma or non-adenocarcinoma. T stage was classified as T1 *vs.* T2. Period was classified as 2007–2009 or 2010–2013 because staging was changed since 2010. Use of PET, systemic therapy, and previous cancer was classified as yes or no. We used the national death registry to determine survival status and used OS as our endpoint, as initially completed in the SPACE trial.¹⁰ This study was approved by the Research ethics committee at our institute (CMUH104-REC-002).

Statistical analysis

We used the Kaplan-Meier method and log-rank test to compare crude OS between patients treated with SABR *vs.* CFRT. We further used inverse probability weighting (IPW) based on the propensity score (PS) as the primary means of analysis to address the nonrandomization of treatment.²⁷ We modeled the use of SABR *vs.* CFRT as the dependent variable and the above covariates as independent variables and used logistic regression to model the probability of receiving SABR. Then we used the logit of the probability as the PS, as described previously.²⁷ Tabulation and standardized differences were used to assess the balance of covariates between treatment groups.^{27,28} We used a weighted Cox model to compare OS between treatment groups for the entire follow-up period (censored on December 31, 2015).^{27,29} We used bootstrap analysis to obtain confidence intervals and p-values, as described previously.³⁰ For OS results with statistical significance, we further calculated the E-factor to evaluate the robustness of our finding regarding potential unmeasured confounder[s] as suggested in the recent literature.³¹

Supplementary analyses

In the first supplementary analysis (SA-1), we constructed a subgroup based on PS matching and used a robust variance estimator to compare OS and lung cancer-specific survival of patients treated with SABR *vs.* CFRT. We also used cause of death to obtain lung cancer-specific survival (LCSS). In the second supplementary analysis (SA-2), we constructed another subgroup by PS matching limited to cases from 2011 to 2013 to use the additional covariate (performance status, classified as Eastern Cooperative Oncology Group [ECOG] 0–2 *vs.* 3–4) in PS modeling to compare the survival of patients treated with SABR *vs.* CFRT. We limited to this period [2011–2013] because performance in-

formation was available in Taiwan cancer registry since 2011. SAS 9.4 (SAS Institute, Cary, NC) was used for all analyses.

Results

Identification of study cases

As shown in Figure 1, we found 238 clinical stage I NSCLC patients who received either SABR or CFRT from 2007 to 2013 were included in our primary analysis. The characteristics of these patients are described in Table 1. Although an imbalance in covariate distribution was observed before PS weighting such as higher percentage of patients with comorbidity received SABR [32%] than those without comorbidity [17%], a good balance of covariates and small standardized differences (≤ 0.25) were observed for all covariates after we adjusted for PS weighting.^{28,32}

Primary analysis

After a median follow-up of 28 months (range 2–105), 171 patients were found to have died (40 SABR and 131 CFRT). We found that SABR led to higher crude OS compared to CFRT, as shown in Figure 2. The 5-year OS rates for SABR and CFRT were 31% and 20%, respectively (log-rank test, $p = 0.0008$). After IPW, OS was not significantly different between those treated with SABR *vs.* CFRT (SABR *vs.* CFRT: IPW adjusted hazard ratio [HR] 0.586, 95% confidence interval 0.264–1.101, $p = 0.102$).

Supplementary analyses

In SA-1, a good balance of covariates was observed with small standardized differences (≤ 0.25) for the PS-matched subgroup ($n = 120$; see Table 2). Compared to CFRT, the OS (HR 0.672, $p = 0.039$) and LCSS (HR 0.529, $p = 0.007$) of patients receiving SABR were superior. The observed HR 0.672 for OS could be explained away by an unmeasured confounder that was associated with both selections of SABR/CFRT and live/death by a risk ratio of 1.96 fold each, but weaker confounding could not do so. The OS curve is shown in Figure 3. In SA-2, well-balanced covariates were observed with small standardized differences (≤ 0.25) when cases were limited to 2011 to 2013 with an available performance status ($n = 52$; see Table 3), although there were some imbalances before matching such as those with poor performance status [ECOG 3–4] were more likely to

TABLE 2. Patient characteristics in the first supplementary analysis

		SABR		CFRT		Standardized difference (rounded)*
		Number or mean (sd) [†]	(%) [*]	Number or mean (sd) [†]	(%) [*]	
Age		77.47 (8.26)		77.75 (9.79)		0.03
Sex	Female	18	(30)	24	(40)	0.21
	Male	42	(70)	36	(60)	
Residency	Non-north	29	(48)	30	(50)	0.03
	North	31	(52)	30	(50)	
Comorbidity	Without	9	(15)	8	(13)	0.05
	With [†]	51	(85)	52	(87)	
Histology	Adenocarcinoma	37	(62)	41	(68)	0.14
	Non-adenocarcinoma	23	(38)	19	(32)	
T stage	T1	30	(50)	31	(52)	0.03
	T2	30	(50)	29	(48)	
Period	2007–2009	15	(25)	15	(25)	0.00
	2010–2013	45	(75)	45	(75)	
Use of PET	Yes	30	(50)	31	(52)	0.03
	No	30	(50)	29	(48)	
Use of systemic therapy	Yes	10	(17)	13	(22)	0.13
	No	50	(83)	47	(78)	
Previous cancer	Yes	8	(13)	7	(12)	0.05
	No	52	(87)	53	(88)	

CFRT = conventional fractionated radiotherapy; PET = positron emission tomography; SABR = stereotactic ablative radiotherapy; sd = standard deviation; [†] modified Carlson comorbidity score ≥ 1; * rounded at the second

receive SABR [60%] than those with acceptable performance status [33%]. We found SABR was associated with further improvement in hazard for death (HR 0.381, $p = 0.016$) compared to CFRT, as seen in Figure 4. The observed HR 0.381 for OS could be explained away by an unmeasured confounder that was associated with both selections of SABR/CFRT and live/death by a risk ratio of 3.29 fold each, but weaker confounding could not do so.

Discussion

In this population-based PS-adjusted analysis, we provide the first empirical evidence from Asia regarding non-operated early-stage NSCLC patients treated with either SABR or CFRT. We found that OS was not significantly different between those treated with SABR vs. CFRT in the primary analysis, although statistical significance was observed in the supplementary analyses.

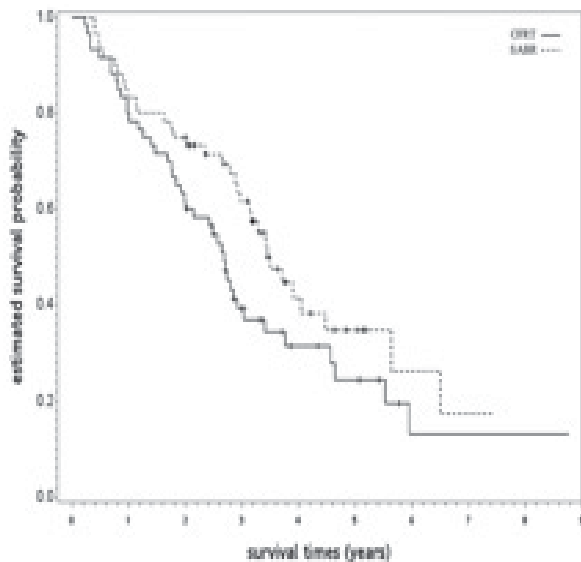


FIGURE 3. Kaplan-Meier survival curve for the first supplementary analysis.

CFRT = conventional fractionated radiotherapy; SABRT = stereotactic ablative radiotherapy

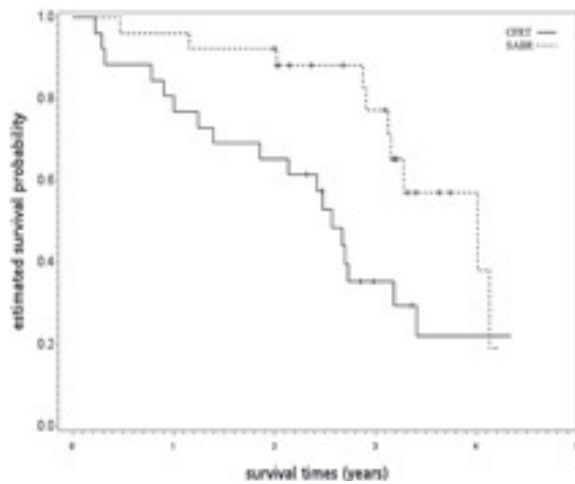


FIGURE 4. Kaplan-Meier survival curve for the second supplementary analysis.

CFRT = conventional fractionated radiotherapy; SABRT = stereotactic ablative radiotherapy

Our results may be interpreted as compatible with the SPACE trial in that OS was not significantly different between those treated with SABR *vs.* CFRT. On the contrary, because the point estimate of HR for death was around 0.6, SABR may lead to better OS, but the statistical significance was limited by the moderate sample size. The statistical significance found in our SA supported this hypothesis, as reported in other studies from Europe and North America, and indirect comparison in a previous meta-analysis showed that SABR led to better survival.¹²⁻¹⁸ Therefore, our results should not be interpreted as conclusive.

Our study provides additional evidence for practitioners considering SABR in addition to conventional CFRT for non-operated early-stage NSCLC.³³ Although the available randomized data did not support the superior efficacy of SABR compared to CFRT, the power of that study was limited and is not compatible with previous retrospective data.¹⁰ Although the results of our primary analysis were not significant, the trend was in favor of SABR (HR 0.59), and similar trends with statistical significance were observed in SA. Furthermore, we observed that patients with comorbidity or poor performance status were more likely to receive SABR in the pre-matched population (*i.e.*, SABR patients were possibly prone to die from competing death), so it is possible that SABR had improved LCSS [HR 0.529] but OS benefit was less obvious [HR 0.72] as seen in our SA-1. Therefore, our study may be used by practitioners to select treatment for non-operated early-stage NSCLC

while awaiting results from ongoing RCTs (such as NCT01968941 or NCT01014130).

There are some limitations to our study. First, the sample size was moderate, particularly in both supplementary analyses, which severely limits statistical power [around 0.5 ~ 0.8 in the setting of our SA]. Second, identification of the study population may be inhomogeneous because a higher dose may be more effective, although we used the NCCN criteria to classify SABR *vs.* CFRT.³⁴ Third, treatment selection was not random or specified. The reason for choosing radiotherapy but not surgery was not available due to data limitation. In addition, the reason for choosing SABR or CFRT remains unclear. Unobservable bias is possible in retrospective studies, and results of the aforementioned ongoing trials are required. For example, the location of the primary tumor (central *vs.* peripheral) or lung function test results were not known and could have been unbalanced, even after we matched for observable covariates.³⁵ Epidermal growth factor receptor (EGFR) status may also have been unbalanced. Population variation in treatment response is an emerging issue, and highly prevalent EGFR mutations in Asia (including Taiwan) is a well-known example.³⁶ Adjuvant EGFR-directed treatment may even improve the outcomes of resected NSCLC.³⁷ However, we found our result was somehow robust [E-factor 3.29] to potential unmeasured confounder(s). Fourth, other endpoints such as local control were not available due to data limitation, although no difference in local control was reported in the SPACE trial.¹⁰

Conclusions

In this population-based PS-adjusted analysis, we provide the first empirical evidence from Asia regarding non-operated early-stage NSCLC patients treated with either SABR or CFRT. We found that OS was not significantly different in the primary analysis between those treated with SABR *vs.* CFRT, although statistical significance was observed in supplementary analyses. Thus, the results of ongoing randomized controlled studies are required.

Acknowledgements

The data analyzed in this study was provided by the Health and Welfare Data Science Center, Ministry of Health and Welfare, Taiwan. This

TABLE 3. Patient characteristics in the second supplementary analysis

		SABR		CFRT		Standardized difference (rounded)*
		Number or mean (sd)*	(%)*	Number or mean (sd)*	(%)*	
Age		76.92 (8.84)		77.73 (9.19)		0.09
Sex	Female	8	(31)	7	(27)	0.09
	Male	18	(69)	19	(73)	
Residency	Non-north	16	(62)	18	(69)	0.16
	North	10	(38)	8	(31)	
Comorbidity	Without	#		#		0.13
	With†	#		#		
Histology	Adenocarcinoma	14	(54)	15	(58)	0.08
	Non-adenocarcinoma	12	(46)	11	(42)	
T stage	T1	11	(42)	11	(42)	0.00
	T2	15	(58)	15	(58)	
Use of PET	Yes	13	(50)	12	(46)	0.08
	No	13	(50)	14	(54)	
Use of systemic therapy	Yes	#		#		0.13
	No	#		#		
Previous cancer	Yes	3	(12)	3	(12)	0.00
	No	23	(88)	23	(88)	
Performance status	ECOG (0-2)	#		#		0.00
	ECOG (3-4)	#		#		

CFRT = conventional fractionated radiotherapy; ECOG = Eastern Cooperative Oncology Group; PET = positron emission tomography; SABR = stereotactic ablative radiotherapy; sd = standard deviation; † modified Carlson comorbidity score ≥ 1; * rounded at the second; # Exact numbers are not reported because the Health and Welfare Data Science Center (HWDC) database center policy is to avoid numbers in single cells ≤ 2

work was supported by China Medial University Hospital [DMR-105-046]. The corresponding author would like to thank Dr. Ya-Chen Tina Shih for her suggestions in study design. The authors thank “Textcheck” for professional writing assistance.

References

- National Comprehensive Cancer Network Guideline for Non-Small Cell Lung Cancer, version 8. 2017. [Cited 14 Jul 2017]. Available at: https://www.nccn.org/professionals/physician_gls/pdf/nscl.pdf.
- Baker S, Dahele M, Lagerwaard FJ, Senan S. A critical review of recent developments in radiotherapy for non-small cell lung cancer. *Radiat Oncol* 2016; **11**: 115. doi: 10.1186/s13014-016-0693-8
- Ricardi U, Badellino S, Filippi AR. Stereotactic body radiotherapy for early stage lung cancer: history and updated role. *Lung Cancer* 2015; **90**: 388-96. doi: 10.1016/j.lungcan.2015.10.016
- Guckenberger M, Andratschke N, Alheit H, Holy R, Moustakis C, Nestle U, et al. Definition of stereotactic body radiotherapy: principles and practice for the treatment of stage I non-small cell lung cancer. *Strahlenther Onkol* 2014; **190**: 26-33. doi: 10.1007/s00066-013-0450-y
- Murray P, Franks K, Hanna GG. A systematic review of outcomes following stereotactic ablative radiotherapy in the treatment of early-stage primary lung cancer. *Br J Radiol* 2017; **90**: 20160732. doi: 10.1259/bjr.20160732
- Timmerman R, Paulus R, Galvin J, Michalski J, Straube W, Bradley J, et al. Stereotactic body radiation therapy for inoperable early stage lung cancer. *JAMA* 2010; **303**: 1070-6. doi: 10.1001/jama.2010.261
- Chang JY, Senan S, Paul MA, Mehran RJ, Louie AV, Balter P, et al. Stereotactic ablative radiotherapy versus lobectomy for operable stage I non-small-cell lung cancer: a pooled analysis of two randomised trials. *Lancet Oncol* 2015; **16**: 630-7. doi: 10.1016/S1470-2045(15)70168-3
- Dionisi F, Guarneri A, Dell'Acqua V, Leonardi M, Niespolo R, Macchia G, et al. Radiotherapy in the multidisciplinary treatment of liver cancer: a survey on behalf of the Italian Association of Radiation Oncology. *Radiol Med* 2016; **121**: 735-43. doi: 10.1007/s11547-016-0650-5
- Matsuo Y, Yoshida K, Nishimura H, Ejima Y, Miyawaki D, Uezono H, et al. Efficacy of stereotactic body radiotherapy for hepatocellular carcinoma with portal vein tumor thrombosis/inferior vena cava tumor thrombosis: evaluation by comparison with conventional three-dimensional conformal radiotherapy. *J Radiat Res* 2016; **57**: 512-23. doi: 10.1093/jrr/rrw028
- Nyman J, Hallqvist A, Lund J, Brustugun OT, Bergman B, Bergström P, et al. SPACE - a randomized study of SBRT vs conventional fractionated radiotherapy in medically inoperable stage I NSCLC. *Radiother Oncol* 2016; **121**: 1-8. doi: 10.1016/j.radonc.2016.08.015
- Wang SW, Ren J, Yan YL, Xue CF, Tan L, Ma XW. Effect of image-guided hypofractionated stereotactic radiotherapy on peripheral non-small-cell lung cancer. *Onco Targets Ther* 2016; **9**: 4993-5003. doi: 10.2147/OTT.S101125
- Grutters JP, Kessels AG, Pijls-Johannesma M, De Ruyscher D, Joore MA, Lambin P. Comparison of the effectiveness of radiotherapy with photons, protons and carbon-ions for non-small cell lung cancer: a meta-analysis. *Radiother Oncol* 2010; **95**: 32-40. doi: 10.1016/j.radonc.2009.08.003

13. Jeppesen SS, Schytte T, Jensen HR, Brink C, Hansen O. Stereotactic body radiation therapy versus conventional radiation therapy in patients with early stage non-small cell lung cancer: an updated retrospective study on local failure and survival rates. *Acta Oncol* 2013; **52**: 1552-8. doi: 10.3109/0284186X.2013.813635
14. Widder J, Postmus D, Ubbels JF, Wiegman EM, Langendijk JA. Survival and quality of life after stereotactic or 3D-conformal radiotherapy for inoperable early-stage lung cancer. *Int J Radiat Oncol Biol Phys* 2011; **81**: e291-7. doi: 10.1016/j.ijrobp.2011.03.052
15. Shirvani SM, Jiang J, Chang JY, Welsh JW, Gomez DR, Swisher S, et al. Comparative effectiveness of 5 treatment strategies for early-stage non-small cell lung cancer in the elderly. *Int J Radiat Oncol Biol Phys* 2012; **84**: 1060-70. doi: 10.1016/j.ijrobp.2012.07.2354
16. Liu HW, Gabos Z, Ghosh S, Roberts B, Lau H, Kerba M. Outcomes in stage I non-small cell lung cancer following the introduction of stereotactic body radiotherapy in Alberta - A population-based study. *Radiation Oncol* 2015; **11**: 71-6. doi: 10.1016/j.radonc.2015.08.027
17. Lanni TB Jr, Grills IS, Kestin LL, Robertson JM. Stereotactic radiotherapy reduces treatment cost while improving overall survival and local control over standard fractionated radiation therapy for medically inoperable non-small-cell lung cancer. *Am J Clin Oncol* 2011; **34**: 494-8. doi: 10.1097/JCO.0b013e3181ec63ae
18. Mitera G, Swaminath A, Rudoler D, Seereeram C, Giuliani M, Leigh N, et al. Cost-effectiveness analysis comparing conventional versus stereotactic body radiotherapy for surgically ineligible stage I non-small-cell lung cancer. *J Oncol Pract* 2014; **10**: e130-6. doi: 10.1200/JOP.2013.001206
19. The Health and Welfare Data Science Center database (in Chinese). [Cited 18 Jul 2017]. Available at: <http://dep.mohw.gov.tw/DOS/np-2497-113.html>.
20. Chiang CJ, You SL, Chen CJ, Yang YW, Lo WC, Lai MS. Quality assessment and improvement of nationwide cancer registration system in Taiwan: a review. *Jpn J Clin Oncol* 2015; **45**: 291-6. doi: 10.1093/jco/hyu211
21. Universal Health Coverage in Taiwan. [Cited 15 Jul 2017]. Available at:
22. National Health Insurance. 2016-2017 Annual report. Chapter 2. Comprehensive services, reasonable payments. Available at https://www.nhi.gov.tw/Resource/webdata/21717_1_UniversalHealthCoverage-2.pdf.
23. von Elm E, Altman DG, Egger M, Pocock SJ, Gøtzsche PC, Vandenbroucke JP, et al. The Strengthening the Reporting of Observational Studies in Epidemiology (STROBE) Statement: guidelines for reporting observational studies. *Int J Surg* 2014; **12**: 1495-9. doi: 10.1016/j.ijsu.2014.07.013
24. Hsia TC, Tu CY, Fang HY, Liang JA, Li CC, Chien CR. Cost and effectiveness of image-guided radiotherapy for non-operated localized lung cancer: a population-based propensity score-matched analysis. *J Thorac Dis* 2015; **7**: 1643-9. doi: 10.3978/j.issn.2072-1439.2015.09.36
25. Chien CR, Pan IW, Tsai YW, Tsai T, Liang JA, Buchholz TA, et al. Radiation therapy after breast-conserving surgery: does hospital surgical volume matter? A population-based study in Taiwan. *Int J Radiat Oncol Biol Phys* 2012; **82**: 43-50. doi: 10.1016/j.ijrobp.2010.09.025
26. Jelercic S, Rajer M. The role of PET-CT in radiotherapy planning of solid tumours. *Radiation Oncol* 2015; **49**: 1-9. doi: 10.2478/raon-2013-0071
27. Schroeder MC, Tien YY, Wright K, Halfdanarson TR, Abu-Hejleh T, Brooks JM. Geographic variation in the use of adjuvant therapy among elderly patients with resected non-small cell lung cancer. *Lung Cancer* 2016; **95**: 28-34. doi: 10.1016/j.lungcan.2016.02.010
28. Austin PC. The use of propensity score methods with survival or time-to-event outcomes: reporting measures of effect similar to those used in randomized experiments. *Stat Med* 2014; **33**: 1242-58. doi: 10.1002/sim.5984
29. Austin PC, Stuart EA. Moving towards best practice when using inverse probability of treatment weighting (IPTW) using the propensity score to estimate causal treatment effects in observational studies. *Stat Med* 2015; **34**: 3661-79. doi: 10.1002/sim.6607
30. Cole SR, Hernán MA. Adjusted survival curves with inverse probability weights. *Comput Methods Programs Biomed* 2004; **75**: 45-9. doi:10.1016/j.cmpb.2003.10.004
31. Austin PC. Variance estimation when using inverse probability of treatment weighting (IPTW) with survival analysis. *Stat Med* 2016; **35**: 5642-55. doi: 10.1002/sim.7084.
32. VanderWeele TJ, Ding P. Sensitivity analysis in observational research: introducing the E-Value. *Ann Intern Med* 2017; **167**: 268-74. doi: 10.7326/M16-2607
33. Garrido MM, Kelley AS, Paris J, Roza K, Meier DE, Morrison RS, et al. Methods for constructing and assessing propensity scores. *Health Serv Res* 2014; **49**: 1701-20. doi: 10.1111/1475-6773.12182
34. Rosenbaum PR. Reasons for Effects. In: Rosenbaum PR, editor. Design of observational studies (Springer Series in Statistics). New York: Springer; 2010. p. 104-7. doi: 10.1007/978-1-4419-1213-8
35. Koshy M, Malik R, Weichselbaum RR, Sher DJ. Increasing radiation therapy dose is associated with improved survival in patients undergoing stereotactic body radiation therapy for stage I non-small-cell lung cancer. *Int J Radiat Oncol Biol Phys* 2015; **91**: 344-50. doi: 10.1016/j.ijrobp.2014.10.002
36. Chang JY, Bezjak A, Mornex F; IASLC Advanced Radiation Technology Committee. Stereotactic ablative radiotherapy for centrally located early stage non-small-cell lung cancer: what we have learned. *J Thorac Oncol* 2015; **10**: 577-85. doi: 10.1097/JTO.0000000000000453
37. Ma BB, Hui EP, Mok TS. Population-based differences in treatment outcome following anticancer drug therapies. *Lancet Oncol* 2010; **11**: 75-84. doi: 10.1016/S1470-2045(09)70160-3
38. Wu YL, Zhong W, Wang Q, Xu ST, Mao WM, Wu L, et al. Gefitinib (G) versus vinorelbine+cisplatin (VP) as adjuvant treatment in stage II-IIIA (N1-N2) non-small-cell lung cancer (NSCLC) with EGFR-activating mutation (ADJUVANT): a randomized, Phase III trial (CTONG 1104). [Abstract]. 2017 ASCO Annual Meeting; *J Clin Oncol* 2017; **35**(15 Suppl): 8500. doi: 10.1200/JCO.2017.35.15_suppl.8500

Survival and stability of patients with urothelial cancer and spinal bone metastases after palliative radiotherapy

Robert Foerster^{1,3}, Katharina Hees², Thomas Bruckner², Tilman Bostel^{1,3}, Ingmar Schlamp^{1,3}, Tanja Sprave^{1,3}, Nils H. Nicolay^{1,3}, Juergen Debus^{1,3}, Harald Rief^{1,3}

¹ Department of Radiation Oncology, University Hospital Heidelberg, Heidelberg, Germany

² Department of Medical Biometry, University Hospital Heidelberg, Heidelberg, Germany

³ National Center for Radiation Research in Oncology (NCRO), Heidelberg Institute for Radiation Oncology (HIRO), Heidelberg, Germany

Radiol Oncol 2018; 52(2): 189-194.

Received 9 June 2017

Accepted 14 August 2017

Correspondence to: Harald Rief, M.D., Ph.D., Department of Radiation Oncology, University Hospital Heidelberg, Im Neuenheimer Feld 400, 69120 Heidelberg, Germany. Phone: +49 6221 56 8202; Fax: +49 6221 56 5353; E-mail: harald.rief@gmx.at

Disclosure: No potential conflicts of interest were disclosed.

Background. The aim of the study was to analyze survival and stability of patients with urothelial cell cancer and spinal bone metastases (SBM) after radiotherapy (RT). Furthermore, to assess the effects of RT on bone mineral density (BMD) as a local response in SBM after RT.

Patients and methods. Survival of 38 patients with 132 SBM from urothelial cancer, treated from January 2000 to January 2012, was calculated. Stability of irradiated thoracic and lumbar SBM was retrospectively evaluated in computed tomography (CT) scans using the validated Taneichi *et al.* score. Difference in BMD, measured in Hounsfield units (HU), of the SBM before and at 3 and 6 months after RT was analyzed.

Results. All patients died during follow-up. Overall survival (OS) after 6 months, 1 year and 2 years was 90%, 80% and 40%, respectively. Bone survival (BS) was 85%, 64% and 23% after 6 months, 1 year and 2 years, respectively. Survival from start of RT (RTS) was 42% after 6 months, 18% after 1 year and 5% after 2 years. Only 11% received bisphosphonates. Stability did not improve at 3 or 6 months after RT. BMD increased by 25.0 HU \pm 49.7 SD after 3 months ($p = 0.001$) and by 24.2 HU \pm 52.2 SD after 6 months ($p = 0.037$). Pain relief (≥ 2 points on the visual analogue scale) was achieved in only 27% of patients.

Conclusions. Benefit from palliative RT of painful or unstable SBM is limited in these patients and they should be carefully selected for RT. Shorter fractionation schedules may be preferred and outcome may improve with concomitant bisphosphonates.

Key words: bone density; bone metastases; stability; survival; urothelial cancer

Introduction

Approximately one quarter of patients with metastatic urothelial cancer present with bone metastases.¹ Spinal bone metastases (SBM) are commonly associated with drug-resistant pain, pathological fractures and neurological complications, resulting in substantial morbidity and reduced quality of life (QoL).

Treatment of these patients requires an interdisciplinary approach and palliative radiotherapy

(RT) remains the most important treatment option, particularly for persistent pain, existing or impending instability and neurological symptoms due to malignant spinal cord compression.² The bone stability score introduced by Taneichi *et al.* has been validated to provide an instrument to estimate the probability of collapse of bone metastases.³ The usage of a validated scoring tool for the assessment of SBM stability may prevent physicians from overdiagnosis of instability and hence improve QoL

A Taneichi score for the thoracic spine

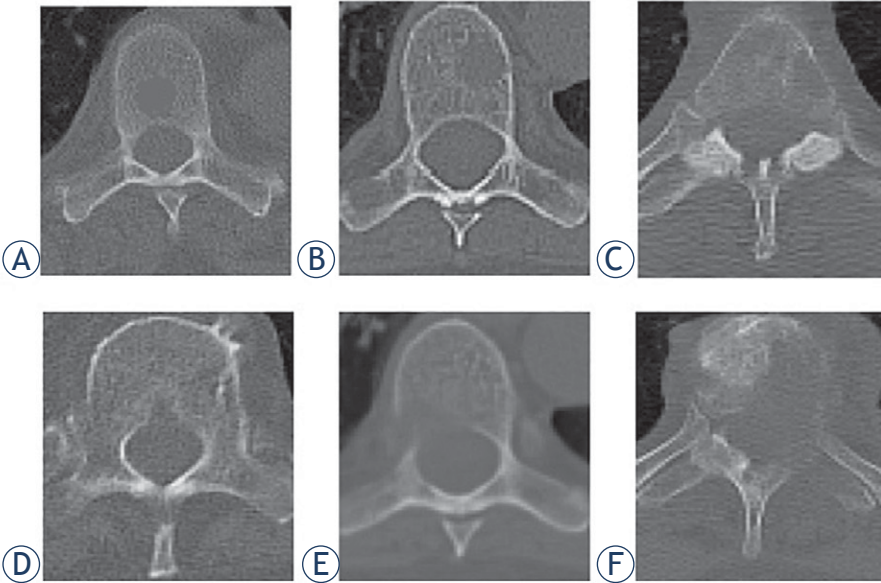
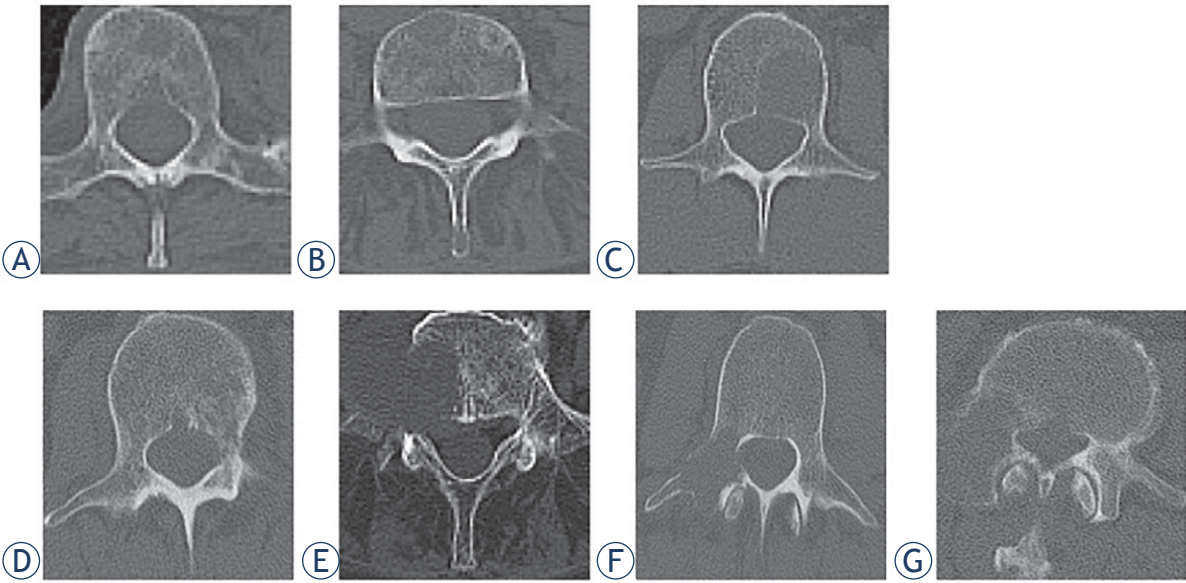


FIGURE 1. Taneichi *et al.* score for spinal bone metastases of the (A) thoracic and (B) lumbar spine.

B Taneichi score for the lumbar spine



A Taneichi score for the thoracic spine						
	A	B	C	D	E	F
Tumor occupancy vertebral body	30%	60%	30%	60%	30%	60%
Costovertebral joint destruction	No	No	Yes	Yes	Yes	Yes
Pedicle destruction	No	No	No	No	Yes	Yes
Posterior elements destruction	No	No	No	No	No	Yes
Predicted probability of collapse	0.13	0.68	0.57	0.96	0.71	0.98

B Taneichi score for the lumbar spine							
	A	B	C	D	E	F	G
Tumor occupancy vertebral body	20%	30%	40%	40%	60%	5%	20%
Pedicle destruction	No	No	No	Yes	Yes	Yes	Yes
Posterior elements destruction	No	No	No	No	Yes	Yes	Yes
Predicted probability of collapse	0.07	0.25	0.60	0.99	0.99	0.06	0.38

of palliative patients. In earlier studies, we demonstrated that re-ossification and stability can be improved by RT in patients with SBM from non-small cell lung cancer (NSCLC), breast cancer, and gynecologic malignancies.^{4,6} We were also able to show that quantification of bone density within metastases can be accurately and easily used to evaluate local response after RT.^{7,8} However, in two studies with patients suffering from renal cancer and malignant melanoma, stabilization of SBM was not achieved.^{9,10} With this retrospective study, we aimed to analyze survival and clinical outcome of patients with SBM from urothelial cancer as well as to systematically assess bone mineral density (BMD) and stability before and after RT in SBM of these patients.

Patients and methods

All patients were treated with palliative RT for SBM from histologically diagnosed urothelial cancer at the Department of Radiation Oncology, University Hospital Heidelberg between January 2000 and January 2012. Patients' data including survival status were collected from the institutional cancer registry. Patients received regular clinical follow-up examinations and computed tomography (CT) scans at 3 and 6 months after RT. All patients were included in the survival analyses.

Nineteen patients with osteolytic SBM of the thoracic or lumbar spine, and a minimum duration of follow-up to treatment of 6 months were included in the stability analyses. For each patient, the most severe metastasis according to the Taneichi *et al.* score was evaluated in the analysis. Bone metastases were diagnosed by CT, magnetic-resonance imaging or bone-scintigraphy scans. Treatment planning CT scans were used to assess stability based on the Taneichi *et al.* score prior to RT; at 3 and 6 months after RT, stability was reassessed using follow-up CT imaging. Osteolytic metastases were rated on a scale from A to G. Subtypes A to C were defined as stable and subtypes D to G as unstable (Figure 1). Height reduction by at least 20% or visible fracture lines were defining for a new pathological fracture. New partial fractures of a vertebral body did not mandatorily influence the stability score. To assess BMD, we measured Hounsfield units (HU) within the bone metastases by manual regions of interest setting (Figure 2) before RT and 3 months as well as 6 months after RT.

This study was conducted in accordance with the declaration of Helsinki and was approved by

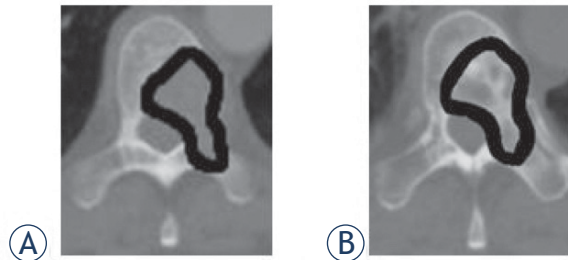


FIGURE 2. Bone mineral density measurement in Hounsfield units by manual region of interest setting (A) before radiotherapy and (B) after radiotherapy within the spinal bone metastases.

the independent ethics committee of the University of Heidelberg on 22 October 2012 (# S-513/2012). The requirement of informed consent was waived by the ethics committee, due to the retrospective nature of the study.

Patients' characteristics

RT was performed for osseous instability in 18.5% (n = 7), for pain in 78.9% (n = 30), and for neurological symptoms in 2.6% (n = 1) of patients. Pain and neurological deficits as well as their alterations after RT were recorded during the follow-up examinations, in case they were linked to the irradiated area. Prior fractures affecting the vertebrae in the treated area were detected in the treatment planning CT scans in 10 patients (26.3%). In 1 patient (3%), a new fracture was found after RT. Nine patients (24%) also had distant metastases in other organs. Most patients were males (n = 30, 79%) and had a Karnofsky performance status (KPS) < 80% (n = 29; 76.3%). Fourteen patients (37%) had received chemotherapy (ChT) with cisplatin and gemcitabine prior to RT. Only 4 patients (10.5%) received concomitant bisphosphonates (Table 1).

Radiotherapy

RT planning was performed based on CT scans, and treatment was performed using a posterior photon field with an energy of 6 MV. The planning target volume (PTV) covered the affected vertebral body as well as those immediately above and below. The fractionation schedule was selected individually for each patient, depending on the patient's general state of health, the current staging, response to current therapy and the respective prognosis. The most frequent fractionation schedule was 10 × 3 Gy (Table 1).

TABLE 1. Patients' characteristics of all patients with urothelial cancer and spinal bone metastases

Patients' characteristics		
Age		
Median	70 years	
Range	35–82 years	
	n	%
Gender		
Female	8	21.0%
Male	30	79.0%
Karnofsky performance status		
40–60%	12	31.6%
70%	17	44.7%
80%	9	23.7%
Histology		
Urothelial carcinoma	38	100%
Localization of metastases		
Thoracic	18	47.4%
Lumbar	20	52.6%
Number of metastases		
Single	15	39.5%
Multiple	23	60.5%
Distant extra-osseous metastases		
Overall	9	23.7%
Lungs	6	15.8%
Liver	5	13.2%
Brain	2	5.3%
Surgical corset		
Yes	6	15.8%
No	32	84.2%
Treatment indications		
Instability	7	18.4%
Neurological symptoms	1	2.6%
Pain	30	79.0%
Radiotherapy schedule		
10 x 3 Gy	24	63.2%
14 x 2.5 Gy	3	7.9%
20 x 2 Gy	11	28.9%
Systemic therapy		
Chemotherapy	14	36.8%
Bisphosphonates	4	10.5%

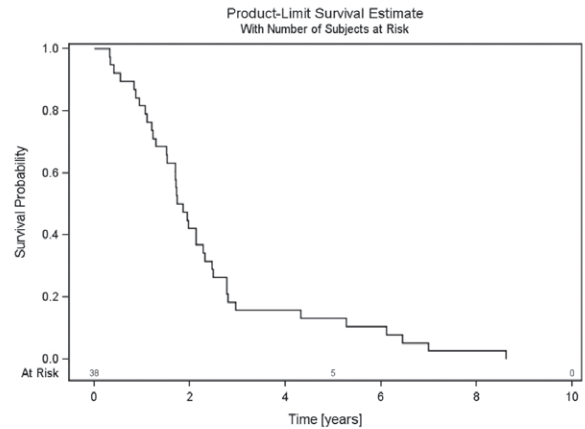


FIGURE 3. Overall survival - survival of all patients with urothelial cancer and spinal bone metastases from first diagnosis of urothelial cancer until death.

Statistical analyses

Survival was calculated with the Kaplan-Meier method and presented graphically. Patients, who were lost to follow-up, were censored for statistical analyses. Overall survival (OS) was defined as the time from initial diagnosis of urothelial cancer until death and “bone survival” (BS) as the time from first diagnosis of SBM until death. “Radiotherapy survival” (RTS) was defined as the time between start of RT and death. For the assessment of the distribution of Taneichi *et al.* score subtypes before and at 6 months after RT, Bowker test was used. Kappa statistics were calculated to detect possible asymmetry in the distribution of the Taneichi *et al.* score over time. BMD was measured in HU. Mean values and the standard deviation (SD) were calculated for BMD before RT as well as at 3 and

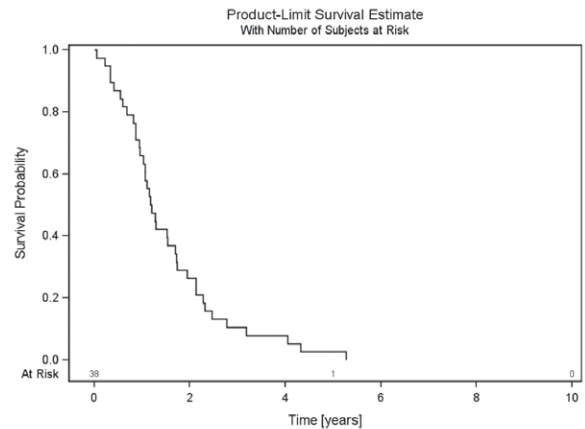


FIGURE 4. Bone survival - survival of all patients with urothelial cancer and spinal bone metastases from first diagnosis of spinal bone metastases until death.

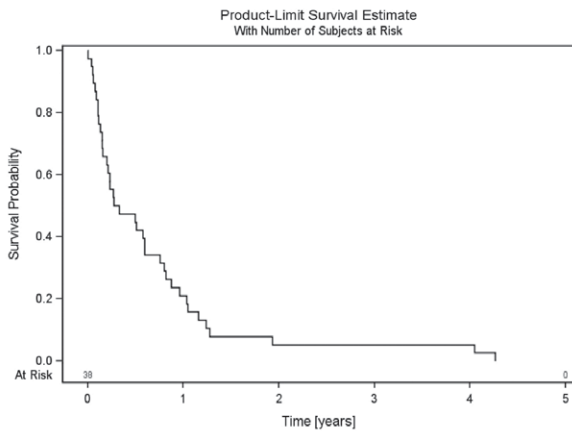


FIGURE 5. Radiotherapy survival - survival of all patients with urothelial cancer and spinal bone metastases from start of palliative radiotherapy until death.

6 months after RT. To statistically analyze the differences in BMD before and after RT, we used the Wilcoxon signed-rank test. A p -value ≤ 0.05 was considered statistically significant. All statistical analyses were performed with SAS software 9.4 (SAS Institute, Cary, NC, USA).

Results

The median follow up of all patients was 1.8 years (mean 2.4 years, range 0.3–8.6 years). All patients died during follow-up. OS after 6 months, 1 year and 2 years was 90%, 80% and 40%, respectively (Figure 3). BS was 85%, 64% and 23% after 6 months, 1 year and 2 years, respectively (Figure 4). RTS after 6 months, 1 year and 2 years was 42%, 18% and 5%, respectively (Figure 5).

Twenty of the 38 patients (52.6%) were classified as unstable before RT. One of the initially unstable metastases was classified as stable at 3 and 6 months after RT. Additionally, one patient with an initially stable metastasis showed progression of the osteolytic lesion with a new pathological fracture after RT and was classified as unstable after 3 and after 6 months. Overall, 10 of the 19 surviving patients (52.6%) were classified as unstable and nine (47.4%) were classified as stable after 3 and after 6 months. The evaluation of the distribution of Taneichi *et al.* subtypes A to G showed no improvement over the course of time. Bowker test confirmed symmetry of the distribution of stability ($p = 1$; Table 2).

Mean calculated metastasis size and mean bone density were $413.8 \text{ mm}^2 \pm \text{SD } 253.6$ and $110.8 \text{ HU} \pm \text{SD } 63.9$ at initial assessment. At 3 months after RT,

TABLE 2. Distribution of subtypes A to G of the Taneichi Score over the course of time (0–6 months)

		6 months after radiotherapy						
		A	B	C	D	E	F	G
before radiotherapy	A	1	0	0	0	0	0	0
	B	1	2	0	0	0	0	0
	C	0	0	5	1	0	0	0
	D	0	0	0	1	0	0	0
	E	0	0	0	0	4	0	0
	F	0	0	0	0	0	4	0
	G	0	0	0	0	0	0	0

we observed a bone density of $125.7 \text{ HU} \pm \text{SD } 82.6$ and after 6 months a bone density of $127.5 \text{ HU} \pm \text{SD } 85.6$. The increase of bone density of $25.0 \text{ HU} \pm 49.7 \text{ SD}$ after 3 months and $24.2 \text{ HU} \pm 52.2 \text{ SD}$ after 6 months was statistically significant ($p = 0.001$; $p = 0.037$).

The documented indication for RT was pain in 30 patients and only 26.7% ($n = 8$) reported pain relief (≥ 2 points on the visual analogue scale). One patient (2.6%) had a neurological deficit with paresthesia of the right laterodorsal thoracic wall and this was unchanged 6 months after RT. None of the patients developed a new neurological deficit.

Discussion

While survival was comparable to previously published data on patients with metastatic urothelial cancer¹¹, we found RTS with 42% after 6 months to be particularly poor. We believe this to be attributable to patients' extensive morbidity, with a KPS $< 80\%$ in 76.3% and additional extra-osseous metastases in 9 out of 38 patients, at the initiation of RT, since earlier publications on different ChT regimens in patients with metastatic urothelial cancer reported visceral metastases as well as reduced performance status to be independent predictors of poor outcome. Moreover, these studies also described the presence of bone metastases to be an independent prognostic factor for survival.^{12,13} Nevertheless, there is only a minor impact of local therapy in these patients.

Generally, in patients with osseous metastases of the vertebral column, pain and instability are

major concerns regularly resulting in reduced QoL. Instability, especially when requiring a prescribed surgical corset, leads to reduced activity in daily life and further impairment of patients' QoL. Taneichi *et al.* developed a validated scoring system for the probability of vertebral body collapse based on risk factors such as tumor size, costovertebral joint involvement and pedicle destruction.³ The use of such a score may aid physicians in the evaluation of vertebral body stability and stabilization after RT. In recent studies on patients with SBM and different primary tumor entities, we found stabilization to be largely dependent on the primary tumor histology. While women with breast cancer and gynecologic malignancies as well as patients with NSCLC may benefit from stabilizing RT, patients with malignant melanoma and renal cancer died before stabilization was achieved.^{4-6,9,10} In our current study, none of the patients with urothelial cancer and initially unstable SBM could be classified as stable 6 months after RT. This poor local response to palliative RT is underlined by our findings regarding BMD. While we were able to demonstrate a statistically significant increase of $25.0 \text{ HU} \pm 49.7 \text{ SD}$ ($p = 0.001$) after 3 months and of $24.2 \pm 52.2 \text{ SD}$ ($p = 0.037$) after 6 months, BMD did not further improve between 3 months and 6 months after RT ($-1.7 \text{ HU} \pm 17.6 \text{ SD}$). Additionally, increase in HU was small when compared to our previous studies.^{7,8} Furthermore, pain relief was reached in only 26.7% of the patients with painful SBM. Previous studies on patients with bone metastases from our own institution^{10,14,15} as well as in the international literature¹⁶ found substantially better response rates. Besides, only 10.5% of the patients in our study had received concomitant bisphosphonates. A small randomized trial on patients with bladder cancer and bone metastases found pain response, incidence of skeletal-related events and survival to be improved by zoledronic acid.¹⁷ Therefore, our patients may have benefitted from concomitant bisphosphonate treatment as well. Only one patient had a neurological deficit before RT and there was no improvement during follow-up. We were unable to elucidate, whether this was due to poor response to palliative RT or due to the duration of symptoms before RT.

Benefit from sole palliative RT of painful or unstable SBM in patients with urothelial cancer is limited. Given the short survival and poor local response, patients should be carefully selected for palliative RT based on their KPS, and longer fractionation schedules, as used in our patients, should be avoided. However, concomitant bisphospho-

nates may improve outcome in terms of re-ossification, pain relief and survival.

References

- Bianchi M, Roghmann F, Becker A, Sukumar S, Briganti A, Menon M, et al. Age-stratified distribution of metastatic sites in bladder cancer: A population-based analysis. *Can Urol Assoc J* 2014; **8**: E148-58. doi:10.5489/auaj.787
- Lutz S, Berk L, Chang E, Chow E, Hahn C, Hoskin P, et al. Palliative radiotherapy for bone metastases: an ASTRO evidence-based guideline. *Int J Radiat Oncol Biol Phys* 2011; **79**: 965-76. doi:10.1016/j.ijrobp.2010.11.026
- Taneichi H, Kaneda K, Takeda N, Abumi K, Satoh S. Risk factors and probability of vertebral body collapse in metastases of the thoracic and lumbar spine. *Spine (Phila Pa 1976)* 1997; **22**: 239-45.
- Foerster R, Habermehl D, Bruckner T, Bostel T, Schlamp I, Welzel T, et al. Spinal bone metastases in gynecologic malignancies: a retrospective analysis of stability, prognostic factors and survival. *Radiat Oncol* 2014; **9**: 194. doi:10.1186/1748-717X-9-194
- Rief H, Bischof M, Bruckner T, Welzel T, Askoxylakis V, Rieken S, et al. The stability of osseous metastases of the spine in lung cancer - a retrospective analysis of 338 cases. *Radiat Oncol* 2013; **8**: 200. doi:10.1186/1748-717X-8-200
- Schlamp I, Rieken S, Habermehl D, Bruckner T, Förster R, Debus J, et al. Stability of spinal bone metastases in breast cancer after radiotherapy: a retrospective analysis of 157 cases. *Strahlenther Onkol* 2014; **190**: 792-7. doi:10.1007/s00066-014-0651-z
- Foerster R, Eisele C, Bruckner T, Bostel T, Schlamp I, Wolf R, et al. Bone density as a marker for local response to radiotherapy of spinal bone metastases in women with breast cancer: a retrospective analysis. *Radiat Oncol* 2015; **10**: 62. doi:10.1186/s13014-015-0368-x
- Rief H, Petersen LC, Omlor G, Akbar M, Bruckner T, Rieken S, et al. The effect of resistance training during radiotherapy on spinal bone metastases in cancer patients - a randomized trial. *Radiother Oncol* 2014; **112**: 133-9. doi:10.1016/j.radonc.2014.06.008
- Bostel T, Förster R, Schlamp I, Wolf R, Serras AF, Mayer A, et al. Stability, prognostic factors and survival of spinal bone metastases in malignant melanoma patients after palliative radiotherapy. *Tumori* 2016; **102**: 156-61. doi:10.5301/tj.5000382
- Schlamp I, Lang H, Förster R, Wolf R, Bostel T, Bruckner T, et al. Stability of spinal bone metastases and survival analysis in renal cancer after radiotherapy. *Tumori* 2015; **101**: 614-20. doi:10.5301/tj.5000370
- Abe T, Shinohara N, Harabayashi T, Sazawa A, Maruyama S, Suzuki S, et al. Impact of multimodal treatment on survival in patients with metastatic urothelial cancer. *Eur Urol* 2007; **52**: 1106-13. doi:10.1016/j.eururo.2007.02.052
- Bellmunt J, Albanell J, Paz-Ares L, Climent MA, Gonzalez-Larrriba JL, Carles J, et al. Pretreatment prognostic factors for survival in patients with advanced urothelial tumors treated in a phase I/II trial with paclitaxel, cisplatin, and gemcitabine. *Cancer* 2002; **95**: 751-7. doi:10.1002/cncr.10762
- Saxman SB, Propert KJ, Einhorn LH, Crawford ED, Tannock I, Raghavan D, et al. Long-term follow-up of a phase III intergroup study of cisplatin alone or in combination with methotrexate, vinblastine, and doxorubicin in patients with metastatic urothelial carcinoma: a cooperative group study. *J Clin Oncol* 1997; **15**: 2564-9. doi:10.1200/jco.1997.15.7.2564
- Habermehl D, Haase K, Rieken S, Debus J, Combs SE. Defining the role of palliative radiotherapy in bone metastasis from primary liver cancer: an analysis of survival and treatment efficacy. *Tumori* 2011; **97**: 609-13. doi:10.1700/989.10720
- Rief H, Heinhold M, Bruckner T, Schlamp I, Förster R, Welzel T, et al. Quality of life, fatigue and local response of patients with unstable spinal bone metastases under radiation therapy—a prospective trial. *Radiat Oncol* 2014; **9**: 133. doi:10.1186/1748-717X-9-133
- Chow R, Hoskin P, Chan S, Mesci A, Hollenberg D, Lam H, et al. Efficacy of multiple fraction conventional radiation therapy for painful uncomplicated bone metastases: A systematic review. *Radiother Oncol* 2017; **122**: 323-31. doi:10.1016/j.radonc.2016.12.031
- Zaghloul MS, Boutrus R, El-Hossieny H, Kader YA, El-Attar I, Nazmy M. A prospective, randomized, placebo-controlled trial of zoledronic acid in bony metastatic bladder cancer. *Int J Clin Oncol* 2010; **15**: 382-9. doi:10.1007/s10147-010-0074-5

Prognostic value of plasma EBV DNA for nasopharyngeal cancer patients during treatment with intensity-modulated radiation therapy and concurrent chemotherapy

Chawalit Lertbutsayanukul¹, Danita Kannarunimit¹, Anussara Prayongrat¹, Chakkapong Chakkabat¹, Sarin Kitpanit¹, Pokrath Hansasuta²

¹ Division of Radiation Oncology, Department of Radiology, Faculty of Medicine, Chulalongkorn University, King Chulalongkorn Memorial Hospital, Bangkok, Thailand

² Division of Virology, Department of Microbiology, Faculty of Medicine, Chulalongkorn University, Bangkok, Thailand

Radiol Oncol 2018; 52(2): 195-203.

Received 21 December 2017

Accepted 4 February 2018

Correspondence to: Danita Kannarunimit, Division of Radiation Oncology, Department of Radiology, Faculty of Medicine, Chulalongkorn University, King Chulalongkorn Memorial Hospital, 1873 Rama IV Road, Pathumwan, Bangkok, 10330, Thailand. Phone: +662-256-4334; Fax: +662-256-4590; E-mail: danita.k@chula.ac.th

Disclosure: No potential conflicts of interest were disclosed.

Background. Plasma EBV DNA concentrations at the time of diagnosis (pre-EBV) and post treatment (post-EBV) have significant value for predicting the clinical outcome of nasopharyngeal cancer (NPC) patients. However, the prognostic value of the EBV concentration during radiation therapy (mid-EBV) has not been vigorously studied.

Patients and methods. This was a post hoc analysis of 105 detectable pre-EBV NPC patients from a phase II/III study comparing sequential (SEQ) versus simultaneous integrated boost (SIB) intensity-modulated radiation therapy (IMRT). Plasma EBV DNA concentrations were measured by PCR before commencement of IMRT, at the 5th week of radiation therapy and 3 months after the completion of IMRT. The objective was to identify the prognostic value of mid-EBV to predict overall survival (OS), progression-free survival (PFS) and distant metastasis-free survival (DMFS).

Results. A median pre-EBV was 6880 copies/ml. Mid-EBV and post-EBV were detectable in 14.3% and 6.7% of the patients, respectively. The median follow-up time was 45.3 months. The 3-year OS, PFS and DMFS rates were 86.0% vs. 66.7% ($p = 0.043$), 81.5% vs. 52.5% ($p = 0.006$), 86.1% vs. 76.6% ($p = 0.150$), respectively, for those with undetectable mid-EBV vs. persistently detectable mid-EBV. However, in the multivariate analysis, only persistently detectable post-EBV was significantly associated with a worse OS (hazard ratio (HR) = 6.881, 95% confident interval (CI) 1.699-27.867, $p = 0.007$), PFS (HR = 5.117, 95% CI 1.562-16.768, $p = 0.007$) and DMFS (HR = 129.071, 95%CI 19.031-875.364, $p < 0.001$).

Conclusions. Detectable post-EBV was the most powerful adverse prognostic factor for OS, PFS and DMFS; however, detectable mid-EBV was associated with worse OS, PFS especially Local-PFS (LPFS) and may facilitate adaptive treatment during the radiation treatment period.

Key words: plasma EBV; nasopharyngeal cancer; IMRT; Prognosis during treatment

Introduction

Epstein-Barr virus (EBV) is associated with nasopharyngeal carcinoma (NPC) in an endemic area. The plasma EBV DNA concentration at the time of diagnosis and after treatment can be used as a biomarker for screening, monitoring and predicting clinical outcomes in NPC.^{1,2} Peng identified a pre-

treatment plasma EBV DNA (pre-EBV) cut-off value of 2010 copies/ml in predicting disease-free survival, overall survival, loco-regional relapse-free survival and distant metastasis-free survival when NPC patients were treated with intensity-modulated radiation therapy (IMRT).³ Others confirmed the prognostic value of pre-EBV in predicting clinical outcomes despite the different pre-EBV cut-off

values.⁴⁻¹¹ The persistent post-treatment EBV DNA concentration (post-EBV) has the strongest risk of disease relapse and distant metastasis^{4,7,12-14} and may help in treatment modification, such as the intensification of adjuvant chemotherapy regimens.¹⁵

In recent decades, the use of concurrent chemotherapy with IMRT has shifted the pattern of recurrence from locoregional recurrence toward distant metastasis alone.¹⁶⁻¹⁹ The mid-treatment plasma EBV-DNA may be useful in adaptive treatment, such as reducing treatment intensity in patients with early response or giving more intensified treatment to those without response. However, studies on the plasma EBV DNA during radiation treatment (mid-EBV) were scarce, and patients were not uniformly treated with IMRT or concurrent chemoradiation.^{20,21} Our primary endpoint was to identify the prognostic value of mid-EBV to predict the overall survival, progression-free survival and distant metastasis-free survival rates.

Patients and methods

This study was a secondary analysis of a prospective randomized controlled trial that compared the utility of sequential (SEQ) or simultaneous integrated boost (SIB) IMRT in non-metastatic nasopharyngeal cancer.²² This study was approved by the institutional review board. Informed consent was obtained from every patient before entry into the study. One hundred and twenty-three patients had detectable pre-EBV. After excluding 18 patients because of missing blood samples at any of the three time-points, there were 105 patients in this study.

Chemotherapy consisted of weekly treatments of 40 mg/m² cisplatin given concurrently with 70 Gy IMRT in 33-35 fractions to those with more than T1 or positive nodal disease for a maximum of 7 cycles. Adjuvant chemotherapy, consisting of 80 mg/m² cisplatin and 1000 mg/m²/per day 5-fluorouracil (5-FU) over a 96-hour continuous infusion, was given at 4-week intervals for 3 cycles.

Quantitative measurement of plasma EBV DNA level

Plasma EBV DNA concentrations were evaluated before treatment (pre-EBV), at the 5th week of the radiation course (mid-EBV) and 3 months after the completion of radiation treatment (post-EBV). We elected to test the mid-EBV in the 5th week of IMRT because it was the best time to perform re-simula-

tion and in accordance with Leung's study which tested mid-EBV at completion of 4 weeks of radiation therapy.²¹ The EBV nucleic acids were purified from the plasma samples using the QIASymphony SP in combination with the QIASymphony DSP Virus/Pathogen Midi Kit (QIAGEN, Germany) using the manufacturer's recommended protocol. After extraction, the eluates in the 96-microwell plates were transferred to the module for assembly with the master mix (QIAGEN artus EBV QS RGQ kit) by the instrument. The aliquoted reactions were subsequently put in a Rotor-Gene Q. The amplification parameters were as follows: 95°C for 10 min and 45 cycles of 95°C for 15 s, 65°C for 30 s, and 72°C for 20 s. The plasma DNA samples were quantified for EBV DNA using an RTQ-PCR system targeting the BamHI-W fragment region of the EBV genome. A plasma EBV DNA concentration of < 316 copies/ml was defined as an undetectable level in our institution. Note that in the following section, values of 0 represent an undetectable plasma EBV DNA concentration.

Statistical analysis

Local progression-free survival (LPFS), regional progression-free survival (RPFS), distant metastasis-free survival (DMFS), progression-free survival (PFS) and overall survival (OS) were analyzed using the Kaplan–Meier method and the log-rank test. Cox proportional hazard models with univariate and multivariate analyses were performed to identify the predictors for OS, PFS and DMFS. The factors, including age, sex, stage, pre-EBV, mid-EBV, post-EBV, WHO subtypes, and IMRT techniques, were included as covariates in this exploratory analysis. Factors with a *P*-value of < 0.25 in the univariate analysis were entered into the multivariate Cox regression model. All tests were two-sided, and a *P*-value of < 0.05 was considered statistically significant. Statistical analyses were performed using IBM SPSS statistics (version 22.0, SPSS Inc., Chicago, Ill).

Results

Between October 2010 and September 2015, 105 NPC patients who had detectable pre-EBV and completed blood sampling between RT and 3 months after RT were included. The median age was 50 years. Patient characteristics are outlined in Table 1. The median follow-up time was 45.3 months. Most patients were stage III-IVb. The ma-

TABLE 1. Patient characteristics

	N = 105
Age < 45	34 (32.4%)
Age ≥ 45	71 (67.6%)
Sex	
Male	82 (78.1%)
Female	23 (21.9%)
T-stage	
1	30 (28.6%)
2	28 (26.7%)
3	29 (27.6%)
4	18 (17.1%)
N-stage	
0	1 (1.0%)
1	26 (24.8%)
2	57 (54.3%)
3	21 (20.0%)
Stage grouping (AJCC 2010)	
II	14 (13.3%)
III	54 (51.4%)
IVa-b	37 (35.2%)
WHO subtypes	
2A	11 (10.5%)
2B	94 (89.5%)
Mid-EBV	
undetectable	90 (85.7%)
detectable	15 (14.3%)
Post-EBV	
undetectable	98 (93.3%)
detectable	7 (6.7%)

majority had undifferentiated squamous cell carcinoma and male gender. Patients received a median of 6 cycles of concurrent weekly cisplatin (88.6% received ≥ 5 cycles) and a median of 3 cycles of adjuvant chemotherapy (76.2% completed 3 cycles).

Plasma EBV DNA level correlated with disease and treatment outcomes

Median pre-EBV was 6880 copies/ml. (interquartile range, IQR, 2555–14600 copies/ml). The corresponding values for stage II, III and IV were 3690 copies/ml (Interquartile range (IQR), 1462–8885), 6880 copies/ml. (IQR, 2407–16475) and 5620 copies/ml (IQR, 3735–17200), respectively. Fifteen patients (14.3%) had persistent mid-EBV, 4 of whom had residual post-EBV. Among the remaining 90 patients who had undetectable mid-EBV, 3 patients had rebound detectable post-EBV. A total of 7 patients (6.7%) had residual post-EBV.

Survival outcomes

During the follow-up period, a total of 24 (22.9%) patients died, 39 (37.1%) had progressive disease, and 27 (25.7%) developed distant metastases. The 3-year OS, PFS and DMFS for the patients were 83.2%, 77.4%, 84.7%, respectively. The overall survival rates for stages II, III, and IV were 85.1%, 88.7% and 75.0%, respectively ($p = 0.253$), while the PFS was 85.1%, 83% and 67.3%, respectively ($p = 0.070$). The corresponding DMFS was 100%, 88.5% and 74.2%, respectively ($p = 0.102$) (Figure 1).

Using a pre-EBV cut-off of 2010 copies/ml³, the 3-year OS, PFS and DMFS rates were 88.4% *vs.* 82.1% ($p = 0.360$), 82.9% *vs.* 76.2% ($p = 0.114$), and 82.9% *vs.* 85.2% ($p=0.390$), respectively, for those with pre-EBV < 2010 copies/ml *vs.* ≥ 2010 copies/ml (Figure 1). The 3-year OS, PFS and DMFS rates were 86.0% *vs.* 66.7% ($p = 0.043$), 81.5% *vs.* 52.5% ($p = 0.006$), and 86.1% *vs.* 76.6% ($p = 0.150$), respectively, for those with undetectable mid-EBV *vs.* persis-

TABLE 2. Overall survival (OS), progression-free survival (PFS), distant metastasis-free survival (DMFS), local progression-free survival (LPFS) and regional progression-free survival (RPFS) rates among different plasma EBV time points

	3-year OS (95%CI)	p-value	3-year PFS (95%CI)	p-value	3-year DMFS (95%CI)	p-value	3-year LPFS (95%CI)	p-value	3-year RPFS (95%CI)	p-value
Pre-EBV < 2010	88.4 (73.1–103.7)	0.360	82.9 (65.3–100.5)	0.114	82.9 (62.3–100.5)	0.386	100	0.328	100	0.475
Pre-EBV ≥ 2010	82.1 (73.9–90.3)		76.2 (67.0–85.4)		85.2 (77.0–93.4)		94.4 (89.1–99.6)		96.6 (91.9–101.3)	
Undetectable mid-EBV	86.0 (78.5–93.4)	0.040	81.5 (73.3–89.7)	0.006	86.1 (78.5–93.7)	0.15	97.5 (94.0–101.0)	0.01	98.6 (95.9–101.3)	0.113
Detectable mid-EBV	66.7 (42.8–90.6)		52.5 (26.8–78.2)		76.6 (52.9–100.3)		79.5 (53.8–105.2)		87.5 (64.6–110.4)	
Undetectable post-EBV	86.1 (79.0–93.2)	< 0.001	79.9 (71.9–87.9)	< 0.001	88.2 (81.3–95.1)	< 0.001	97.6 (94.3–100.9)	< 0.001	97.2 (93.5–100.9)	0.841
Detectable post-EBV	42.9 (6.3–79.6)		42.9 (6.3–79.6)		22.9 (15.7–61.5)		33.3 (20.0–86.6)		100	

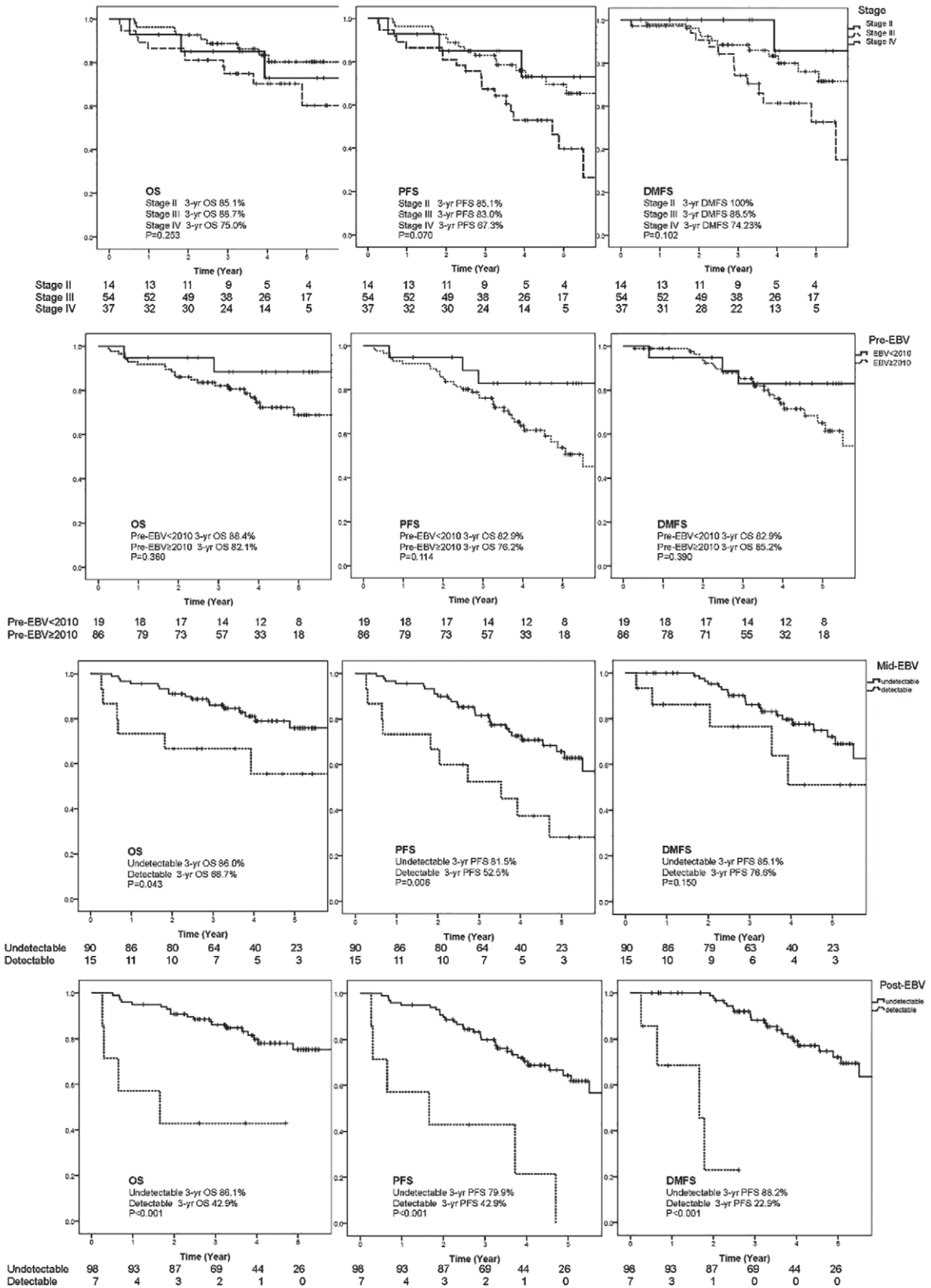


FIGURE 1. Kaplan-Meier curves for the overall survival (OS), progression-free survival (PFS), distant metastasis-free survival (DMFS) stratified by stage and plasma EBV DNA at different time points.

TABLE 3. Univariate analyses for the clinical parameters and EBV values associated with the overall survival (OS), progression-free survival (PFS), distant metastasis-free survival (DMFS)

	Hazard ratio for OS	Univariate			p-value	Hazard ratio for PFS	Univariate			p-value	Hazard ratio for DMFS	Univariate		
		95.0% CI		p-value			95.0% CI		p-value			95.0% CI		p-value
		Lower	Upper				Lower	Upper				Lower	Upper	
Age <45 vs. ≥45	0.497	0.185	1.331	0.164	0.655	0.319	1.346	0.250	0.807	0.353	1.845	0.611		
Sex Male vs. Female	1.442	0.493	4.222	0.504	1.623	0.679	3.879	0.276	1.078	0.434	2.677	0.872		
WHO type IIA vs. IIB	1.344	0.399	4.532	0.633	1.795	0.748	4.31	0.190	2.101	0.719	6.141	0.175		
T Stage				0.152				0.026				0.119		
T1 vs. T4	0.155	0.031	0.773	0.023	0.176	0.055	0.564	0.003	0.212	0.05	0.89	0.034		
T2 vs. T4	0.73	0.257	2.073	0.555	0.523	0.224	1.222	0.134	0.617	0.204	1.862	0.391		
T3 vs. T4	0.667	0.223	1.991	0.468	0.73	0.319	1.671	0.457	0.93	0.316	2.743	0.896		
N Stage				0.740				0.501				0.188		
N1 vs. N3	1.222	0.386	3.865	0.733	0.887	0.368	2.138	0.789	0.587	0.208	1.657	0.314		
N2 vs. N3	0.844	0.297	2.4	0.750	0.651	0.302	1.406	0.275	0.445	0.187	1.063	0.068		
Stage				0.253				0.070				0.102		
Stage II vs. IVa-b	0.888	0.281	2.8	0.839	0.491	0.166	1.449	0.198	0.326	0.073	1.451	0.141		
Stage III vs. IVa-b	0.484	0.2	1.17	0.107	0.472	0.242	0.92	0.028	0.47	0.214	1.034	0.061		
Tech SIB vs. SEQ	1.619	0.707	3.71	0.255	1.309	0.693	2.472	0.407	1.461	0.674	3.167	0.336		
Concurrent chemotherapy 0-5 vs. 6-7 cycles	1.172	0.525	2.616	0.699	0.795	0.418	1.514	0.486	0.632	0.287	1.393	0.255		
Adjuvant chemotherapy 0-2 vs. 3 cycles	1.089	0.432	2.748	0.856	1.101	0.536	2.263	0.793	0.937	0.377	2.327	0.888		
Pre-EBV ≥ 2010 vs. < 2010	1.760	0.524	5.915	0.360	2.309	0.819	6.512	0.114	1.595	0.550	4.625	0.390		
Mid-EBV detectable vs undetectable	2.600	1.031	6.556	0.043	2.746	1.337	5.640	0.006	2.041	0.772	5.397	0.15		
Post-EBV detectable vs. undetectable	5.923	1.989	17.638	0.001	5.961	2.457	14.465	<0.001	29.758	8.155	108.593	<0.001		

tently detectable mid-EBV (Figure 1). In comparing the patients with residual post-EBV *vs.* undetectable post-EBV, the OS, PFS and DMFS are demonstrated in Figure 1. Details on the OS, PFS, DMFS, LPFS and RPFS regarding the different pre-EBV, mid-EBV and post-EBV subgroups are presented in Table 2.

Among the 39 patients who had progressive disease, persistent mid-EBV and post-EBV were observed in 25.6% and 15.4% of these patients, respectively. There were 4 patients who had both persistent mid-EBV and post-EBV, and their 3-year OS, PFS and DMFS rates were 25%, 25% and 37.5%, respectively, which were significantly worse than those of the 11 patients who had detectable mid-EBV but undetectable post-EBV. The 3-year OS, PFS and DMFS rates in the latter group were 81.8%, 62.3% and 88.9%, respectively. Among the 3 patients who had undetectable mid-EBV but had rebound detectable post-EBV, the 3-year OS, PFS and DMFS rates were 66.7%, 66.7% and 33.3%, respectively. The best prognostic group was the

patients who had both undetectable mid-EBV and post-EBV, and their 3-year OS, PFS and DMFS rates were 86.7%, 82.1% and 88.2%, respectively.

The unadjusted univariate analyses for the clinical parameters and the EBV-value associated with the OS, DMFS and PFS are shown in Table 3. Undetectable mid-EBV was significantly associated with better OS and PFS but not DMFS, while undetectable post-EBV was significantly associated with better OS, PFS and DMFS. T-stage was a significant prognostic factor for PFS only ($p = 0.026$). In the multivariate analysis (Table 4), only detectable post-EBV was significantly associated with a worse OS (hazard ratio (HR) = 6.881, 95% confident interval (CI) 1.699–27.867, $p = 0.007$), PFS (HR = 5.117, 95% CI 1.562–16.768, $p = 0.007$) and DMFS (HR = 129.071, 95%CI 19.031–875.364, $p < 0.001$)

Zhang¹ proposed the risk stratification into 4 groups based on the stage and mid-EBV as follows: (1) patients who had stage I-II with undetectable mid-EBV; (2) patients who had stage III-IV with undetectable mid-EBV; (3) patients who had stage

TABLE 4. Multivariate analyses for the clinical parameters and EBV values associated with the overall survival (OS), progression-free survival (PFS), distant metastasis-free survival (DMFS)

	Hazard ratio for OS	95.0% CI for OS		P-value
		Lower	Upper	
Age < 45 vs. ≥ 45	0.409	0.140	1.190	0.101
T				0.305
T1 vs. T4	0.286	0.052	1.570	0.150
T2 vs. T4	1.214	0.361	4.078	0.754
T3 vs. T4	1.177	0.341	4.069	0.796
Mid-EBV undetectable vs detectable	1.620	0.617	4.251	0.327
Post-EBV undetectable vs. detectable	6.881	1.699	27.867	0.007
	Hazard ratio for PFS	95.0% CI for PFS		
		Lower	Upper	
Age <45 vs. ≥ 45	0.422	0.180	0.988	0.047
WHO type IIA vs. IIB	1.354	0.441	4.159	0.597
T Stage				0.101
T1 vs. T4	0.497	0.104	2.375	0.381
T2 vs. T4	1.660	0.450	6.125	0.446
T3 vs. T4	2.099	0.646	6.825	0.218
Stage				0.099
Stage II vs. IVa-b	1.016	0.256	4.035	0.982
Stage III vs. IVa-b	0.416	0.170	1.021	0.055
EBV < 2010 vs. ≥ 2010	0.370	0.113	1.211	0.100
Mid-EBV undetectable vs. detectable	1.427	0.630	3.234	0.394
Post-EBV undetectable vs. detectable	5.117	1.562	16.768	0.007
	Hazard ratio for DMFS	95.0% CI for DMFS		
		Lower	Upper	
WHO type IIA vs. IIB	1.653	0.470	5.810	0.433
T Stage				0.113
T1 vs. T4	0.945	0.068	13.158	0.966
T2 vs. T4	5.632	0.388	81.647	0.205
T3 vs. T4	4.628	0.384	55.737	0.228
N Stage				0.410
N1 vs. N3	4.484	0.305	65.955	0.274
N2 vs. N3	2.018	0.151	26.935	0.595
Stage				0.340
Stage II vs. IVa-b	0.090	0.003	2.435	0.153
Stage III vs. IVa-b	0.150	0.009	2.474	0.185
Mid-EBV undetectable vs detectable	1.583	0.517	4.843	0.421
Post-EBV undetectable vs. detectable	129.071	19.031	875.364	0.000

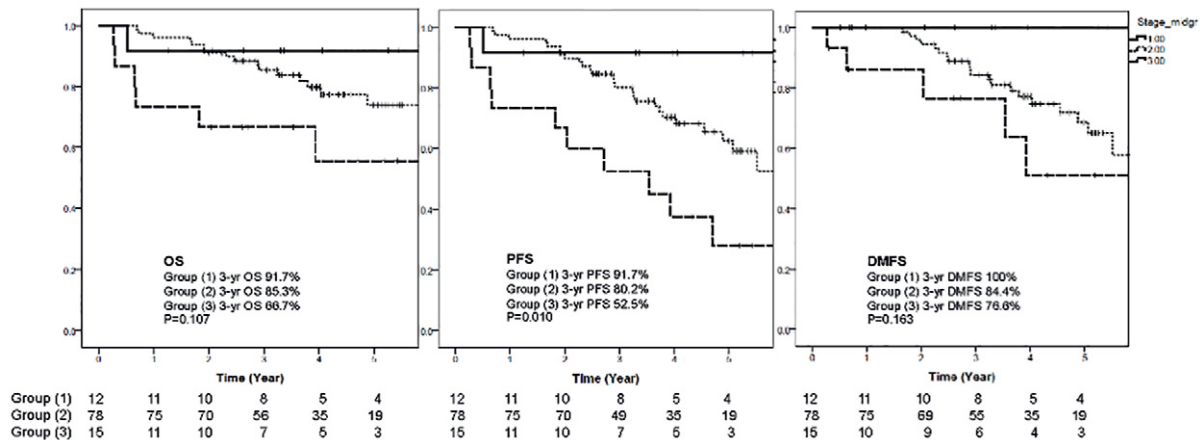


FIGURE 2. Kaplan-Meier curves for the overall survival (OS), progression-free survival (PFS), distant metastasis-free survival (DMFS) stratified by a combination of stage and mid-EBV concentration.

II-IV with detectable mid-EBV; and (4) patients who had stage I with detectable mid-EBV. In our study, there were no patients in group (4). Thus, we analyzed the survival in group (1)-(3). The overall survival rates for group (1), (2), and (3) were 91.7%, 85.3% and 66.7%, respectively ($p = 0.107$), while the PFS rates were 91.7%, 80.2% and 52.5%, respectively ($p = 0.010$). The corresponding DMFS rates were 100%, 84.4% and 76.6%, respectively ($p = 0.163$) (Figure 2).

Discussion

The plasma EBV DNA concentration has been identified as a prognostic biomarker and is correlated with the overall survival in NPC. Pre-EBV concentration has been evaluated in many studies. A higher concentration was associated with a higher mortality, poorer PFS and poorer DMFS.^{1,4-10,12,23} Leung *et al.*⁵ retrospectively reviewed 376 NPC patients who were treated with conventional RT. In their multivariate analysis, pre-EBV was an independent prognostic factor for OS ($p = 0.0053$) and DMFS ($p = 0.0002$). Note that there was no mid-EBV or post-EBV testing in their study. Two recent meta-analyses reported pooled HRs for an OS of 3.01 (95%CI = 2.25–4.02; $P < 0.001$)²³ and 2.81 (95%CI 2.44–3.24, $p < 0.00001$)¹, indicating that the higher levels of pre-EBV were associated with higher mortality, while our study revealed a corresponding HR of 1.76 (95%CI 0.52–5.92).

Other than the pre-EBV, mid-EBV may provide additional information on the risk of disease failure. To our knowledge, there is only one prospective trial that studied the prognostic value of mid-

EBV. Leung *et al.* found that persistent mid-EBV at the completion of the 4th week of chemoradiation was associated with a worse OS (HR 3.29, 95% CI 1.37–7.89), worse PFS (HR 4.05, 95%CI 1.89–8.67) and more distant failure (HR 12.02, 95%CI 2.78–51.93).²¹ Although Leung *et al.* study had a long median follow-up time and involved stage IIB–IVB NPC (AJCC 1997 edition), only 78 of the 107 patients received concurrent chemotherapy. No patient received adjuvant chemotherapy, and an unknown proportion of patients were treated with conventional 2D RT or IMRT. In accordance with Leung *et al.* study, we also found that the detectable mid-EBV value was a predictor for OS (HR 2.60, 95%CI 1.03–6.56), PFS (HR 2.75 95%CI 1.34–5.64) and DMFS (HR 2.01 95%CI 0.77–5.40). In our study, the number of concurrent or adjuvant chemotherapy cycles did not affect OS, PFS or DMFS. However, in a multivariate analysis, the prognostic value of mid-EBV was lower compared to the persistent post-EBV. It was noted that post-EBV was not incorporated into the multivariate analysis in Leung *et al.* study.²¹ Mid-EBV was not a predictive factor for locoregional failure in Leung's study, but mid-EBV was a significant factor in predicting LPFS in our study ($p = 0.01$). Among the 4 patients who had local progression, 3 patients were T4 and 2 patients had detectable mid-EBV. We hypothesized that those patients who had detectable mid-EBV might benefit from the adaptive radiotherapy, such as dose escalation for better local control. The high locoregional failures of 18% in the patients who had detectable mid-EBV, but undetectable post-EBV, and 11% in the patients who had both undetectable mid-EBV and post-EBV in Leung *et al.* study²¹ reflected the pattern of recurrence in

the pre-IMRT era. In contrast, we uniformly used IMRT and concurrent cisplatin-based chemotherapy followed by adjuvant cisplatin and 5FU which gave very high rates of LPFS and RPFS.²² In our previous report of phase III study comparing SEQ and SIB IMRT, both IMRT techniques provided excellent survival outcomes with few late toxicities. There were no statistically significant differences in the cumulative incidence of grade 3–4 acute and late toxicities.²⁴ We acknowledged that the effect of mid-EBV evaluation in adaptive treatment during chemoradiation still has to be investigated in the future.

A meta-analysis confirmed the significant value of mid-EBV in terms of the OS, PFS and DMFS¹; however, detectable post-EBV was a stronger prognostic factor than pre-EBV and mid-EBV. The HRs for the OS, PFS and DMFS of post-EBV were 4.26 (95%CI 3.26–5.57), 5.21 (95%CI 3.29–8.27) and 7.54 (95%CI 3.39–16.77), respectively. Peng *et al.*³ retrospectively reviewed 584 NPC patients treated with IMRT. Overall, 77.7% of patients had detectable pre-EBV, and 8.6% of patients had detectable post-EBV. Among patients who had pre-EBV \geq 2010 copies/ml, the 3-year OS, PFS and DMFS rates were 92.3%, 78.1% and 85.5% in Peng *et al.* study, which were slightly better than the corresponding percentages of 82.1% 76.2% and 85.2%, respectively, in our patient population. In contrast to Peng *et al.* study, which demonstrated statistically significant values of pre-EBV and post-EBV to OS, PFS and DMFS in the multivariate analysis, we found that only the post-EBV was an independent predictor for OS, PFS and DMFS. By comparing between pre-EBV \geq 4000 copies/ml and post-EBV $>$ 500 copies/ml in 170 NPC patients treated with conventional RT, Chan *et al.*⁴ found that only post-EBV $>$ 500 copies was associated with the DMFS (RR 2.1 95% CI 0.70–6.58, $p = 0.182$) in their multivariate analysis, while the HR for DMFS was 129.07, with a 95% CI from 19.03–875.36, $p < 0.001$ in our study. The HRs predicting the DMFS were 3.89, 12.02 and 7.54 in high pre-EBV, detectable mid-EBV and detectable post-EBV, respectively¹, in a meta-analysis. The corresponding HRs for the DMFS in our patient population were 1.60, 2.04 and 29.7, respectively.

We further compared the patient groups according to the risk stratification proposed by Zhang *et al.*¹ Zhang *et al.* regarded patients in group (1) as having modified stage I. In concordance with Zhang *et al.*, this group had the best 3-year OS, PFS and DMFS at approximately 91.7%–100% in our study. The survival rates were also comparable to the 5-year disease-specific survival and DMFS

rates of 97.3% and 100%, respectively, in early stage NPC reported by Su *et al.*²⁵ and the 5-year OS and DMFS rates for those in stage T1N0 of 96.6% and 94.9% as reported by Xiao *et al.*²⁶ This group might not need adjuvant chemotherapy. Patients in group (2) were regarded as having modified stage II by Zhang *et al.*; however, the OS, PFS and DMFS in group (2) were closer to the stage III survivals in our study. The OS, PFS and DMFS in group (3) were 66.7%, 52.5% and 76.6%, respectively, which compared unfavorably to stage IV patients [OS, PFS and DMFS of 75%, 67.3% and 74.2% in stage IV patients]. The above results suggested that patients in group (2) and (3) should be regarded as higher risk than those proposed by Zhang *et al.* Moreover, the combination of stage and mid-EBV was more powerful in discriminating PFS than stage alone.

A limitation of our study is that the follow-up time was relatively short. The prognostic value of mid-EBV was not our primary objective in our randomized controlled trial comparing the different IMRT techniques, which may not have adequate power to detect the prognostic significance of mid-EBV on DMFS. However, the strength of our study was the uniform use of the IMRT technique and concurrent cisplatin-based chemotherapy followed by adjuvant cisplatin and 5FU in a prospective randomized trial.

In conclusion, detectable EBV during chemoradiation was an adverse prognostic factor for OS and PFS; however, it was not as a strong prognostic factor as post-EBV. Prospective clinical trials are warranted to allow evidence-based recommendations for adaptive treatment based on mid-EBV.

References

1. Zhang W, Chen Y, Chen L, Guo R, Zhou G, Tang L, et al. The clinical utility of plasma Epstein-Barr virus DNA assays in nasopharyngeal carcinoma: the dawn of a new era?: a systematic review and meta-analysis of 7836 cases. *Medicine (Baltimore)* 2015; **94**: e845. doi: 10.1097/md.0000000000000845
2. Chan KCA, Woo JKS, King A, Zee BCY, Lam WKJ, Chan SL, et al. Analysis of plasma Epstein-Barr Virus DNA to screen for nasopharyngeal cancer. *N Engl J Med* 2017; **377**: 513–22. doi: 10.1056/NEJMoa1701717
3. Peng H, Guo R, Chen L, Zhang Y, Li WF, Mao YP, et al. Prognostic impact of plasma Epstein-Barr Virus DNA in patients with nasopharyngeal carcinoma treated using intensity-modulated radiation therapy. *Sci Rep* 2016; **6**: 22000. doi: 10.1038/srep22000
4. Chan AT, Lo YM, Zee B, Chan LY, Ma BB, Leung SF, et al. Plasma Epstein-Barr virus DNA and residual disease after radiotherapy for undifferentiated nasopharyngeal carcinoma. *J Natl Cancer Inst* 2002; **94**: 1614–9.
5. Leung SF, Zee B, Ma BB, Hui EP, Mo F, Lai M, et al. Plasma Epstein-Barr viral deoxyribonucleic acid quantitation complements tumor-node-metastasis staging prognostication in nasopharyngeal carcinoma. *J Clin Oncol* 2006; **24**: 5414–8. doi: 10.1200/jco.2006.07.7982

6. Tang LQ, Li CF, Chen QY, Zhang L, Lai XP, He Y, et al. High-sensitivity C-reactive protein complements plasma Epstein-Barr virus deoxyribonucleic acid prognostication in nasopharyngeal carcinoma: a large-scale retrospective and prospective cohort study. *Int J Radiat Oncol Biol Phys* 2015; **91**: 325-36. doi: 10.1016/j.ijrobp.2014.10.005
7. Lin JC, Wang WY, Chen KY, Wei YH, Liang WM, Jan JS, et al. Quantification of plasma Epstein-Barr virus DNA in patients with advanced nasopharyngeal carcinoma. *N Engl J Med* 2004; **350**: 2461-70. doi: 10.1056/NEJMoa032260
8. Twu CW, Wang WY, Liang WM, Jan JS, Jiang RS, Chao J, et al. Comparison of the prognostic impact of serum anti-EBV antibody and plasma EBV DNA assays in nasopharyngeal carcinoma. *Int J Radiat Oncol Biol Phys* 2007; **67**: 130-7. doi: 10.1016/j.ijrobp.2006.07.012
9. Alfieri S, Iacovelli NA, Marcegaglia S, Lasorsa I, Resteghini C, Taverna F, et al. Circulating pre-treatment Epstein-Barr virus DNA as prognostic factor in locally-advanced nasopharyngeal cancer in a non-endemic area. *Oncotarget* 2017; **8**: 47780-9. doi: 10.18632/oncotarget.17822
10. Wei W, Huang Z, Li S, Chen H, Zhang G, Li S, et al. Pretreatment Epstein-Barr virus DNA load and cumulative cisplatin dose intensity affect long-term outcome of nasopharyngeal carcinoma treated with concurrent chemotherapy: experience of an institute in an endemic area. *Oncol Res Treat* 2014; **37**: 88-95. doi: 10.1159/000360178
11. Wang WY, Twu CW, Chen HH, Jan JS, Jiang RS, Chao JY, et al. Plasma EBV DNA clearance rate as a novel prognostic marker for metastatic/recurrent nasopharyngeal carcinoma. *Clin Cancer Res* 2010; **16**: 1016-24. doi: 10.1158/1078-0432.ccr-09-2796
12. Prayongrat A, Chakkabat C, Kannarunimit D, Hansasuta P, Lertbutsayanukul C. Prevalence and significance of plasma Epstein-Barr Virus DNA level in nasopharyngeal carcinoma. *J Radiat Res* 2017; **58**: 509-16. doi: 10.1093/jrr/rw128
13. Hou X, Zhao C, Guo Y, Han F, Lu LX, Wu SX, et al. Different clinical significance of pre- and post-treatment plasma Epstein-Barr virus DNA load in nasopharyngeal carcinoma treated with radiotherapy. *Clin Oncol (R Coll Radiol)* 2011; **23**: 128-33. doi: 10.1016/j.clon.2010.09.001
14. Lee VH, Kwong DL, Leung TW, Choi CW, Lai V, Ng L, et al. Prognostication of serial post-intensity-modulated radiation therapy undetectable plasma EBV DNA for nasopharyngeal carcinoma. *Oncotarget* 2017; **8**: 5292-308. doi: 10.18632/oncotarget.14137
15. Twu CW, Wang WY, Chen CC, Liang KL, Jiang RS, Wu CT, et al. Metronomic adjuvant chemotherapy improves treatment outcome in nasopharyngeal carcinoma patients with postradiation persistently detectable plasma Epstein-Barr virus deoxyribonucleic acid. *Int J Radiat Oncol Biol Phys* 2014; **89**: 21-9. doi: 10.1016/j.ijrobp.2014.01.052
16. Al-Sarraf M, LeBlanc M, Giri PG, Fu KK, Cooper J, Vuong T, et al. Chemoradiotherapy versus radiotherapy in patients with advanced nasopharyngeal cancer: phase III randomized Intergroup study 0099. *J Clin Oncol* 1998; **16**: 1310-7. doi: 10.1200/jco.1998.16.4.1310
17. Wee J, Tan EH, Tai BC, Wong HB, Leong SS, Tan T, et al. Randomized trial of radiotherapy versus concurrent chemoradiotherapy followed by adjuvant chemotherapy in patients with American Joint Committee on Cancer/International Union against cancer stage III and IV nasopharyngeal cancer of the endemic variety. *J Clin Oncol* 2005; **23**: 6730-8. doi: 10.1200/jco.2005.16.790
18. Lee AW, Tung SY, Chua DT, Ngan RK, Chappell R, Tung R, et al. Randomized trial of radiotherapy plus concurrent-adjuvant chemotherapy vs. radiotherapy alone for regionally advanced nasopharyngeal carcinoma. *J Natl Cancer Inst* 2010; **102**: 1188-98. doi: 10.1093/jnci/djq258
19. Chen L, Hu CS, Chen XZ, Hu GQ, Cheng ZB, Sun Y, et al. Adjuvant chemotherapy in patients with locoregionally advanced nasopharyngeal carcinoma: Long-term results of a phase 3 multicentre randomised controlled trial. *Eur J Cancer* 2017; **75**: 150-8. doi: 10.1016/j.ejca.2017.01.002
20. Lo YM, Leung SF, Chan LY, Chan AT, Lo KW, Johnson PJ, et al. Kinetics of plasma Epstein-Barr virus DNA during radiation therapy for nasopharyngeal carcinoma. *Cancer Res* 2000; **60**: 2351-5.
21. Leung SF, Chan KC, Ma BB, Hui EP, Mo F, Chow KC, et al. Plasma Epstein-Barr viral DNA load at midpoint of radiotherapy course predicts outcome in advanced-stage nasopharyngeal carcinoma. *Ann Oncol* 2014; **25**: 1204-8. doi: 10.1093/annonc/mdu117
22. Songthong AP, Kannarunimit D, Chakkabat C, Lertbutsayanukul C. A randomized phase II/III study of adverse events between sequential (SEQ) versus simultaneous integrated boost (SIB) intensity modulated radiation therapy (IMRT) in nasopharyngeal carcinoma; preliminary result on acute adverse events. *Radiat Oncol* 2015; **10**: 166. doi: 10.1186/s13014-015-0472-y
23. Liu TB, Zheng ZH, Pan J, Pan LL, Chen LH. Prognostic role of plasma Epstein-Barr virus DNA load for nasopharyngeal carcinoma: a meta-analysis. *Clin Invest Med* 2017; **40**: E1-e12.
24. Lertbutsayanukul C, Prayongrat A, Kannarunimit D, Chakkabat C, Netsawang B, Kitpanit S. A randomized phase III study between sequential versus simultaneous integrated boost intensity-modulated radiation therapy in nasopharyngeal carcinoma. *Strahlenther Onkol* 2018. doi: 10.1007/s00066-017-1251-5. [Epub ahead of print]
25. Su SF, Han F, Zhao C, Chen CY, Xiao WW, Li JX, et al. Long-term outcomes of early-stage nasopharyngeal carcinoma patients treated with intensity-modulated radiotherapy alone. *Int J Radiat Oncol Biol Phys* 2012; **82**: 327-33. doi: 10.1016/j.ijrobp.2010.09.011
26. Xiao WW, Han F, Lu TX, Chen CY, Huang Y, Zhao C. Treatment outcomes after radiotherapy alone for patients with early-stage nasopharyngeal carcinoma. *Int J Radiat Oncol Biol Phys* 2009; **74**: 1070-6. doi: 10.1016/j.ijrobp.2008.09.008

Early cardiotoxicity after adjuvant concomitant treatment with radiotherapy and trastuzumab in patients with breast cancer

Tanja Marinko¹, Simona Borstnar², Rok Blagus³, Jure Dolenc⁴, Cvetka Bilban-Jakopin¹

¹ Department of Radiation Oncology, Institute of Oncology Ljubljana, Ljubljana, Slovenia

² Department of Medical Oncology, Institute of Oncology Ljubljana, Ljubljana, Slovenia

³ Department of Cardiology, University Medical Centre Ljubljana, Ljubljana, Slovenia

⁴ Institute for biostatistics and medical informatics, University of Ljubljana, Slovenia

Radiol Oncol 2018; 52(2): 204-212.

Received 4 December 2017

Accepted 12 December 2017

Correspondence to: Assist. Tanja Marinko, M.D., Ph.D., Department of Radiation Oncology, Institute of Oncology Ljubljana; Zaloška 2, 1000 Ljubljana, Slovenia. Phone: +386 1 5879 550; Fax: +386 1 5879 400; Email: tmarinko@onko-i.si

Disclosure: No potential conflicts of interest were disclosed

Background. The purpose of the study was to find out whether there is a difference in the early parameters of cardiotoxicity (left ventricular ejection fraction [LVEF] and N-terminal pro-B-type natriuretic peptide [NT-proBNP]) between the two groups of patients: the patients treated for left breast cancer (left breast cancer group) and those treated for the right breast cancer (right breast cancer group), after the treatment had been completed.

Patients and methods. The study included 175 consecutive patients with human epidermal growth factor receptor-2 (HER2) positive early breast cancer, treated concurrently with trastuzumab and radiotherapy (RT), between June 2005 and December 2010. Echocardiography with LVEF measurement was performed before adjuvant RT (LVEF₀) and after the completed treatment (LVEF₁). After the treatment NT-proBNP measurement was done as well. The difference (Δ) between LVEF₀ and LVEF₁ was analysed (Δ LVEF = LVEF₀ - LVEF₁) and compared between the two groups.

Results. There were 84 patients in the left and 91 in the right breast cancer group. Median observation time was 57 (37–71) months. Mean Δ LVEF (%) was -1.786% in the left and -2.607% in the right breast cancer group ($p = 0.562$, CI: -2.004 to 3.648). Median NT-proBNP were 111.0 ng/l in the left and 90.0 ng/l in the right breast cancer group ($p = 0.545$). Echocardiography showed that the patients in the left breast cancer group did not have significantly worse systolic and diastolic left ventricular function in comparison with the patients in the right breast cancer group, but, they had higher incidence of pericardial effusion (9 [11%] vs. 1 [1%]) ($p = 0.007$).

Conclusions. We did not find any significant differences in the early parameters of cardiotoxicity (LVEF, NT-proBNP) between the observed groups. Patients who received left breast/chest wall irradiation had higher incidence of pericardial effusion.

Key words: trastuzumab; breast cancer; Radiotherapy; cardiotoxicity; echocardiography

Introduction

The advent of trastuzumab, a humanized monoclonal antibody against the extracellular domain of human epidermal growth factor receptor-2 (HER2), represented a major breakthrough in the treatment of patients with HER2-positive breast cancer. Long term follow-up from the initial large adjuvant tri-

als with trastuzumab continue to show some remarkably positive results.¹ The current standard adjuvant systemic treatment of early HER2-positive breast cancer consists of chemotherapy (CT) plus 12 months of trastuzumab, with or without endocrine therapy.²⁻⁴ The patients treated with adjuvant radiotherapy (RT) of the breast or chest wall receive trastuzumab concurrently with RT. Treatment with

trastuzumab results in a small to modest cardiotoxicity risk.⁵⁻⁷ RT could be cardiotoxic as well.⁸⁻¹⁰ Long-term effects of concomitant treatment with trastuzumab and RT have not yet been known, the most important of which is the issue of cardiotoxicity.

Reduced left ventricular ejection fraction (LVEF) and elevated N-terminal pro-B-type natriuretic peptide (NT-proBNP) levels represent early parameters of cardiotoxicity. LVEF is the golden standard for monitoring cardiac function in patients receiving cardiotoxic therapy.¹¹ Trastuzumab-related cardiotoxicity is most often manifested by an asymptomatic decrease in LVEF, and less often by clinical heart failure.¹²⁻¹⁴ NT-proBNP represents a sensitive biomarker for both: systolic and diastolic heart failure, not just as a diagnostic tool, but also as a prognostic tool.¹⁵ Elevated levels can be detected early in the asymptomatic stage of the disease, or in patients with the preserved ejection fraction.¹⁶ Changes in NT-proBNP usually occur earlier than changes in LVEF.¹⁷

There are two widely used methods for measuring LVEF: radionuclide ventriculography and echocardiography. The first method provides solely the information regarding the LVEF, while the second one provides also the information concerning chamber dimensions, heart valves, and pericardium. This data is very important because a reduction in LVEF is not that sensitive and it occurs later than left ventricular diastolic dysfunction. Some patients with heart failure never develop ventricular systolic dysfunction (heart failure with preserved ejection fraction).¹⁷⁻¹⁹

The main purpose of this study was to find out whether there is a significant difference in the early parameters of cardiotoxicity between the two groups of patients: those who received adjuvant trastuzumab and concurrent postoperative RT to the left (left breast cancer group) or to the right (right breast cancer group) breast/chest wall, after the completed treatment.

The study was designed as an equivalence study. Our hypothesis was that there were no significant differences between the left breast cancer and the right breast cancer group regarding some early cardiotoxicity parameters (LVEF and NT-proBNP).

Materials and methods

Patients and treatment

In a prospective observational monocentric population study, we included 175 consecutive patients with HER2-positive breast cancer (stage I-III) with-

out disease recurrence, who received adjuvant treatment with trastuzumab and RT to the breast/chest wall between June 2005 and December 2010 at the Institute of Oncology in Ljubljana.

All patients were treated according to the clinical guidelines, namely with surgery, CT, endocrine therapy in case of hormone receptor positive disease, trastuzumab, and RT. Trastuzumab treatment started before RT or on the first day of RT at the latest. Altogether, 203 consecutive patients with HER2-positive breast cancer were invited to participate in the study, among them 28 patients refused to be involved in the study. Informed consent was obtained from all individual participants included in the study. The study was internationally registered at ClinicalTrial.gov (identifier NCT 01572883), and it was approved by the Republic of Slovenia National Medical Ethics Committee.

In the study framework, between December 2011 and July 2012, after the treatment with trastuzumab had been completed, we performed clinical examinations, echocardiographic measurements of LVEF, and measurements of NT-proBNP levels in all patients. Baseline LVEF was determined either by means of echocardiography or by radionuclide ventriculography. Before the clinical examination took place patients had fulfilled the questionnaires about smoking, concomitant diseases, and problems related to cardio-vascular diseases. All other data were collected from the patients' records. Patients were classified in New York Heart Association (NYHA) classes, according to the NYHA classification, as well as in World Health Organisation (WHO) performance classes, according to the WHO classification.

Systemic treatment

The criteria for the adjuvant treatment with trastuzumab regarding tumour, nodal stage and cardiac function were the same as in pivotal adjuvant trials: tumours larger than 2 cm if node negative disease, any tumour size if node positive disease, WHO performance status zero or one, no serious concomitant cardiac disease, and treatment with adjuvant CT.⁴

Loco regional treatment

According to clinical guidelines patients were operated with either breast conservation surgery or mastectomy and either sentinel node biopsy or axillary dissection. After the operation and CT they were irradiated on the Cobalt machine or on the

linear accelerator. Two-dimensional RT (2D RT) or three-dimensional conformal RT (3D CRT) were mostly used. Some of the patients received electron-beam chest wall irradiation, sometimes in combination with concomitant photon-beam irradiation of the periclavicular region (regional RT). Whole breast RT was required in all patients who underwent breast cancer surgery. In addition to the irradiation of the breast/thoracic wall all patients with 4 or more positive axillary lymph nodes also received regional RT. Parasternal lymph nodes were not specifically included in the irradiated area.

Patients were irradiated with a total dose (TD) = 25×2 Gy, 5 fractions per week. A minority received RT with TD = 17 or 18×2.5 Gy, 5 fractions per week. RT was performed 3 or more weeks after CT had been completed and concurrently with trastuzumab treatment as well as hormonal therapy in case of hormone receptor positive breast cancer.

Echocardiography and radionuclide ventriculography

At the beginning of the primary systemic therapy baseline echocardiography was performed at different clinical institutions according to the shortest waiting time for the examination. Contrary to this, all control echocardiographies were performed in one institution (Department of Cardiology, University Medical Centre Ljubljana) by three cardiologists, and they were carried out on the same device (Aloka SSD- α 10, Tokyo, Japan). Conventional and tissue-Doppler echocardiography was performed on each patient.^{20,21} Normal range for LVEF was 50% or more.

All radionuclide ventriculographs were performed at the Institute of Oncology in Ljubljana (Gamma Cam Siemens; erythrocytes were labelled with in vivo method, activity 740-952 MBq) Normal range for LVEF was 50% or more. LVEF was calculated with the programme Intermedical/Medicview.

NT-proBNP

NT-proBNP was determined with the analyser Cobas e 411 (Roche). According to the instructions of the manufacturer, the values of the NT-proBNP below 125 ng/l exclude heart dysfunction.

Pathology methods

HER2 immuno histochemistry (IHC) expression was scored as follows: 0, no staining or faint mem-

brane staining in $\leq 10\%$ of tumour cells; 1+, incomplete membrane staining that is faint perceptible in $>10\%$ of tumour cells; 2+, incomplete and/or weak to moderate membrane staining in $>10\%$ of tumour cells or complete and intense staining in $\leq 10\%$ of tumour cells; and 3+, complete, intense circumferential membrane staining in $>10\%$ of tumour cells. HER2 scores of 0 and 1+ were considered negative. All IHC2+ tumours were tested for gene amplification by fluorescent in situ hybridization (FISH). HER2 IHC 3+ and FISH-amplified tumours were considered positive.

Statistical methods

The study was designed as an equivalence study. For the purpose of the analysis the patients were divided into two groups: (1) left breast cancer group: patients irradiated on the left side of the chest (breast cancer of the left breast) and (2) right breast cancer group: patients irradiated on the right side of the chest (breast cancer of the right breast).

In both group we compared the difference between LVEF, measured at the beginning of the adjuvant systemic therapy (LVEF₀), and LVEF measured after the treatment with trastuzumab (LVEF₁) had been completed. The difference between the two measurements was marked as Δ LVEF = LVEF₀ - LVEF₁, and we made comparisons between the two groups. A 95% confidence interval for the difference of means (CI) was estimated. Groups were labelled as equivalent if 95 % CI did not include Δ LVEF of 10 percentage points, but it included the value 0.

In calculating the necessary sample size we assumed that there were no differences in the population between the investigated groups, and that the standard deviation of the difference of Δ LVEF would be 10 percentage points. The level of significance was set to 5% and the desired power to at least 80%. We considered the difference Δ LVEF of 10 percentage points or less as clinically irrelevant. The calculation using PASS (version 12) showed that under these assumptions the equivalence study enrolling 20 patients per group would have 86% power. In addition to the primary objective we, namely, wanted to analyse also echocardiographic parameters at the control examination after the completed treatment with trastuzumab and RT. The data is presented as mean (standard deviation, SD) or median (interquartile range Q1-Q3) for continuous variables as appropriate, and number (%) for categorical variables.

The difference between the groups (the left breast cancer group and the right breast cancer

TABLE 1. Patients and tumour characteristics, concomitant diseases

		All N = 175 (100%)	Left BC group N = 84 (48%)	Right BC group N = 91 (52%)	p value
Age in years (Median [Q1–Q3])		58 (49–64)	59 (52–67)	55 (46–63)	0.0096
Menopause status	Premenopause	90 (51.4%)	38 (45.2%)	52 (57.1%)	0.155
	Postmenopause	85 (48.5%)	46 (54.8%)	39 (42.9%)	
Histological type	Ductal invasive	168 (96%)	81 (96.4%)	87 (95.6%)	1
	Lobular invasive	4 (2.3%)	2 (2.4%)	2 (2.2%)	
	Other	3 (1.7%)	1 (1.2%)	2 (2.2%)	
Histo-pathological grade	G 1	2 (1.1%)	0	2 (2.2%)	0.337
	G 2	48 (27.4%)	21 (25%)	27 (29.7%)	
	G 3	125 (71.5%)	63 (75%)	62 (68.1%)	
Hormonal receptors	ER positive	97 (55.4%)	53 (63%)	44 (48.3%)	0.851
	PR positive	82 (46.8%)	43 (51.2%)	39 (42.8%)	
	ER in PR negative	73 (41.7%)	28 (33.3%)	45 (49.4%)	
Concomitant disease	Smoking	33 (19%)	13 (15%)	20 (22%)	0.365
	Arterial hypertension	35 (20%)	21 (25%)	14 (15.4%)	0.161
	Diabetes	3 (1.7%)	3 (3.4%)	0	0.108
	Hyperlipidemia	30 (17.1%)	16 (19%)	14 (15.4%)	0.658
	Known heart disease*	4 (2.3%)	1 (1.2%)	3 (3.3%)	0.621

BC = breast cancer; ER = estrogens receptor; PR = progesterone receptor; Q1–Q3 = quartiles

*All diseases had been already present at diagnosis of breast cancer. Group 1: mild aortic stenosis; Group 2: mitral valve prolapse; compensated hypertonic heart and symptomatic angina pectoris; undefined cardiomyopathy

group) for continuous variables was tested with t-test, Welch t-test, or Mann-Whitney test as appropriate. The assumption of normality was verified with Shapiro-Wilks test, and Bartlett test was used to test the assumption of variance equality.

The association between the two groups (left breast cancer and right breast cancer group) and categorical variables was tested with χ^2 test, as well as with Yates continuity correction of Fischer exact test as appropriate.

A p-value of less than 0.05 was considered as statistically significant. The analysis was performed with R language for statistical computing (R version 3.0.1).²²

Results

Patient characteristics

There were 84 patients (48%) in the left breast cancer group, and 91 patients (52%) in the right breast cancer group. Median age was 59 (52–67) years in the left breast cancer group, and 55 (46–63) years in the right breast cancer group ($p = 0.009$). Median observation time was 57 (37–71) months. Patients and tumour characteristics as well as the associated diseases are described in Table 1. Among all the patients, 35 of them (20%) had arterial hypertension,

but there were no significant differences between the two groups.

Local and systemic treatments

All patients received CT. Among all of them 95 patients (54.3% of all the patients) received one of the following CT schemes: doxorubicin, cyclophosphamide (AC) / epirubicin, cyclophosphamide (EC) / 5-FU, doxorubicin, cyclophosphamide (FAC) / 5-FU, epirubicin, and cyclophosphamide (FEC) with a sequence of taxanes, and 69 patients (39.4% of all the patients) received one of the following schemes: AC / EC / FAC / FEC without taxanes. Only 11 patients (6.3% of all the patients) did not receive any anthracyclines (6 patients in the left breast cancer group and 5 patients in the right breast cancer group). None of the patients received concomitant anthracyclines and trastuzumab. There were no significant differences found in the CT schemes used, hormone therapies, and in the mean received cumulative doses of anthracyclines, taxanes, cyclophosphamide, and trastuzumab between the two groups. Systemic treatment is described in detail in Table 2.

Among all the patients, 39 patients (79.4% of all the patients) were treated with 2D RT technique, and 25 patients (14.3%) with 3D CRT technique. RT treatment features are presented in Table 3.

TABLE 2. Systemic treatment and surgical characteristics

	All (N = 175) (%)	Left BC Group (N = 84) (%)	Right BC Group (N = 91) (%)	P value
Anthracyclines				
Cumulative dose- mg/m ² BSA (Median [Q1–Q3])	350 (292–499)	352 (295–497)	349 (290–499)	0.799
Taxanes				
Cumulative dose- mg/m ² BSA (Median [Q1–Q3])	297 (276–594)	297 (281–422)	298 (273–768)	0.783
Cyclophosphamide				
Cumulative dose- mg/m ² BSA (Median [Q1–Q3])	2316 (1758–2924)	2344 (1763–2992)	2268 (1758–2829)	0.482
CT Scheme				
AC/EC/FAC/FEC + taxanes	95 (54.3%)	40 (47.6%)	55 (60.4%)	0.235
AC/EC/FAC/FEC without taxanes	69 (39.4%)	38 (45.3%)	31 (34.1%)	
Other	11 (6.3%)	6 (7.1%)	5 (5.5%)	
Endocrine therapy				
Tamoxifen	39 (22.3%)	21 (25%)	18 (19.8%)	0.652
Aromatase inhibitor	45 (25.7%)	26 (30.9%)	19 (20.8%)	
Other	10 (5.7%)	7 (8.3%)	3 (3.3%)	
Trastuzumab				
Cumulative dose- mg/kg BSA (Median [Q1–Q3])	105 (97–114)	105 (97–116)	105 (97–112)	0.658
Type of surgery				
Mastectomy	91 (52%)	38 (45.2%)	53 (58.2%)	0.116
Breast conserving surgery	84 (48%)	46 (54.8)	38 (41.8%)	

AC = doxorubicin, cyclophosphamide; BC = breast cancer; BSA = body surface area (The Du Bois formula was used for the calculation); CT = chemotherapy; EC = epirubicin, cyclophosphamide; FAC = 5-FU, doxorubicin, cyclophosphamide; FEC = 5-FU, epirubicin, and cyclophosphamide; Q1–Q3 = quartiles

TABLE 3. Radiotherapy treatment features

	All (N = 175) (%)	Left BC group (N = 84) (%)	Right BC group (N = 91) (%)	p value
RT field*				
Breast	70 (40%)	38 (45.3%)	32 (35.2%)	0.434
Breast + scl	17 (9.7%)	9 (10.7%)	8 (8.8%)	
Thoracic wall	17 (9.7%)	8 (9.5%)	9 (9.9%)	
Thoracic wall + scl	71 (40.6%)	29 (34.5%)	42 (46.1%)	
RT technique				
2D RT	139 (79.4%)	69 (82.1%)	70 (76.9%)	0.256
3D CRT	25 (14.3%)	12 (14.3%)	13 (14.3%)	
Electrons +/- photons	11 (6.3%)	3 (3.6%)	8 (8.8%)	
RT scheme				
25 x 2 Gy	14 (8.6%)	73 (86.9%)	75 (82.4%)	0.540
17 or 18 x 2.5 Gy	27 (15.4%)	11 (13.1%)	16 (17.6%)	

BC = breast cancer; RT = radiotherapy; scl = periclavicular nodes; 2D RT = two-dimensional radiotherapy; 3D CRT = three-dimensional conformal radiotherapy

* parasternal lymph nodes were not included in the irradiated area

Early cardiotoxicity parameters (LVEF and NT-proBNP)

The analysis showed no statistically significant differences between initial and control LVEF in the observed groups. Data is presented in detail in Table 4.

The time between the introduction of trastuzumab and the beginning of RT, the time between LVEF₀ measurement and the time between LVEF₀ and LVEF₁ did not differ between the observed groups (p = 0.596, 0.506 and 0.089, respectively).

Overall, we found an important reduction of the LVEF (a decrease of LVEF for 10 percent points or

TABLE 4. Analysis of the difference in left ventricular ejection fractions (Δ LVEF)

	All (N = 175)	Left BC Group (N = 84)	Right BC Group (N = 91)	P value
LVEF₀ (%) (Median [Q1–Q3])	65 (60–69)	65 (61–70)	63 (59.5–67)	0.0208
LVEF₁ (%) (Median [Q1–Q3])	66 (62–70)	67 (64–70)	65 (60–70.5)	0.117
Analysis of Δ LVEF	(n = 149)	(n = 70)	(n = 79)	0.562
LVEF ₀ (%)–LVEF ₁ (%) = Δ LVEF (Mean [SD])	-2.22 (8.69)	-1.78 (7.85)	-2.60 (9.4)	95% CI: -2.004 – 3.648

BC = breast cancer; CI = confidential interval; LVEF₀ = measurement of LVEF before RT; LVEF₁ = measurement of LVEF after the adjuvant treatment with T; Q1–Q3 = quartiles; SD = standard deviation

more or a final value of LVEF < 50) in 9 patients (6%) (4 patients in the left breast cancer and 5 in the right breast cancer group), of which 8 patients were classified as NYHA class 1.

Median NT-proBNP, measured after the completed treatment with trastuzumab, was 111.0 (56.7–182) ng/l in the left breast cancer group, and 90.0 (58–170) ng/l in the right breast cancer group ($p = 0.545$).

Echocardiographic parameters

Echocardiographic parameters are presented in Table 5. A comparison of echocardiographic parameters showed that the patients who received RT to the left breast/thoracic wall did not have significantly worse systolic or diastolic left ventricular function.

We found significantly more pericardial effusions (9 [11%]) in the left breast cancer group than in the right breast cancer group (1 [1%]) ($p = 0.007$). The thickness of pericardial effusion was > 1cm in 1 patient in the left breast cancer group, all others were < 1 cm.

Discussion

Thanks to treatment with trastuzumab, patients with HER2 positive breast cancer nowadays live longer than ever. In the framework of the oncological treatment they received a very successful therapy that in many cases prevents cancer recurrence, but could also have an impact on their health and therefore on the quality of their life a few or many years after the treatment. It is very important to analyse such sequels of a treatment, especially if they could be successfully treated at the very beginning, and if the exacerbation could be stopped before it affects the quality of life.

Concomitant treatment with trastuzumab and RT has been a part of a standard adjuvant treatment of HER2 positive breast cancer at our institution since 2005, which means from the very beginning of the “adjuvant trastuzumab era”. In that time 2D RT technique was used at our institution for breast cancer patients, and most patients from our study were irradiated with this technique. Later more accurate 3D CRT technique was available for adjuvant RT in breast cancer patients. None

TABLE 5. Echocardiographic parameters (n = 175)

	Left BC Group (n = 84) (median [Q1–Q3])	Right BC Group (n = 91) (median [Q1–Q3])	p value
LV EDD (cm)	4.6 (4.4–4.9)	4.6 (4.4–4.8)	0.913 95% CI (-0.10–0.10)
LV ESD (cm)	2.9 (2.6–3.1)	2.8 (2.5–3.2)	0.541 95% CI (-0.19–0.10)
LA tr (cm)	3.4 (3.2–3.8)	3.4 (3.2–3.7)	0.830 95% CI (-0.10–0.10)
LA long (cm)	4.4 (4.0–4.8)	4.5 (4.2–4.6)	0.979 95% CI (-0.10–0.10)
RA tr (cm)	3.2 (3.0–3.6)	3.4 (3.0–3.7)	0.298 95% CI (-0.20–0.00)
RA long (cm)	4.1 (3.8–4.4)	4.3 (3.9–4.4)	0.226 95% CI (-0.20–0.09)
LVEF (%)	68.5 (64–74.2)	68.0 (63.0–72.5)	0.758 95% CI (-2.0–3.00)
E/A	1.07 (0.80–1.23)	1.08 (0.87–1.32)	0.113 95% CI (-0.18–0.02)
E/E_m	7.15 (6.27–9.26)	7.40 (6.18–8.68)	0.918 95% CI (-0.52–0.66)
s/d	1.368 (1.065–1.600)	1.149 (0.94–1.35)	0.002 95% CI (0.07–0.29)
TDI Sm (cm/s)	8.0 (7.0–9.1)	8.0 (7.0–9.1)	0.985 95% CI (-0.50–0.50)
TDI Em (cm/s)	10.0 (7.82–11.37)	10.0 (8.05–11.8)	0.547 95% CI (-0.10–0.50)

CI = confidential interval; E/A = mitral valve annulus ratio of early diastolic and atrial flow velocities; E/E_m = ratio between the early diastolic blood flow velocity on the mitral valve annulus and early diastolic tissue Doppler velocity at the mitral ring; LA long – left atrial longitudinal diameter; LA tr = left atrial transversal diameter; LV EDD = left ventricular end diastolic diameter; LVEF = left ventricular ejection fraction; LV ESD = left ventricular end systolic diameter; Q1–Q3 = quartiles; RA long – right atrial longitudinal diameter; RA tr = right atrial transversal diameter; s/d = ratio of systolic and diastolic blood flow velocities in the pulmonary vein; TDI Sm – systolic tissue Doppler velocity at the mitral ring; TDI Em = early diastolic tissue Doppler velocity at the mitral ring

TABLE 6. Pericardial effusion

	ECHO	All (N = 174) (%)	Left BC Group (N = 83) (%)	Right BC Group (N = 91) (%)	p value
Pericard	Normal Effusion	164 (94.3%) 10 (5.7%)	74 (89%) 9 (11%)	90 (99%) 1 (1%)	0.007

BC = breast cancer; ECHO = echocardiography

of the patients included in the study received RT specifically to the parasternal lymph nodes. This fact is important for the interpretation of the results, because RT in that region may raise the dose received by the heart.²³

All the patients included in the study were treated with CT. Only 11 patients did not receive CT with anthracyclines, which is not surprising, especially if taking into account the well-known benefits of the anthracycline treatment.²⁴ There were no significant differences in the CT scheme used, endocrine therapy, and in the mean received cumulative doses of anthracyclines, taxanes, cyclophosphamide, and trastuzumab between the two groups ($p > 0.05$). These results suggest that cardiotoxic effect of specific systemic oncological treatment was similar in both groups that were analysed. In the framework of the adjuvant treatment received by the patients, the only factor that could affect the difference in cardiotoxic parameters measured in both groups was the cardiotoxic effect of the adjuvant RT.

The prevalence of smoking, hyperlipidemia, and arterial hypertension was approximately the same in both groups (around 20 %). Only 3 patients had diabetes, all of them had breast cancer of the right breast. Among all the patients, 4 patients had already been diagnosed with heart diseases at the time of breast cancer diagnosis (specified in Table 1). One 70-year-old patient acquired atrial fibrillation two years after being diagnosed with breast cancer, but she had had arterial hypertension for 18 years already. According to this data, the influence of cardiovascular disease predisposing factors was similar in both groups.

The differences in Δ LVEF between the two groups were not statistically significant. The acquired data shows that the median value of the LVEF in both groups was slightly lower at the beginning of the treatment in comparison with the LVEF value measured after the treatment. This could be explained by the time that passed from the introduction of trastuzumab to the measurement of LVEF (mean time 62 days in the left breast cancer group and 66 days in the right breast cancer

group. $p = 0.591$). It was reported that LVEF value could reversibly decrease during treatment with trastuzumab.²⁵

Among all the patients, we found an important reduction of the LVEF (a decrease of LVEF for 10 percent points or more or a final value of LVEF < 50) in 9 patients (6%). There were more such patients in the right breast cancer group (6.3%) than in the left breast cancer group (5.7%); therefore, we concluded that left breast/chest wall irradiation was not the key factor that would significantly affect the reduction of LVEF.

The analysis showed no statistically significant differences in NT-proBNP between the two groups. According to the instructions of the diagnostic test manufacturer, the values of the NT-proBNP below 125 ng/l exclude heart failure, so we decided to mark all the values of NT-proBNP 125 ng/l or higher as an event. There were no significant differences in the number of such events in both groups. Among all the patients there were 69 patients (39%) with NT-proBNP 125 ng/l or more, 35 patients (41.7%) in the left breast cancer group, 34 patients (37.4%) in the right breast cancer group; $p = 0.669$. Based on these results we concluded that left breast/chest wall irradiation did not have a considerable impact on the measured values of NT-proBNP after the treatment had been completed.

Certain parameters of left ventricular diastolic dysfunction, such as mitral valve E/A ratio, E/Em ratio, and pulmonary vein s/d ratio, are more sensitive and can be detected before the LVEF reduction. Left ventricular diastolic dysfunction therefore can represent an early sign of cardiotoxicity, and thus, since it is more timely, proves to be more effective than LVEF estimation.^{26,27} Among patients included in our study 42% had left ventricular diastolic dysfunction, mostly mild. One patient in the left breast cancer and 5 patients in the right breast cancer group had moderate diastolic dysfunction, none of the patients had severe diastolic dysfunction. Baseline diastolic function was not determined. We found significantly lower s/d ratio in the right breast cancer group, suggesting worse diastolic function compared to the left breast cancer group.

Since s/d ratio is largely dependent on the hemodynamic status it cannot be used as a sole diastolic function predictor. There were no significant differences in other left ventricular diastolic function parameters between the observed groups. That is why we presumed that RT had no significant influence on the left ventricular diastolic function in the observed time interval.

The analysis of echocardiographic parameters showed that patients in both groups had heart cavities of normal size and a normal systolic function of the left ventricle. The patients irradiated on the left breast/thoracic wall did not have significantly worse systolic or diastolic function of the left ventricle.

The data showed that the patients with left breast cancer had significantly higher incidence of pericardial effusion after the stated observation time. It is well known that irradiation could damage pericardium and that acute pericarditis is the most common heart damage caused by irradiation. It is rare and most commonly develops in the first year after the RT treatment.²⁸

In conclusion, we did not find any significant differences in the early parameters of cardiotoxicity (LVEF, NT-proBNP) between the two observed groups. The patients with the left breast cancer that were irradiated on the left breast/thoracic wall four and a half years after the treatment did not have significantly worse systolic or diastolic function of the left ventricle compared to the patients with the right breast cancer that were irradiated on the right breast/thoracic wall, but, left breast cancer patients had significantly higher incidence of pericardial effusion. RT did not have an important impact on the function of the left ventricle after the stated observation time.

So far, this is the first study evaluating early cardiotoxicity with the echocardiographic parameters and NT-proBNP in breast cancer patients after the completed concomitant treatment with RT and trastuzumab.

Our observation of higher incidence of pericardial effusion in left breast cancer was limited by a small number of included patients. In the future studies with a larger number of patients are to be carried out to confirm our findings.

In the following studies, it would be necessary to determine whether the changes in the pericardium are more frequent, more pronounced, or may be last longer if patients receive RT concurrently with trastuzumab.

References

1. Cameron D, Piccart-Gebhart MJ, Gelber RD, Procter M, Goldhirsch A, de Azambuja E, et al. Herceptin Adjuvant (HERA) Trial Study Team. 11 years' follow-up of trastuzumab after adjuvant chemotherapy in HER2-positive early breast cancer: final analysis of the HERceptin Adjuvant (HERA) trial. *Lancet* 2017; **389**: 1195-205. doi: 10.1016/S0140-6736(16)32616-2
2. Pinto AC, Ades F, de Azambuja E, Piccart-Gebhart M. Trastuzumab for patients with HER2 positive breast cancer: delivery, duration and combination therapies. *Breast* 2013; **22**: 152-5. doi: 10.1016/j.breast.2013.07.029
3. Mathew A, Romond EH. Systemic therapy for HER2-positive early-stage breast cancer. *Curr Probl Cancer* 2016; **40**: 106-16. doi: 10.1016/j.cuprob-cancer.2016.09.002
4. Matos E, Zakotnik B, Kuhar CG. Effectiveness of adjuvant trastuzumab in daily clinical practice. *Radiol Oncol* 2014; **48**: 403-7. doi: 10.2478/raon-2013-0081
5. Zamorano JL, Lancellotti P, Muñoz DR, Aboyans V, Asteggiano R, Galderisi M, et al. 2016 ESC Position Paper on cancer treatments and cardiovascular toxicity developed under the auspices of the ESC Committee for Practice Guidelines: The Task Force for cancer treatments and cardiovascular toxicity of the European Society of Cardiology (ESC). *Eur Heart J* 2016; **37**: 2768-801. doi: 10.1093/eurheartj/ehw211
6. Jawa Z, Perez RM, Garlie L, Singh M, Qamar R, Khandheria BK, et al. Risk factors of trastuzumab-induced cardiotoxicity in breast cancer: a meta-analysis. *Medicine (Baltimore)* 2016; **95**: e5195. doi: 10.1097/MD.0000000000005195
7. Piccart-Gebhart MJ, Procter M, Leyland-Jones B, Goldhirsch A, Untch M, Smith I, et al. Trastuzumab after adjuvant chemotherapy in HER-2 positive breast cancer. *N Engl J Med* 2005; **353**: 1659-72. doi: 10.1056/NEJMoa052306
8. Darby SC, McGale P, Taylor CW, Peto R. Long-term mortality from heart disease and lung cancer after radiotherapy for early breast cancer: prospective cohort study of about 300,000 women in US SEER cancer registries. *Lancet Oncol* 2005; **6**: 557-65. doi: 10.1016/S1470-2045(05)70251-5
9. Henson KE, McGale P, Taylor C, Darby SC. Radiation-related mortality from heart disease and lung cancer more than 20 years after radiotherapy for breast cancer. *Br J Cancer* 2013; **108**: 179-82. doi: 10.1038/bjc.2012.575
10. Sardar P, Kundu A, Chatterjee S, Nohria A, Nairooz R, Bangalore S, et al. Long-term cardiovascular mortality after radiotherapy for breast cancer: a systematic review and meta-analysis. *Clin Cardiol* 2017; **40**: 73-81. doi: 10.1002/clc.22631
11. Jacob J, Belin L, Gobillion A, Daveau-Bergerault C, Dendale R, Beuzeboc P, et al. [Prospective monocentric study of the toxicity and the efficacy of concurrent trastuzumab and radiotherapy]. [French]. *Cancer Radiother* 2013; **17**: 183-90. doi: 10.1016/j.canrad.2012.12.006
12. Keefe DL. Trastuzumab-associated cardiotoxicity. *Cancer* 2002; **95**: 1592-600. doi: 10.1002/cncr.10854
13. Perez EA, Rodeheffer R. Clinical cardiac tolerability of trastuzumab. *J Clin Oncol* 2004; **22**: 322-9. doi: 10.1200/JCO.2004.01.120
14. Fiuza M. Cardiotoxicity associated with trastuzumab treatment of HER2+ breast cancer. *Adv Ther* 2009; **26(Suppl 1)**: S9-17. doi: 10.1007/s12325-009-0048-z
15. Guarneri V, Lenihan DJ, Valero V, Durand JB, Broglio K, Hess KR, et al. Long-term cardiac tolerability of trastuzumab in metastatic breast cancer: the M.D. Anderson Cancer Center experience. *J Clin Oncol* 2006; **24**: 4107-15. doi: 10.1200/JCO.2005.04.9551
16. Steel GG. *Basic clinical radiobiology*. 3rd edition. London: Arnold; 2002. p. 217-39.
17. Zethelius B, Berglund L, Sundström J, Ingelsson E, Basu S, Larsson A, et al. Use of multiple biomarkers to improve the prediction of death from cardiovascular causes. *N Engl J Med* 2008; **358**: 2107-16. doi: 10.1056/NEJMoa0707064
18. Kinnunen P, Vuolteenaho O, Ruskoaho H. Mechanisms of atrial and brain natriuretic peptide release from rat ventricular myocardium: Effect of stretching. *Endocrinology* 1993; **132**: 1961-70. doi: 10.1210/endo.132.5.8477647

19. Raymond I, Groenning BA, Hildebrandt PR, Nilsson JC, Baumann M, Trawinski J, et al. The influence of age, sex and other variables on the plasma level of N-terminal pro brain natriuretic peptide in a large sample of the general population. *Heart* 2003; **89**: 745-51.
20. Marinko T, Dolenc J, Bilban-Jakopin C. Cardiotoxicity of concomitant radiotherapy and trastuzumab for early breast cancer. *Radiol Oncol* 2014; **48**: 105-12. doi: 10.2478/raon-2013-0040
21. Marinko T. Impact of concurrent radiotherapy and treatment with trastuzumab on cardiotoxicity of breast cancer patients. [Dissertation]. Ljubljana: Faculty of Medicine, University of Ljubljana; 2014.
22. R Core Team. R: A language and environment for statistical computing. Vienna: R Foundation for Statistical Computing; 2013. [cited 2017 Nov 15]. Available at <http://www.R-project.org/>
23. Hoening MJ, Botma A, Aleman BM, Baaijens MH, Bartelink H, Klijn JG, et al. Long-term risk of cardiovascular disease in 10-year survivors of breast cancer. *J Natl Cancer Inst* 2007; **99**: 365-75. doi: 10.1093/jnci/djk064
24. National Comprehensive Cancer Network Clinical Practice Guidelines in Oncology: Breast Cancer. Version 2.2017. [cited 2017 Nov 7]. Available at: https://www.nccn.org/professionals/physician_gls/pdf/breast.pdf
25. Ewer MS, Tan-Chiu E. Reversibility of trastuzumab cardiotoxicity: is the concept alive and well? *J Clin Oncol* 2007; **25**: 5532-3. doi: 10.1200/JCO.2007.14.0657
26. Giannuzzi P, Temporelli PL, Bosimini E, Silva P, Imparato A, Corrà U, et al. Independent and incremental prognostic value of Doppler-derived mitral deceleration time of early filling in both symptomatic and asymptomatic patients with left ventricular dysfunction. *J Am Coll Cardiol* 1996; **28**: 383-90. doi: 10.1016/0735-1097(96)00163-5
27. Suzuki J, Yanagisawa A, Shigejama T, Tsubota J, Yasumura T, Shimoyama K, et al. Early detection of anthracycline-induced cardiotoxicity by radionuclide angiocardiology. *Angiology* 1999; **50**: 37-45. doi: 10.1177/000331979905000105
28. Hall EJ, Giaccia AJ. *Radiobiology for the radiologist*. Chapter 20. 7th edition. Philadelphia: Lippincott Williams & Wilkins, Wolters Kluwer; 2012. p 343.

Ocular changes in metastatic melanoma patients treated with MEK inhibitor cobimetinib and BRAF inhibitor vemurafenib

Ana Ursula Gavric¹, Janja Ocvirk^{2,3}, Polona Jaki Mekjavic^{1,3}

¹ Eye Hospital, University Medical Centre Ljubljana, Ljubljana, Slovenia

² Department of Medical Oncology, Institute of Oncology Ljubljana, Ljubljana, Slovenia

³ Faculty of Medicine, University of Ljubljana, Ljubljana, Slovenia

Radiol Oncol 2018; 52(2): 213-219.

Received 4 October 2017

Accepted 20 November 2017

Correspondence to: Assoc. Prof. Polona Jaki Mekjavič, M.D., Ph.D.; Eye Hospital, University Medical Centre Ljubljana, Grablovičeva 46, 1000 Ljubljana. Phone: +386 1 522 1750; Fax: +386 1 522 1940; E-mail: polona.jaki@guest.arnes.si

Disclosure: No potential conflicts of interest were disclosed.

Background. Mitogen-activated protein kinase kinase (MEK) inhibitor cobimetinib and V-raf murine sarcoma viral oncogene homolog B1 (BRAF) inhibitor vemurafenib have significantly improved the prognosis of BRAF-mutated metastatic melanoma. Some ocular symptoms and signs were recently recognized to follow this treatment. The study was aimed to investigate ocular toxicity in patients with metastatic melanoma treated with cobimetinib in combination with vemurafenib.

Patients and methods. In the prospective, observational study, patients with BRAF-mutated metastatic melanoma treated with cobimetinib in combination with vemurafenib at the Institute of Oncology Ljubljana were asked to participate. Ophthalmic examination was performed including measurement of visual acuity and intraocular pressure, slit lamp examination, funduscopy (CF), infrared-reflectance (IR) imaging and optical coherence tomography (OCT).

Results. Five out of 7 patients noticed changes in vision few days after starting the therapy with cobimetinib. In all patients, small circular lesions, described as MEKAR lesions, were documented in outer retinal layers demonstrated with OCT, IR, and CF. Changes were in the center and/or scattered over the retina almost symmetrical in both eyes in 6 patients, and asymmetrical in one patient, the latter presented also with unilateral anterior uveitis and cystoid macular edema.

Conclusions. Multiple bilateral foveal and extrafoveal small retinal lesions in the outer retinal layers develop in patients treated with MEK inhibitor in combination with BRAF inhibitor. Ophthalmologists and oncologists need to be aware of this common, yet relatively benign and often transient ocular side effect to avoid needless intervention, including the discontinuance of a potentially life-prolonging therapy.

Key words: metastatic malignant melanoma; eye; MEKAR; MEK inhibitor

Introduction

Malignant melanoma is a significant health problem, the incidence of melanoma is steadily increasing, fastest among all cancers.¹ At diagnosis, metastases are present in approximately 2-5% of patients.²

In recent years several new targeted drugs and immunotherapy have been approved for the treatment of metastatic melanoma. Mitogen-activated

protein kinase kinase (MEK) inhibitors and V-raf murine sarcoma viral oncogene homolog B1 (BRAF) inhibitors are a newer group of drugs that act on the target enzymes of MAPK / ERK signaling pathway. The combination treatment with BRAF and MEK inhibitors is amongst the current standard of care for stage IIIc/IV BRAF-mutated melanoma. Combined BRAF and MEK inhibition seems to provide a greater benefit than BRAF or MEK inhibitor monotherapy.^{3,4}

The BRAF protein is a key part of “mitogen-activated protein kinase signaling pathway” (MAPK), which regulates the division and proliferation of cells and plays a central role in the progression of melanoma. MEK inhibitors inhibit the mitogen-activated protein kinase kinase MEK1 and/or MEK2. A specific mutation in the BRAF gene causes excessive activity, leading to uncontrolled growth and cell division. About 50% of melanomas harbors activating BRAF mutations.⁵ Therapy with the selective inhibitor of mutant BRAF Val600, vemurafenib in combination with MEK inhibitor cobimetinib showed major tumor responses, resulting in improved progression-free and overall survival in patients with metastatic disease, compared with chemotherapy.^{3,6}

MEK inhibitors have been associated with changes in retina by means of small localized serous neuroretinal detachments, which have been named MEK inhibitor-associated retinopathy (MEKAR).^{7,8} The most common ocular side effect associated with BRAF inhibitor vemurafenib in monotherapy are uveitis, conjunctivitis and dry eyes.⁹

When used cobimetinib in combination with vemurafenib the most commonly observed adverse effects in the coBRIM phase III trial were rash,

photosensitivity, MEKAR, alopecia, hyperkeratosis, diarrhea, nausea, arthralgia, fatigue, vomiting, blood creatine phosphokinase (CPK) increase and alanine aminotransferase (ALT) increase. Most adverse effects occurred within the first treatment cycle and decrease substantially over time.¹⁰

A pattern of ocular toxicity has followed these drugs through clinical trials and their association with ocular toxicity is only just beginning to be recognized.

The aim of our study was to look prospectively at the incidence, symptomatology, course, and reversibility of ocular toxicity in patients with BRAFV600 metastatic melanoma treated with MEK/BRAF inhibitor cobimetinib plus vemurafenib.

Patients and methods

Patients

All patients with BRAFV600 metastatic melanoma treated at the Institute of Oncology Ljubljana with MEK/BRAF inhibitor cobimetinib and vemurafenib from January to June 2017, were offered the chance to be included in the study at Eye Hospital of University Medical Centre Ljubljana. Seven out of eight patients were willing to participate. The

TABLE 1. Patient characteristics

Patient N°	1	2	3	4	5	6	7
Sex	M	M	F	M	M	M	M
Age (years)	41	58	64	74	71	45	55
N° of cycles at first eye exam	2	11	15	3	3	3	6
N° of cycles at last eye exam	3	13	24	8	5	4	7
Change in dosage	yes*	no	no	no	no	no	no
BCVA RE	1.0	1.0	1.0	0.7 – 0.9	0.8	1.0	1.0
BCVA LE	1.0	1.0	1.0	0.7 – 0.9	0.7	1.0	1.0
Symptoms	circle centrally	blurred vision	no	blurred vision	floaters in LE, blurred vision	circle centrally	no
Occurrence of symptoms after starting the therapy	1 week	1 week	-	1 week	1 month	1 week	-
Fluctuations of symptoms	spontan. resolution	no	-	different spectacles needed	better after topical therapy	spontan. resolution	needs spectacles
OCT changes in the fovea	elongation of IZ	SRF	SRF	SRF	elongation of IZ in RE, SRF in LE	SRF	SRF
Extrafoveal SRF	multiple bilateral	multiple bilateral	multiple bilateral	multiple bilateral	no	no	multiple bilateral
Other ocular findings	-	-	-	incipient senile cataract ou	uveitis in LE; incipient cataract ou	-	dilatated conjunctival vessels in the RE

* adjusted dose = lower dose due to the cutaneous side effects; BCVA = best corrected visual acuity; F = female; IZ = interdigitation zone; LE = left eye; M = male, OCT = optical coherence tomography; ou = both eyes; RE = right eye; SRF = subretinal fluid.

study adhered to the tenets of the Declaration of Helsinki and was submitted and approved by The Slovenian National Medical Ethics Committee. All patients signed an informed consent form and all attended the ophthalmology visits.

Treatment

All patients received BRAF/MEK inhibitor combination therapy for metastatic melanoma, vemurafenib (Zelboraf, Roche Products Ltd, Hertfordshire, UK) plus cobimetinib (Cotellic, Roche Products Ltd, Hertfordshire, UK) in the standard doses: cobimetinib 60 mg orally once daily on days 1-21 of an every 28-day cycle and vemurafenib 960 mg orally twice daily on days 1-28. Doses were reduced in the course of the treatment in one patient due to a severe cutaneous side effect.

Outcome measures

All patients had undergone a complete ophthalmologic examination, including best-corrected visual acuity (BCVA) and intraocular pressure measurement, slit-lamp biomicroscopy, funduscopy, and noninvasive imaging: color fundus photography (Topcon Fundus Camera), fundus autofluorescence (FAF), infrared-reflectance (IR) and spectral-domain optical coherent tomography (SD-OCT). Images were obtained with the Heidelberg Spectralis HRA+OCT (Heidelberg Engineering, Heidelberg, Germany). Every patient had at least two examinations in Eye Hospital of University Medical Centre Ljubljana.

Information about primary cancer diagnosis, other adjuvant treatments, the number of cycles, and the dosage of chemotherapy was collected from medical charts.

Results

Patient characteristics

There were 7 participants with BRAF mutated metastatic melanoma. The mean age was 58.3 years (\pm 9.8 years) with a median age of 58 years (range of 41–74 years). Time from the beginning of the therapy to the last control ranged from 2 to 24 months. Patient characteristics are shown in Table 1.

Ophthalmic characteristics

Ocular adverse effects were documented in all of the patients, giving an incidence of 100%. Bilateral

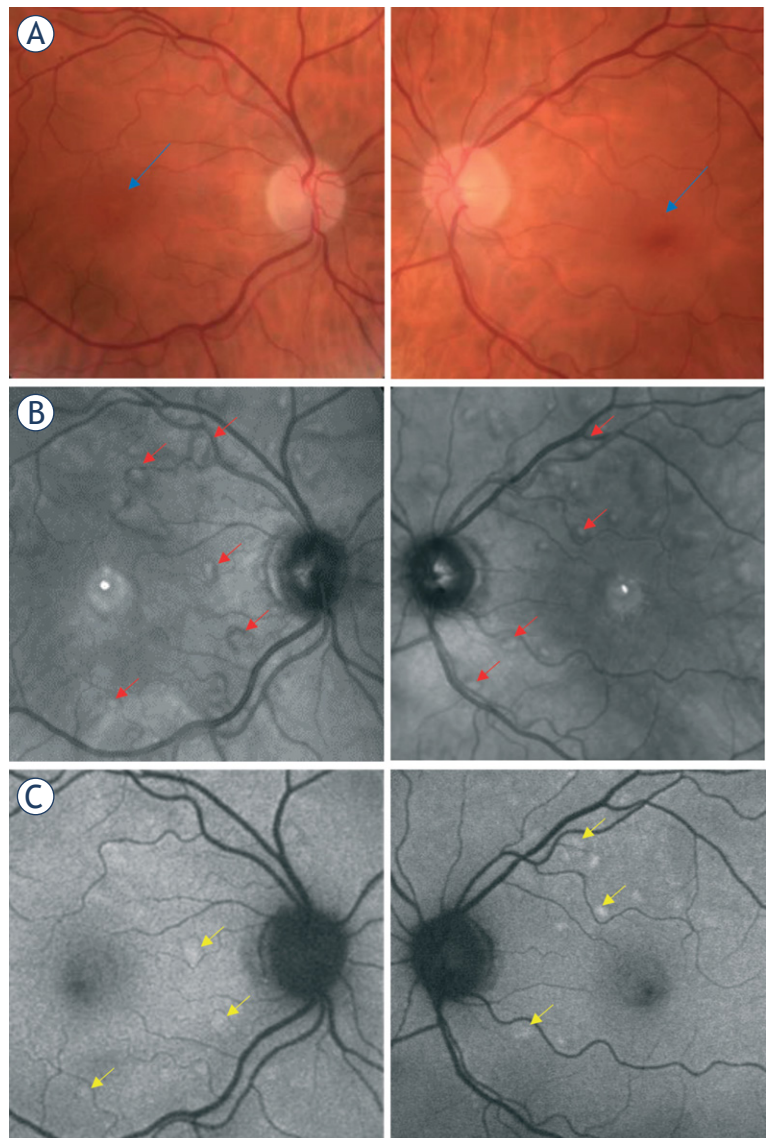


FIGURE 1. (A) Discrete bilateral lesions in the fovea seen on fundus photography (blue arrows); (B) Infrared reflectance imaging showing lesions with a hyperreflective center, surrounded by a hyporeflexive zone scattered throughout the posterior pole (some are marked with red arrows); (C) Some lesions showed increased signal in autofluorescence imaging (some are marked with yellow arrows).

serous neuroretinal detachments were observed in all 7 patients, additionally, in 1 eye, there was an associated anterior uveitis with cystoid macular edema (CME).

Five patients reported eye symptoms, 3 had fluctuations of blurry vision and 2 reported a circle centrally in the visual field. Best corrected visual acuity (BCVA) was 1.0 in 5 patients. Two patients had reduced BCVA; one presented with incipient senile cataract, his BCVA fluctuated from 0.7 to 0.9 in both eyes, another patient presented with unilateral uveitis and cataract in both eyes, he has

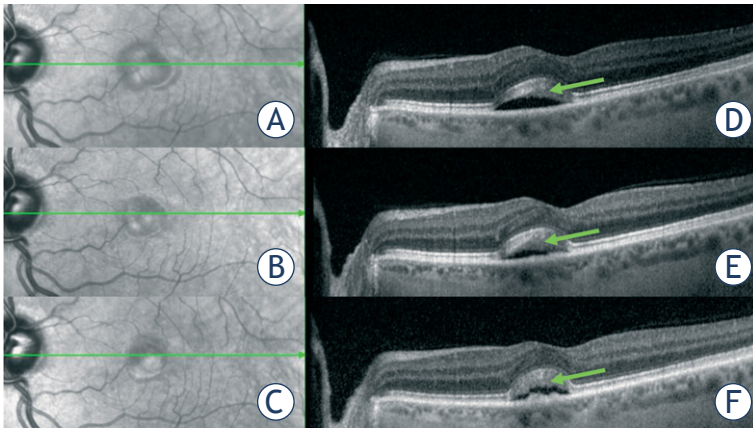


FIGURE 2. (A-C) IR imaging of foveal lesion during cycles; (D-F) OCT showed fluctuations of dome-shaped accumulation of subretinal fluid with elongation of interdigitation zone (green arrows) in the foveal region; A+D = imaging during 3rd cycle; B+E = imaging during 6th cycle; C+F = imaging during 8th cycle.

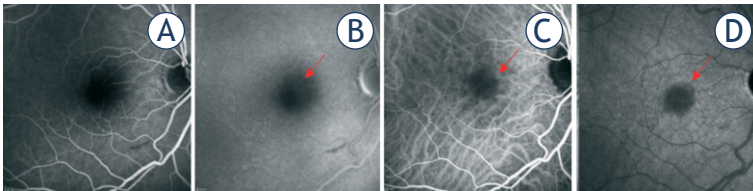


FIGURE 3. Fluorescein (A,B) and indocyanine green (C,D) angiography showed only mild masking effect of subretinal fluid on the location of lesions (red arrows).

BCVA of 0.6. IOP remained stable in all patients (from 14 to 22 mmHg).

Ophthalmoscopy revealed discrete bilateral transparent to yellowish lesions of less than 1/3 of the disc diameter in the fovea and extrafoveally. Not all lesions were seen with ophthalmoscopy (Figure 1A).

IR imaging showed lesions with a hyper reflective center, surrounded by a hyporeflective zone and multiple smaller lesions with similar reflectance characteristics scattered throughout the posterior pole. The location and number of lesions were relatively symmetrical between both eyes (Figure 1B).

Some lesions showed increased signal in autofluorescence imaging (Figure 1C).

Dome-shaped accumulations of subretinal fluid (SRF) with elongation of outer part of the interdigitation zone of photoreceptors into hyporeflective SRF were detected on OCT. During the following cycles of therapy, OCT findings showed fluctuations (Figure 2).

One patient presented with anterior uveitis and cystoid macular edema in the left eye, which re-

solved after a 3-week course of topical 0.1% dexamethasone.

Besides noninvasive imaging, fluorescein and indocyanine green (ICG) angiography was performed in one patient, showing no vascular abnormalities, no leakage or staining, only mild masking effect of subretinal fluid on the location of lesions was observed (Figure 3).

Discussion

We studied the incidence, symptoms and clinical characteristics of ocular toxicity in patients with BRAFV600 metastatic melanoma treated with cobimetinib in combination with vemurafenib.

Our results show 100% incidence of MEKAR in our patients. In contrast, in the coBRIM study patients were receiving the same therapy, but MEKAR was reported in only 26% of patients.¹¹ The authors of this study do not specify the day and hour of the examination, which according to Urner-Bloch is very relevant. On the basis of our observations, we concur with Urner-Bloch that the fluctuations in the MEKAR lesions are also dependent of the day within the treatment cycle.⁷ In patients that were also examined during the inter-treatment interval, we noted a decrease in the magnitude of the lesions. Some patients reported fluctuation of the symptoms, and one of them was able to compensate fluctuated blurry vision with different hyperopic refractive correction.

The results of a meta-analysis of the ocular safety of MEK inhibitors reveals an increased risk for ocular problems, particularly disturbed vision, and retinal changes such as “chorioretinopathy and retinal detachment”. They did not report any statistically significant increase in the risk for uveitis or eye hemorrhage.¹²

Similar results to ours were reported in a prospective observational study, in which 62 melanoma patients were treated with MEK inhibitor binimetinib in monotherapy or in combination with BRAF inhibitor. Bilateral retinopathy was diagnosed in 92% of patients on monotherapy and 100% in those with combination therapy. Retinopathy was described as dose- and time-dependent and was reversible in all patients.⁷

There is some confusion regarding the description of MEKAR in the literature. Some groups and authors have defined MEKAR as “chorioretinopathy”, “retinal pigment epithelium detachment (PED)” or “central serous retinopathy-like”.¹²⁻¹⁵

By means of optical coherent tomography (OCT) which became widely used diagnostic tool for retina, the morphology of MEKAR lesions is clarified. Lesions in MEKAR are not PED, because RPE is not detached and the fluid is accumulated above it. It is also not chorioretinopathy, as there are no visible changes in the choroid, no pachycoroid is observed in MEKAR and also no observable changes on ICG angiography. All mentioned changes are typical for central serous chorioretinopathy.⁸

Characteristically, in MEKAR, the choroidal thickness is normal, and focal lesions in the outer retinal layers are notable. The ellipsoid layer is unchanged and is clearly distinguishable from interdigital zone (IZ) which has elongations into sub-IZ space. Sub-IZ is filled with hypo reflective fluid (SRF). RPE layer is not disturbed. During the cycles hypo reflective sub-IZ fluid fluctuates, can vanish, but elongations of IZ remain (Figure 2). Previous studies have described similar retinal lesions associated with other MEK inhibitors treatment.^{7,16,17}

If lesion is located in the strict center of the macula, in the foveola, patients can describe symptoms such as a circle centrally in the visual field or blurred near vision. Accumulation of SRF thickens retina in the place of lesion hence the axial length of the eye is shortened. That results in blurred near vision due to induced hyperopia. Patients complain of difficulty reading without or with inappropriate reading glasses. Because lesions in MEKAR are thin, changes in vision are not dramatic and do not importantly influence patients' quality of life. If the symptoms are disturbing, they can be corrected with mild hyperopic correction.

One patient noticed a circle centrally in the visual field few days after starting the therapy. The therapy was promptly discontinued due to cutaneous side effects and after cessation of the therapy, the ocular symptoms also disappeared. Two weeks later patient started taking low dose therapy (cobimetinib 40 mg/day for 3 weeks, and vemurafenib 720 mg/12 h) and the ocular symptoms did not reappear. Morphological changes were present but barely detectable (Figure 4). It has been reported that patients treated with MEK inhibitor binimetinib experience visual disturbances, particularly in the first 4 weeks of treatment. Subsequent treatment, initiated after a given interval, causes less pronounced symptoms.⁷ It has not been reported whether the dosage within a given cycle influences the occurrence of the symptoms or the amount of sub-IZ fluid.

The mechanism of MEK inhibitor ocular toxicity still remains unresolved. Dysfunction of retinal

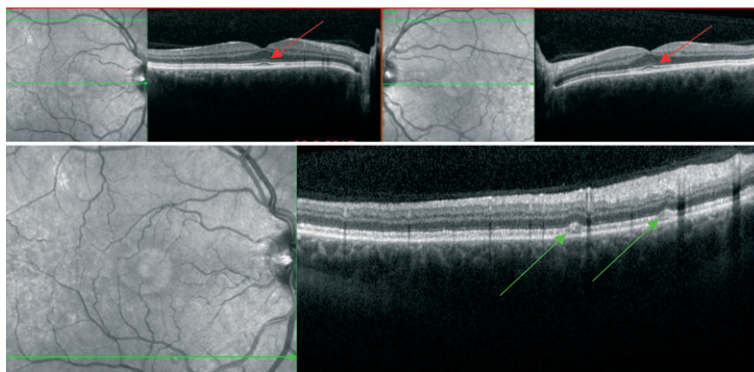


FIGURE 4. Discrete morphological changes with focal elongations of interdigital zone in the fovea (red arrows) and near the vascular arcades (green arrows) seen on OCT.

pigmented epithelium (RPE) may play a major role in pathogenesis.¹⁸ Ophthalmoscopy revealed multiple barely noticeable lesions of less than 1/3 of the disc diameter distributed in the posterior part of the both eyes, in the fovea and scattered around it extrafoveally, mainly near the vascular arcades. It is speculated that these are the sites where the concentration of the drug is the highest.⁸ Prior pre-clinical studies showed that MEK inhibition leads to acute RPE toxicity, which results in RPE hyper permeability and breakdown of the retinal-blood barrier.^{19,20} RPE is an epithelial barrier that maintains the outer blood-retinal barrier. Adherent and tight junctions, facilitated and active transporters perform important barrier functions in the physiological processes of the retina, by transporting nutrients, water, and ions, and removing metabolic wastes. The removal of excessive water from the subretinal space to the choriocapillaris, which is critical to the health of the retina, is regulated by the active transport systems in the RPE.²¹ Inappropriate function of RPE may lead to SRF accumulation observed in MEKAR. Lesions in the foveola are observed to be thicker than extrafoveally. The possible explanation for that might be the fact that in the fovea the concentration of photoreceptors is the greatest, hence this is the region of greatest active transport from the retina to choroid.

OCT reveals some changes in outer retinal layers, observed changes are focal: clearly distinguishable IZ with elongations into sub-IZ space, sub-IZ space can be additionally thickened due to accumulation of hyporeflexive SRF above RPE layer which remains unchanged.

During the subsequent treatment, OCT findings showed minimal fluctuations in SRF. In our patients, the follow-up was up to 2 years from the

beginning of the treatment. During this time, lesions did not completely resolve. Despite persistent SRF, no permanent changes in RPE layer were observed in this short-term follow up. Van Dijk *et al.* analyzed the molecular mechanism and cell proliferation using neuroretina and cell models of RPE treated with MEK inhibitor binimetinib *in vitro* and found that cell proliferation was not inhibited during treatment and retinal cells were able to regain the activation after binimetinib treatment, mimicking the reversibility of the retinopathy.¹⁶ The effect on RPE on long-term follow up is to be studied further.

We also observed discrete focal dilatation of conjunctival vessels by slit lamp microscopy in one patient. These changes were not previously reported in the literature and could be the result of local irritation due to some other factor.

Patient number 5 presented with reduced vision in his left eye. His BCVA was reduced to 0.7, and he observed floaters. We found cells in the anterior chamber with posterior synechiae as well as slight macular edema. After topical corticosteroid therapy, the signs and symptoms resolved. This is in line with previous case reports of patients with metastatic melanoma and clinical signs of inflammation in both eyes. The bilateral uveitis was reported as an adverse effect of vemurafenib therapy, which was treated with topical corticosteroid therapy.^{22,23} In our patient number 5, MEKAR with lesions in both foveas was observed three weeks after the onset of inflammation in the left eye. Previous studies have reported that the most common ocular toxicity associated with BRAF inhibitor monotherapy is uveitis, occurring in 2.1% of patients receiving vemurafenib and in 1% of patients treated with dabrafenib across clinical trials. Current algorithms suggest management with a temporary dose interruption, ophthalmological review, a course of topical steroids and in most cases a dose reduction.¹³

We have observed a high incidence of ocular side effects in this small group of patients taking combined cobimetinib and vemurafenib. They were mild and prone to spontaneous resolution. Morphological changes were located in outer retinal layers. They did not significantly effect visual function. Overall, we have shown that therapy with MEK/BRAF inhibitor combination therapy is safe with respect to ocular adverse effects, for a duration of up to 2 years. However, the results of the present study must be viewed as a hypothesis-generating pilot study, and the results interpreted with caution, because of the small sample sizes.

We would recommend that patients treated with MEK and BRAF inhibitors have regular ophthalmologic examinations, which include BCVA, slit lamp examination, and OCT of macular region, and when available IR imaging. The long-term follow-up of MEK inhibitor therapy is to be studied to evaluate the potential irreversible effects of MEK on outer retinal layers, which could permanently influence visual function.

Retinal changes named MEKAR are observed in metastatic melanoma patients treated with MEK inhibitor in combination with BRAF inhibitor. Lesions are either solitary or multiple bilateral foveal and extrafoveal serous neurosensory retinal detachments. MEKAR lesions can be recognized and differentiated from serous retinal detachments of other etiology using noninvasive diagnostic imaging methods such as OCT and IR imaging. They have no, or only mild influence on visual function and are self-limited.

Ophthalmologists and oncologists need to be aware of this common, yet relatively benign and often transient ocular side effect of treatment with MEK inhibitor in combination with BRAF inhibitor to avoid needless intervention, including the discontinuance of a potentially life-prolonging therapy.

References

1. Arnold M, Holterhues C, Hollestein LM, Coebergh JWW, Nijsten T, Pukkala E, et al. Trends in incidence and predictions of cutaneous melanoma across Europe up to 2015. *J Eur Acad Dermatol Venereol JEADV* 2014; **28**: 1170-8. doi: 10.1111/jdv.12236
2. Garbe C, Peris K, Hauschild A, Saiag P, Middleton M, Bastholt L, et al. Diagnosis and treatment of melanoma. European consensus-based interdisciplinary guideline – Update 2016. *Eur J Cancer* 2016; **63**: 201-17. doi: 10.1016/j.ejca.2016.05.005
3. Larkin J, Ascierto PA, Dréno B, Atkinson V, Liskay G, Maio M, et al. Combined vemurafenib and cobimetinib in BRAF-mutated melanoma. *N Engl J Med* 2014; **371**: 1867-76. doi: 10.1056/NEJMoa1408868
4. Dummer R, Hauschild A, Lindenblatt N, Pentheroudakis G, Keilholz U. Cutaneous melanoma: ESMO Clinical Practice Guidelines for diagnosis, treatment and follow-up. *Ann Oncol* 2015; **26**: v126-32. doi: 10.1093/annonc/mdv297
5. Ascierto PA, Kirkwood JM, Grob J-J, Simeone E, Grimaldi AM, Maio M, et al. The role of BRAF V600 mutation in melanoma. *J Transl Med* 2012; **10**: 85. doi: 10.1186/1479-5876-10-85
6. Jang S, Atkins MB. Which drug, and when, for patients with BRAF-mutant melanoma? *Lancet Oncol* 2013; **14**: e60-9. doi: 10.1016/S1473-2045(12)70539-9
7. Urner-Bloch U, Urner M, Jaberg-Bentele N, Frauchiger AL, Dummer R, Goldinger SM. MEK inhibitor-associated retinopathy (MEKAR) in metastatic melanoma: Long-term ophthalmic effects. *Eur J Cancer* 2016; **65**: 130-8. doi: 10.1016/j.ejca.2016.06.018
8. Francis JH, Habib LA, Abramson DH, Yannuzzi LA, Heinemann M, Gounder MM, et al. Clinical and morphologic characteristics of MEK inhibitor-associated retinopathy: differences from central serous chorioretinopathy. *Ophthalmology* 2017. doi:10.1016/j.ophtha.2017.05.038. [Epub ahead of print]

9. Choe CH, McArthur GA, Caro I, Kempen JH, Amaravadi RK. Ocular toxicity in BRAF mutant cutaneous melanoma patients treated with vemurafenib. *Am J Ophthalmol* 2014; **158**: 831-837.e2. doi: 10.1016/j.ajo.2014.07.003
10. Dréno B, Ribas A, Larkin J, Ascierto PA, Hauschild A, Thomas L, et al. Incidence, course, and management of toxicities associated with cobimetinib in combination with vemurafenib in the coBRIM study. *Ann Oncol* 2017; **28**: 1137-44. doi: 10.1093/annonc/mdx040
11. de la Cruz-Merino L, Di Guardo L, Grob J-J, Venosa A, Larkin J, McArthur GA, et al. Clinical features of serous retinopathy observed with cobimetinib in patients with BRAF-mutated melanoma treated in the randomized coBRIM study. *J Transl Med* 2017; **15**: 146. doi: 10.1186/s12967-017-1246-0
12. Alves C, Ribeiro I, Penedones A, Mendes D, Batel Marques F. Risk of ophthalmic adverse effects in patients treated with MEK inhibitors: A systematic review and meta-analysis. *Ophthalmic Res* 2017; **57**: 60-9. doi: 10.1159/000446845
13. Welsh SJ, Corrie PG. Management of BRAF and MEK inhibitor toxicities in patients with metastatic melanoma. *Ther Adv Med Oncol* 2015; **7**: 122-36. doi: 10.1177/1758834014566428
14. Schoenberger SD, Kim SJ. Bilateral multifocal central serous-like chorioretinopathy due to MEK inhibition for metastatic cutaneous melanoma. *Case Rep Ophthalmol Med* 2013; **2013**: 1-3. doi: 10.1155/2013/673796
15. Michalarea V, de Miguel Luken MJ, Diamantis N, Garg A, Maubon L, Yap TA, et al. Ocular toxicity with MEK inhibitors in phase I trials: A single centre experience across six clinical trials. *J Clin Oncol* 2015; **33**: 11090-90. doi: 10.1200/jco.2015.33.15_suppl.11090
16. van Dijk EHC, van Herpen CML, Marinkovic M, Haanen JBAG, Amundson D, Luyten GPM, et al. Serous retinopathy associated with mitogen-activated protein kinase inhibition (Binimetinib) for metastatic cutaneous and uveal melanoma. *Ophthalmology* 2015; **122**: 1907-16. doi: 10.1016/j.ophtha.2015.05.027
17. Weber ML, Liang MC, Flaherty KT, Heier JS. Subretinal fluid associated with MEK inhibitor use in the treatment of systemic cancer. *JAMA Ophthalmol* 2016; **134**: 855-62. doi: 10.1001/jamaophthalmol.2016.0090
18. Stjepanovic N, Velazquez-Martin JP, Bedard PL. Ocular toxicities of MEK inhibitors and other targeted therapies. *Ann Oncol* 2016; **27**: 998-1005. doi: 10.1093/annonc/mdw100
19. Jiang Q, Cao C, Lu S, Kivlin R, Wallin B, Chu W, et al. MEK/ERK pathway mediates UVB-induced AQP1 downregulation and water permeability impairment in human retinal pigment epithelial cells. *Int J Mol Med* 2009; **23**: 771-7.
20. Huang W, Yang AH, Matsumoto D, Collette W, Marroquin L, Ko M, et al. PD0325901, a mitogen-activated protein kinase kinase inhibitor, produces ocular toxicity in a rabbit animal model of retinal vein occlusion. *J Ocul Pharmacol* 2009; **25**: 519-30. doi: 10.1089/jop.2009.0060
21. Runkle EA, Antonetti DA. The blood-retinal barrier: Structure and functional significance. In: Nag S, editor. *Blood-Brain Neural Barriers*, vol. 686, Totowa, NJ: Humana Press; 2011. p. 133-48.
22. Niro A, Strippoli S, Alessio G, Sborgia L, Recchimurzo N, Guida M. Ocular toxicity in metastatic melanoma patients treated with mitogen-activated protein kinase inhibitors: a case series. *Am J Ophthalmol* 2015; **160**: 959-67.e1. doi: 10.1016/j.ajo.2015.07.035
23. Guedj M, Quéant A, Funck-Brentano E, Kramkimel N, Lellouch J, Monnet D, et al. Uveitis in patients with late-stage cutaneous melanoma treated with vemurafenib. *JAMA Ophthalmol* 2014; **132**: 1421-5. doi: 10.1001/jamaophthalmol.2014.3024

Sclerosing melanocytic lesions (sclerosing melanomas with nevoid features and sclerosing nevi with pseudomelanomatous features) - an analysis of 90 lesions

Biljana Grcar-Kuzmanov¹, Emanuela Bostjancic², Juan Antonio Contreras Bandres¹,
Joze Pizem²

¹ Department of Pathology, Institute of Oncology, 1000 Ljubljana, Slovenia

² Institute of Pathology, Faculty of Medicine, University of Ljubljana, 1000 Ljubljana, Slovenia

Radiol Oncol 2018; 52(2): 220-228

Received 17 October 2017

Accepted 20 December 2017

Correspondence to: Prof. Jože Pižem, M.D., PhD., Institute of Pathology, Medical Faculty, University of Ljubljana, Korytkova 2, 1000 Ljubljana, Slovenia. Phone: +386 1 543 7103; Fax: +386 1 543 7104; E-mail: joze.pizem@mf.uni-lj.si

Disclosure: No potential conflicts of interest were disclosed.

Background. Sclerosing melanocytic lesions, which are characterized by either focal or diffuse sclerosis in the dermal component and atypical proliferation of predominantly nevoid melanocytes, remain poorly defined. Our aim was to analyze systematically their morphologic spectrum, especially the distinction between sclerosing melanocytic nevus and sclerosing melanoma, which has not been well documented.

Patients and methods. We collected 90 sclerosing melanocytic lesions, occurring in 82 patients (49 male, 33 female; age range from 21 to 89 years). A four probe fluorescent *in situ* hybridization (FISH) assay was performed in 41 lesions to substantiate the diagnosis of sclerosing melanomas.

Results. A prominent full-thickness pagetoid spread of melanocytes was identified in 44 (48%) lesions, and a melanoma *in situ* adjacent to the sclerosis in 55 (61%) lesions. In the intrasclerotic component, maturation was absent in 40 (44%) and mitotic figures were identified in 18 (20%) lesions. Of the 90 lesions, 26 (29%) were diagnosed morphologically as nevi and 64 (71%) as melanomas (Breslow thickness from 0.4 to 1.8 mm), including 45 (50%) melanomas with an adjacent nevus. A four-probe FISH assay was positive in the sclerotic component in 14 of 25 lesions diagnosed morphologically as melanomas and none of 16 nevi. A sentinel lymph node biopsy was performed for 17 lesions and was negative in all cases.

Conclusions. Sclerosing melanocytic lesions form a morphologic spectrum and include both nevi and melanomas. The pathogenesis of sclerosis remains obscure but seems to be induced by melanocytes or an unusual host response in at least a subset of lesions.

Key words: sclerosing melanoma; sclerosing nevus; fibrosis; regression; trauma

Introduction

Fibrosis or sclerosis can be found in various types of melanocytic lesions, including persistent/recurrent nevi (partially excised or treated with other modalities)¹⁻⁵, traumatized nevi^{6,7}, desmoplastic nevi^{8,9}, nevi arising against a background of lichen sclerosis or epidermolysis bullosa¹⁰⁻¹², melanomas with regression and desmoplastic melanomas.^{13,14} In addition, there is a subset of morphologically

distinct and diagnostically challenging melanocytic lesions with focal or more diffuse sclerosis, which are characterized by an atypical intraepidermal proliferation of melanocytes that often resembles or is diagnostic for a melanoma *in situ*, frequent effacement of the rete ridge pattern, atypical proliferation of nevoid melanocytes in the sclerotic area, and frequent remnants of a morphologically banal nevus adjacent to or beneath the sclerosis, creating a trizonal pattern (atypical intraepider-

mal component, sclerotic dermal component and remnants of a banal looking melanocytic nevus below the sclerosis).¹⁵⁻¹⁷ Although the sclerosis may resemble regression or changes after previous trauma, its pathogenesis remains obscure. Fabrizio *et al.* first reported a series of 19 such lesions, which they designated as “sclerosing nevi with pseudomelanomatous features”.¹⁵ The authors concluded that, despite their worrisome clinical and morphologic features, the lesions were probably benign nevi.

Although it has been suggested that a subset of sclerosing melanocytic lesions may represent melanomas (“sclerosing melanomas with nevoid features”), the full morphologic and biologic spectrum of sclerosing melanocytic lesions remains unknown and sclerosing melanomas have not been well characterized.¹⁵⁻¹⁷ We present a series of 90 sclerosing melanocytic lesions collected prospectively, with a systematic morphologic, immunohistochemical analysis, fluorescent *in situ* hybridization (FISH) and follow-up. Our aim was to analyze the morphologic spectrum of sclerosing melanocytic lesions, especially the distinction between sclerosing melanocytic nevus and sclerosing melanoma, which has not been well documented.

Patients and methods

Case selection in histopathologic analysis

Ninety sclerosing melanocytic lesions, occurring in 82 patients, were included in the study; 76 lesions were seen in routine practice and 14 lesions were outside consultation cases. Eighty-six lesions were collected from 2006 (when we first paid attention to this type of lesion) to 2014. After histopathologic revision of all other known excised melanocytic lesions in the 82 patients, four additional sclerosing melanocytic lesions were identified and included in the study. There was no history of previous treatment or trauma in relation to any of the lesions.

The inclusion criterion was the presence of focal or diffuse dermal sclerosis within a melanocytic lesion, surrounding predominantly nests rather than single melanocytes of usually nevoid melanocytes. Lesions with large areas of fibrosis or sclerosis lacking melanocytes, or with greatly reduced numbers of melanocytes, were not included (excluding lesions with classical features of recurrent or previously traumatized nevi, or melanocytic lesions with regression).^{1,4-7} Sclerotic areas were not typical of regression in melanomas since there was dense

sclerosis with mostly preserved melanocytes, although there could be small adjacent areas suggestive of regression.¹⁴

All lesions were histopathologically re-evaluated by two of the authors (BGK and JP) in 2015. The following features were assessed histopathologically: 1) atypical features of the intraepidermal portion of the lesion above the sclerosis (effacement of the rete ridge pattern, cytological atypia of melanocytes, lentiginous proliferation, upward migration of melanocytes and presence of irregular intraepidermal nests of melanocytes), 2) extension of an atypical intraepidermal melanocytic proliferation outside the sclerosis, 3) maximum thickness of the sclerosis, 4) atypical features within the sclerosis (absence of maturation, presence of prominent nucleoli, deep pigmentation, mitotic activity, distribution of melanocytic nests within the sclerosis), 5) presence of an unequivocal accompanying melanocytic nevus outside the sclerotic area, and 6) intraepithelial extension of melanocytes along the eccrine ducts. The number of mitoses in the sclerotic dermal component was reported per square millimeter according to the protocol for assessment of mitotic activity in malignant melanomas.¹⁸ Inflammatory infiltrate in the dermis was assessed as absent/mild or marked. Special attention was paid to possible more cellular foci in the sclerosis, a lamellar configuration of the sclerosis around the rete ridges and any features that would suggest regression (areas of more cellular sclerosis/fibrosis devoid of melanocytes, more pronounced inflammation, proliferation of small vessels, fibrosis arranged parallel to the surface).

Melanocytic lesions were on morphological grounds, together with HMB-45 expression and Ki67 proliferative activity when available (but without knowing the FISH results) categorized into one of three categories: nevus, melanoma, or melanoma with an accompanying nevus. The most important criteria in favor of a melanoma were: 1) extension of atypical intraepidermal melanocytic proliferation, diagnostic for an *in situ* melanoma beyond the sclerotic area, 2) prominent upward migration of intraepidermal melanocytes above the sclerosis, 3) severe cytological atypia of intraepidermal melanocytes above the sclerosis, 4) presence of mitoses within the sclerosis, 5) absence of maturation, 6) prominent nucleoli in the sclerosis, 7) patchy or irregular diffuse HMB-45 positivity in the deepest part of the sclerotic component (*i.e.*, absence of maturation) and 8) presence of Ki67 proliferative activity in the melanocytes of the lower half of the sclerotic component.^{15,19}

Clinical data including data on sentinel lymph node biopsies and follow-up data were collected from patients' medical records and national Cancer Registry. The study was performed on the archival tissue slides and blocks; therefore, no consent was required for this study. The study was approved by the Republic of Slovenia National Medical Ethics Committee (N23k/03/12 bis; date 03-13-2012).

Immunohistochemistry

A representative tissue block, when available, was selected for immunohistochemistry, including double Ki67/melan A staining (Ki67: DAKO, Glostrup, Denmark, clone MIB-1, dilution 1:50; melan A: DAKO, Glostrup, Denmark, clone A103, dilution 1:10) and HMB-45 (DAKO, Glostrup, Denmark, clone HMB-45, dilution 1:20). Deparaffinization, antigen retrieval, and staining with antibodies were performed in an automatic immunostainer (Benchmark XT, Ventana Medical Systems Inc., Tucson, USA) in combination with treating sections with secondary antibodies and color development with horseradish peroxidase (ultraVIEW DAB Detection Kit, Ventana Medical Systems Inc., Tucson, USA) for Ki67 and alkaline phosphatase (ultraVIEW Red Detection Kit, Ventana Medical Systems Inc., Tucson, USA) for HMB-45 and melan A.

Fluorescence *in situ* hybridization (FISH)

FISH analysis was performed using a four-probe assay from Abbott Molecular, Inc. (Des Plaines, IL, USA) targeting Ras responsive element binding protein-1 on 6p25 (Vysis®LSI® RREB1-Spectrum Red), V-myb myeloblastosis viral oncogene homolog on 6q23 (Vysis®LSI® MYB-Spectrum Gold), cyclin D1 on 11q13 (Vysis®LSI® CCND1-Spectrum Green) and centromeric enumeration probe control for chromosome 6 (Vysis®LSI® CEP6-Spectrum Aqua). The FISH analysis was performed on 5 µm thick sections prepared from formalin fixed and paraffin embedded tissue according to the manufacturer's recommendations and using criteria as previously described.^{20,21} The analysis was done on melanocytes in the sclerotic dermal component in 41 lesions with available tissue. A lesion was considered to have a positive FISH result if any of the following criteria were met: 1) gain in RREB1 relative to CEP6 in more than 55% of tumor cell nuclei, 2) gain in RREB1 in more than 29% of tumor cell nuclei, 3) loss of MYB relative to CEP6 in more than 40% of tumor cell nuclei or 4) gain in CCND1 in more than 38% of tumor cell nuclei.^{20,21} To deter-

mine the sensitivity and specificity of the test, we analyzed 19 morphologically obvious melanomas (non-sclerosing superficial spreading and nodular) and 18 nevi (common acquired and with congenital features). The assay was positive in 16 of 19 melanomas and in 4 of 18 nevi, with 84% sensitivity and 78% specificity.^{20,21}

Statistical analysis

Statistical analysis was performed with IBM SPSS Statistics 20 (International Business Machines Corp., New York, NY). Differences among groups in relation to other clinicopathologic parameters were analyzed by the Kruskal-Wallis test and χ^2 test.

Results

Ninety sclerosing melanocytic lesions occurred in 82 patients; 33 (40%) females and 49 (60%) males (four patients had 2 lesions each and two patients had 3 lesions each). The age of the patients ranged from 21 to 89 years (median, 48 years). The lesions were most frequently located on the back (46 lesions), followed by abdomen (18 lesions), chest excluding breast (12 lesions), breast (5 lesions), lower extremities (4 lesions), inguinal region (2 lesions), retroauricular region (2 lesions) and upper extremities (1 lesion). Clinical diagnoses, available for 74 lesions, included nevus (18 lesions), dysplastic nevus (21 lesions), melanoma (29 lesions) and non-melanocytic lesion (6 lesions). Thirteen patients (16%), including three with multiple sclerosing melanocytic lesions, had at least one additional (two patients had 3 and two patients had 2) non-sclerosing superficial spreading melanoma, diagnosed previously, simultaneously or subsequently.

Histopathologic interpretation was difficult in most of the lesions (Figures 1-4). Morphologically, twenty-six lesions (29%) were diagnosed on revision as nevi (8 ordinary, 10 dysplastic, 6 congenital, 2 Spitz), 19 lesions (21%) as melanomas and 45 lesions (50%) as melanomas with an adjacent nevus (10 ordinary, 6 dysplastic, 29 congenital). On revision, 8 lesions originally diagnosed as melanomas (with or without an adjacent nevus) were reclassified as nevi and 1 lesion originally diagnosed as a nevus was reclassified as a melanoma.

Of the 64 melanomas (with or without an accompanying nevus), one was an *in situ* melanoma, 3 Clark level 2, 29 Clark level 3 and 31 Clark level 4. The Breslow thickness of the 63 invasive melano-

mas ranged from 0.4 to 1.8 mm (median, 0.75 mm). It corresponded to the thickness of sclerosis in all except one case, in which the Breslow thickness exceeded the thickness of the sclerosis. Of the 45 melanomas with an accompanying nevus outside the sclerosis, the nevus was located below the sclerosis in 22 cases, adjacent to it in 11 cases or both in 12 cases. No ulceration was present in any of the lesions.

Key clinical, morphologic and immunohistochemical features, and the FISH results in relation to the three diagnostic categories are shown in Table 1. Among 14 lesions diagnosed on morphological grounds as melanomas and positive FISH results, one FISH criterion was met in 6, two criteria in 6 and three criteria in 2 cases. Gain in RREB1 in more than 29% of tumor cell nuclei was found in 9 lesions, gain in RREB1 relative to CEP6 in more than 55% of tumor cell nuclei in 6 lesions, loss of MYB relative to CEP3 in more than 40% of tumor cell nuclei in 7 lesions, and gain in CCND1 in more than 38% of tumor cell nuclei in 2 lesions. Clinical and histopathologic parameters in relation to FISH results in 41 lesions with FISH analysis of the sclerotic component are shown in Table 2.

Sclerosis in the dermis was diffuse (involving the entire dermal part of the lesion) in 39 lesions (43%), including 15 of 26 nevi (58%), 17 of 19 melanomas (89%) and 7 of 45 melanomas with an accompanying nevus (16%), and focal in other lesions. It never extended beyond a melanocytic lesion. The thickness of sclerosis ranged from 0.3 to 1.8 mm (median, 0.7 mm) and did not differ among the three diagnostic groups. A trizonal pattern (atypical intraepidermal component, sclerotic dermal component and remnants of a banal nevus below the sclerosis) was noted in 43 lesions (48%) (Figures 1, 3 and 4). Sclerotic areas were generally hypocellular, except for 3 melanomas in which the sclerosis was focally more cellular and edematous, indicating an early stage of sclerosis. A lamellar configuration of sclerosis around rete ridges was noted in 8 lesions (9%) (Figure 2). Very focal areas suggestive of regression were noted in 26 lesions (32%), predominantly melanomas.

There was partial or complete effacement of the rete ridge pattern in 38 (42%) and 43 (44%) of the cases, respectively. Except for 2 Spitz nevi and 3 melanomas, melanocytes within the sclerosis were relatively small, nevoid, with various degrees of hyperchromasia and variously prominent nucleoli (Table 1, Figures 3C, 3D, 4C). Compared to the surrounding nevus outside the sclerosis (when present), melanocytes within the sclerosis were usu-

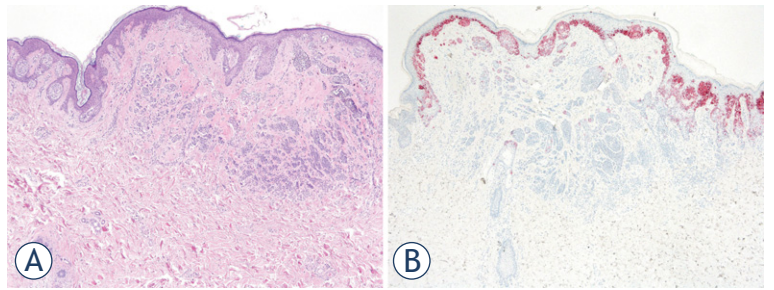


FIGURE 1. Sclerosing melanocytic nevus from the abdomen of a 22-year-old woman, with negative FISH assay. **(A)** There is a trizonal pattern, maturation and an atypical intraepidermal component above the sclerosis, which does not extend beyond the sclerosis. **(B)** HMB-45 stain shows maturation in the dermal component.

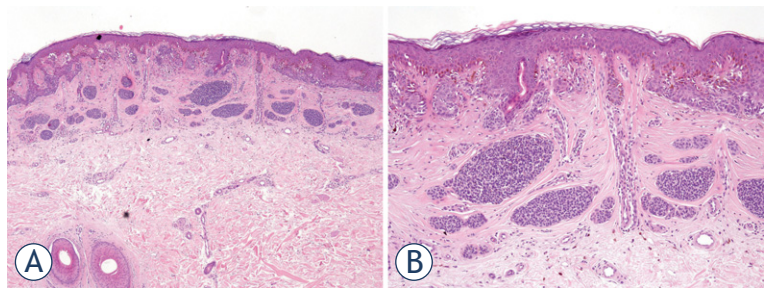


FIGURE 2. Sclerosing melanocytic nevus from the abdomen of a 53-year-old man, with negative the FISH assay. **(A), (B)** There is lamellar-type sclerosis involving the entire dermal component.

ally slightly larger, with more conspicuous pale cytoplasm (Figure 4C). Dermal mitotic figures within the sclerosis were found in 17 of 64 melanomas (1 per square millimeter in 11 lesions, 2 in 2 lesions and 3 in 1 lesion) and in 1 of the 26 nevi (1 per square millimeter) (Table 1). Nests in the sclerosis varied in size, but very large expansive nodules were absent. In some lesions, nests were oriented parallel to the surface of the skin. Extension of melanocytes along the eccrine ducts (not used as a diagnostic criterion) was found significantly more frequently in melanomas (Figure 3B, Table 1).

All lesions were treated by surgical excision. A re-excision was performed in 65 of 85 (76%) lesions with available information. A sentinel lymph node biopsy was performed for 17 lesions (16 melanomas, including all 13 melanomas with Breslow thickness ≥ 1 mm, and 1 nevus that was initially interpreted as a melanoma) and was negative in all cases. The Breslow thickness of melanomas with sentinel lymph node biopsies ranged from 0.6 to 1.8 mm (median, 1.2 mm) and was ≥ 1 mm in 13 cases and > 1.5 mm in only one case.

Follow-up data for disease free survival were available for 66 lesions, with a follow-up period

TABLE 1. Clinical and histopathologic parameters in relation to morphological diagnostic categories

Parameter, n (%)	All	Nevus	Melanoma	Melanoma with nevus	P -value
N (%)	90	26 (29)	19 (21)	45 (50)	
Age of the patients (years) (median; range)	48; 21-89	38; 22-53	60; 21-89	51; 26-85	< 0.001
Maximum diameter* (mm) (median; range)	9; 2-29	7; 2-14	8; 3-29	11; 4-25	0.014
Location					0.076
Back	46 (51)	9 (35)	9 (47)	28 (62)	
Other	44 (49)	17 (65)	10 (53)	17 (38)	
Extension along eccrine ducts**	49/77 (64)	5/21 (24)	14/17 (82)	30/39 (77)	< 0.001
Evidence of regression	29 (32)	1 (4)	12 (63)	16 (36)	/
Lamellar sclerosis	8 (9)	6 (23)	0	2 (4)	/
Marked inflammation in the sclerosis	27 (30)	2 (8)	6 (32)	19 (42)	/
Maturation in the sclerosis	50 (56)	25 (96)	8 (42)	17 (38)	/
Dermal mitoses present	18 (20)	1 (4)	4 (21)	13 (29)	/
Prominent nucleoli in the sclerosis	52 (58)	5 (19)	16 (84)	31 (69)	/
Intraepidermal component adjacent to the sclerosis					/
Not atypical	18 (20)	17 (65)	1 (5)	0	
Atypical	17 (19)	9 (35)	1 (5)	7 (16)	
Melanoma in situ	55 (61)	0	17 (89)	38 (84)	
Severe cytological atypia in the epidermis above the sclerosis	68 (76)	9 (35)	19 (100)	40 (89)	/
Lentiginous growth above the sclerosis	82 (91)	19 (73)	19 (100)	44 (98)	/
Upward migration in the epidermis above the sclerosis					/
No	12 (13)	9 (35)	1 (5)	2 (4)	
Lower half	11 (12)	7 (27)	1 (5)	3 (7)	
Focally in the upper half	23 (26)	9 (35)	5 (26)	9 (20)	
Prominent full thickness	44 (48)	1 (4)	12 (63)	31 (69)	
HMB-45 in the sclerotic component	60	19	11	30	/
Patchy, irregular	37 (62)	6 (32)	10 (91)	21 (70)	
Maturation or completely absent	23 (38)	13 (68)	1 (9)	9 (30)	
Ki67 in the sclerotic component	66	19	13	34	
No positivity in the lower half	51 (77)	19 (100)	8 (62)	24 (71)	/
Some positive melanocytes in the lower half, <5% overall	13 (20)	0	4 (31)	9 (26)	
>5%, no gradient with the depth	2 (3)	0	1 (7)	1 (3)	
Four-probe FISH in the sclerotic component	41	16	7	18	0.001
Positive	14 (34)	0	3 (43)	11 (61)	
Negative	27 (66)	16 (100)	4 (57)	7 (39)	

* available for 81 lesions; **no eccrine ducts were identified within or adjacent to sclerotic dermal component in 13 lesions

from 1 to 106 months (median, 19 months), and for overall disease specific survival for 75 lesions, with a follow-up period from 12 to 131 months (median, 77 months). During the follow up period, there was no evidence of disease progression in any of the patients that could undoubtedly be attributed to the lesions studied.

Discussion

We present 90 melanocytic lesions, which we designated morphologically as sclerosing melanocytic nevi or sclerosing melanomas. The lesions are characterized by an area of sclerosis in the dermis, with nests of atypical, in most cases nevoid

melanocytes, an atypical intraepidermal component and, in more than half of the cases, a banal looking nevus beneath or adjacent to the sclerosis. Sclerosing melanocytic lesions are most striking when banal looking nevus remnants are present beneath the sclerosis (in 48% of our lesions), creating a trizonal pattern. Fabrizio *et al.* reported 19 similar lesions, which they called sclerosing nevi with pseudomelanomatous features.¹⁵ However, the authors included in their study only lesions with the presence of a nevus below or adjacent to the sclerosis, an absence of cytological atypia or prominent nucleoli in sclerotic areas and an absence of significant mitotic activity. Forty-two lesions, selected on the basis of features of dysplastic nevus and pronounced fibrosis, were reported by Ko *et al.* and termed dysplastic nevi with florid fibroplasia and pseudomelanomatous features.¹⁶ We collected our cases prospectively and included all lesions with an area of sclerosis in the dermis (similar to the sclerosis described in the above mentioned studies), which was different from what one classically observes in regressing melanomas or recurrent/previously traumatized nevi.^{1-4,7,14} Our series therefore broadens the spectrum of sclerosing melanocytic lesions, including lesions with sclerosis of the entire dermal component (without an adjacent remnant of banal nevus), and more prominent cytological and architectural atypia.¹⁵⁻¹⁷

Histopathologic interpretation of most sclerosing lesions is challenging because of overlapping features between an atypical nevus and a melanoma.^{15,17,22,23} Morphologic interpretation may depend on the point of view of whether the sclerosis represents regression, previous chronic trauma, exaggerated lamellar fibrosis seen in dysplastic nevi, or other unknown factors.^{15-17,24} Most difficult and clinically important is interpretation of the melanocytic component in the sclerotic area. Many sclerosing melanocytic lesions display morphologic features that are in the routine practice used to differentiate melanomas from nevi, including presence of a melanoma in situ adjacent to the sclerosis (61% of our lesions), prominent full-thickness pagetoid spread above the sclerosis (48% of our lesions), absence of maturation (44% of our lesions), presence of prominent nucleoli (58% of our lesions) and mitotic activity in the sclerotic area (20% of our lesions). Patchy or irregular diffuse positivity for HMB-45 in the dermal component and an absence of a gradient in Ki67 labeling have been considered useful clues for melanoma.¹⁹ However, there is overlap in the staining patterns between nevi and melanomas and their discriminatory value may

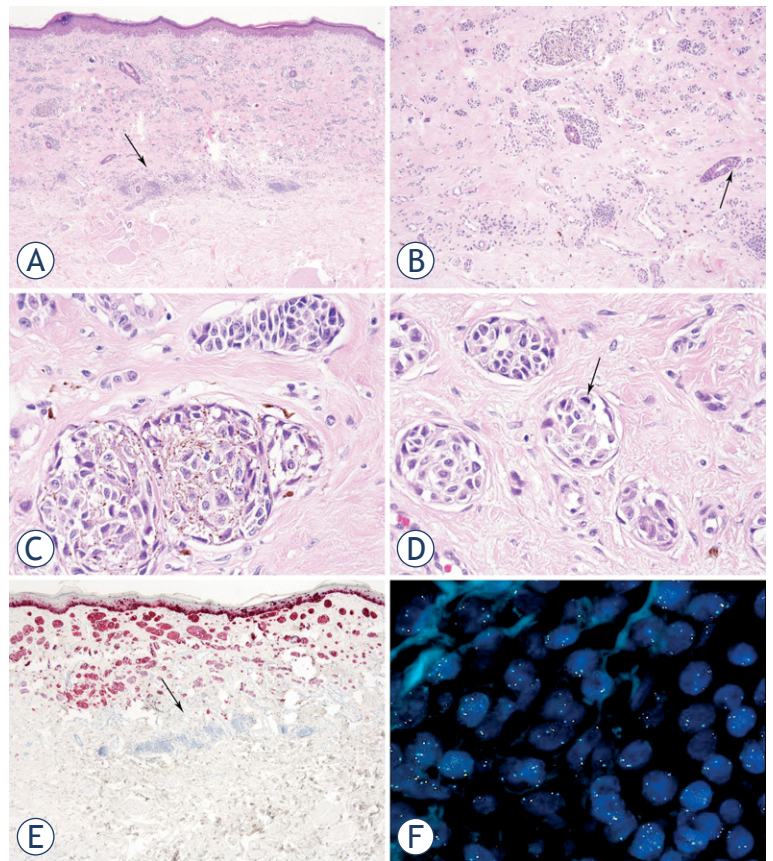


FIGURE 3. Sclerosing melanoma from the abdomen of a 67-year-old man. **(A)** There are remnants of a nevus below the melanoma (arrow) and a trizonal pattern. **(B)** Some melanocytes are in the epithelium of an eccrine duct (arrow). **(C)** Melanocytes within sclerosis are atypical, with prominent nucleoli. **(D)** There is a mitotic figure (arrow). **(E)** HMB-45 staining is irregular diffuse in the sclerotic dermal component (melanoma) but negative in the nevus below (arrow). There is prominent pagetoid spread in the epidermis. **(F)** The FISH assay was positive, showing loss of MYB (gold) relative to CEP6 (aqua) in 57% of tumor cell nuclei.

be lower in thin, ambiguous and diagnostically difficult lesions.²⁵ An aberrant, irregular diffuse expression of HMB-45 was found in melanocytic nevi after liquid nitrogen cryotherapy.¹⁹ Although it is frequently stated that the Ki67 index is typically more than 5% in invasive melanomas, Ki67 labelling may be less than 5% or even completely absent in the invasive component in a significant proportion of thin melanomas (Breslow thickness of less than 1 mm).²⁵ In most of our lesions, it was less than 5%, usually with only a few positive melanocytes.

Although an atypical proliferation of intraepidermal melanocytes above the sclerosis can, similarly to recurrent/persistent or previously traumatized nevi, be attributed to the sclerosis itself, cytological atypia and, in particular, prominent pagetoid growth in our sclerosing melanocytic le-

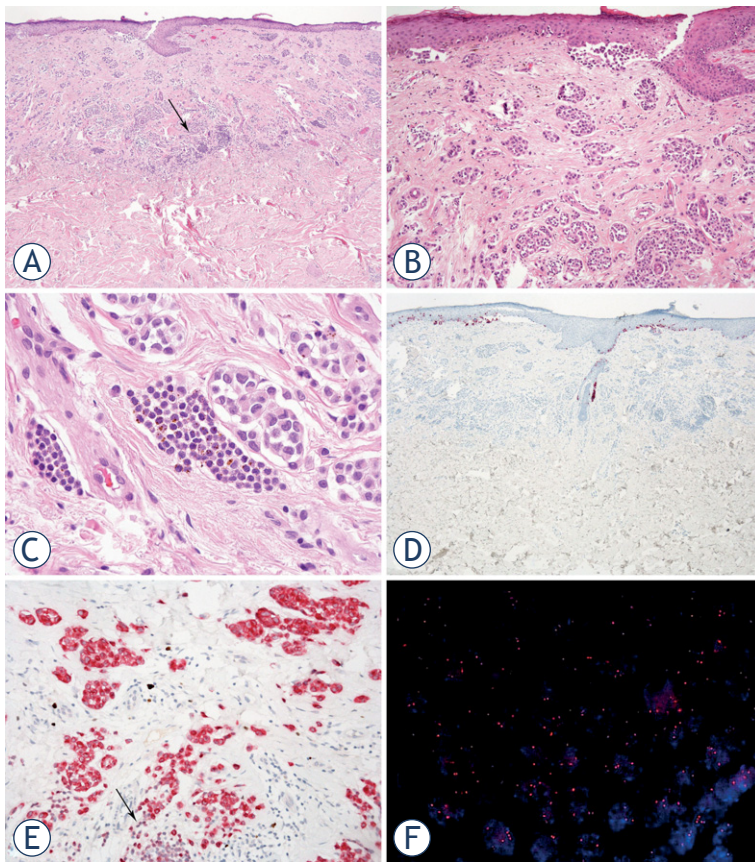


FIGURE 4. Sclerosing melanoma from the back of a 70-year-old female. **(A)** There are remnants of a nevus below sclerosis (arrow). **(B)** Melanocytes in the sclerosis do not show maturation and **(C)** are larger with irregular nuclei and prominent nucleoli compared to melanocytes in the adjacent nevus (left). **(D)** HMB-45 stain shows pagetoid spread in the epidermis, but is completely negative in the dermis. **(E)** Ki67 (brown)/melan A (red) shows no proliferative activity in the melanocytes in the deepest aspect of the sclerotic component; note less intense melan A positivity in the nevus below the melanoma (arrow). **(F)** The FISH assay was positive, showing gain in RREB1 (red) in 30% of tumor cell nuclei.

sions frequently exceeded atypical features seen in recurrent or previously traumatized nevi.^{1,3,4,6,17} In a large series of recurrent melanocytic nevi, pagetoid growth was observed in 6% of the lesions, in contrast to 87% of our sclerosing lesions.⁴ In two previous studies of sclerosing melanocytic nevi, some degree of pagetoid spread was identified in 24% and 47% of cases, respectively.^{15,16} In previous studies, the morphologic features of the intraepidermal melanocytic component outside the sclerosis were not specifically reported; in our series, it was atypical in 80% of cases, and in 61% to the degree of a melanoma in situ. Although atypia above the sclerotic process in the dermis and may therefore be less relevant for morphologic interpretation, an atypical intraepidermal component that extends

outside the area of sclerosis is strongly suggestive of a melanoma in situ.^{4,19} We also noted significantly more frequent extension of melanocytes along the eccrine ducts in lesions that we diagnosed as melanomas.¹

The four-probe FISH assay was positive in 14 of 25 (56%) of the lesions diagnosed morphologically as melanomas and in none of 16 nevi, providing additional evidence that sclerosing melanocytic lesions include both nevi and melanomas. Although the four-probe FISH assay has been reported to have a sensitivity of about 85% for diagnosing unequivocal melanomas, its sensitivity is much lower (about 50%) in ambiguous melanocytic lesions and in some melanoma types, including desmoplastic melanoma.^{20,21,26} Negative FISH results do not therefore rule out a melanoma. Nevertheless, although the sensitivity of the FISH assay for sclerosing melanomas may be lower than for unequivocal ordinary melanomas, it is likely that some of our lesions had been morphologically overdiagnosed as melanomas. Although the FISH assay has been reported to be relatively specific in differentiating melanomas from nevi (with reported specificity around 95%, and 78% specificity in our test series of 18 nevi), a positive FISH assay *per se* is not diagnostic for a melanoma and should be interpreted in correlation with morphologic features.^{20,21,26}

The thickness of sclerosis ranged from 0.3-1.8 mm (median 0.7 mm).¹⁵⁻¹⁷ Sclerosis was either focal (57%) or diffuse (43%), involving the entire dermal part of the melanocytic lesion. The etiology of sclerosis remains elusive. There is usually no history of previous trauma or treatment, and the pattern of sclerosis usually differs from scars after previous mechanical trauma, surgery or other treatment modalities such as cryotherapy.^{1,4,5-7,15-17} In recurrent nevi, fibrosis tends to be more cellular, with larger areas devoid of melanocytes.⁴ Although sclerosis can be related to previous unnoticed or chronic trauma, it is our impression that the sclerosis cannot be explained by previous trauma in most of our lesions.¹⁵ In contrast to our lesions, cytological atypia and pagetoid spread tend to be only rarely and focally present in traumatized nevi.⁶ Sclerosis sometimes displays a lamellar configuration (in 9% of our lesions), suggesting an exaggerated lamellar fibrosis, as seen in dysplastic nevi.^{16,27} Sclerosis in sclerosing melanocytic lesions differs from fibrosis typically seen in regressing melanomas. It usually has a very dense, sclerotic quality, lacks vascular proliferation and, most of all, melanocytes in the sclerotic areas tend to be preserved.^{4,13-15} Nevertheless, small areas sugges-

TABLE 2. Clinical and histopathologic parameters in relation to FISH results in 41 lesions with FISH analysis of the sclerotic component

Parameter, n (%)	All	FISH-positive	FISH-negative	P -value
N (%)	41	14	27	
Age of the patients (years) (median; range)	48; 22-89	51; 42-89	48; 22-77	0.196
Thickness of sclerosis (mm) (mean; range)	0.85; 0.5-1.5	1.0; 0.7-1.5	0.8; 0.5-1.3	0.002
Location				0.096
Back	25 (61)	11 (79)	14 (52)	
Other	16 (39)	3 (21)	13 (48)	
Extension along eccrine ducts	21/38 (55)	11/14 (71)	10/24 (42)	0.026
Evidence of regression	8 (20)	4 (29)	4 (15)	0.411
Maturation in the sclerosis	29 (71)	7 (50)	22 (81)	0.068
Dermal mitoses present	10 (24)	5 (36)	5 (19)	0.267
Prominent nucleoli in the sclerosis	20 (49)	11 (79)	9 (33)	0.009
Melanoma in situ adjacent to the sclerosis	23 (56)	13 (93)	10 (39)	0.001
Severe cytological atypia in the epidermis above the sclerosis	27 (66)	12 (86)	15 (56)	0.053
Prominent full thickness upward migration in the epidermis above the sclerosis	19 (22)	10 (71)	9 (33)	0.026
Patchy irregular HMB-45 in the sclerotic component	22/38 (58)	11/13 (85)	11/25 (44)	0.016
No Ki67 positivity in the lower half of the sclerotic component	28/39 (72)	7/14 (50)	21/25 (84)	0.033

tive of regression have been found adjacent to sclerotic areas in one third of cases.¹⁷ In some lesions, the contours of the sclerosis follow perfectly the contours of the melanocytic lesion, and sclerosis typically does not extend beyond the confines of sclerosing melanocytic lesions. This argues against a post-traumatic sclerosis and suggests that there may be some melanocyte-related factors inducing sclerosis.

The lesions described in the present study share some features with desmoplastic nevi (also called sclerotic and sometimes sclerosing); however, there are several distinctive features.^{8,9,24} Desmoplastic nevi tend to be predominantly dermal, the junctional component is not atypical, sclerosis involves the entire dermal component and is symmetrically distributed. Single melanocytes predominate, particularly in the deepest aspects of the lesion.

The age distribution of sclerosing melanocytic lesions is wide, from 18-91 years, with a male to female ratio of approximately 1.5-2:1.¹⁵⁻¹⁷ From 37% to 72% of the lesions are located on the back, although they can be located at many other sites.¹⁵⁻¹⁷ The lesions are relatively large; their largest diameter ranges from 2-29 mm, with a median of approximately 10 mm.¹⁵ In our series, lesions diagnosed morphologically as melanomas were significantly larger than nevi and occurred in significantly older patients than nevi. Clinically, the lesions are often

suspicious for a melanoma because of an uneven pigmentation and whitish areas suggestive of regression.^{15,16,19,24} Remnants of nevus tissue beneath or adjacent to the sclerosis are of congenital, common acquired, dysplastic, and rarely Spitz type.¹⁵⁻¹⁷

We could not prove progression of the disease attributable to the sclerosing melanomas in any of our patients. However, the median follow-up for recurrence-free survival was relatively short and the number of cases with sentinel lymph node biopsy small. Additionally, on the basis of classic prognostic parameters in melanoma, sclerosing melanomas tend to be low-risk lesions, since the Breslow thickness is < 1 mm in most lesions, ulceration is not present and mitotic activity is identified in only a minority of cases.¹⁸ The absence of disease progression does not therefore in itself argue against sclerosing melanomas.^{15,17}

Conclusions

In conclusion, we present a large series of rare but peculiar, diagnostically challenging and not widely recognized sclerosing melanocytic lesions. The pathogenesis of sclerosis remains obscure. It may be in some lesions (nevi) related to chronic unnoticed trauma, but it seems to be induced by melanocytes or an unusual host response in at

least a subset of lesions. Many sclerosing melanocytic lesions display morphologic features that are suggestive or diagnostic for a melanoma, including the presence of a melanoma in situ extending beyond the sclerotic area, prominent full-thickness pagetoid spread above the sclerosis and an absence of maturation in the sclerotic area, with atypical melanocytes, prominent nucleoli and sometimes mitoses. Approximately half of the more atypical lesions also show a positive four-probe FISH assay, providing additional evidence in favor of sclerosing melanomas. Although we could not prove progression of the disease attributable to the lesions diagnosed as sclerosing melanomas, our study provides strong evidence, based on morphological criteria and a positive four-probe FISH assay, that sclerosing melanocytic lesions include both nevi and melanomas. A four-probe FISH assay may assist in diagnosing these lesions when they cannot be confidently diagnosed as either nevus or melanoma by morphologic features. An awareness of the morphologic features of sclerosing melanocytic lesions and their overlap between nevus and melanoma is important for a more cautious histopathologic interpretation. It may be more appropriate to use the terms “atypical sclerosing melanocytic lesion” or “sclerosing melanocytic lesion with unknown malignant potential” when a sclerosing melanocytic lesion cannot be confidently classified as either a nevus or a melanoma.

Acknowledgements

The research was funded by the Slovenian Research Agency, under the research program codes P3-0054 and P3-0289.

References

- Hoang MP, Prieto VG, Burchette JL, Shea CR. Recurrent melanocytic nevus: histologic and immunohistochemical evaluation. *J Cutan Pathol* 2001; **28**: 400-6. doi: 10.1034/j.1600-0560.2001.028008400.x
- Sommer LL, Barcia SM, Clarke LE, Helm KF. Persistent melanocytic nevi: a review and analysis of 205 cases. *J Cutan Pathol* 2011; **38**: 503-7. doi: 10.1111/j.1600-0560.2011.01692.x
- Fox JC, Reed JA, Shea CR. The recurrent nevus phenomenon. A history of challenge, controversy, and discovery. *Arch Pathol Lab Med* 2011; **135**: 842-6. doi: 10.1043/2010-0429-RAR.1
- King R, Hayzen BA, Page RN, Googe PB, Zeagler D, Mihm MC Jr. Recurrent nevus phenomenon; a clinicopathologic study of 357 cases and histologic comparison with melanoma with regression. *Mod Pathol* 2009; **22**: 611-7. doi: 10.1038/modpathol.2009.22
- Adeniran AJ, Prieto VG, Chon S, Duvic M, Diwan AH. Atypical histologic and immunohistochemical findings in melanocytic nevi after liquid nitrogen cryotherapy. *J Am Acad Dermatol* 2009; **61**: 341-5. doi: 10.1016/j.jaad.2009.01.038. Epub 2009 Apr 11.
- Selim MA, Vollmer RT, Herman CM, Pham TTN, Turner JW. Melanocytic nevi with nonsurgical trauma; a histopathologic study. *Am J Dermatopathol* 2007; **29**: 134-136. doi: 10.1097/01.dad.0000246176.81071.a6
- Leleux TM, Prieto VG, Diwan AH. Aberrant expression of HMB-45 in traumatized melanocytic nevi. *J Am Acad Dermatol* 2011; **67**: 446-50. doi: 10.1016/j.jaad.2011.11.927
- Ferrara G, Brasiello M, Annese P, Francione S, Giorgio CM, Moscarella E, et al. Desmoplastic nevus: clinicopathologic keynotes. *Am J Dermatopathol* 2009; **31**: 718-22. doi: 10.1097/DAD.0b013e3181a9f0ee
- Harris GR, Shea CR, Horenstein MG, Reed JA, Burchette JL Jr, Prieto VG. Desmoplastic (sclerotic) nevus; an underrecognized entity that resembles dermatofibroma and desmoplastic melanoma. *Am J Surg Pathol* 1999; **23**: 786-94. doi: 10.1097/00000478-199907000-00006
- Carlson JA, Mu XC, Slominski A, Weismann K, Crowson AN, Malfetano J, et al. Melanocytic proliferations associated with lichen sclerosis. *Arch Dermatol* 2002; **138**: 77-87. doi:10.1001/archderm.138.1.77
- Natsuga K, Akiyama M, Sato-Matsumura KC, Tsuchiya K, Shimizu H. Two cases of atypical melanocytic lesions in recessive dystrophic epidermolysis bullosa infants. *Clin Exp Dermatol* 2005; **30**: 336-9. doi: 10.1111/j.1365-2230.2005.01822.x
- Gallardo F, Toll A, Malvehy J, Mascaro-Galy JM, Lloreta J, Barranco C, et al. Large atypical melanocytic nevi in recessive dystrophic epidermolysis bullosa; clinicopathological, ultrastructural, and dermoscopic study. *Pediatric Dermatol* 2005; **22**: 338-43. doi: 10.1111/j.1525-1470.2005.22412.x
- Massi G, Leboit PE, editors. *Histological diagnosis of nevi and melanoma*. Darmstadt: Steinkopff Verlag; 2004.
- Kang S, Barnhill RL, Mihm MC Jr, Sober AJ. Histologic regression in malignant melanoma: an interobserver concordance study. *J Cutan Pathol* 1993; **20**: 126-9. doi: 10.1111/j.1600-0560.1993.tb00228.x
- Fabrizi G, Pennacchia I, Pagliarello C, Massi G. Sclerosing nevus with pseudomelanomatous features. *J Cutan Pathol* 2008; **35**: 995-1002. doi: 10.1159/000228317. Epub 2009 Jul 8.
- Ko CJ, Bologna JL, Glusac EJ. “Clark/dysplastic” nevi with florid fibroplasia associated with pseudomelanomatous features. *J Am Acad Dermatol* 2011; **64**: 346-51. doi: 10.1016/j.jaad.2010.02.046
- Ferrara G, Amantea A, Argenziano G, Broganelli P, Cesinaro AM, Donate P, et al. Sclerosing nevus with pseudomelanomatous features and regressing melanoma with nevoid features. *J Cutan Pathol* 2009; **36**: 913-5. doi: 10.1111/j.1600-0560.2008.01176.x
- Edge SB ed. *AJCC cancer staging manual*. New York: Springer; 2010.
- Adeniran AJ, Prieto VG, Chon S, Duvic M, Diwan AH. Atypical histologic and immunohistochemical findings in melanocytic nevi after liquid nitrogen cryotherapy. *J Am Acad Dermatol* 2009; **61**: 341-5. doi: 10.1016/j.jaad.2009.01.038
- Gerami P, Jewell SS, Morrison LE, Blondin B, Schulz J, Ruffalo T, et al. Fluorescence in situ hybridization (FISH) as an ancillary diagnostic tool in the diagnosis of melanoma. *Am J Surg Pathol* 2009; **33**: 1146-56. doi: 10.1097/PAS.0b013e3181a1ef36
- Gerami P, Belfuss B, Haghighat Z, Fang Y, Jhanwar S, Busam KJ. Fluorescence in situ hybridization as an ancillary method for the distinction of desmoplastic melanomas from sclerosing melanocytic nevi. *J Cutan Pathol* 2011; **38**: 329-34. doi: 10.1111/j.1600-0560.2010.01666.x
- Zalaudek I, Argenziano G, Ferrara G, Soyer HP, Corona R, Sera F, et al. Clinically equivocal melanocytic skin lesions with features of regression: a dermoscopic-pathological study. *Br J Dermatol* 2004; **150**: 64-71. doi: 10.1111/j.1365-2133.2004.05657.x
- Ferrara G, Argenziano G, Soyer HP, Corona R, Sera F, Brunetti B, et al. Dermoscopic and histopathologic diagnosis of equivocal melanocytic skin lesions. An interdisciplinary study of 107 cases. *Cancer* 2002; **95**: 1094-100. doi: 10.1002/cncr.10768
- Ferrara G, Giorgio CM, Zalaudek I, Broganelli P, Pellacani G, Tomasini C, et al. Sclerosing nevus with pseudomelanomatous features (nevus with regression-like fibrosis): clinical and dermoscopic features of a recently characterized histopathologic entity. *Dermatology* 2009; **219**: 202-8. doi: 10.1159/000228317
- Gimotty PA, Van Belle P, Elder DE, Murry T, MONTONE KT, Xu X, et al. Biologic and prognostic significance of dermal Ki67 expression, mitoses, and tumorigenicity in thin invasive cutaneous melanoma. *J Clin Oncol* 2005; **23**: 8048-56. doi: 10.1200/JCO.2005.02.0735
- Gaiser T, Kutzner H, Palmedo G, Siegelin MD, Wiesner T, Bruckner T, et al. Classifying ambiguous melanocytic lesions with FISH and correlation with clinical long-term follow up. *Mod Pathol* 2010; **23**: 413-9. doi: 10.1038/modpathol.2009.177
- Ko CJ, Glusac EJ, McNiff JM. Elastin staining of “Clark/dysplastic” nevi with florid fibroplasia associated with pseudomelanomatous features. *J Cutan Pathol* 2011; **38**: 593-4. doi: 10.1111/j.1600-0560.2011.01672.x
- Kiuru M, Patel RM, Busam KJ. Desmoplastic melanocytic nevi with lymphocytic aggregates. *J Cutan Pathol* 2012; **39**: 940-4. doi: 10.1111/j.1600-0560.2012.01962.x

An evaluation of the ICON® mask fixation: curing characteristics of the thermoplastic fixation and implications for patient workflow

Samendra Prasad^{1,2}, Matthew Podgorsak¹, Robert Plunkett^{3,4}, Dheerendra Prasad^{1,3,4}

¹ Department of Radiation Medicine, Roswell Park Cancer Institute, Buffalo, NY, USA

² Departments of Biomedical and Civil Engineering, University of Virginia, Charlottesville, VA, USA

³ Department of Neurosurgery, Roswell Park Cancer Institute, Buffalo, NY, USA

⁴ Department of Neurosurgery, Jacobs School of Medicine and Biological Sciences, Buffalo, NY, USA

Radiol Oncol 2018; 52(2): 229-232.

Received 15 September 2018

Accepted 30 September 2018

Correspondence to: Prof. Dheerendra Prasad, Roswell Park Cancer Institute Elm and Carlton Streets, Buffalo, NY, Jacobs School of Medicine and Biological Sciences, Buffalo, NY, USA. E-mail: d.prasad@roswellpark.org

Disclosure: No potential conflicts of interest were disclosed.

Background. Thermoplastic mask immobilization is used to perform hypo-fractionated treatments with the Gamma Knife ICON®.

Materials and methods. We evaluated the curing characteristics of the ICON® Nanor mask using force sensing resistors coupled with a data logging tool designed by us.

Results. For patients being treated with masks made the same day as the treatment, often in the same sitting with no removal and replacement of the patient from the treatment cradle, based on the curves 80% of the force of fixation is reached at 30 minutes.

Conclusions. Allowing for curing over 10-15 minutes and the subsequent localizing and delivery Cone beam CT (CBCT)s as well as the plan evaluation this is a reasonable time to start of therapy. For more exacting targets that are still requiring hypo-fractionation a cure period of 15 hours or greater will ensure that maximum rigidity of fixation is achieved.

Key words: thermoplastic mask; immobilization; hypo-fractionated; Gamma Knife ICON®

Introduction

The Leksell Gamma Knife ICON was introduced in 2015 and first installed in the US in 2016. This model of the Gamma Knife added a relocatable thermoplastic based fixation with an integrated Cone beam CT (CBCT) system that allows for hypo-fractionated radiosurgery. Since the traditional Gamma Knife user base has been accustomed to the submillimeter accuracy inherent in the frame based stereotactic radiosurgery (SRS) system there has been interest in comparing the relative accuracy of the two approaches. Several aspects of the system have been evaluated including the accuracy of the CBCT based stereotactic space¹ and frame and CBCT co-localization accuracy.² One significant as-

pect of the fixation is the thermoplastic mask itself and its characteristics. We present here a simple analysis of the force characteristics of a curing thermoplastic mask and have correlated these findings with a few cases from our clinical practice.

Materials and methods

In order to record the curing characteristics of the ICON Nanor® mask (Art. No 1514925, Elekta Inc. Atlanta, GA, USA) we created a phantom using a head mannequin (Amazon.com: search term:15" Tall Male Mannequin Head Durable Plastic Flesh [50013]). On the mannequin, we attached 5 and 15 mm FSR 400 force sensing resistors (FSR) (Interlink

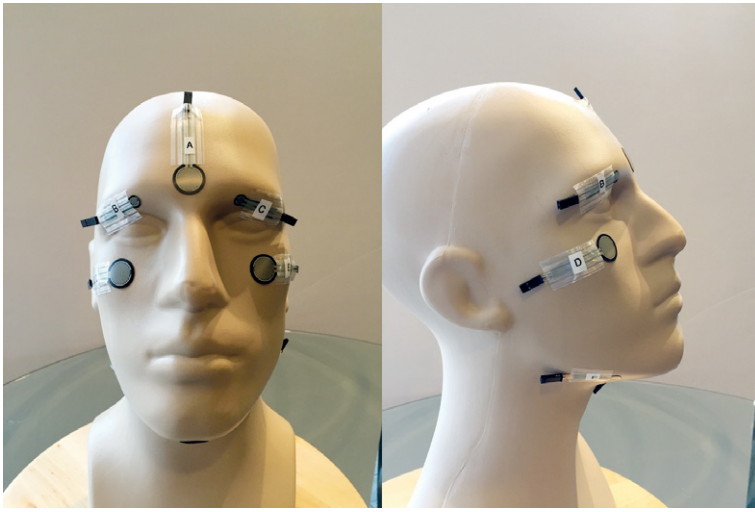


FIGURE 1. Mannequin with FSR 400 sensors mounted at forehead (A), supra-orbital ridge (B & C), malar eminence (D & E) and chin (F).

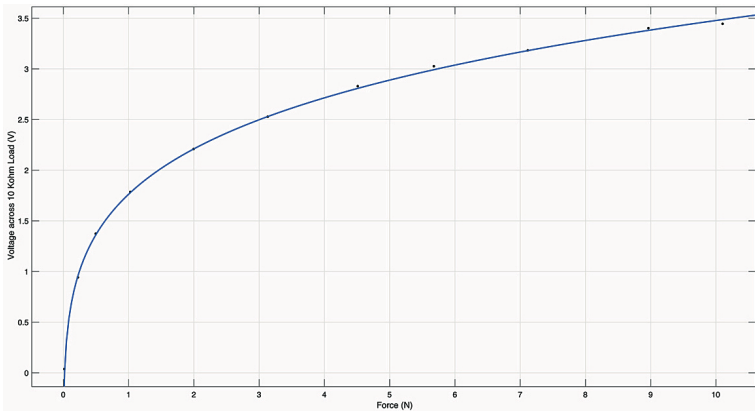


FIGURE 2. Force response curve for a FSR 400 with a 5 V supply and 10 K resistive load.⁵



FIGURE 3. Data-logger assembly to record sensor data together with mask temperature and timestamp.



FIGURE 4. Mannequin in position for measurement.

Electronics, Inc. Westlake Village, CA, USA) as depicted in Figure 1. This FSR was chosen for its relative stability over the measured temperature range and small size. The output of the FSR400 is correlated to the force applied, load resistance across the FSR (10Kohms) and the voltage applied to the measuring circuit (5V in this case).

The correlation is depicted in Figure 2 and corresponds to a two term power curve fit using Non-linear least squares method and the Levenberg-Marquardt algorithm:³

$$force(N) = 2.052 * 10^{-2} (volts)^{-0.15} - 0.023$$

Inter-FSR variation is less than 2% within one batch. All FSRs used in this design were from the same manufacturing batch. The mannequin with mounted sensors is shown in Figure 1.

The reading from the sensors was captured together with a timestamp and mask temperature using a data logger. The data logger (Figure 3) was constructed based on an Arduino® board equipped with an SD card socket, temperature probe, LCD display, and connectors for the FSRs.

The mannequin was then placed on the mold-care pillow which was formed to its shape. After verification of the connections data acquisition was initiated. A heated Nanor® mask (165 °F [73.9

°C] for 11 minutes) was then placed by two operators and molded to the mannequin as it would be to a real patient (Figure 4). The mask was then allowed to cure overnight in that position. Pressure and temperature readings were acquired every 200 milliseconds.

Results

The force recordings (Figures 5 and 6) revealed that the force recorded at the sensors increases as the mask cools and hardens or cures. Maximum force is recorded at the chin, followed by the supra-orbital ridges and the malar eminences. The forehead recordings were the lowest and showed the most drift. This was ascribed to the fact that the mannequin had a somewhat depressed forehead profile (Figure 1) and lacked the skin and elasticity of a normal human head – perhaps resulting in intermittent contact with the FSR.

In the first hour of recording (Figure 5) all sensors recorded increasing force at a rapid rate between 2 and 12 minutes and slowed at approximately 24 minutes. Extended force recordings over 24 hours (Figure 6) revealed that force stabilized after approximately 16 hours at the chin and supra-orbital regions. The malar eminence and forehead regions reach their peak values within the first hour and then show no further increase.

Discussion

Immobilization with a thermoplastic mask is not novel in radiation therapy and LINAC SRS. Thermoplastic immobilization has been used for stereotactic localization in neurosurgery as well.⁴

To our knowledge this is the first report of its kind evaluating the curing characteristics of the ICON Nanor thermoplastic mask and its implication on the pressure sensation experienced by the patient. Our findings are in keeping with the observation that patients find that their masks feel considerably tighter on day 2 and beyond of a multi-session treatment.

The Nanor® material is a nanoparticle composite that is specifically designed to provide molding at low temperatures (145 °F [62.8 °C] and up) and high strength and precision with a short curing time. Another desirable characteristic of the nanoparticle composite masks is reduced shrinkage, enhancing comfort for the patient while retaining a high flexural modulus which ensures precision.

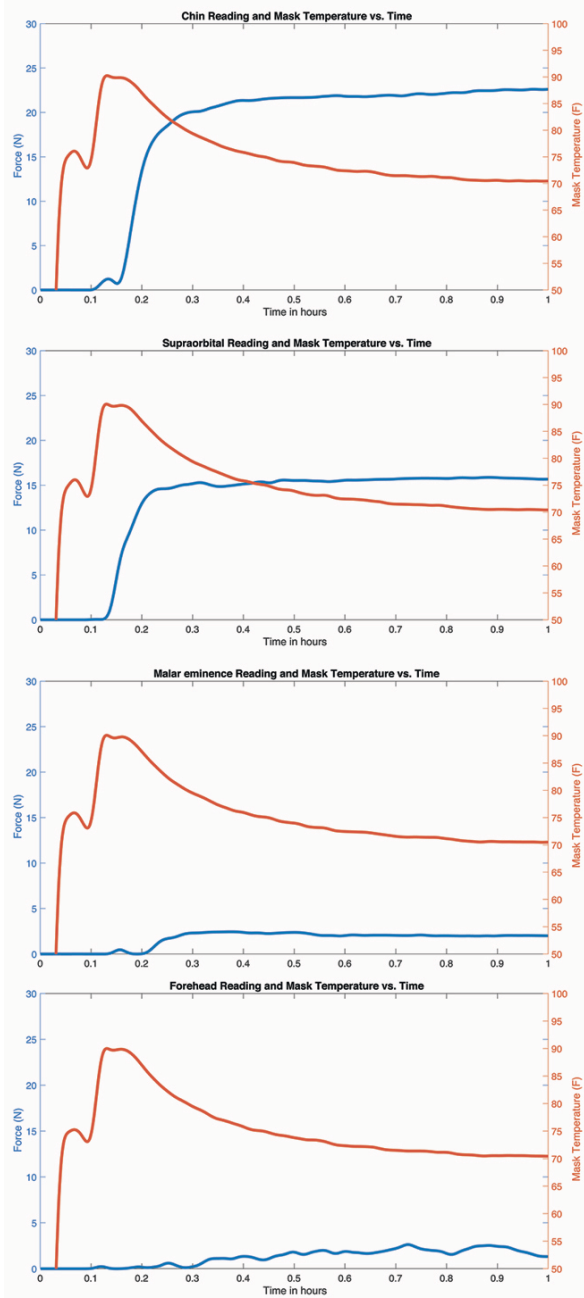


FIGURE 5. First hour force readings at the chin, supra-orbital ridges, malar eminences and forehead (50 °F = 10 °C; 100 °F = 37.8 °C).

The curing characteristics provide insight into the planning of treatment for patients treated on the ICON®. For patients being treated with masks made the same day as the treatment, often in the same sitting with no removal and replacement of the patient from the treatment cradle, based on the curves 80% of the force of fixation is reached at 30 minutes. Allowing for curing over 10–15 minutes

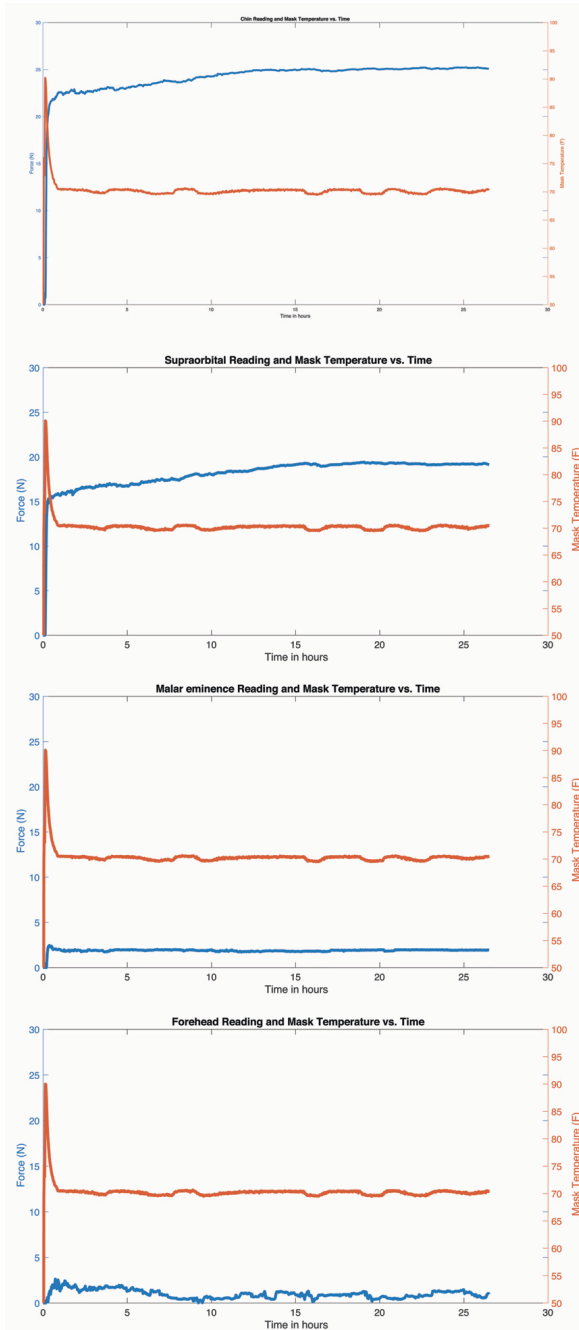


FIGURE 6. Extended 24-hour force recordings at the chin, supra-orbital ridges, malar eminences and forehead (50 °F = 10 °C; 100 °F = 37.8 °C).

and the subsequent localizing and delivery CBCTs as well as the plan evaluation this is a reasonable time to start of therapy. For more exacting targets that are still requiring hypo-fractionation a cure period of 15 hours or greater will ensure that maximum rigidity of fixation is achieved. For practical considerations in our practice, we make the mask on the first day of a multi-session treatment.

The authors recognize that patient position and stability is a function of multiple factors which include the patient clinical condition, pain and discomfort level, anxiety, treatment duration as well as fixation. When a very high premium is placed on precise location based on the indication being treated, a stereotactic frame is preferable. Understanding the curing characteristics of the mask can help in determining the best treatment schedule for a patient. These characteristics are also critical to identifying the patient population most suitable for frameless radiosurgery delivered with fixation using similar thermoplastic masks.

Conclusions

There is a longer curing period for the ICON Nanor® mask than the published Nanor material characteristics indicate. While a rigid reproducible fixation is rapidly achieved for added stability of position overnight curing of the mask may be preferred.

References

1. Aldahlawi I, Prasad D, Podgorsak MB. Evaluation of stability of stereotactic space defined by cone-beam CT for the Leksell Gamma Knife Icon. *J Appl Clin Med Phys* 2017; **18**: 67-72. doi:10.1002/acm2.12073
2. Li W, Bootsma G, Von Schultz O, Carlsson P, Laperriere N, Millar BA, et al. Preliminary evaluation of a novel thermoplastic mask system with intra-fraction motion monitoring for future use with image-guided gamma knife. *Cureus* 2016; **8**: e531. doi: 10.7759/cureus.531
3. Marquardt DW. An algorithm for least-squares estimation of nonlinear parameters. *J Soc Indust Appl Math* 1963; **11**: 431-41. doi: doi.org/10.1137/0111030
4. Pilipuf MN, Goble JC, Kassell NF. A noninvasive thermoplastic head immobilization system. Technical note. *J Neurosurg* 1995; **82**: 1082-5. doi: 10.3171/jns.1995.82.6.1082
5. Interlink. *FSR(R) 400 series datasheet*. Westlake Village, CA USA: Interlink Inc.; 2015.

Radiol Oncol 2018; 52(2): 121-128.
doi: 10.2478/raon-2018-0023

Radioterapija pri glioblastomu 15 let po prelomni Stuppovi raziskavi. Več nedorečenosti kot standardov?

Kazda T, Dziacky A, Burkon P, Pospisil P, Slavik M, Rehak Z, Jancalek R, Stampa P, Slaby O, Lakomy R

Izhodišča. Standardno zdravljenje glioblastoma, najpogostejšega možganskega tumorja pri odraslih, je nespremenjeno že več kot desetletje. Vseeno je bilo doseženo nekaj izboljšav v izidu zdravljenja, kar je posledic moderne kirurgije, izboljšanja radioterapije in sodobne obravnave stranskih učinkov zdravljenja. Bolniki, zdravljeni v kontrolnih rokah (s standardno sočasno kemoradioterapijo in adjuvantno kemoterapijo s temozolamidom) nedavnih kliničnih raziskav, so imeli boljše rezultate zdravljenja v primerjavi s srednjim preživetjem 14,6 mesecev, doseženim v prelomni Stuppovi raziskavi leta 2005. Izvedba radioterapije v Stuppovi raziskavi, ki še vedno sodi v standardno zdravljenje, ni več na mestu. Potrebno je posodobiti smernice za potrebe vsakodnevne radioterapije, ki bi upoštevale obstoječe nedorečenosti v načrtovanju radioterapije.

Namen tega pregleda je spodbuditi kritično razmišljanje o potencialnih nedorečenih vidikih radioterapije glioblastoma, ki med drugim vključuje opredelitev tarče, tehniko s simultanim integriranim dodatkom doze in ščitenje hipokampusa.

Zaključki. Vloga adjuvantne radioterapije bo opredeljena v kontekstu novih pristopov k zdravljenju, kot sta obsevalno tumorsko območje (angl. tumor-treating fields) in imunoterapija. Moderni radioterapevtski sistemi omogočajo individualen pristop tudi v dnevni radioterapevtski praksi.

Radiol Oncol 2018; 52(2): 129-135.
doi: 10.2478/raon-2018-0024

Ultrazvočna elastografija lahko prikaže nepravilnosti tkiva posteljice

Hasegawa T, Kuji N, Notake F, Tsukamoto T, Sasaki T, Shimizu M, Mukaida K, Ito H, Isaka K, Nishi H

Izhodišča. Namen raziskave je bil preveriti koristnost elastografije pri oceni placentalne funkcije in stanja ploda.

Bolniki in metode. V prospektivno kohortno raziskavo smo vključili 111 nosečnic v tretjem trimesečju. Opravili smo ultrazvočni pregled, ki je vključeval elastografijo placente. Izmerili smo placentalni indeks (PI), s katerim smo kvantitativno ocenili trdoto placentalnega tkiva. Trdnost posameznih delov placente smo ocenili tudi kvalitativno s tristopenjsko lestvico HT (hardness of placental tissue score). Patohistološko smo pregledali 40 placent.

Rezultati. Povprečen PI je bil v skupini z majhno ultrazvočno ocenjeno telesno težo plodov za gestacijsko starost (SGA) 44,3 (\pm 29,4), kar je statistično pomembno višje kot v skupini z normalno ocenjeno telesno težo plodov (8,8 (\pm 10,0); $p < 0,01$). Povezava med PI in z vrednostjo ocenjene telesne teže ploda je bila statistično pomembna ($r = -0,55$; $p < 0,01$). Prav tako je bila statistično pomembna povezava med PI in z vrednostjo porodne teže novorojenca ($r = -0,39$; $p < 0,01$). Patohistološki znaki placentalne ishemije so bili prisotni v 67 % (6 od 9) primerov s HT tretje stopnje in le v 20 % (3 od 15) primerov s HT prve stopnje.

Zaključki. Trdnost placentalnega tkiva, ki jo lahko opredelimo z elastografijo, je povezana z manjšo porodno težo. Z elastografijo bi lahko pridobili koristne informacije o delovanju placente in stanju ploda v maternici.

Radiol Oncol 2018; 52(2): 136-142.

doi: 10.2478/raon-2018-0006

Ali je togost karotidnih arterij možen zgodnji kazalec možganske kapi pri bolnikih, ki smo jih zdravili zaradi raka v otroštvu z obsevanjem vratu?

Zdravec Zaletel L, Popit M, Zaletel M

Izhodišča. Tveganje za pozne možganskožilne posledice je med bolniki, ki so preboleli raka v otroštvu, pomembno. V literaturi ne opisujejo, ali je kateri označevalec pri takšnih bolnikih zanesljiv za zgodnje odkrivanje možganskožilnih bolezni. Namen raziskave je bil analizirati togost karotidnih arterij in debeline kompleksa intime medije kot možnih zgodnjih kazalcev možganske kapi.

Bolniki in metode. V raziskavo smo vključili 23 bolnikov, ki smo jih zdravili zaradi bolezni v otroštvu. Obsevali smo jim predel vratu z odmerkom 20–65 (srednja vrednost 30) Gy. V primerjalno skupino smo vključili 26 zdravih preiskovancev, ki so se s skupino bolnikov ujemale v starosti, spolu, indeksu telesne mase, arterijski hipertenziji, kajenju in vrednosti skupnega holesterola. Pri vseh smo opravili visoko ločljiv barvni in močnostni Doppler vratnega žilja ter izmerili debelino kompleksa intime medije, število in kvaliteto plakov. Izračunali smo kazalce arterijske togosti.

Rezultati. Plake in/ali kalcinacije arterijske stene vratnega žilja smo našli pri 24 od 43 (55,8 %) obsevanih žil pri bolnikih in pri nobenem od 26 zdravih preiskovancev ($p < 0,01$). Ugotovili smo značilno razliko v vrednostih vseh parametrov arterijske togosti med skupino bolnikov in kontrolno skupino ($P < 0,05$), nismo pa videli razlike v debelini intime medije med skupinama ($p = 0,92$). V multivariatnem modelu je bila hitrost pulznega vala pozitivno povezana s kajenjem.

Zaključki. Togost karotidnih arterij bi lahko v bodoče služila kot zgodnji kazalec za možgansko kap pri bolnikih, ki so preboleli raka v otroštvu in smo jim obsevali predel vratu. Kajenje bi lahko imelo dodaten negativen učinek na staranje žilja v skupini bolnikov po obsevanju vratu.

Radiol Oncol 2018; 52(2): 143-151.

doi: 10.2478/raon-2018-002

Spremembe magnetnoresonančnih perfuzijskih vrednosti morfološko normalne možganovine pri bolnikih z glioblastomom, ki smo jih zdravili z radioterapijo, lahko vplivajo na oceno uspešnosti zdravljenja

Fahlström M, Blomquist E, Nyholm T, Larsson EM

Izhodišča. Namen raziskave je bil oceniti zgodnje in zgodaj zakasnjene poobsevalne spremembe možganovine z magnetnoresonančno (MR) perfuzijo in njihovo odvisnost od doze frakcionirane radioterapije.

Bolniki in metode. V prospektivno raziskavo smo vključili 17 bolnikov z gliomom, ki so imeli gradus po Svetovni zdravstveni organizaciji (WHO) III-IV in smo jih zdravili s frakcionirano radioterapijo. Sedem bolnikov je bilo zaradi neustreznega protokola zdravljenja in manjkajočih preiskav MR izključenih iz raziskave. Dinamično kontrastno dozjetne preiskave MR in poudarjene sekvence 3D-T1 s kontrastnim sredstvom smo naredili pri vseh bolnikih pred in po frakcionirani radioterapiji (standardna deviacija), v povprečju po 3,1 (3,3), 34,4 (9,5) in 103,3 (12,9) dneh. Sekvence 3D-T1 pred radioterapijo smo segmentirali v belo in sivo možganovino. Izračunane karte možganske prostornine krvi in pretoka krvi smo ko-registrirali s sekvencami 3D-T1 pred radioterapijo. Ustvarili smo sedem področij, ki so prejela različne doze obsevanja: 0–5 Gy, 5–10 Gy, 10–20 Gy, 20–30 Gy, 30–40 Gy, 40–50 Gy in 50–60 Gy. V vsaki izmed naštetih področij smo izračunali srednjo vrednost možganske prostornine krvi in pretoka krvi in ju normalizirali do srednje vrednosti v beli in sivi možganovini pri 0–5 Gy.

Rezultati. Področni in celotni srednji vrednosti možganske prostornine krvi in pretoka krvi v beli in sivi možganovini sta se po radioterapiji zmanjšali, čemur je sledila težnja izboljšanja. Spremembe so bile odvisne od obsevalne doze v beli možganovini ne pa tudi v sivi.

Zaključki. Rezultati raziskave dokazujejo, da imajo možgani normalnega videza na preiskavi MR po frakcionirani radioterapiji spremembe perfuzije, ki jih lahko pripisujemo stanju po obsevanju. To lahko vodi do napačne ocene oziroma precenjenosti perfuzije v samem tumorju, kar pomembno vpliva na oceno uspešnosti zdravljenja.

Radiol Oncol 2018; 52(2): 152-159.
doi: 10.2478/raon-2018-0014

Učinkovitejši *in silico* selekcijski pristop razvoja DNA aptamer za subpopulacijo celic nedrobno celičnega pljučnega adenocarcinoma A549 z lastnostmi matičnosti

Vidic M, Tina Šmuc T, Janež N, Blank B, Accetto T, Mavri J, Nascimento IC, Nery AA, Ulrich H, Lah TT

Izhodišča. Ugotavljanje krožečih celic pljučnega raka z lastnostmi matičnosti lahko predstavlja bolj učinkovito diagnostično orodje za napovedovanje poteka bolezni. Obstoječe metode, ki temelje na protitelesih, niso zadovoljive. Tako smo uporabili metodo celične sistemske evolucije ligandov za eksponencialno obogatitev (SELEX) za razvoj oligonukleotidnih DNA aptamer. Te prepoznavajo površinske označevalce celic nedrobno celičnega pljučnega raka.

Material in metode. Za selekcijo sedmih ciklov SELEX-a smo uporabili humano celično linijo nedrobno celičnega pljučnega raka A549. Kot negativno selekcijo smo uporabili človeške levkocite iz krvi in kot pozitivno selekcijo vezavo protiteles označevalca matičnih celic pljučnega raka, membranskega proteina CD90 na celice A549.

Rezultati. Dobljene oligonukleotidne sekvence po sedmem krogu SLELEX-a smo analizirali s tremi neodvisnimi bioinformatičnimi pristopi, ki so izbrali dva sorodna aptamerna kandidata glede na konsenzualne sekvence, strukturne motive in vezavno afiniteto (Kd) ter stabilnost vezave (ΔG). Izbrali in identificirali smo aptamero A15_18, ki ima zelo dobre vezavne lastnosti in veže apramero protiteles membranskega označevalca CD90. Izračunano filogenetsko drevo je pokazalo, da je naša izbrana aptamer A155_18 zelo sorodna že objavljeni aptameri S6 za A549 celice, ki nam je služila kot pozitivna kontrola. Sekvenčna analiza MEME je pokazala, da imata ti dve aptameri skupne motive, ki so bili različni od ostalih dobljenih aptamernih sekvenc.

Zaključki. Aptamero A155_18 ima močno afiniteto za vezavo na A459 celično linijo nedrobno celičnega pljučnega raka in izraža CD90, kar kaže na matične značilnosti te linije, oz. njene subpopulacije. To aptamero bi lahko uporabili za ugotavljanje krožečih celic nedrobno celičnega pljučnega raka.

Radiol Oncol 2018; 52(2): 160-166.
doi: 10.2478/raon-2018-0005

Polimorfizmi matriksnih metaloproteinaz kot dejavnik tveganja za nastanek malignega plevralnega mezotelioma

Štrbac D, Goričar K, Dolžan V, Kovač V

Izhodišča. Maligni mezoteliom je redka bolezen, povezana z izpostavljenostjo azbestu pri več kot 80 % primerov. Matriksne metaloproteinaze (MMP) preoblikujejo tumorsko mikrookolje in sodelujejo pri karcinogenezi. Polimorfizme genov za MMP so preučevali kot možne biološke označevalce za napovedovanje časa do napredovanja bolezni in celokupnega preživetja. Namen raziskave je bil preučiti polimorfizme izbranih MMP kot dejavniki tveganja za nastanek malignega plevralnega mezotelioma v povezavi z drugimi dejavniki tveganja, zlasti z izpostavljenostjo azbestu.

Bolniki in metode. V raziskavo smo vključili 236 bolnikov in kontrolno skupino 161 zdravih krvodajalcev. S postopkom kompetitivne alelni specifične verižne reakcije polimerizacije (KASPar) smo analizirali deset izbranih genskih polimorfizmov v treh genih za matriksne metaloproteinaze: MMP2 rs243865, rs243849 in rs7201, MMP9 rs17576, rs17577, rs2250889 in rs20544, ter MMP14 rs1042703, rs1042704 in rs743257. Zvezne spremenljivke smo opisali s srednjo vrednostjo in razponom (25–75 %), kategorične pa s frekvencami. Odklone od Hardy-Weinbergovega genetskega ravnotežja (HWE) smo izračunali s pomočjo standardnega testa hi-kvadrat. V statističnih analizah smo uporabili aditivni in dominantni genetski model. Povezavo med genetskimi polimorfizmi in tveganjem za maligni mezoteliom smo izračunali z metodo logistične regresije in jo prikazali z razmerjem obovet (OR) s 95 % intervalom zaupanja (CI).

Rezultati. Nosilci vsaj enega alela MMP2 rs243865 so imeli nižje tveganje za nastanek malignega plevralnega mezotelioma (OR = 0,66, 95 % CI = 0,44–1,00; P = 0,050). Ta povezava je bila najbolj izražena pri bolnikih z znano izpostavljenostjo azbestu; med njimi so nosilci vsaj enega polimorfnega alela imeli statistično značilno nižje tveganje za nastanek malignega mezotelioma (OR = 0,55, 95% CI = 0,35–0,86, P = 0,009). Ostali preučevani polimorfizmi niso bili povezani s tveganjem za nastanek malignega plevralnega mezotelioma.

Zaključki. Polimorfizem MMP2 rs243865 se je v raziskavi pokazal kot zaščitni dejavnik pri tveganju za nastanek malignega plevralnega mezotelioma. Zaščitna vloga je bila bolj izražena pri bolnikih, ki so bili izpostavljeni azbestu, kar kaže na povezavo med genskimi in okoljskimi dejavniki.

Radiol Oncol 2018; 52(2): 167-172.

doi: 10.2478/raon-2018-0010

Glioblastom pri bolnikih starejših od 70 let

Smrdel U, Skoblar Vidmar M, Smrdel A

Izhodišča. V zadnji 20 letih opazamo počasen a stalen porast incidence glioblastoma. Porast incidence je najbolj opazen v skupini bolnikov starejših od 70 let. Ti imajo tudi značilno slabše preživetje kot mlajši bolniki in jih obravnavamo kot posebno skupino bolnikov z glioblastomom. Njihovo zdravljenje pogosto prilagodimo modificiranim napovednim dejavnikom, ki jih v zadnjem obdobju dopolnjujejo genetske in epigenetske informacije o tumorju. Namen raziskave je je bil analizirati sedanje zdravljenje bolnikov z glioblastomom starejših od 70 let in oceniti pomen kliničnih napovednih dejavnikov.

Bolniki in metode. Med bolniki z glioblastomom zdravljenimi na Onkološkem inštitutu v Ljubljani med leti 1997 in 2015 smo poiskali starejše od 70 let. Teh bolnikov je bilo 207. Analizirali smo njihovo preživetje ter klinične napovedne dejavnike (starost, stanje zmogljivosti) in zdravljenje (obseg resekcije, odmerki sevanja prejet pri radioterapiji in sistemska terapija).

Rezultati. Srednje preživetje bolnikov starejših od 70 let je bilo 5,3 mesecev, kar je slabše kot preživetje mlajših bolnikov ($p < 0,001$). Med napovednimi dejavniki so na preživetje najmočnejše vplivali stanje splošne zmogljivosti ($p < 0,001$), obseg resekcije ($p < 0,001$), dodatek temozolomida ($p < 0,001$) in radioterapija ($p = 0,006$). Bolniki, ki so prejeli sočasno radiokemoterapijo s temozolomidom, so imeli enako preživetje kot bolniki, ki so bili obsevani brez temozolomida, so pa ga prejeli po obsevanju ($p = 0,64$).

Zaključki. Porast števila starejših bolnikov z glioblastomom sovпада z podaljšanjem pričakovane življenjske dobe, v Sloveniji pa tudi z večjo dostopnostjo diagnostičnih postopkov. Klinični napovedni dejavniki so nam v pomoč pri odločitvi glede tega, kako agresivno naj bo zdravljenje. Radioterapija in temozolomid imata največji učinek na preživetje, ki pa je pri radioterapiji manjši. Pri izbranih bolnikih je možno, da za optimalni učinek zadošča sistemska terapija. Bolniki, ki so bili v boljšem stanju zmogljivosti, bili bolj radikalno operirani in so prejeli temozolomid, so imeli najboljše preživetje. Pri sistemskem temozolomidu pa različne sheme prejetja niso pokazale različnega vpliva na preživetje. Glede na rezultate naše analize, lahko potrdimo smiselnost uporabe RPA razredov pri odločitvi o zdravljenju.

Radiol Oncol 2018; 52(2): 173-180.

doi: 10.2478/raon-2018-0020

Primerjalna analiza kliničnega in patološkega stadija področnih bezgavk pri bolnikih s ploščatoceličnim rakom glave in vratu zdravljenih v Splošni bolnišnici Dunaj

Eder-Czembirek C, Erlacher B, Thurnher D, M. Erovic B, Selzer E, Formanek M

Izhodišča. Rezultati v objavljenih raziskavah, ki so ocenjevale neujemanje med kliničnimi podatki o stadiju in patološkimi podatki, so pokazali, da pomembno število bolnikov s ploščatoceličnim rakom glave in vratu ni pravilno razvrščenih. Namen retrospektivne raziskave je bil analizirati možne razlike med radiološko oceno in patološkimi podatki o prizadetosti področnih bezgavk in primerjati rezultate s podatki iz literature.

Bolniki in metode. V retrospektivno analizo smo vključili bolnike s ploščatoceličnim rakom glave in vratu, ki smo jih zdravili z operacijo in pooperativno radioterapijo med leti 2002 in 2012. Obvezni podatki za vključitev v raziskavo so bili popolni podatki o predoperativnem, klinično določenem obsegu bolezni, vključno z bezgavčnim statusom in patohistološka navedbe o zajetih bezgavčnih ložah ter podatki o preživetju. Vključili smo 87 bolnikov (UICC stadij III-IV 90,8 %), za katere smo pridobili zgoraj naštetih podatke in so bile narejene preiskave s CT-jem ali MR-jem. Celokupno preživetje smo ocenili z metodo po Kaplan-Meierju. Izračunali smo Pearsonov oz. Spearmanov (nelinearen odnos) korelacijski koeficient.

Rezultati. Neujemanje na ravni ocene celokupnega stadija tumorja je bilo ugotovljeno pri 27,5 % primerov. Med njimi je bilo 5,7 % posledica patohistološke razvrstitve primarnega tumorja v višji (*up-staging*) oz nižji (*down-staging*) stadij. Na ravni bezgavk je bilo 11,5 % bolnikov prerazporejenih v nižji stadij in 10,3 % v višji stadij.

Zaključki. Rezultati raziskave kažejo, da se pri približno petini bolnikov (21,8 %) ocena prizadetosti bezgavk s CT-jem ali MR-jem razlikuje od patohistološkega stadija, kar se sklada z ugotovitvami več drugih raziskovalnih skupin.

Radiol Oncol 2018; 52(2): 181-188.
doi: 10.1515/raon-2017-0058

Populacijska raziskava učinkovitosti stereotaktičnega ablativnega obsevanja v primerjavi s konvencionalnim frakcioniranim obsevanjem pri bolnikih z nedrobnoceličnim pljučnim rakom stadija I

Tu CY, Hsia TC, Fang HY, Liang JA, Yang ST, Li CC, Chien CR

Izhodišča. Stereotaktično ablativno obsevanje (SABR) je obetavno zdravljenje neoperabilnega zgodnjega stadija nedrobnoceličnega raka pljuč v primerjavi s konvencionalno frakcionirano radioterapijo (CFRT). Vendar pa rezultati randomiziranih kontroliranih preskušanj še niso na voljo. Namen raziskave je bil primerjati učinkovitost SABR in CFRT pri neoperabilnem nedrobnoceličnem raku pljuč zgodnjega stadija.

Bolniki in metode. Neoperirane bolnike z nedrobnoceličnim rakom pljuč stadija I, ki so bili zdravljeni s SABR ali CFRT in diagnosticirani med leti 2007 in 2013 v Tajvanu, smo poiskali v celoviti populacijski zbirki podatkov. Uporabili smo inverzno verjetnostno tehtanje in stopnjo nagnjenja za primarno analizo, ker smo primerjali nerandomizirani zdravljenji. V dopolnilnih analizah smo izdelali podskupine, ki so se ujemale glede stopnje nagnjenja, da bi primerjali preživetje med bolniki, zdravljenimi s SABR in CFRT.

Rezultati. S primarno analizo smo ugotovili 238 bolnikov. Dobro razmerje med spremenljivkami je bilo doseženo s ponderiranjem ocene naklona. Celokupno preživetje se ni pomembno razlikovalo med bolniki, zdravljenimi s SABR v primerjavi s CFRT (stopnja tveganja, prilagojena glede na razmerje obolev [HR] 0,586, 95% interval zaupanja 0,26–1,101, $p = 0,102$). Vendar pa je pokazal SABR bistveno prednost v dopolnilnih analizah.

Zaključki. V populacijski analizi, prilagojeni na podlagi nagnjenja, smo ugotovili, da v primarni analizi celokupno preživetje ni bilo bistveno drugačno pri bolnikih, zdravljenih s SABR, v primerjavi s CFRT. Nasprotno pa se je v dodatnih analizah preživetje statistično pomembno razlikovalo v korist SABR. Naše rezultate je potrebno razlagati previdno glede na nerandomiziran pristop do podatkovnih baz uporabljen v raziskavi. Potrebne so nadaljnje raziskave za preučitev učinkovitosti obeh metod zdravljenja.

Radiol Oncol 2018; 52(2): 189-194.
doi:10.1515/raon-2017-0038

Preživetje bolnikov in stabilnost hrbtenice pri bolnikih z rakom urotelijskih celic in zasevki v hrbtenici, ki smo jih zdravili s paliativno radioterapijo

Foerster R, Hees K, Bruckner T, Bostel T, Schlamp I, Sprave T, Nicolay NH, Debus J, Rief H

Izhodišča. Namen raziskave je bil analizirati preživetje bolnikov in stabilnost hrbtenice pri bolnikih z rakom urotelijskih celic in z zasevki v hrbtenici, ki smo jih zdravili s paliativno radioterapijo (RT). Dodatno smo želeli ugotoviti, kakšen je učinek RT na mineralno kostno gostoto (MKG) kot lokalni odziv zasevkov v hrbtenici.

Bolniki in metode. Izračunali smo preživetje 38 bolnikov z rakom urotelijskih celic in s 132 zasevki v hrbtenici, ki smo jih zdravili od januarja 2000 do januarja 2012. Retrospektivno smo analizirali stabilnost hrbtenice v področju obsevanih zasevkov prsne in ledvene hrbtenice s pomočjo računalniške tomografije (CT) in z uporabo lestvice Taneichi *et al.* Mineralno kostno gostoto v hrbteničnih zasevkih smo izmerili pred RT ter 3 in 6 mesecev po njej. Razlike v mineralni kostni gostoti smo izrazili v Hounsfieldovih enotah (HU).

Rezultati. Vsi bolniki so med raziskavo umrli. Celokupno preživetje (OS) po 6 mesecih je bilo 90 %, po 1 letu 80 % in po 2 letih 40 %. Preživetje od ugotovitve kostnih zasevkov je bilo po 6 mesecih 85 %, po 1 letu 64 % in po 2 letih 23 %. Preživetje od začetka radioterapije je bilo 42 % po 6 mesecih, 18 % po enem letu in 5 % po dveh letih. Bifosfonate je dobivalo le 11 % bolnikov. Stabilnost hrbtenice se po 3 ali 6 mesecih po radioterapiji ni izboljšala. Mineralna kostna gostota se je povečala za 25,0 HU ($\pm 49,7$ standardna deviacija [SD]) po 3 mesecih ($p = 0,001$) in za 24,2 HU ($\pm 52,2$ SD) po 6 mesecih ($p = 0,037$). Olajšanje bolečine (≥ 2 točki po vidni analogni lestvici) je bilo doseženo le pri 27 % bolnikov.

Zaključki. Koristi bolnikov po paliativni radioterapiji pri bolnikih z rakom urotelijskih celic in z bolečimi hrbteničnimi zasevki ali z nestabilno hrbtenico v področju zasevkov so omejene. Svetujemo, da skrbno izberemo bolnike, ki so primerni za radioterapijo. Priporočamo krajšo frakcionirano radioterapijo, dodatno prejetje bisfosfonatov pa bi lahko povečalo učinkovitost zdravljenja.

Radiol Oncol 2018; 52(2): 195-203.

doi: 10.2478/raon-2018-0016

Napovedni pomen plazemske EBV DNA pri bolnikih z rakom nosnega žrela med zdravljenjem z intenzitetno moduliranim obsevanjem in sočasno kemoterapijo

Lertbutsayanukul C, Kannarunimit D, Prayongrat A, Chakkabat C, Kitpanit S, Hansasuta P

Izhodišča. Plazemske koncentracije EBV DNA ob diagnozi (pre-EBV) in po zdravljenju (po-EBV) so pomembne za napoved kliničnega izida pri bolnikih z rakom nosnega žrela. Napovedni pomen koncentracije EBV med obsevanjem (med-EBV) do sedaj niso obširneje preučevali.

Bolniki in metode. Naredili smo naknadno analizo 105 bolnikov z rakom nosnega žrela in merljivo koncentracijo pre-EBV, vključenih v raziskavo faze II/III, ki je primerjala zaporedno in simultano integrirano aplikacijo dodatne doze pri intenzitetno moduliranem obsevanju (IMRT). Plazemske koncentracije EBV DNA smo določili s PCR pred pričetkom IMRT, 5. teden obsevanja in 3 mesece po zaključku IMRT. Namen je bil opredeliti prognostično vrednost med-EBV za napoved celokupnega preživetja, preživetja brez ponovitve bolezni in za preživetja brez oddaljenih zasevkov.

Rezultati. Srednja vrednost pre-EBV je bila 6880 kopij/ml. Merljive koncentracije med-EBV in po-EBV smo ugotovili pri 14,3 % oz. 6,7 % bolnikov. Srednji čas sledenja je znašal 45,3 mesece. Pri bolnikih z nemerljivo oz. merljivo koncentracijo med-EBV je bilo 3-letno celokupno preživetje, preživetje brez ponovitve bolezni in preživetje brez oddaljenih zasevkov 86,0 % oz. 66,7 % ($p = 0,043$), 81,5 % oz. 52,5 % ($p = 0,006$) in 86,1 % oz. 76,6 % ($p = 0,150$). V multivariatni analizi so bile le merljive koncentracije po-EBV statistično pomembno povezane s slabšim celokupnim preživetjem (razmerje obovetov (RO) = 6,881, 95 % interval zaupanja (IZ) 1,699–27,867, $p = 0,007$), preživetjem brez ponovitve bolezni (RO = 5,117, 95 % IZ 1,562–16,768, $p = 0,007$) in preživetjem brez oddaljenih zasevkov (RO = 129,071, 95 % IZ 19,031–875,364, $p < 0,001$).

Zaključki. Merljive koncentracije po-EBV so najmočnejši negativni napovedni dejavnik za celokupno preživetje, preživetje brez ponovitve bolezni in preživetje brez oddaljenih zasevkov. Merljive koncentracije med-EBV so bile povezane s slabšim celokupnim preživetjem in preživetjem brez ponovitve bolezni, še posebej lokalno ter bi lahko prispevale k prilagoditvi zdravljenja v času obsevanja.

Radiol Oncol 2018; 52(2): 204-212.

doi: 10.2478/raon-2018-0011

Zgodnja kardiotoksičnost po sočasnem dopolnilnem zdravljenju z obsevanjem in trastuzumabom pri bolnicah z rakom dojke

Marinko T, Borštnar S, Blagus R, Dolenc J, Bilban-Jakopin C

Izhodišča. Z raziskavo smo želeli preveriti ali je med bolnicami, ki so ob zdravljenju s trastuzumabom kooperativno obsevale levo (skupina 1) oziroma desno (skupina 2) dojko/prsno steno, po zaključenem zdravljenju pomembna razlika v zgodnjih kazalcih kardiotoksičnosti. To smo merili z iztisnim deležem levega prekata (LVEF) in N-končnim pro-B natriuretičnim peptidom [NT-proBNP].

Bolniki in metode. V raziskavo smo vključili 175 zaporednih bolnic s pozitivnim HER2 rakom dojke, ki so v okviru dopolnilnega zdravljenja med junijem 2005 in decembrom 2010 prejemale trastuzumab ter smo jim sočasno kooperativno obsevali dojko/prsno steno. Vsem bolnicam smo ob začetku dopolnilnega zdravljenja naredili izhodiščno preiskavo srca, bodisi ehokardiografijo ali radioizotopno ventrikulografijo (LVEF₀) ter naredili kontrolne meritve po zaključenem zdravljenju (LVEF₁), hkrati pa smo jim določili vrednosti NT-proBNP. Analizirali smo razliko med LVEF₀ in LVEF₁ (Δ LVEF = LVEF₀ - LVEF₁) ter ju primerjali med skupinama.

Rezultati. V skupini 1 je sodelovalo 84, v skupini 2 pa 91 bolnic. Mediani čas sledenja bolnic je bil 57 (37–71) mesecev. V skupini 1 je bila srednja vrednost Δ LVEF (%) -1,786 %, v skupini 2 pa -2,607 % ($p = 0,562$; interval zaupanja [CI]: od -2,004 do 3,648). Srednja vrednost NT-proBNP je bila 111,0 ng/l v skupini 1 in 90,0 ng/l v skupini 2 ($p = 0,545$). Primerjava ehokardiografskih kazalcev je pokazala, da bolnice iz skupine 1 niso imele pomembno slabše sistolične in diastolične funkcije levega prekata kot bolnice iz skupine 2, imele pa so pomembno več perikardnih izlivov (9 [11 %]) kot bolnice v skupini 2 (1 [1 %]) ($p = 0,007$).

Zaključki. Med opazovanima skupinama nismo našli značilnih razlik v zgodnjih kazalcih kardiotoksičnosti (LVEF, NT-proBNP). Bolnice, pri katerih smo obsevali levo dojko/prsno steno, so imele značilno več perikardnih izlivov.

Radiol Oncol 2018; 52(2): 213-219.

doi: 10.2478/raon-2018-0002

Očesne spremembe pri bolnikih z metastatskim malignim melanomom zdravljenih z zaviralcem MEK cobimetinibom in zaviralcem BRAF vemurafinibom

Gavrić AU, Ocvirk J, Jaki Mekjavić P

Izhodišča. Zdravljenje z zaviralcem MEK cobimetinibom v kombinaciji z zaviralcem BRAF vemurafinibom je pomembno izboljšalo preživetje bolnikov z metastatskim malignim melanomom z mutacijo V600E v genu BRAF. To je novejša oblika zdravljenja, ob kateri se pogosto pojavijo do sedaj slabo raziskani očesni stranski učinki. Namen raziskave je bil ugotoviti očesne stranske učinke pri bolnikih z metastatskim malignim melanomom zdravljenih s kobimetinibom v kombinaciji z vemurafinibom.

Bolniki in metode. V prospektivno opazovalno raziskavo smo vključili bolnike z BRAF-mutiranim metastatskim melanomom, ki smo jih zdravili s cobimetinibom v kombinaciji z vemurafinibom na Onkološkem inštitutu Ljubljana. Opravili smo oftalmološki pregled, ki je vključeval določanje vidne ostrine, merjenje znotrajočesnega tlaka, pregled s špranjsko svetilko ter slikanje očesnega ozadja, ki je vsebovalo barvno slikanje (FF), slikanje z infrardečo svetlobo (IR) in slikanje avtofluorescence (AF). Na koncu smo izvedli tudi optično koherentno tomografijo (OCT) mrežnice.

Rezultati. Pet od 7 bolnikov (71 %) je opazilo spremembe v vidu nekaj dni po začetku zdravljenja s cobimetinibom. Pri vseh bolnikih (100 % oči) so bile prisotne manjše krožne lezije v zunanji plasti mrežnice, vidne na OCT, IR in FF, t.i. MEKAR. Lezije so bile v centralnem delu in / ali pa so bile razpršene po zadnjem polu, simetrično v obeh očeh; nesimetrična prizadetost je bila le pri enem bolniku, pri katerem je bil prisoten tudi anteriorni uveitis s cistoidnim edemom v makuli.

Zaključki. Pri bolnikih zdravljenih s cobimetinibom v kombinaciji z vemurafinibom se pojavljajo fovealne in ektrafovelne spremembe v zunanji plasti mrežnice, imenovane MEKAR. Oftalmologi in onkologi moramo poznati ta pogost, vendar relativno blag očesni stranski učinek zdravljenja, da bi se izognili nepotrebnim posegom, vključno s prekinitvijo za življenje potrebne terapije.

Radiol Oncol 2018; 52(2): 220-228.

doi: 10.2478/raon-2018-0003

Sklerozirajoče melanocitne lezije - sklerozirajoči melanomi z nevoidnimi značilnostmi in sklerozirajoči nevusi s psevdo-melanomskimi značilnostmi. Analiza 90 primerov

Grčar-Kuzmanov B, Boštjančič E, Contreras Bandres JA, Pižem J

Izhodišča. Sklerozirajoče melanocitne lezije, s fokalno ali difuzno sklerozo v dermalni komponenti ter atipično proliferacijo pretežno nevoidnih melanocitov, so še vedno slabo opredeljene. Cilj raziskave je bil sistematično analizirati njihov morfološki spekter, zlasti razlikovanje med sklerozirajočim melanocitnim nevusom in sklerozirajočim melanomom, ki v dosedanjih raziskavah ni bil opredeljen.

Bolniki in metode. Analizirali smo 90 sklerozirajočih melanocitnih lezij pri 82 bolnikih (49 moških, 33 žensk, starih med 21 in 89 let). Za dodatno potrditev diagnoze sklerozirajočih melanomov smo opravili fluorescenčno *in situ* hibridizacijo (FISH) s štirimi sondami pri 41 primerih.

Rezultati. Izrazito pagetoidno širjenje melanocitov je bilo prisotno v 44 (48 %) lezijah, melanom *in situ* ob skleroziji v 55 (61 %) lezijah. V intrasklerotični komponenti je bilo zorenje odsotno v 40 (44 %) lezijah, mitoze so bile prisotne v 18 (20 %) lezijah. Med 90 lezijami je bilo glede na morfološke kriterije 26 (29 %) nevusov ter 64 (71 %) melanomov (z debelino po Breslowu od 0,4 do 1,8 mm), med katerimi je bilo 45 (50 %) melanomov s spremljajočim nevusom. Preiskava FISH s štirimi sondami je bila pozitivna v sklerotični komponenti 14 od 25 lezij, ki so bile morfološko opredeljene kot melanom, in nobenem od 16 nevusov. Biopsija varovalne bezgavke je bila narejena pri 17 lezijah, v vseh primerih je bila negativna.

Zaključki. Sklerozirajoče melanocitne lezije tvorijo morfološki spekter in vključujejo tako nevuse kot melanome. Patogeneza skleroze ni jasna, vendar se zdi, da jo vsaj v nekaterih lezijah sprožijo melanociti ali je posledica odgovora organizma.

Radiol Oncol 2018; 52(2): 229-232.

doi: 10.2478/raon-2018-0019

Ovrednotenje termoplastične fiksacije bolnika z masko ICON® pri obsevanju z nožem gama

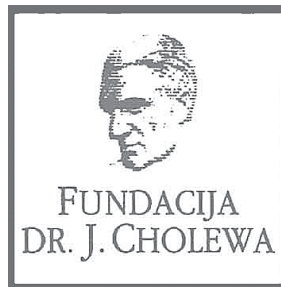
Prasad S, Podgorsak M, Plunkett R, Prasad D

Izhodišča. Za izvedbo hipofrakcioniranega zdravljenja z nožem gama ICON uporabljamo imobilizacijo s termoplastičnimi maskami.

Materiali in metode. Karakteristike strjevanja maske ICON Nanor smo ovrednotili z uporovnim detektorjem sile, priključnim na napravo za zajem podatkov lastne zasnove.

Rezultati. Pri bolnikih, obsevanih isti dan, pogosto v isti seansi brez odstranitve in vnovične namestitve maske, smo glede na izmerjene krivulje dosegli 80 % fiksacijske sile v 30 minutah.

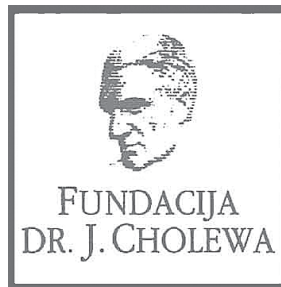
Zaključki. Čas strjevanja vsaj 10–15 minut, ki mu sledi nastavitev bolnika s konusnožarčno računalniško rentgensko tomografijo zadošča za začetek obsevanja. Za natančnejše hipofrakcionirano obsevanje tarč pa čas strjevanja vsaj 15 ur zagotavlja maksimalno togost fiksacijske maske.



FUNDACIJA "DOCENT DR. J. CHOLEWA"
JE NEPROFITNO, NEINSTITUCIONALNO IN NESTRANKARSKO
ZDRUŽENJE POSAMEZNIKOV, USTANOV IN ORGANIZACIJ, KI ŽELIJO
MATERIALNO SPODBUJATI IN POGLABLJATI RAZISKOVALNO
DEJAVNOST V ONKOLOGIJI.

DUNAJSKA 106
1000 LJUBLJANA

IBAN: SI56 0203 3001 7879 431



Activity of “Dr. J. Cholewa” Foundation for Cancer Research and Education - a report for the second quarter of 2018

Dr. Josip Cholewa Foundation for cancer research and education continues with its planned activities in the second quarter of 2018. Its primary focus remains the provision of grants, scholarships, and other forms of financial assistance for basic, clinical and public health research in the field of oncology. In parallel, it also makes efforts to provide financial and other support for the organisation of congresses, symposia and other forms of meetings to spread the knowledge about prevention and treatment of cancer, and finally about rehabilitation for cancer patients. In Foundation’s strategy, the spread of knowledge should not be restricted only to the professionals that treat cancer patients, but also to the patients themselves and to the general public.

The Foundation continues to provide support for »Radiology and Oncology«, a quarterly scientific magazine with a respectable impact factor that publishes research and review articles about all aspects of cancer. The magazine is edited and published in Ljubljana, Slovenia. »Radiology and Oncology« is an open access journal available to everyone free of charge. Its long tradition represents a guarantee for the continuity of international exchange of ideas and research results in the field of oncology for all in Slovenia that are interested and involved in helping people affected by many different aspects of cancer.

The Foundation will continue with its activities in the future, especially since the problems associated with cancer affect more and more people in Slovenia and elsewhere. Ever more treatment that is successful reflects in results with longer survival in many patients with previously incurable cancer conditions. Thus adding many new dimensions in life of cancer survivors and their families.

Tomaž Benulič, M.D.
Andrej Plesničar, M.D., M.Sc.
Viljem Kovač M.D., Ph.D.
Borut Štabuc, M.D., Ph.D.

➤ PRVA REGISTRIRANA TERAPIJA
V 2. LINIJI ZA ZDRAVLJENJE
ADENOKARCINOMA ŽELODCA ALI
GASTRO-EZOFAGEALNEGA PREHODA¹


CYRAMZA[®]
(ramucirumab)

UKREPAJTE ZDAJ

**USPOSOBLJENI
ZA SPREMEMBE,
ZA NEPRIMERLJIVE
IZKUŠNJE**

Skrajšan povzetek glavnih značilnosti zdravila

▼ Za to zdravilo se izvaja dodatno spremljanje varnosti. Tako bodo hitreje na voljo nove informacije o njegovi varnosti. Zdravstvene delavce naprošamo, da poročajo o katerem koli domnevnem neželenem učinku zdravila.

Cyramza 10 mg/ml koncentrat za raztopino za infundiranje

En mililiter koncentrata za raztopino za infundiranje vsebuje 10 mg ramucirumaba. Ena 10-mililitrska viala vsebuje 100 mg ramucirumaba. **Terapevtske indikacije** Zdravilo Cyramza je v kombinaciji s paklitakselom indicirano za zdravljenje odraslih bolnikov z napredovalim rakom želodca ali adenokarcinomom gastro-efozagealnega prehoda z napredovalo boleznijo po predhodni kemoterapiji, ki je vključevala platino in fluoropirimidin. Monoterapija z zdravilom Cyramza je indicirana za zdravljenje odraslih bolnikov z napredovalim rakom želodca ali adenokarcinomom gastro-efozagealnega prehoda z napredovalo boleznijo po predhodni kemoterapiji s platino ali fluoropirimidinom, za katere zdravljenje v kombinaciji s paklitakselom ni primerno. Zdravilo Cyramza je v kombinaciji s shemo FOLFIRI indicirano za zdravljenje odraslih bolnikov z metastatskim kolorektalnim rakom (mCRC), z napredovanjem bolezni ob ali po predhodnem zdravljenju z bevacizumabom, oksaliplatinom in fluoropirimidinom. Zdravilo Cyramza je v kombinaciji z docetakselom indicirano za zdravljenje odraslih bolnikov z lokalno napredovalim ali metastatskim nedrobnoceličnim pljučnim rakom, z napredovanjem bolezni po kemoterapiji na osnovi platine. **Odmerjanje in način uporabe** Zdravljenje z ramucirumabom morajo uvesti in nadzirati zdravniki z izkušnjami v onkologiji. **Odmerjanje Rak želodca in adenokarcinom gastro-efozagealnega prehoda** Priporočeni odmerek ramucirumaba je 8 mg/kg 1. in 15. dan 28-dnevnega cikla, pred infuzijo paklitaksela. Priporočeni odmerek paklitaksela je 80 mg/m² in se daje z intravenskim infundiranjem, ki traja približno 60 minut, 1., 8. in 15. dan 28-dnevnega cikla. Pred vsakim infundiranjem paklitaksela je treba pri bolnikih pregledati celotno krvno sliko in izvide kemičnih preiskav krvi, da se oceni delovanje jeter. Priporočeni odmerek ramucirumaba kot monoterapije je 8 mg/kg vsaka 2 tedna. **Kolorektalni rak** Priporočeni odmerek ramucirumaba je 8 mg/kg vsaka 2 tedna, dan z intravensko infuzijo pred dajanjem sheme FOLFIRI. Pred kemoterapijo je treba bolnikom odvzeti kri za popolno krvno sliko. **Nedrobnocelični pljučni rak (NSCLC)** Priporočeni odmerek ramucirumaba je 10 mg/kg na 1. dan 21-dnevnega cikla, pred infuzijo docetakselo. Priporočeni odmerek docetakselo je 75 mg/m², dan z intravensko infuzijo v približno 60 minutah na 1. dan 21-dnevnega cikla. **Premedikacija** Pred infundiranjem ramucirumaba je priporočljiva premedikacija z antagonistom histaminskih receptorjev H1. **Način uporabe** Po redčenju se zdravilo Cyramza daje kot intravenska infuzija v približno 60 minutah. Zdravila ne dajajte v obliki intravenskega bolusa ali hitre intravenske injekcije. Da boste dosegli zahtevano trajanje infundiranja približno 60 minut, največja hitrost infundiranja ne sme preseči 25 mg/minuto, saj morate sicer podaljšati trajanje infundiranja. Bolnika je med infundiranjem treba spremljati glede znakov reakcij, povezanih z infuzijo, zagotoviti pa je treba tudi razpoložljivost ustrezne opreme za oživiljanje. **Kontraindikacije** Pri bolnikih z NSCLC je ramucirumab kontraindiciran, kjer gre za kavitacijo tumorja ali prepletanost tumorja z glavnimi žilami. **Posebna opozorila in previdnostni ukrepi** Trajno prekinite zdravljenje z ramucirumabom pri bolnikih, pri katerih se pojavijo resni arterijski tromboembolični dogodki, gastrointestinalne perforacije, krvavitve stopnje 3 ali 4, če zdravstveno pomembne hipertenzije ni mogoče nadzirati z antihipertenzivnim zdravljenjem ali če se pojavi fistula, raven beljakovin v urinu > 3 g/24 ur ali v primeru nefrotskega sindroma. Pri bolnikih z neuravnavano hipertenzijo zdravljenja z ramucirumabom ne smete uvesti, dokler oziroma v kolikor obstoječa hipertenzija ni uravnavana. Pri bolnikih s ploščatocelično histologijo obstaja večje tveganje za razvoj resnih pljučnih krvavitve. Če se pri bolniku med zdravljenjem razvijejo zapleti v zvezi s celjenjem rane, prekinite zdravljenje z ramucirumabom, dokler rana ni povsem zaceljena. V primeru pojava stomatitisa je treba takoj uvesti simptomatsko zdravljenje. Pri bolnikih, ki so prejeli ramucirumab in docetaksel za zdravljenje napredovalnega NSCLC z napredovanjem bolezni po kemoterapiji na osnovi platine, so opazili trend manjše učinkovitosti z naraščajočo starostjo. **Medsebojno delovanje z drugimi zdravili in druge oblike interakcij** Med ramucirumabom in paklitakselom niso opazili medsebojnega delovanja. **Plodnost, nosečnost in dojenje** Ženskam v rodni dobi je treba svetovati, naj se izognejo zanositvi med zdravljenjem z zdravilom Cyramza in jih je treba seznaniti z možnim tveganjem za nosečnost in plod. Ni znano, ali se ramucirumab izloča v materino mleko. **Neželeni učinki Zelo pogosti (≥ 1/10)** nevropenija, levkopenija, trombocitopenija, hipoalbuminemija, hipertenzija, epistaksa, gastrointestinalne krvavitve, stomatitis, driska, proteinurija, utrujenost/astenija, periferni edem, bolečina v trebuhu. **Pogosti (≥ 1/100 do < 1/10)** hipokaliemija, hiponatriemija, glavobol. **Rok uporabnosti 3 leta** **Posebna navodila za shranjevanje** Shranjujte v hladilniku (2 °C–8 °C). Ne zamrzujte. Vialo shranjujte v zunanji ovojnini, da zagotovite zaščito pred svetlobo. **Pakiranje** 2 viali z 10 ml **IMETNIK DOVOLJENJA ZA PROMET Z ZDRAVILOM** Eli Lilly Nederland B.V., Papendorpseweg 83, 3528 BJ Utrecht, Nizozemska **DATUM ZADNJE REVIZIJE BESEDILA** 25.01.2016 Režim izdaje: Predpisovanje in izdaja zdravila je le na recept, zdravilo pa se uporablja samo v bolnišnicah.

Pomembno obvestilo:

Pričujoče gradivo je namenjeno **samo za strokovno javnost**. Zdravilo Cyramza se izdaja le na recept, zdravilo pa se uporablja samo v bolnišnicah. Pred predpisovanjem zdravila Cyramza vs vladno prosimo, da preberete celotni Povzetek glavnih značilnosti zdravila Cyramza. Podrobnejše informacije o zdravilu Cyramza in o zadnji reviziji besedila Povzetka glavnih značilnosti zdravila so na voljo na sedežu podjetja Eli Lilly (naslov podjetja in kontaktni podatki spodaj) in na spletni strani European Medicines Agency (EMA): www.ema.europa.eu. in na spletni strani European Commission <http://ec.europa.eu/health/documents/community-register/html/atregister.htm>.

Eli Lilly farmacevtska družba, d.o.o., Dunajska cesta 167, 1000 Ljubljana, telefon: (01) 5800 010, faks: (01) 5691 705

Referenca: 1. <https://pharmaphorum.com/news/lilly-s-cyramza-approved-in-eu-for-stomach-cancer/?epoch=1505121044344>

PP-RB-SI-0002, 17.11.2017.

Lilly

Bi se težko poslovili od svojega zvestega avtomobila? Razumemo.

PRI ZDRAVLJENJU JE DRUGAČE. ČAS JE, DA GREMO NAPREJ Z ZDRAVILOM GAZYVARO.



* Izsledki kliničnih raziskav faze III so pokazali, da GAZYVARO[®] v kombinaciji s kemoterapijo pomembno podaljša preživetje brez napredovanja bolezn (PFS) v primerjavi z rituksimabom v kombinaciji s kemoterapijo.

G
GAZYVARO[®]
obinutuzumab

KLL*

GAZYVARO[®] je v kombinaciji s klorambucilom indiciran za zdravljenje odraslih bolnikov s predhodno nezdravljeno kronično limfocitno levkemijo (KLL), pri katerih zdravljenje s polnim odmerkom fludarabina zaradi pridruženih bolezn ni primerno.

Referenca:
Povzetek glavnih značilnosti zdravila GAZYVARO. Dostopano (9.03.2018) na http://www.ema.europa.eu/docs/sl_SI/document_library/EPAR_-_Product_Information/human/002799/WC500171594.pdf

Za to zdravilo se izvaja dodatno spremljanje varnosti. Tako bodo hitreje na voljo nove informacije o njegovi varnosti. Zdravstvene delavce naprošamo, da poročajo o katerem koli domnevnem neželenem učinku zdravila. Kako poročati o neželenih učinkih, si poglejte skrajšani povzetek glavnih značilnosti zdravila pod "Poročanje o domnevnih neželenih učinkih".

1L FL*

GAZYVARO[®] je v kombinaciji s kemoterapijo, čemur pri odzivnih bolnikih sledi vzdrževalno zdravljenje z zdravilom Gazyvaro, indiciran za zdravljenje bolnikov s predhodno nezdravljenim napredovalim folikularnim limfomom (FL).

R/R FL

GAZYVARO[®] je v kombinaciji z bendamustinom ter s poznejšo vzdrževalno uporabo zdravila Gazyvaro indiciran za zdravljenje bolnikov s folikularnim limfomom (FL), ki se na zdravljenje z rituksimabom ali shemo, ki je vključevala rituksimab, niso odzvali ali jim je bolezen med ali v 6 mesecih po takšnem zdravljenju napredovala.

Skrajšan povzetek glavnih značilnosti zdravila GAZYVARO[®] (obinutuzumab) 1000 mg koncentrat za raztopino za infundiranje

Ime zdravila: Gazyvaro 1000 mg koncentrat za raztopino za infundiranje
Kakovostna in klinična sestava: Etna viala s 40 ml koncentrata vsebuje 1000 mg obinutuzumaba; to ustreza koncentraciji 25 mg/ml pred razreditvijo. Obinutuzumab je humanizirano anti-CD20 monoklonsko protiteleso tipa IgG1, pridobljeno s humanizacijo parentalnega protitelesa B-Ly1 in proizvedeno v celični liniji jajčnika kitajskega hrčka s tehnologijo rekombinantne DNA. **Terapevtske indikacije:** **Kronična limfocitna levkemija:** Zdravilo Gazyvaro je v kombinaciji s klorambucilom indicirano za zdravljenje odraslih bolnikov s predhodno nezdravljeno kronično limfocitno levkemijo (KLL), pri katerih zdravljenje s polnim odmerkom fludarabina zaradi pridruženih bolezn ni primerno. **Folikularni limfom:** Zdravilo Gazyvaro je v kombinaciji s kemoterapijo, čemur pri odzivnih bolnikih sledi vzdrževalno zdravljenje z zdravilom Gazyvaro, indicirano za zdravljenje bolnikov s predhodno nezdravljenim napredovalim folikularnim limfomom. Zdravilo Gazyvaro je v kombinaciji z bendamustinom ter s poznejšo vzdrževalno uporabo zdravila Gazyvaro indicirano za zdravljenje bolnikov s folikularnim limfomom (FL), ki se na zdravljenje z rituksimabom ali shemo, ki je vključevala rituksimab, niso odzvali ali jim je bolezen med ali v 6 mesecih po takšnem zdravljenju napredovala. **Odmerjanje in način uporabe:** Dajanje zdravila Gazyvaro mora potekati pod natančnim nadzorom izkušenega zdravnika in v okolju, kjer je takoj na voljo vse potrebno za obvladnje. **Odmerjanje:** **Profilaksa in prepreževanje sindroma razpada tumorja:** Bolniki z velikim tumorskim bremenom in/ali velikim številom limfocitov v krvnem obtoku in/ali ledvično okvaro imajo večje tveganje za sindrom razpada tumorja in morajo prejeti profilakso. To naj sestavljata ustrezna hidracija in dajanje urikostatikov ali primerno alternativno zdravljenje, kot je uratna oksidaza. **Profilaksa reakcij, povezanih z infuzijo, in premedikacija zanje:** Premedikacija s kortikosteroidi je v prvem ciklu za bolnike s FL priporočljiva, za bolnike s KLL pa obvezna. Med intravenskim infundiranjem zdravila Gazyvaro se lahko kot simptom reakcij, povezanih z infuzijo, pojavi hipotenzija. Zato je treba uporabo antihipertenzivnih zdravil zadržati v obdobju 12 ur pred infundiranjem zdravila Gazyvaro, med celotnim infundiranjem in še prvo uro po koncu dajanja zdravila. **Odmerki:** **KLL: 1. cikel:** Priporočeni odmerki zdravila Gazyvaro v kombinaciji s klorambucilom je 1000 mg, ki ga dajemo na 1. in 2. dan (ali v nadaljevanju 1. dne) ter 8. in 15. dan prvega 28-dnevnega cikla zdravljenja. Za infundiranje 1. in 2. dan je treba pripraviti dve infuzijski vrečki (1000 mg za 1. dan in 900 mg za 2. dan). Če med dajanjem prve vrečke ni bilo treba prilagoditi hitrosti infundiranja ali infundiranja prekiniti, je mogoče drugo vrečko uporabiti isti dan. Če je med dajanjem prvih 100 mg treba spremeniti hitrost infundiranja ali infundiranje prekiniti, je treba drugo vrečko dati naslednji dan. **2. do 6. cikel:** Priporočeni odmerki zdravila Gazyvaro v kombinaciji s klorambucilom je 1000 mg, uporabljen 1. dan vsakega cikla. **Trajanje zdravljenja:** Šest ciklov zdravljenja, od katerih vsak traja 28 dni. **Folikularni limfom:** Bolniki s predhodno nezdravljenim FL. **Indukcija:** Zdravilo Gazyvaro aplicirano v kombinaciji s kemoterapijo šest 28-dnevnih ciklov v kombinaciji z bendamustinom ali šest 21-dnevnih ciklov v kombinaciji s CHOP, ki jim sledita 2 dodatna cikla zdravila Gazyvaro v monoterapiji, ali osem 21-dnevnih ciklov v kombinaciji s CVP. **Vzdrževanje:** Bolniki, ki dosežejo popolni ali delni odgovor na indukcijsko zdravljenje z zdravilom Gazyvaro v kombinaciji s kemoterapijo, nadaljujejo z monoterapijo z zdravilom Gazyvaro 1000 mg kot vzdrževalnim zdravljenjem enkrat na 2 meseca v obdobju 2 let ali do napredovanja bolezni. Bolniki s FL, ki se na zdravljenje z rituksimabom ali shemo, ki je vključevala rituksimab, niso odzvali ali jim je bolezen med ali v 6 mesecih po takšnem zdravljenju napredovala. **Indukcija:** Zdravilo Gazyvaro se mora aplicirati v šestih 28-dnevnih ciklih v kombinaciji z bendamustinom. **Vzdrževanje:** Bolniki, ki dosežejo popolni ali delni odgovor na indukcijsko zdravljenje z zdravilom Gazyvaro v kombinaciji z bendamustinom ali imajo stabilno bolezen, nadaljujejo z monoterapijo z zdravilom Gazyvaro 1000 mg kot vzdrževalnim zdravljenjem enkrat na 2 meseca v obdobju 2 let ali do napredovanja bolezni. **Trajanje zdravljenja:** Približno šestmesečno indukcijsko zdravljenje, ki mu sledi vzdrževalno zdravljenje enkrat na 2 meseca v obdobju 2 let ali do napredovanja bolezni. **Način uporabe:** za intravensko uporabo. Po razreditvi ga je treba dati kot intravensko infuzijo po posebni liniji. Infuzija zdravila Gazyvaro se ne sme dati v obliki hitre intravenske infuzije ali kot bolus. **Kontraindikacije:** Preobčutljivost na učinkovino ali katero koli pomembno sestavo. **Posebna opozorila in previdnostni ukrepi:** Za težabnejše sledilnosti bioloških zdravil je treba zaščiteno ime in številko serije uporabljene zdravila jasno zabeležiti v bolnikovi dokumentaciji. **Reakcije, povezane z infuzijo:** Najpogostejše opaženi neželeni učinki pri bolnikih, ki so prejeli zdravilo Gazyvaro, so bile reakcije, povezane z infuzijo, ki so se pretežno pojavile med infundiranjem prvih 1000 mg. Reakcije, povezane z infuzijo, so lahko povezane s sindromom sprostitve citokinov. Za zmanjšanje reakcij, povezanih z infuzijo, je treba uporabiti ukrepe za ublažitve. Incidenca in trajnostni simptomi reakcij, povezanih z infuzijo, se je bistveno zmanjšala po infundiranju prvih 1000 mg in večina bolnikov med nadaljnjo uporabo zdravila Gazyvaro reakcij, povezanih z infuzijo, ni imela. Pri večini bolnikov ne glede na indikacijo so bile reakcije, povezane z infuzijo, blage do zmerno in jih je bilo mogoče obvladati z uporabo snovi ali časno prekinjivo prve infundiranja. Vendar pa so poročali tudi o hudih in življenju ogrožajočih reakcijah, povezanih z infuzijo, ki so zahtevale simptomatsko zdravljenje. Reakcije, povezane z infuzijo, so lahko klinično nerazločljive od alergijskih reakcij. Bolnike z ledvično okvaro imajo večje tveganje za nevtropenijo. **Trombocitopenija:** Med zdravljenjem z zdravilom Gazyvaro so poročali o hudih in življenju ogrožajočih nevtropenijah. Pri hudi ali življenju ogrožajoči nevtropeniji je treba razmisliti o preložitvi odmerka na kasnejši čas. Pojavijo se lahko zapoznela nevtropenija ali dolgotrajna nevtropenija. Bolniki z ledvično okvaro imajo večje tveganje za nevtropenijo. **Trombocitopenija:** Med zdravljenjem z zdravilom Gazyvaro so poročali o hudih in življenju ogrožajočih trombocitopenijah, vključno z akutno trombocitopenijo. Bolniki z ledvično okvaro imajo večje tveganje za trombocitopenijo. Pri bolnikih, zdravljenih z zdravilom Gazyvaro, so bile v 1. ciklu opisane tudi krvavitve s smrtnim izidom. Javne poročevane med trombocitopenijo in krvavitvami niso ugotovili. Bolnike je treba natančno spremljati glede trombocitopenije, zlasti v prvem ciklu; izvajati je treba redne laboratorijske preiskave krvne slike, dokler dopokde ne mine, pri hudi ali življenju ogrožajoči trombocitopeniji pa je treba razmisliti o preložitvi odmerka na kasnejši čas. Upoštevati je treba tudi sočasno uporabo katerih koli zdravil, ki lahko poslabšajo s trombocitopenijo povezane dogodke, na primer zaviralce trombocitov in antikoagulantov; to je treba še zlasti upoštevati v prvem ciklu. **Poslabšanje obstoječih srčnih bolezn:** Pri bolnikih z obstoječo srčno boleznijo so se med zdravljenjem z zdravilom Gazyvaro pojavile motnje ritma srca, angina pektoris, akutni koronarni sindrom, akutni miokardni infarkt in srčno popuščanje. Ti dogodki se lahko pojavijo kot deli reakcij, povezanih z infuzijo, in so lahko smrtni. Zato je treba bolnike z anamnezo srčne bolezni natančno nadzirati. Poleg tega je treba pri teh bolnikih hidracijo izvajati previdno, da bi preprečili možno preobremenitev s tekočino. **Okužbe:** Zdravilo Gazyvaro se ne sme uporabiti pri bolnikih z aktivno okužbo, pri bolnikih z anamnezo ponavljajočih se ali kroničnih okužb pa je pri razmisleku o uporabi zdravila Gazyvaro potrebna previdnost. Med zdravljenjem z zdravilom Gazyvaro in po njem se lahko pojavijo resne bakterijske, glivične in nove ali reaktivirane virusne okužbe. Poročali so o okužbah s smrtnim izidom. Bolniki, ki imajo hkrati CRP > 6 in očitek kreatinina < 70 ml/min, imajo večje tveganje za okužbe, vključno s hudimi okužbami. V študijah folikularnega limfoma so v vseh fazah, vključno z obdobjem spremljanja, opazili visoko incidenco okužb; najvišjo incidenco so zaznali pri bolnikih v vzdrževalni fazi. Med obdobjem spremljanja so dokumentirali več okužb. 3. do 5. stopnje pri bolnikih, ki so v fazi indukcije prejeli zdravilo Gazyvaro v kombinaciji z bendamustinom. **Reaktivacija hepatitisa B:** Bolnikom, zdravljenim s protitelesi proti CD20 (vključno z zdravilom Gazyvaro), se lahko pojavi reaktivacija virusa hepatitisa B. V nekaterih primerih s posledičnim fulminantnim hepatitisom, jetrno odpovedjo in smrtjo. Pred začetkom zdravljenja z zdravilom Gazyvaro je treba pri vseh bolnikih opravi presajeno testiranje za HBV. Bolnikov z aktivnim hepatitisom B se ne sme zdraviti z zdravilom Gazyvaro. Bolniki s pozitivnimi serološkimi izvidi za hepatitis B se morajo pred začetkom zdravljenja posvetovati s specialista za jetrne bolezni; treba jih je nadzorovati in voditi v skladu z lokalnimi zdravilnimi standardi, da bi preprečili reaktivacijo hepatitisa. **Progressivna multifokalna levkoencefalopatija (PMLE):** Pri bolnikih, zdravljenih z zdravilom Gazyvaro, je bila opisana PMLE. Na diagnozo PMLE je treba pomisliti pri vsakem bolniku s novonastalimi nevrološkimi spremembami ali spremembi že obstoječih nevroloških stanj. Simptomi PMLE so nespecifični in se lahko razlikujejo glede na prizadetost možganov. **Ovrednotenje PMLE:** vključuje posvet z nevrologom, magnetnoresonančno slikanje možganov in lumbalno punkcijo. Med preskovanjem suma na PMLE je treba zdravljenje z zdravilom Gazyvaro prekiniti, če je PMLE potrjena, pa je treba trajno prekiniti. V postev pride tudi prenehanje ali zmanjšanje morebitne sočasne kemoterapije ali imunosupresivnega zdravljenja. **Imunizacija:** Varnost imunizacije z živimi ali oslabljenimi virusnimi cepivi po zdravljenju z zdravilom Gazyvaro ni raziskana in cepljenje z živimi virusnimi cepivi med zdravljenjem in do okrevanja celic B ni priporočljivo. **Medsebojno delovanje z drugimi zdravili in druge oblike interakcij:** Farmakokinetično medsebojno delovanje: Obinutuzumab ni substrat, zaviralec ali induktor CYP450, encimov UGT ali prenašalec, kakršen je P-glikoprotein. Zato pri pričakovani farmakokinetični medsebojni delovanju z zdravili, ki se presnavljajo s temi encimskimi sistemi. Sočasno dajanje zdravila Gazyvaro in imelo vpliva na farmakokinetiko bendamustina, FC, klorambucila ali posameznih učinkovin v CHOP. Dodatno ni bilo vidnih učinkov bendamustina, FC, klorambucila ali CHOP na farmakokinetiko zdravila Gazyvaro. **Farmakodinamično medsebojno delovanje:** Zaradi imunosupresivnega učinka obinutuzumaba cepjenje z živimi virusnimi cepivi ni priporočljivo med zdravljenjem in do okrevanja celic B. Kombinacija obinutuzumaba s klorambucilom, bendamustinom, CHOP ali CVP lahko poveča tveganje za nevtropenijo. **Neželeni učinki:** Povzetek neželenih učinkov iz kliničnih študij, ki so se pojavili z večjo incidenco (razlika ≥ 2 %), v primerjavi s skupino, ki je prejela ustrezno primerjalno zdravilo v svoji eni od ključnih študij. Zelo pogosto: okužba zgornjih dihal, sinusitis, okužba sečil, pljučnica, herpes zoster, nevtropenija, trombocitopenija, anemija, levkopenija, glavobol, nespečnost, kašelj, diareja, zaprtost, alopecija, srbecica, artralgija, bolečina v hrbtu, zvišana telesna temperatura, astenija in reakcije, povezane z infuzijo. Pogosto: herpes usne volnine, nitis, faringitis, okužba pljuč, gripa, nazofarngitis, plekzotocelčni rakom kože, bolečina v bezgavki, sindrom razpada tumorja, hiperurikemija, hipokalemija, depresija, tesnoba, okusna hipermija, atrijska fibrilacija, srčno popuščanje, hipertenzija, nazalna kongestija, rinoreja, orofaringealna bolečina, dispneja, kolitis, hemoroidi, nočno potenje, ekcem, mišično-skeletna bolečina v prsnem košu, bolečina v okončinah, bolečina v kosteh, dihidrogena, bolečina v prsnem košu, zmanjšanje števila belih krvnih celic, zmanjšanje števila nevtrofilcev in povečanje telesne mase. **Poročanje o domnevnih neželenih učinkih:** Poročanje o domnevnih neželenih učinkih zdravila po izdaji dovoljenja za promet je pomembno. Omogoča namreč stalno spremljanje razmerja med koristmi in tveganji zdravila. Od zdravstvenih delavcev se zahteva, da poročajo o katerem koli domnevnem neželenem učinku zdravila na: Javna agencija Republike Slovenije za zdravila in medicinske pripomočke. Sektor za farmakovigilanco, Nacionalni center za farmakovigilanco, Slovenčeva ulica 22, SI-1000 Ljubljana, Tel: +386 (0)8 2000 500, Faks: +386 (0)8 2000 510, e-pošta: h-farmakovigilanca@zjzpz.si, wjzjz.pz.si. Za zagotavljanje sledljivosti zdravila je pomembno, da pri izpolnjevanju obrazca o domnevnih neželenih učinkih zdravila navedete številko serije biološkega zdravila. **Režim izdaje zdravila:** H. **Imetnik dovoljenja za promet:** Roche Registration GmbH, Emil-Barell-Strasse 1, 79639 Grenzach-Wyhlen, Nemčija. **Verzija:** 1.0/18. **Informacija pripravljena:** april 2018

Samo za strokovno javnost

DODATNE INFORMACIJE SO NA VOLJO PRI: Roche farmacevtska družba d.o.o., Vodovodna cesta 109, 1000 Ljubljana



PM-0013-2108-HMC

Zdravilo za predhodno že zdravljene bolnike z mKRR

Več časa za trenutke, ki štejejo


trifluridin/tipiracil

Spremeni zgodbo predhodno že zdravljenih bolnikov z mKRR

LONSURF® (trifluridin/tipiracil) je indiciran za zdravljenje odraslih bolnikov z metastatskim kolorektalnim rakom (mKRR), ki so bili predhodno že zdravljeni ali niso primerni za zdravljenja, ki so na voljo. Ta vključujejo kemoterapijo na osnovi fluoropirimidina, oksaliplatina in irinotekana, zdravljenje z zaviralci žilnega endotelijskega rastnega dejavnika (VEGF) in zaviralci receptorjev za epidermalni rastni dejavnik (EGFR).

Družba Servier ima licenco družbe Taiho za zdravilo Lonsurf®. Pri globalnem razvoju zdravila sodelujeta obe družbi in ga tržita na svojih določenih področjih.

 TAIHO PHARMACEUTICAL CO., LTD.

 SERVIER

Skrajsan povzetek glavnih značilnosti zdravila: Lonsurf 15 mg/6,14 mg filmsko obložene tablete in Lonsurf 20 mg/8,19 mg filmsko obložene tablete

▼ Za to zdravilo se izvaja dodatno spremljanje varnosti. **SESTAVA***: Lonsurf 15 mg/6,14 mg: Ena filmsko obložena tableta vsebuje 15 mg trifluridina in 6,14 mg tipiracila (v obliki klorida). Lonsurf 20 mg/8,19 mg: Ena filmsko obložena tableta vsebuje 20 mg trifluridina in 8,19 mg tipiracila (v obliki klorida). **TERAPEVTSKE INDIKACIJE***: Zdravilo Lonsurf je indicirano za zdravljenje odraslih bolnikov z metastatskim kolorektalnim rakom, ki so bili predhodno že zdravljeni ali niso primerni za zdravljenja, ki so na voljo. Ta vključujejo kemoterapijo na osnovi fluoropirimidina, oksaliplatina in irinotekana, zdravljenje z zaviralci žilnega endotelijskega rastnega dejavnika (VEGF - Vascular Endothelial Growth Factor) in zaviralci receptorjev za epidermalni rastni dejavnik (EGFR - Epidermal Growth Factor Receptor). **ODMERJANJE IN NAČIN UPORABE***: Priporočeni začetni odmerek zdravila Lonsurf pri odraslih je 35 mg/m²/odmerek peroralno dvakrat dnevno na 1. do 5. dan in 8. do 12. dan vsakega 28-dnevnega cikla zdravljenja, najpozneje 1 uro po zaključku jutranjega in večernega obroka. Odmerjanje, izračunano glede na telesno površino, ne sme preseči 80 mg/odmerek. Možne prilagoditve odmerka glede na varnost in prenašanje zdravila: dovoljena so največ 3 zmanjšanja odmerka na najmanjši odmerek 20 mg/m² dvakrat dnevno. Potem ko je bil odmerek zmanjšan, povečanje ni dovoljeno. **PROSTORNA VARNOST***: Med zdravljenjem se lahko pojavijo utrujenost, omotica ali splošno slabo počutje. **NEZELI ENČINI***: Zelo pogosti: nevtropenija, levkopenija, anemija, trombocitopenija, zmanjšan apetit, diareja, navzea, bruhanje, utrujenost. **Pogosti**: okužba spodnjih dihal, okužba zgornjih dihal, febrilna nevtropenija, limfopenija, monocitoza, hipalbuminemija, nespečnost, disgevgija, periferna nevropatija, omotica, glavobol, vročinski oblivi, dispneja, kašelj, bolečina v trebuhu, zaprtje, stomatitis, boleznj ustne votline, hiperbilirubinemija, sindrom palmarne plantarne eritrodesezestije, izpuščaj, alopecija, pruritus, suha koža, proteinurija, pireksija, edem, vnetje sluznice, bakterijska okužba, okužba, bolečina zaradi raka, pancitopenija, granulocitopenija, monocitopenija, eritropenija, levkocitoza, dehidracija, hiperglikemija, hiperkalemija, hipotenzija, hiponatremija, hipokalcemija, protin, anksioznost, nevrološki sindrom, disestezija, hiperestezija, hipoestezija, sinkopa, parestezija, pekoč občutek, letargija, zmanjšana ostrina vida, zamajen vid, diplopija, katarakta, konjunktivitis, suho oko, vrtoglavica, neugodje v ušesu, angina pectoris, aritmija, palpitanje, embolija, hipertenzija, hipotenzija, pljučna embolija, plevralni izliv, izcedek iz nosu, distonija, orofaringealna bolečina, epistaksa, hemoragični enterokolitis, krvavitev v prebavilih, akutni pankreatitis, ascites, ileus, subileus, kolitis, gastritis, refleksni gastritis, ezofagitis, moteno praznjenje želodca, abdominalna distenzija, analno vnetje, razjede v ustih, dispneja, gastrozofagealna refleksna bolezen, proktalgija, bukalni polip, krvavitev dlesni, glossitis, parodontalna bolezen, bolezen zob, siljenje na bruhanje, flatulenca, slab zadah, hepatotoksičnost, razširitev žolčnih vodov, luščenje kože, urtikarija, preobčutljivostne reakcije na svetlobo, eritem, akne, hiperhidroza, žulj, boleznj nohtov, otekanje sklepov, artralgijska bolečina v kosteh, mialgija, mišično-skeletna bolečina, mišična oslabelost, mišični krči, bolečina v okončinah, občutek teže, ledvična odpoved, neinfektivni cistitis, motnje mikcije, hematurija, levkociturija, motnje menstruacije, poslabšanje splošnega zdravstvenega stanja, bolečina, občutek spremembe telesne temperature, kseroza, zvišanje kreatinina v krvi, podaljšanje intervala QT na elektrokardiogramu, povečanje mednarodnega umerjenega razmerja (INR), podaljšanje aktiviranega parcialnega trombotičnega časa (aPTC), zvišanje sečnine v krvi, zvišanje laktatne dehidrogenaze v krvi, znižanje celokupnih proteinov, zvišanje C-reaktivnega proteina, zmanjšan hematokrit. **Post-marketingne izkušnje**: pri bolnikih, zdravljenih z zdravilom Lonsurf na Japonskem, so poročali o primerih intersticijske bolezni pljuč. **PREVELIKO ODMERJANJE***: Neželene učinki, o katerih so poročali v povezavi s prevelikim odmerjanjem, so bili v skladu z uveljavljenim varnostnim profilom. Glavni pričakovani zaplet prevelikega odmerjanja je supresija kostnega mozga. **FARMAKODINAMIČNE LASTNOSTI***: Farmakoterapevtska skupina: zdravila z delovanjem na novotvorbe, antimitotični, oznaka ATC: L01BC59. Zdravilo Lonsurf sestavljata antineoplastični timidinski nukleozidni analog, trifluridin, in zaviralec timidin-fosforilaze (TPaze), tipiracilijev klorid. Po privzetemu v rakave celice timidin-kinaza fosforilira trifluridin. Ta se v celicah nato presnovi v vključen deoksiribonukleinske kisline (DNA), ki se vgradi neposredno v DNA ter tako preprečuje celično proliferacijo. TPaza hitro razgradi trifluridin in njegova presnova po peroralni uporabi je hitra zaradi učinka prvega prehoda, zato je v zdravilo vključen zaviralec TPaze, tipiracilijev klorid. **PAKIRANJE***: 20 filmsko obloženih tablet. **NAČIN PREDPISOVANJA IN IZDAJE ZDRAVILA**: Rg/Spec. **Imetnik dovoljenja za promet**: Les Laboratoires Servier, 50, rue Carnot, 92284 Suresnes cedex, Francija. **Številka dovoljenja za promet z zdravilom**: EU/1/16/1096/001 (Lonsurf 15 mg/6,14 mg), EU/1/16/1096/004 (Lonsurf 20 mg/8,19 mg). **Datum zadnje revizije besedila**: avgust 2017. * Pred predpisovanjem preberite celoten povzetek glavnih značilnosti zdravila. Celoten povzetek glavnih značilnosti zdravila in podrobnejše informacije so na voljo pri: Servier Pharma d.o.o., Podmilščakova ulica 24, 1000 Ljubljana, tel: 01 563 48 11, www.servier.si.

Instructions for authors

The editorial policy

Radiology and Oncology is a multidisciplinary journal devoted to the publishing original and high quality scientific papers and review articles, pertinent to diagnostic and interventional radiology, computerized tomography, magnetic resonance, ultrasound, nuclear medicine, radiotherapy, clinical and experimental oncology, radiobiology, radiophysics and radiation protection. Therefore, the scope of the journal is to cover beside radiology the diagnostic and therapeutic aspects in oncology, which distinguishes it from other journals in the field.

The Editorial Board requires that the paper has not been published or submitted for publication elsewhere; the authors are responsible for all statements in their papers. Accepted articles become the property of the journal and, therefore cannot be published elsewhere without the written permission of the editors.

Submission of the manuscript

The manuscript written in English should be submitted to the journal via online submission system Editorial Manager available for this journal at: www.radioloncol.com.

In case of problems, please contact Sašo Trupej at saso.trupej@computing.si or the Editor of this journal at gsera@onko-i.si

All articles are subjected to the editorial review and when the articles are appropriated they are reviewed by independent referees. In the cover letter, which must accompany the article, the authors are requested to suggest 3-4 researchers, competent to review their manuscript. However, please note that this will be treated only as a suggestion; the final selection of reviewers is exclusively the Editor's decision. The authors' names are revealed to the referees, but not vice versa.

Manuscripts which do not comply with the technical requirements stated herein will be returned to the authors for the correction before peer-review. The editorial board reserves the right to ask authors to make appropriate changes of the contents as well as grammatical and stylistic corrections when necessary. Page charges will be charged for manuscripts exceeding the recommended length, as well as additional editorial work and requests for printed reprints.

Articles are published printed and on-line as the open access (www.degruyter.com/view/j/raon).

All articles are subject to 700 EUR + VAT publication fee. Exceptionally, waiver of payment may be negotiated with editorial office, upon lack of funds.

Manuscripts submitted under multiple authorship are reviewed on the assumption that all listed authors concur in the submission and are responsible for its content; they must have agreed to its publication and have given the corresponding author the authority to act on their behalf in all matters pertaining to publication. The corresponding author is responsible for informing the coauthors of the manuscript status throughout the submission, review, and production process.

Preparation of manuscripts

Radiology and Oncology will consider manuscripts prepared according to the Uniform Requirements for Manuscripts Submitted to Biomedical Journals by International Committee of Medical Journal Editors (www.icmje.org). The manuscript should be written in grammatically and stylistically correct language. Abbreviations should be avoided. If their use is necessary, they should be explained at the first time mentioned. The technical data should conform to the SI system. The manuscript, excluding the references, tables, figures and figure legends, must not exceed 5000 words, and the number of figures and tables is limited to 8. Organize the text so that it includes: Introduction, Materials and methods, Results and Discussion. Exceptionally, the results and discussion can be combined in a single section. Start each section on a new page, and number each page consecutively with Arabic numerals.

The Title page should include a concise and informative title, followed by the full name(s) of the author(s); the institutional affiliation of each author; the name and address of the corresponding author (including telephone, fax and E-mail), and an abbreviated title (not exceeding 60 characters). This should be followed by the abstract page, summarizing in less than 250 words the reasons for the study, experimental approach, the major findings (with specific data if possible), and the principal conclusions, and providing 3-6 key words for indexing purposes. Structured abstracts are required. Slovene authors are requested to provide title and the abstract in Slovene language in a separate file. The text of the research article should then proceed as follows:

Introduction should summarize the rationale for the study or observation, citing only the essential references and stating the aim of the study.

Materials and methods should provide enough information to enable experiments to be repeated. New methods should be described in details.

Results should be presented clearly and concisely without repeating the data in the figures and tables. Emphasis should be on clear and precise presentation of results and their significance in relation to the aim of the investigation.

Discussion should explain the results rather than simply repeating them and interpret their significance and draw conclusions. It should discuss the results of the study in the light of previously published work.

Charts, Illustrations, Images and Tables

Charts, Illustrations, Images and Tables must be numbered and referred to in the text, with the appropriate location indicated. Charts, Illustrations and Images, provided electronically, should be of appropriate quality for good reproduction. Illustrations and charts must be vector image, created in CMYK color space, preferred font "Century Gothic", and saved as .AI, .EPS or .PDF format. Color charts, illustrations and Images are encouraged, and are published without additional charge. Image size must be 2.000 pixels on the longer side and saved as .JPG (maximum quality) format. In Images, mask the identities of the patients. Tables should be typed double-spaced, with a descriptive title and, if appropriate, units of numerical measurements included in the column heading. The files with the figures and tables can be uploaded as separate files.

References

References must be numbered in the order in which they appear in the text and their corresponding numbers quoted in the text. Authors are responsible for the accuracy of their references. References to the Abstracts and Letters to the Editor must be identified as such. Citation of papers in preparation or submitted for publication, unpublished observations, and personal communications should not be included in the reference list. If essential, such material may be incorporated in the appropriate place in the text. References follow the style of Index Medicus, DOI number (if exists) should be included.

All authors should be listed when their number does not exceed six; when there are seven or more authors, the first six listed are followed by "et al.". The following are some examples of references from articles, books and book chapters:

Dent RAG, Cole P. In vitro maturation of monocytes in squamous carcinoma of the lung. *Br J Cancer* 1981; **43**: 486-95. doi: 10.1038/bjc.1981.71

Chapman S, Nakielny R. *A guide to radiological procedures*. London: Bailliere Tindall; 1986.

Evans R, Alexander P. Mechanisms of extracellular killing of nucleated mammalian cells by macrophages. In: Nelson DS, editor. *Immunobiology of macrophage*. New York: Academic Press; 1976. p. 45-74.

Authorization for the use of human subjects or experimental animals

When reporting experiments on human subjects, authors should state whether the procedures followed the Helsinki Declaration. Patients have the right to privacy; therefore the identifying information (patient's names, hospital unit numbers) should not be published unless it is essential. In such cases the patient's informed consent for publication is needed, and should appear as an appropriate statement in the article. Institutional approval and Clinical Trial registration number is required. Retrospective clinical studies must be approved by the accredited Institutional Review Board/Committee for Medical Ethics or other equivalent body. These statements should appear in the Materials and methods section.

The research using animal subjects should be conducted according to the EU Directive 2010/63/EU and following the Guidelines for the welfare and use of animals in cancer research (*Br J Cancer* 2010; 102: 1555 – 77). Authors must state the committee approving the experiments, and must confirm that all experiments were performed in accordance with relevant regulations.

These statements should appear in the Materials and methods section (or for contributions without this section, within the main text or in the captions of relevant figures or tables).

Transfer of copyright agreement

For the publication of accepted articles, authors are required to send the License to Publish to the publisher on the address of the editorial office. A properly completed License to Publish, signed by the Corresponding Author on behalf of all the authors, must be provided for each submitted manuscript.

The non-commercial use of each article will be governed by the Creative Commons Attribution-NonCommercial-NoDerivs license.

Conflict of interest

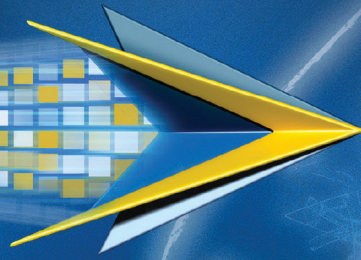
When the manuscript is submitted for publication, the authors are expected to disclose any relationship that might pose real, apparent or potential conflict of interest with respect to the results reported in that manuscript. Potential conflicts of interest include not only financial relationships but also other, non-financial relationships. In the Acknowledgement section the source of funding support should be mentioned. The Editors will make effort to ensure that conflicts of interest will not compromise the evaluation process of the submitted manuscripts; potential editors and reviewers will exempt themselves from review process when such conflict of interest exists. The statement of disclosure must be in the Cover letter accompanying the manuscript or submitted on the form available on www.icmje.org/coi_disclosure.pdf

Page proofs

Page proofs will be sent by E-mail to the corresponding author. It is their responsibility to check the proofs carefully and return a list of essential corrections to the editorial office within three days of receipt. Only grammatical corrections are acceptable at that time.

Open access

Papers are published electronically as open access on www.degruyter.com/view/j/raon, also papers accepted for publication as E-ahead of print.



XALKORI® – I. linija zdravljenja napredovalega, ALK pozitivnega nedrobnoceličnega pljučnega raka¹

ALK = anaplasična limfomska kinaza

BISTVENI PODATKI IZ POVZETKA GLAVNIH ZNAČILNOSTI ZDRAVILA

XALKORI 200 mg, 250 mg trde kapsule

▼ Za to zdravilo se izvaja dodatno spremljanje varnosti. Tako bodo hitreje na voljo nove informacije o njegovi varnosti. Zdravstvene delavce naprošamo, da poročajo o kateremkoli domnevnem neželenem učinku zdravila. Glejte poglavje 4.8 povzetka glavnih značilnosti zdravila, kako poročati o neželenih učinkih.

Sestava in oblika zdravila: Ena kapsula vsebuje 200 mg ali 250 mg krizotiniba. **Indikacije:** Monoterapija za: - prvo linijo zdravljenja odraslih bolnikov z napredovalim nedrobnoceličnim pljučnim rakom (NSCLC – *Non-Small Cell Lung Cancer*), ki je ALK (anaplasična limfomska kinaza) pozitiven; - zdravljenje odraslih bolnikov s predhodno zdravljenim, napredovalim NSCLC, ki je ALK pozitiven; - zdravljenje odraslih bolnikov z napredovalim NSCLC, ki je ROS1 pozitiven. **Odmerjanje in način uporabe:** Zdravilje mora uvesti in nadzorovati zdravnik z izkušnjami z uporabo zdravil za zdravljenje rakavih bolezni. **Preverjanje prisotnosti ALK in ROS1:** Pri izbiri bolnikov za zdravljenje je treba pred zdravljenjem opraviti točno in validirano preverjanje prisotnosti ALK ali ROS1. **Odmerjanje:** Priporočeni odmerek je 250 mg dvakrat na dan (500 mg na dan), bolniki pa morajo zdravilo jemati brez prekinitev. Če bolnik pozabi vzeti odmerek, ga mora vzeti takoj, ko se spomni, razen če do naslednjega odmerka manjka manj kot 6 ur. V tem primeru bolnik pozabljenega odmerka ne sme vzeti. **Prilaganja odmerkov:** Glede na varnost uporabe zdravila pri posameznem bolniku in kako bolnik zdravljenje prenaša, utegne biti potrebna prekinitev in/ali zmanjšanje odmerka zdravila na 200 mg dvakrat na dan; če je potrebno še nadaljnje zmanjšanje, pa znaša odmerek 250 mg enkrat na dan. Za prilaganje odmerkov pri hematološki in nehematološki (povečanje vrednosti AST, ALT, bilirubina; ILD/pnevmonitis; podaljšanje intervala QTc, bradikardija, bolezi oči) toksicitosti glejte priložnici 1 in 2 v povzetku glavnih značilnosti zdravila. **Okvara jeter:** Pri zdravljenju pri bolnikih z okvaro jeter je potrebna previdnost. Pri blagi okvari jeter prilaganje začnega odmerka ni priporočeno, pri zmernih okvari jeter je priporočeni začetni odmerek 200 mg dvakrat na dan, pri hudi okvari jeter pa 250 mg enkrat na dan (za merila glede klasifikacije okvare jeter glejte poglavje 4.2 v povzetku glavnih značilnosti zdravila). **Okvara ledvic:** Pri blagi in zmerni okvari prilaganje začnega odmerka ni priporočeno. Pri hudi okvari ledvic (ki ne zahteva peritonealne dialize ali hemodialize) je začetni odmerek 250 mg peroralno enkrat na dan; po vsaj 4 tednih zdravljenja se lahko poveča na 200 mg dvakrat na dan. **Starjši bolniki (≥ 65 let):** Prilaganje začnega odmerka ni potrebno. **Pediatrična populacija:** Varlost in učinkovitost nista bili dokazani. **Način uporabe:** Kapsule je treba pogoltniti cele, z nekaj vode, s hrano ali brez nje. Ne sme se jih zdrobiti, raztopiti ali odpreti. Izogibati se je treba uživanju grenivk, grenivkinega soka ter uporabi šentjanževke.

Kontraindikacije: Preobčutljivost na krizotinib ali katerokoli pomožni snov. **Posebna opozorila in previdnostni ukrepi:** **Določanje statusa ALK in ROS1:** Pomembno je izbrati dobro validirano in robustno metodologijo, da se izogne močno lažno negativnim ali lažno pozitivnim rezultatom. **Hepatotoksičnost:** V kliničnih študijah so poročali o hepatotoksičnosti, ki jo je povzročilo zdravilo (vključno s primeri s smrtnim izidom). Delovanje jeter, vključno z ALT, AST in skupnim bilirubinom, je treba preveriti enkrat na teden v prvih 2 mesecih zdravljenja, nato pa enkrat na mesec in kot je klinično indicirano. Ponovite preverjanj morajo biti pogostejše pri povečanih vrednostih stopnje 2, 3 ali 4. **Intersticijska bolezen pljuč (ILD)/pnevmonitis:** Lahko se pojavi huda, življenjsko nevarna ali smrtna ILD/pnevmonitis. Bolnike s simptomi ILD/pnevmonitisa je treba spremljati, zdravljenje pa prekiniti ob sumu na ILD/pnevmonitis. **Podaljšanje intervala**

QT: Opažali so podaljšanje intervala QTc. Pri bolnikih z obstoječo bradikardijo, podaljšanjem intervala QTc v anamnezi ali predispozicijo zanj, pri bolnikih, ki jemljejo antiaritmike ali druga zdravila, ki podaljšujejo interval QT, ter pri bolnikih s pomembno obstoječo srčno boleznijo in/ali motnjami elektrolitov je treba krizotinib uporabljati previdno, potrebno je redno spremljanje EKG, elektrolitov in delovanja ledvic, preiskavi EKG in elektrolitov je treba opraviti čim bližje uporabi prvega odmerka, potem se priporoča redno spremljanje. Če se interval QTc podaljša za 60 ms ali več, je treba zdravljenje s krizotinibom začasno prekiniti in se posvetovati s kardiologom. **Bradikardija:** Lahko se pojavi simptomatska bradikardija (lahko se razvije več tednov po začetku zdravljenja); izogibati se je treba uporabi krizotiniba v kombinaciji z drugimi zdravili, ki povzročajo bradikardijo, pri simptomatski bradikardiji je treba prilagoditi odmerek. **Srčno popuščanje:** Poročali so o hudih, življenjsko nevarnih ali smrtnih neželenih učinkih, srčnega popuščanja. Bolnike je treba spremljati glede pojavov znakov in simptomov srčnega popuščanja in ob pojavu simptomov zmanjšati odmerjanje ali prekiniti zdravljenje. **Nevtropenija in levkopenija:** V kliničnih študijah so poročali o nevtropeniji in levkopeniji. V kliničnih študijah so opazili zvišanje ravni kreatinina v krvi in zmanjšanje očistka kreatinina. V kliničnih študijah in v obdobju trženja so poročali tudi o odpovedi ledvic, akutni odpovedi ledvic, primerih s smrtnim izidom, primerih, ki so zahtevali hemodializo in hiperkaliemiji stopnje 4. Voljivi na vid: V kliničnih študijah so poročali o izgubi vidnega polja stopnje 4 z izgubo vida. Če se na novo pojavi huda izguba vida, je treba zdravljenje prekiniti in opraviti oftalmološki pregled. Če so motnje vida trdovratne ali se poslabšajo, je priporočljiv oftalmološki pregled. **Histološka preiskava, ki ne nakazuje adenokarcinoma:** Na voljo so le omejeni podatki pri NSCLC, ki je ALK in ROS1 pozitiven in ima histološke značilnosti, ki ne nakazujejo adenokarcinoma, vključno s ploščatoceličnim karcinomom (SCC). **Medsebojno delovanje z drugimi zdravili in druge oblike interakcij:** Izogibati se je treba sočasni uporabi z močnimi zaviralci CYP3A4, npr. atazanavir, ritonavir, kobicistat, itraconazol, ketokonazol, posakonazol, vorikonazol, klaritromicin, telitromicin in eritromicin (razen če morebitna korist za bolnika odtehta tveganje, v tem primeru je treba bolnike skrbno spremljati glede neželenih učinkov krizotiniba), ter grenivko in grenivkinim sokom, saj lahko povečajo koncentracije krizotiniba v plazmi. Izogibati se je treba sočasni uporabi z močnimi induktorji CYP3A4, npr. karbamazepin, fenobarbital, fenitoin, rifampicin in šentjanževka, saj lahko zmanjšajo koncentracije krizotiniba v plazmi. Učinek zmernih induktorjev CYP3A4, npr. efavirenz in rifabutin, še ni jasn, zato se je treba sočasni uporabi s krizotinibom izogibati. Zdravila, katerih koncentracije v plazmi lahko krizotinib spremeni (midazolam, alfentanil, cisaprid, ciklosporin, derivati ergot alkaloidov, fentanil, pimizod, kinidin, sirolimus, takrolimus, digoksin, dabigatran, kolhicin, pravarstatin; sočasni uporabi s temi zdravili se je treba izogibati oziroma izvajati skrben klinični nadzor; bupropion, efavirenz, peroralni kontraceptivi, raltegravir, irinotekan, morfin, nalokson, metformin, prokainamid). Zdravila, ki

XALKORI®

KRIZOTINIB

podaljšujejo interval QT ali ki lahko povzročijo Torsades de pointes (antiaritmiki skupine IA (kinidin, disopiramid), antiaritmiki skupine III (amiodaron, sotalol, dofetilid, ibutilid), metadon, cisaprid, moksifloksacin, antipsihotiki) – v primeru sočasne uporabe je potreben skrben nadzor intervala QT. Zdravila, ki povzročajo bradikardijo (nedihidropiridinski zaviralci kalcijevih kanalčkov (verapamil, diltiazem), antagonisti adrenergičnih receptorjev beta, klonidin, gvanfacin, digoksin, meflokin, antiholinesteraze, pilokarpin) – krizotinib je treba uporabljati previdno. **Plodnost, nosečnost in dojenje:** Zenske v rodni dobi se morajo izogibati zanositvi. Med zdravljenjem in najmanj 90 dni po njem je treba uporabljati ustrezno kontracepcijo (velja tudi za moške). Zdravilo lahko škoduje plodu in se ga med nosečnostjo ne sme uporabljati, razen če klinično stanje matere ne zahteva takega zdravljenja. Matere naj se med jemanjem zdravila dojenju izogibajo. Zdravilo lahko zmanjša plodnost moških in žensk. **Vpliv na sposobnost vožnje in upravljanja strojev:** Lahko se pojavijo simptomatska bradikardija (npr. sinkopa, omotica, hipotenzija), motnje vida ali utrujenost; potrebna je previdnost. **Neželeni učinki:** Najresnejši neželeni učinki so bili hepatotoksičnost, ILD/pnevmonitis, nevtropenija in podaljšanje intervala QT. Najpogostejši neželeni učinki (≥ 25 %) so bili motnje vida, navzea, diareja, bruhanje, edem, zaprtje, povečane vrednosti transaminaz, utrujenost, pomanjkanje apetita, omotica in nevropatija. Ostali zelo pogosti (≥ 1/10 bolnikov) neželeni učinki so: nevtropenija, anemija, levkopenija, disgeuzija, bradikardija, bolečina v trebuhu in izpuščaji. **Način in režim izdaje:** Predpisovanje in izdaja zdravila je le na recept, zdravilo pa se uporablja samo v bolnišnicah. Izjemoma se lahko uporablja pri nadaljevanju zdravljenja na domu ob odpustu iz bolnišnice in nadaljnjem zdravljenju. **Imetnik dovoljenja za promet:** Pfizer Limited, Ramsgate Road, Sandwich, Kent CT13 9NJ, Velika Britanija. **Datum zadnje revizije besedila:** 25.01.2018

Pred predpisovanjem se seznanite s celotnim povzetkom glavnih značilnosti zdravila.

Vir: 1. Povzetek glavnih značilnosti zdravila Xalkori, 25.01.2018



Pfizer Luxembourg SARL, GRAND DUCHY OF LUXEMBOURG, 51, Avenue J.F. Kennedy, L-1855, Pfizer podružnica Ljubljana, Letališka cesta 3c, 1000 Ljubljana

